A field, geochemical and geochronological perspective on the origin of granitoids and mafic volcanic rocks in the Wecho River area and the nature of ancient crust in the southwestern Slave Province, NWT.

Sara Jaine Buse
B.Sc. Geology

A thesis submitted to the School of Graduate Studies in partial fulfillment of the degree of Master of Science

Department of Earth Sciences
Carleton University
January, 2006

Ottawa, Ontario

Abstract

The Wecho River area, located in the southwestern Slave Province, approximately 100 kilometres north of Yellowknife, NT, is dominated by Neoarchean granitoid rocks with lesser amounts of meta-sedimentary and associated mafic volcanic rocks. The rocks can be divided into 5 groups based on their age and geochemical characteristcs: Central Slave Basement Complex rocks, Group A mafic volcanic rocks, Group B metaluminous plutonic rocks, Group C peraluminous plutonic rocks and the Dauphinee Suite. Plutonism shows a shift from metaluminous to plutonism at 2600 Ma, similar to across the Slave Province. The Nd isotopic data for all groups are consistent with the presence of ancient crust beneath only the eastern side of the Wecho River area at the time of 2608 Ma granite production. The Central Slave Basement complex is thus interpreted to extend into and terminate within the Wecho River area.

Acknowledgements

I would like to thank my supervisor, Brian Cousens who was incredibly helpful and patient. Thanks to Bill Davis for all his knowledge with the geochronology. To Luke Ootes for two great field seasons as well as for his excellent editing. Thanks also to my field assistants over the past two years Dave White, Gord McKercher, Tania (Waffles) Brzozowski and Vance Hachkewich. As well, thanks to Val Jackson and Venessa Bennett for sharing their extensive knowledge with me. A special thanks also goes to Venessa Bennett who helped to define this project.

The Northwest Territories Geoscience Office is thanked for summer employment as well as funding for the project. Carleton University is also thanked for financial support. Thanks to Mike Jackson, the SHRIMP staff at the J.C.Roddick SHRIMP lab, Nicole and Tom, Julie from the picking lab at the GSC, and Lou Ling from the SEM lab at Carleton for their expertise and assistance while I was using the equipment in their labs.

I would also like to thank the Hard Core 4, Wanda, Jen and Robin, for providing excellent social stimulation and some awesome parties. Thanks to my favorite friend Jean-Yves Landry for his support. Lastly, thanks to the best family ever, my parents and brother who are extremely supportive, and to the Edgelow and Irvine families and my grandparents who remained interested and supportive.

TABLE OF CONTENTS

ORIGINAL WORK BY AUTHOR

All field work was done by S.Buse and L.Ootes (NWT Geoscience Office), with assitance from G. McKercher (University of Alberta), Dave White (Aurora Geosciences), Vance Hachkewich, and Tania Brzozowski (Carleton University) and all interpretations of discussed field relations within this thesis are those of the author. All geochronological data collected was done by the author at the Geological Survey of Canada with the help of the staff for the crushing and TIMS geochemistry and mass spectrometry. All grain picking, SHRIMP preparation, analysis and interpretations are those of the author with helpful discussion with B.Davis (GSC Ottawa).

Rock crushing and cutting for geochemical analysis was completed by S. Buse as well as the preparation of fused glass discs for XRF analysis. XRF analysis was carried out at the University of Ottawa and ICP-MS analysis was done by the Ontario Geological Survey. Sm-Nd isotope chemistry and analysis on the mass spectrometers was completed by the author with help from B.Cousens (Carleton University). All interpretations of the data are those of the author with helpful discussion from B. Cousens (Carleton University), B. Davis (GSC Ottawa) and L. Ootes (NWT Geoscience Office).

LIST OF TABLES

LIST OF FIGURES

LIST OF ABBREVIATIONS

ICP-MS	Inductively Coupled Plasma Mass Spectrometry
BSE	Back Scattered Electron
XRF	X-ray Fluorescence
SHRIMP	Sensitive High Resolution Ion Microprobe
LREE	Light Rare Earth Elements
REE	Rare Earth Element
HREE	Heavy Rare Earth Elements
CSBC	Central Slave Basement Complex
CSCG	Central Slave Cover Group
ε_{Nd}^{T}	Epsilon Neodymium at Time of Crystallization
Opx	Orthopyroxene
Cpx	Clinopyroxene
Plag	Plagioclase
Hbl	Hornblende
Mag	Magnetite
Qtz	Quartz
Bt	Biotite
Grdt	Granodiorite
Musc	Muscovite
Ep	Epidote
Cum	Cummingtonite
Chl	Chlorite
Kspar Porph	K-feldspar Porphyritic Granite
Kspar	K-feldspar
HT-LP	High Temperature – Low Pressure Metamorphism

Chapter 1: Introduction

1.1 Introduction

Archean cratons represent important geologic domains of early earth crust formation and growth. In Canada they form a large portion of the lithosphere and host major metallic mineral deposits making them targets for extensive study. The Slave Province is one of the smallest cratons of the Canadian Shield and is a meta-sedimentary and volcanic terrain extensively intruded by granitoid rocks. The granitoid rocks in the Slave Province are excellent contributors to the understanding of crust formation and growth within the craton. They represent large volumes of crust formed by complex melting and assimilation processes sometimes involving very old crust or younger more primitive melts of the lower crust or upper mantle. Within the Slave Province, Mesoarchean basement plays an important role in the formation of granitoid suites, often lending an ancient geochemical signature to younger granitoid melts, indicating that the granitoids formed at least in part by the partial melting of these basement complexes. In the eastern portion of the craton, the extent of the basement is defined by Pb (Thorpe, 1992) and Nd (Davis and Hegner, 1992) isotopic boundaries. The Pb isotopic boundary is based on massive sulfide deposits and the Nd isotopic boundary was determined from granitoid rocks. Supracrustal rocks to the east of these lines have juvenile isotopic signatures, indicating that there was no Mesoarchean basement involved in crust formation, and instead suggest the tectonic accretion of juvenile crust to a nucleus of older continental crust. In the western part of the craton, there has been some work done

to determine if Mesoarchean basement played a role during crust formation, but an isotopic limit to the basement complex has yet to be defined.

The Wecho River area, a granitoid-meta-sedimentary terrain, is located 100 km north of Yellowknife in the Southwestern Slave Province. It is wedged between an area with known basement exposures, the Nardin Complex, and the Snare River domain where there is no evidence for involvement of Mesoarchean basement in the formation of the rocks. The western edge of the Central Slave Basement Complex, the underlying pre-2.8 Ga gneissic basement, has been predicted to terminate in the Wecho River subsurface, but until now no research has been conducted to prove this.

To investigate the Wecho River Area, two seasons of 1:100,000 scale mapping were conducted in 2003 and 2004 to define and describe the various plutonic suites. Intensive rock sampling was done throughout the area with an emphasis on sample quality as well as full representation of units within the map area. Samples were then analyzed for major, trace element and Sm-Nd isotopic geochemistry. Select samples were also collected for U-Pb geochronology in order to constrain the ages of the rocks as well as discern any inheritance within the suites. These analyses will help to describe and contrast the Wecho granitoid suites as well as determine if they can be correlated to other plutonic suites in surrounding areas. The Sm-Nd analyses provide important information on whether the suite has a juvenile or evolved crustal signature, thus giving clues to whether there was interaction between Mesoarchean basement during the formation of any of the suites.

This information is important in understanding how the western Slave Province was formed and how crustal growth continued in comparison to the rest of the craton. It also helps to tie the entire western portion of the craton together, such as the Snare River and Nardin map areas, as well as the Western Plutonic Complex directly south of the study area.

Chapter 2: Regional Geology

2.1 Location of the Slave Craton

The Slave craton, located in central Northwest Territories, is an Archean granite-meta-sedimentary-greenstone terrain (Figure 2-1). It is one of the best exposed Archean cratons in the world and is unlike any other craton in the Canadian Shield due to its volume of meta-sediments and granitoids relative to greenstone belts as well as its lack of komatiites. To the east, the craton is flanked by the Proterozoic Thelon orogen and the Archean Western Churchill Province and to the west is flanked by the Proterozoic Great Bear Magmatic Zone (Hoffman, 1989). A summary of the geologic events within the Slave Province can be found in Figure 2-2.

2.2 The Central Slave Basement Complex and Central Slave Cover Group

The oldest sequence within the Slave craton is the >2.8 Ga Central Slave Basement Complex (CSBC), commonly represented by diorite to tonalite gneisses with migmatitic layering and at least one crosscutting mafic dyke swarm that is also deformed and metamorphosed. Also common are tonalitic to monzogranitic gneisses that are not migmatized but still include multiple generations of mafic dyke swarms (Bleeker et al., 1999a). The CSBC outcrops throughout the central and parts of the southwestern Slave craton including the 4.00 to 4.03 Ga Acasta Gneiss complex, the westernmost basement exposure (Bowring and Williams, 1999), and a gneiss underlying the

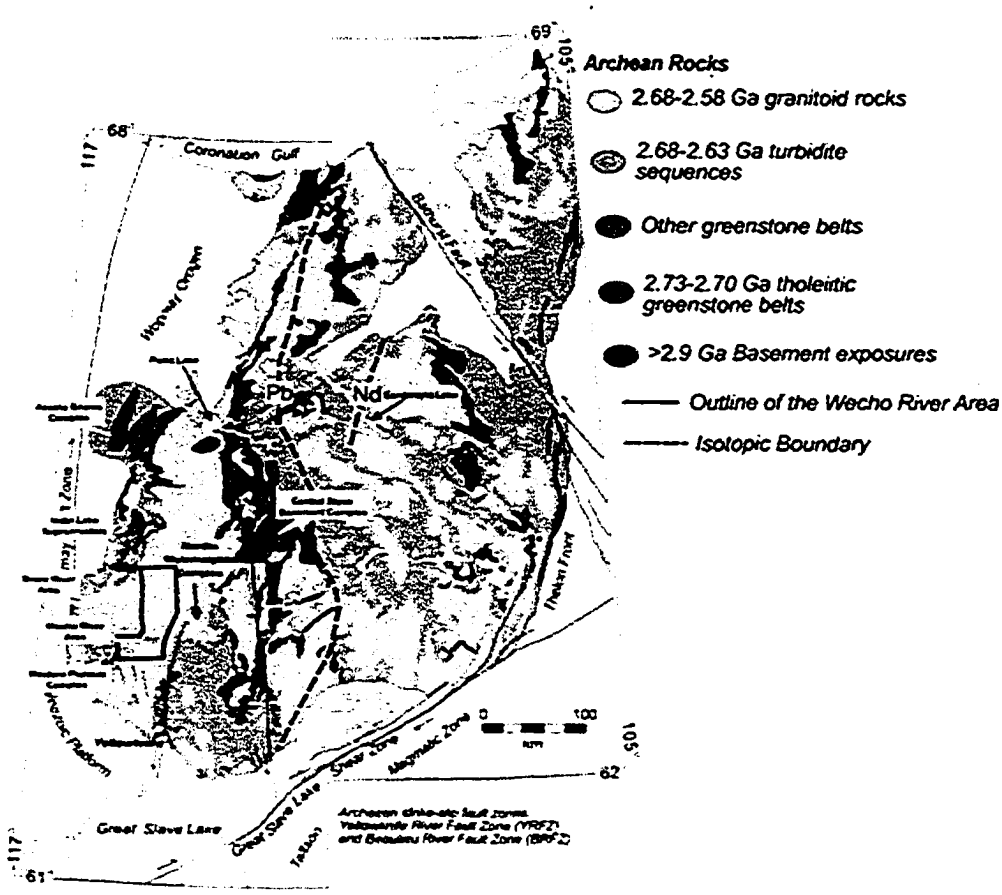

Figure 2-1 Map of the Slave Craton with the location of the Wecho River area and other important geographic locations.

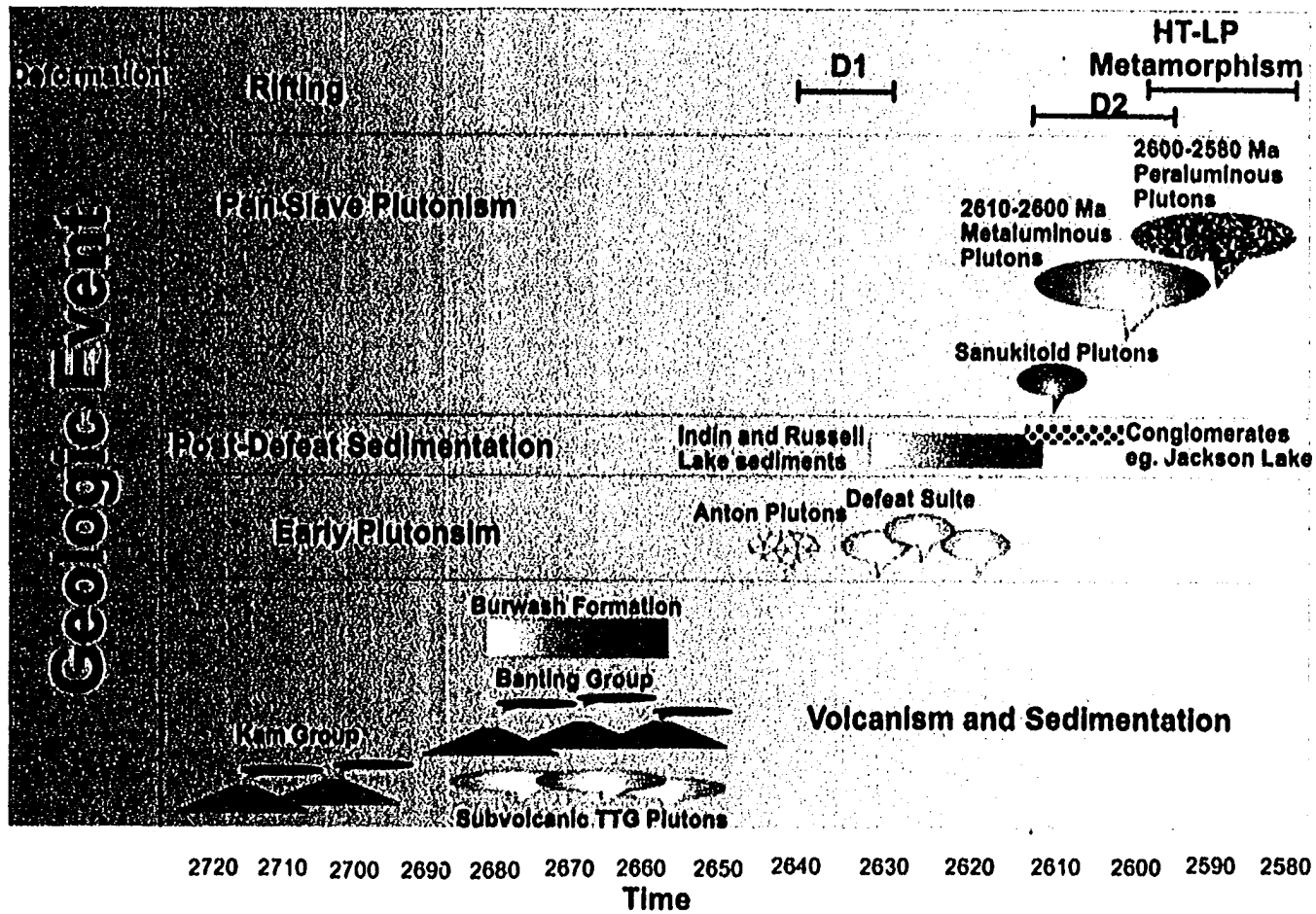

Figure 2-2 Summary of the geologic events in the Slave Craton.

Courageous Lake greenstone belt dated at 3325+/-8 Ma, the easternmost occurrence (Bleeker et al., 1999a). The extent of exposed CSBC is interpreted to be the result of fold interference and later strike-slip faulting along the Beaulieu River and Yellowknife River fault zones.

In the eastern portion of the craton the extent of the CSBC complex is defined by Nd and Pb isotopic boundaries in granitoid rocks and VMS deposits, respectively, as well as other isotopic studies that determine the absence of >2.70 Ga rocks (Isachson and Bowring, 1994). The Nd isotopic boundary of Davis and Hegner (1992) is defined by the Nd isotopic compositions of granitoid rocks in the Contwoyto Lake area, which show unradiogenic signatures in the west and more radiogenic, juvenile signatures to the east. The Pb isotopic boundary is defined by higher $^{207}Pb/^{204}Pb$ ratios (more evolved ancient Pb compositions) in the western and central parts of the craton compared to the eastern Slave indicating that ancient crust was involved in the petrogenesis of rocks in the central Slave craton. East of the Pb isotopic boundary, a more juvenile source is reflected by the lower Pb ratios (Thorpe, 1992).

Overlying the CSBC is the Central Slave Cover Group (CSCG), constrained in age between 2924 and 2734 Ma, and consisting of mafic volcanic flows overlain by a sequence of conglomerates, chromite bearing fuchsitic quartzites and banded iron formation (Bleeker et al., 1999a). The CSCG is interpreted to be the product of rifting and subsidence, resulting in the formation of local shallow shelves where mixed basement and volcanic debris were transported, and banded iron formation could be

deposited (Bleeker et al., 1999a). Both the CSBC and the CSCG are extensively intruded by syn- to post- deformational granites that in some cases destroy the contact between the two sequences.

2.3 Greenstone Belts and Meta-sedimentary Rocks

Greenstone belts in the Slave Province are volumetrically small, but with the sedimentary rocks they overlie the CSBC and CSCG sequences (Bleeker et al., 1999a). Two groups of volcanic rocks make up the Yellowknife Greenstone Belt, the Kam Group and the Banting Group.

The Kam group is represented by tholeiitic mafic volcanic rocks, interpreted to be submarine due to pillow structures, and lesser amounts of felsic tuffaceous volcanic rocks. Dated at 2712 to 2701 Ma with inherited zircons as old as 2820 Ma (Isachson, 1992), and metamorphosed to greenschist facies, the group is divided into four formations, the Chan, Crestaurum, Townsite and Yellowknife Bay, based largely on physical characteristics (Cousens, 2000). Rare earth element (REE) geochemistry of the suite is similar to modern Normal Mid Ocean Ridge Basalt (N-MORB), which is the product of depleted upper mantle melting, with flat to slightly depleted light rare earth elements (LREE) (Cousens, 2000). Nd isotopic data for this suite reflect CSBC contamination, indicated by a range of positive to negative $\varepsilon_{Nd}{}^{T}$ values with increasing silica content and LREE enrichment. Contamination of the lavas by the CSBC occurred as the magmas evolved from mafic to felsic compositions (Cousens, 2000). The proposed

geological setting for this volcanic group is interpreted to be an extensional continental margin setting.

Unconformably overlying the Kam Group are the Banting Group volcanic rocks. The Banting group is divided into the Ingraham and Prosperous formations with U-Pb ages of 2658±2 Ma and 2664±1 Ma (Isachson, 1992). Geochemical analysis of this group by Cousens et al. (2002) indicates that the rocks range from tholeiitic, depleted upper mantle derived melts, similar to those of the Kam group, to felsic rocks with $\varepsilon_{Nd}{}^{T}$ values >-1 and TTG-like geochemical characteristics. These more calc-alkaline rocks of the Banting group are interpreted to have been partially melted from a garnet amphibolite source with residual garnet, accounting for the depletion in HREE (Cousens et al., 2002). Tectonically the Banting Group is interpreted to have formed during waning of an extensional setting, with delamination of the dense lower crust initiating partial melting of the overlying mafic crust (Cousens et al., 2002 and Cousens et al., 2005).

During and previous to the deposition of the Banting group are the 2680-2660 Ma sedimentary rocks of the Burwash and equivalent formations. These are clastic sedimentary rocks, dominantly greywackes, interpreted to be turbidite sequences. These rocks cover approximately 40% of the craton, ranging in metamorphic facies from greenschist to upper amphibolite with rare granulite occurrences, such as those in the Snare River area (Jackson, 2003 and Bennett et al., 2005). There are three ages of sedimentation for the Yellowknife Supergroup: the >2680 Ma George Lake turbidites (van Breeman et al., 1992), the 2660-2680 Ma Burwash and equivalent formations and a

younger formation dated at <2630 Ma, locally known as the Damoti formation in the Indin Lake area, but also found at Russell Lake (Pehrsson and Villeneuve, 1999;Bennett et al., 2005; Ootes et al., 2005).

The two main sequences within the southwestern Slave Province are the 2660 Ma Burwash formation and the ca. 2630 Ma Damoti sequence. A paleocurrent study of the Burwash formation determined that the main direction of flow was from west to east (Henderson, 1975). Zircon within this formation are as old as 3.4 Ga and are interpreted to be a mixture of ~20% mafic-intermediate rocks, ~55% felsic volcanic rocks, and ~25% granitic rocks, interpreted from geochemical data and ε_{Nd}^{T} values of +1.7 to -4.4 (Yamashita and Creaser, 1999).

Unconformably overlying the Banting and Kam Group volcanic rocks are the ca 2600-2590 Ma conglomerates and lithic quartz arenites of the Jackson Lake Formation (Bleeker et al., 1999a). This formation is found across the Slave craton, with correlatives such as the Beaulieu Rapids Formation and the Keskarrah Formation at Point Lake.

2.4 Granitoid Rocks

Granitoid rocks are widespread across the Slave Structural Province and exceed 50% of the surface area. Plutonism in the Neoarchean history of the craton reflects tectonothermal processes that led to the stabilization of the craton. These rocks can be divided into 3 main groups defined by their ages relative to the main deformational

events (labeled D1 and D2 in figure 2-2): the ca. 2689 to 2650 Ma pre-deformational plutons, the syn- to late deformational ca. 2610 to 2600 Ma plutons and the post deformational 2599 to 2580 Ma granitoids (Henderson et al., 1987; van Breeman et al., 1992; Davis et al., 1994; Davis and Bleeker, 1999). Granitoid compositions shift from metaluminous to peraluminous through time, and the later plutonism represents final stitching of the craton connecting the older basement with the over thrust accreted terrains such as the Anialik terrane (van Breeman et al., 1992; Relf et al., 1999; Davis et al., 1994).

Part of the pre-deformational granitoid group in the northeastern portion of the craton near Contwoyto Lake are the ca. 2689-2650 Ma trondjhemites and diorites. Granitoids such as the Hinscliffe domain in the southwestern Slave Province dated at 2654±4 Ma (Villeneuve and Henderson, 1998), the ca. 2680 Ma Cotterhill gneiss complex in the Indin Lake area (Pehrsson and Villeneuve, 1999) as well as the ca. 2680 to 2650 Ma trondjhemite-granodiorite-tonalite (TTG) plutons of the Snare River area (Bennett et al., 2005) are part of the pre-deformational granitoid group. The Anton Complex, once interpreted as part of the CSBC, is composed of 2630 to 2638 Ma foliated granodiorites and granites. It has been determined to be older than the 2630 to 2580 Ma Western Plutonic Complex, but has gradational contacts with the pre-, syn- and post-deformational granitoids (Dudas et al., 1990). These pre-deformational plutons tend to be localized and may not be the result of craton-wide plutonic events like the syn and post deformational granitoid rocks.

The best-studied example of the syn to late deformational granitoids is the Defeat Suite, a diorite to tonalite to granodiorite plutonic suite spread across the Slave craton (Henderson et al., 1987; van Breeman et al., 1992; Yamashita et al., 1999; Davis and Bleeker, 1999; Cousens et al., 2005; Bennett et al., submitted). The Defeat plutons postdate the compressional D1 deformational event and represent plutonism in the southern Slave Province from 2628 to 2615 Ma (Davis and Bleeker, 1999). This suite is thought to be the result of overthickening of the crust due to deformation and melting of garnet amphibolite in the lower crust (Yamashita et al., 1999). Equivalents include the Disco Intrusive Suite in the Snare River area and similar I-type granites on the eastern side of the craton such as in the Walmsley Lake area (Cairns et al., 2005). This suite has been dated at 2628±3 Ma and 2624±3 Ma within the Western Plutonic Complex, an area within the southern Slave Province dominated by Neoarchean granitoids (Davis and Bleeker, 1999), and at 2635 ±8 Ma for the equivalent Disco Intrusive Suite in the Snare River domain (Bennett et al., 2005).

At ca. 2608 Ma, sanukitoid plutons were emplaced in various locations across the craton such as the Contwoyto area (Davis et al., 1994), the Snare River area (Bennett et al., submitted) and the ca. 2614 Ma Margaret Lake Pluton in the Walmsley Lake area (Cairns et al., 2005) as part of the syn- to late- deformational plutonic suite. These rocks are interpreted to be juvenile high Mg andesitic magmas from a depleted mantle source (Davis et al, 1994).

The latest generation of granitoid rocks are interpreted as post-deformational plutonism and include such suites as the 2596±2 Ma Prosperous granite (Davis and Bleeker, 1999), the Awry granite, the 2586±2 Ma Morose Pluton (Davis and Bleeker, 1999), the 2583.5±1 Ma Stagg suite (Davis and Bleeker, 1999), the Contwoyto suite, and the Yamba suite. This plutonism is Pan-Slave, dated between 2600 and 2580 Ma and is contemporaneous with the D2 deformation (Davis and Bleeker, 1999). These granitoids include weakly metaluminous to peraluminous granodiorites, granites, porphyritic granites to syenogranites and two mica granites. This was a period of voluminous magmatism that requires a thermal anomaly such as that due to a lithospheric delamination to drive crustal plutonism (Davis and Bleeker, 1999; Yamashita et al., 1999).

2.5 Deformation and Metamorphism

Deformation within the Slave craton is constrained into two main episodes that both affect the Burwash sediments and are thus post 2660 Ma (Davis and Bleeker,1999). Upright doubly plunging F1 folds, either tight chevrons or isoclinal, represent D1. The D1 event has been constrained between 2660 and 2630 Ma, and is responsible for greenschist grade metamorphism. Events prior to D1 are documented as a high strain zone along the basement-supracrustal boundary of the Sleepy Dragon Complex (Bleeker et al., 1999b). F2 folds are steeply plunging with a dominant S2 crenulation cleavage axial planar to the F2 folds which overprint the F1 generation (Davis and Bleeker,1999). This S2 cleavage is commonly seen refracting around plutons. Peak metamorphism

occurs pre-, syn- to post-F2, between 2.61 and 2.59 Ga. The high temperature-low pressure (HT-LP) metamorphism constrained between 2.60 and 2.58 Ga, is associated with plutonism (Bethune and Carmichael, 1998). Defeat and Prosperous plutonism are spatially associated with metamorphic isograds within the meta-sediments, indicating that the isograds formed at different times over a 30 million year period (Davis and Bleeker, 1999).

A later deformation, D3, is not seen as often and is found as late strike slip faults and steeply plunging folds with an associated S3 crenulation cleavage.

2.6 Growth of the Slave Province

Many authors have explored the assembly of the Slave craton from the formation of the Central Slave Basement Complex, interpreted by some as the result of accretion of continental blocks (eg. Yamashita et al., 2000), to the final assembly of the craton in its present state. In the eastern part of the craton, east-dipping subduction is interpreted to have occurred, accreting arc terranes to the CSBC, such as in the Anialik domain (Relf et al., 1999) where the CSBC is interpreted to have been thrust eastward onto the Anialik arc. In the Contwoyto Lake area, Davis et al. (1994) interprets two eastward dipping subduction zones accreting younger CSBC age rocks onto an older CSBC block followed by accretion of a < 2.71 Ga block onto the CSBC by ca. 2650 Ma. Kusky (1989) interprets the Hackett River arc in the eastern portion of the craton to be thrust westward over the CSBC. Cook et al. (2002) interpret seismic reflections from the SNORCLE

transect to mean that the CSBC was thrust eastward over arc rocks at the time of deformation (ca. 2.65 to 2.58 Ma). The accretion of arc terranes is mapped by the isotopic Pb and Nd boundaries of Thorpe (1992) and Davis and Hegner (1992) respectively because they show roughly where the CSBC terminates and where the juvenile terranes begin. In the western part of the craton Bennett et al. (submitted) suggest an arc-continent collision between the Snare arc, as well as the Indin Lake supracrustal belt (Pehrrson and Villeneuve, 1999) and the CSBC at ca. 2600 Ma.

Chapter 3: Field Relations

3.1 Introduction

The Wecho River area is located in the southwestern Slave Province, approximately 100 kilometres north of Yellowknife, NWT (Figure 3-1) between the Snare River map area to the west (Jackson, 2003), the Nardin Complex to the east (Stubley, 1997), the Western Plutonic Complex to the south and southeast (Henderson, 1985), and the Indin Lake supracrustal belt to the northwest (Pehrsson and Villeneuve, 1999) (Figure 3-2). The Snare River area, directly to the west, is granite-meta-sedimentary terrane with no known Central Slave Basement Complex exposures or evidence for basement based on the geochemistry of its plutonic rocks. The western boundary of the Wecho River area is the eastern edge of the Snare granulite wedge. The Nardin Complex, located to the east of the Wecho River area, is a granite-meta-sedimentary domain metamorphosed to upper amphibolite and granulite grade (mineral assemblage dependant) and it hosts the closest geologically interpreted basement exposure to the Wecho River area. The Wecho River area is a granite-meta-sedimentary terrain with minor occurrences of mafic volcanics (Figure 3-3). It represents an area of the Slave craton with voluminous plutonism and, as such, a record of significant Archean crust formation and growth. It ranges from greenschist to granulite in metamorphic grade.

3.2 Mafic Volcanic Rocks

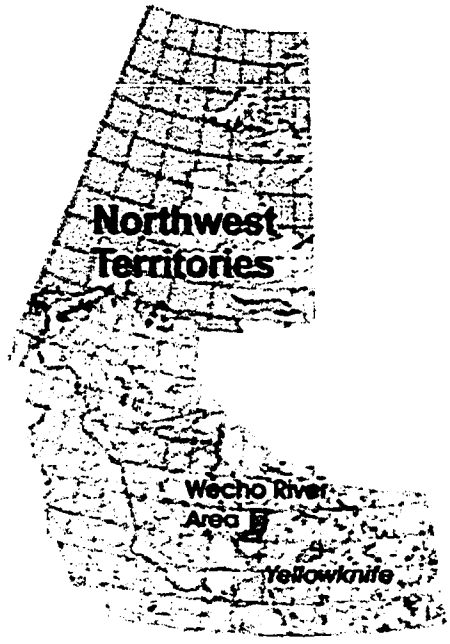

3-1

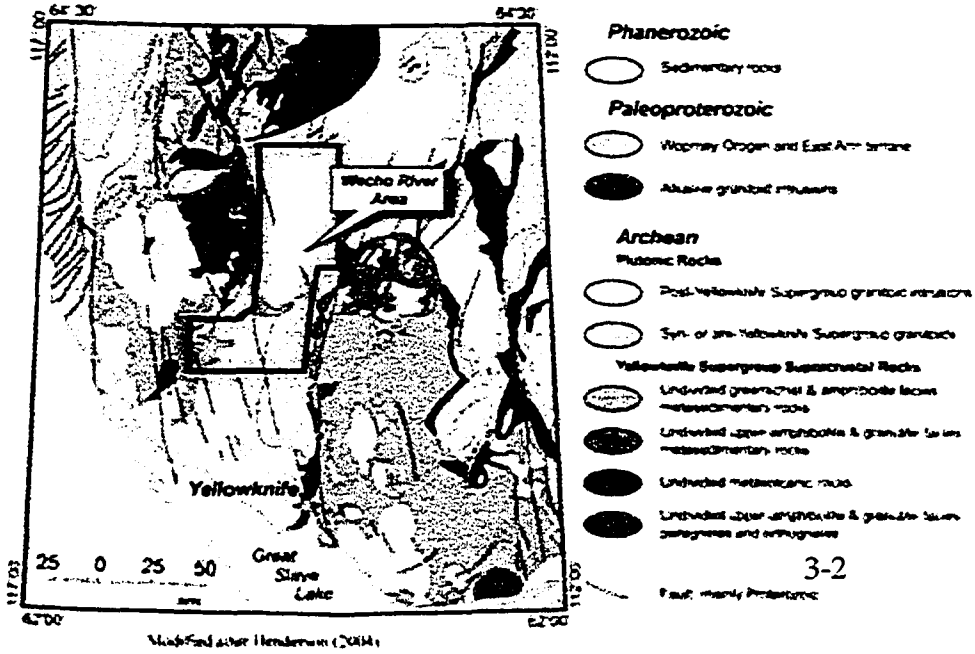

3-2

Figure 3-1 and 3-2. 3-1. Location of the Wecho River area in the NWT. 3-2. Location of the Wecho River map area in the Southwestern Slave Province.

Mafic rocks in the Wecho River occur at two localities, Mosher Lake and Germaine Lake, and were sampled at both. The Mosher Lake volcanic rocks occur in a linear ridge trending NW-SE that extends from south of Mosher Lake into the Snare River area. The rocks are highly sheared, but in some places remnant pillow structures can be seen (Figure 3-4) with rare occurrences of garnet within the selvages. The volcanics are hornblende, plagioclase and chlorite-bearing with local pyrite and sphalerite.

The Germaine Lake mafic volcanic rocks are volumetrically small, are extensively intruded by the Armi Pluton and spatially lie within the Wheeler-Germaine Lake meta-sedimentary belt. Although limited in extent, these volcaniclastic rocks are representative of a lithology present prior to the intrusion of younger granitoids. The rocks are volcaniclastic in origin, consisting of inter-layered mafic and intermediate units (Figure 3-5). It is generally fine grained, but the mafic layers contain coarse-grained hornblende crystals as well as rare garnet. The unit is only several 10s of meters thick.

3.3 Meta-sedimentary Rocks and Deformation

Meta-sedimentary rocks in the Wecho River area range from greenschist to granulite grade and are crop out sporadically throughout the study area. They are commonly found as xenoliths within the granitoid suites. In the far southwestern portion of the map area are the Mosher Lake turbidites. These greywacke-mudstone turbidites are

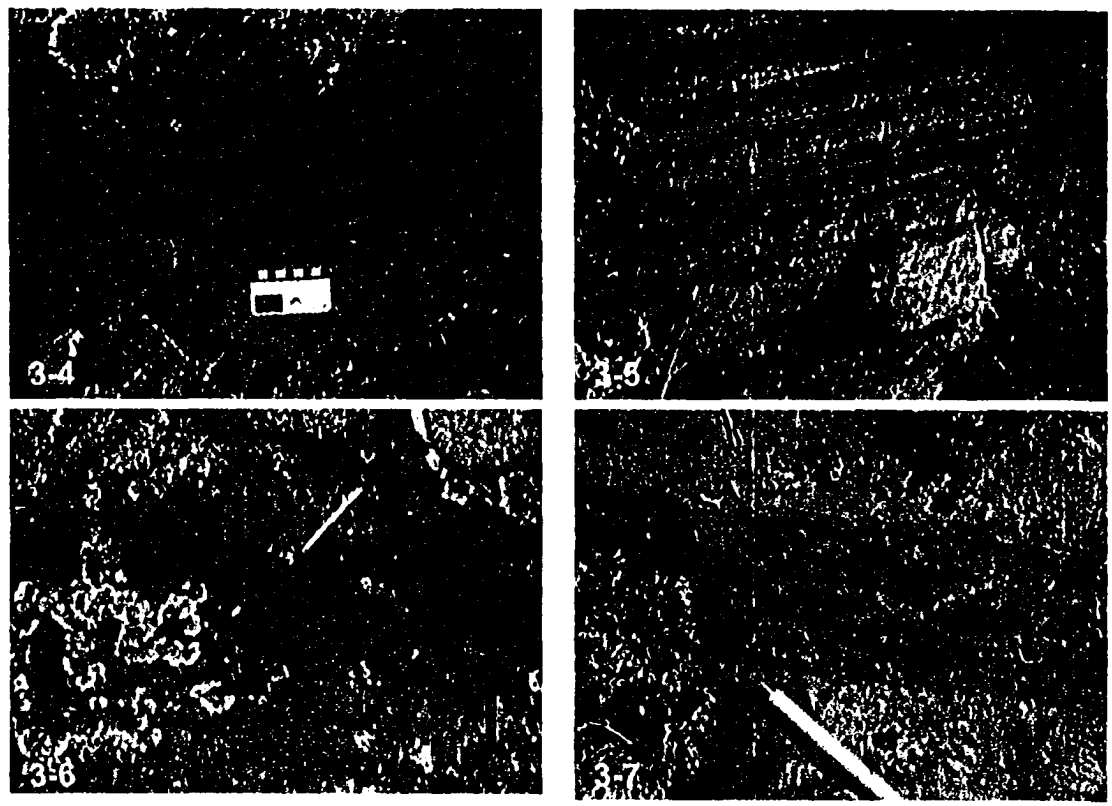

Figures 3-4 to 3-7. 3-4.Remnant pillow salvage within the Mosher Lake volcanics. 3-5. Germaine Lake volcaniclastic rocks. Dark coloured layers are mafic with hornblende and plagioclase and the light coloured layers are intermediate in composition. 3-6. Biotite grade greywacke-turbidites at Mosher Lake. Arrow marks the topping direction of the beds. 3-7. Cordierite grade turbidites. Porphyroblasts of cordierite within muddy layers that have overgrown the S2 cleavage, marked by the direction of the pen magnet.

metamorphosed to biotite and cordierite facies (greenschist to lower amphibolite metamorphic grade) and are distinguished by a cordierite isograd, which is offset by a NW-SE trending fault with sinistral displacement. F1 folding in the turbidites is interpreted utilizing younging directions in the sediments such as cross-bedding, flame structures and other load structures in the biotite facies sediments (Figure 3-6) and by increasing amount of cordierite in the more aluminous fine-grained silty and muddy layers in the cordierite facies sediments. These F1 folds are large-scale isoclinal folds. A local S2 cleavage within the turbidites is overgrown by cordierite indicating that metamorphism was post-deformation (Figure 3-7) (Ootes and Pierce, 2005). F2 and F3 folds (referred to as post-F1) occur as centimetre to metre scale open folds, where the cleavage is generally rotated slightly clockwise to bedding, indicating a larger S-fold structure.

The Mosher Lake turbidites are intruded from the east by large tourmaline-bearing pegmatites that range from decimeters to metres in width and locally exhibit spectacular graphic texture. The metamorphic grade of the meta-sediments increases eastward to upper amphibolite southeast of Inglis Lake. The meta-sediments locally include sulfide minerals such as pyrite and chalcopyrite.

The other large meta-sedimentary belts within the Wecho River area are located northeast of the Mosher Lake meta-sediments at Germaine, Wheeler and Armi Lakes. At Germaine and Wheeler Lakes, meta-sedimentary rocks are biotite + cordierite + sillimanite ± garnet ± andalusite bearing. Sillimanite-bearing outcrops are often

distinguished by small, white bladed sillimanite although some outcrops are quite spectacular with large sillimanite knots. Sillimanite pseudomorphs of andalusite are noted by a pink hue to the crystals as well as the presence of the distinctive chiastolite crosses. This implies that the metamorphism in the Germaine Lake area would have involved the formation of andalusite at low to medium pressure and temperature followed by an increase in at least the temperature to form sillimanite. To the north and northeast of Germaine Lake, the sediments become migmatitic with 10-70%melt.

At both Wheeler and Germaine lakes the meta-sediments are extensively intruded by the Hickey, Armi, Mofee and Wecho granitoids. F1 folding in this part of the map sheet is similar to the Mosher Lake area and is defined by bedding reversals. F2 and F3 deformation are difficult to define because the cordierite/sillimanite growth has destroyed the earlier cleavage relationships. The porphyroblasts define either a S2 or S3 generation cleavage, but are folded around younger open folds associated with S3/S4 foliations (Ootes and Pierce, 2005).

North of Germaine Lake is the Armi Lake meta-sedimentary belt composed of mid- to upper-amphibolite grade meta-sediments and migmatites bearing biotite + sillimanite ± garnet (Figure 3-8). The foliation in these rocks is defined by biotite and sillimanite and is the same as the biotite foliation in the Armi pluton that intrudes the meta-sediments. The northernmost part of the Wecho terrane is metamorphosed to granulite grade, identified by assemblages of cordierite + garnet + K-feldspar in meta-

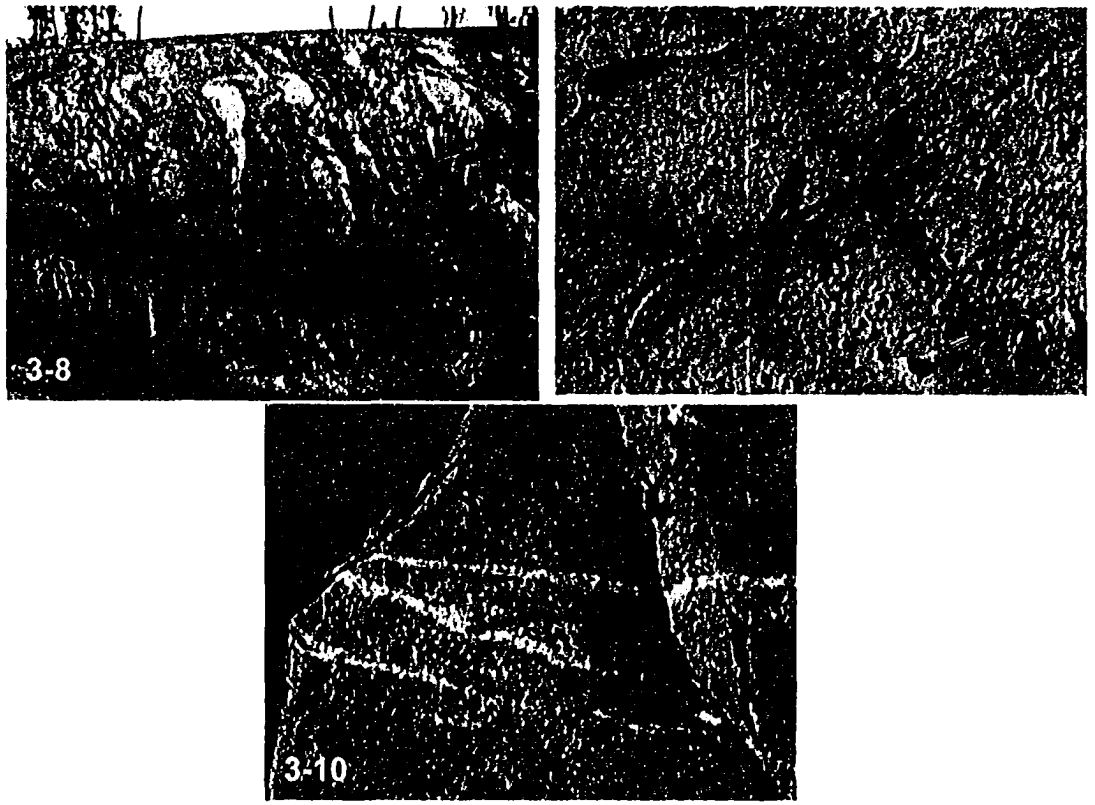

Figures 3-8 to 3-10. 3-8. Migmatites from north of Wheeler Lake. 3-9. A tourmaline bearing pegmatite dyke cross cutting the Old suite, a well deformed hornblende granodiorite. 3-10. Wheeler Lake diorite cross-cut dykes of the Mag Suite and pegmatites.

sedimentary remnants and orthopyroxene-bearing assemblages in mafic rocks. Meta-sedimentary packages in the northern part of the map sheet are largely migmatites, with local occurrences of metatexite and diatexite.

3.4 Granitoids of the Wecho River Area

Granitoids in the Wecho River area are voluminous and the focus of this study. Many of them are either very altered or contain abundant schlerin or enclaves making them poor candidates for geochemical analysis, so not all plutons were sampled. Nine granitoid suites and two mafic volcanic localities were sampled, with an emphasis on metaluminous granitoid suites. Sampling took place over the entire study area to obtain a representative sample suite for the Wecho River area, especially important when looking for evidence of underlying basement. No basement exposures were found within the study area, the closest CSBC exposure being the Nardin Complex, directly east of the Wecho River area. The lack of basement exposures in the Wecho River area means that the only evidence for basement would be found in either the geochronology or isotope geochemistry of the granitoids. The proceeding descriptions are of all the granitoids in the Wecho River area, presented from oldest to youngest.

3.4.1 Old Suite

To the north of Germaine Lake is the Old Suite, a strongly foliated granodiorite bearing biotite ± hornblende. This suite contains granodiorite enclaves and is intruded by

mixed granodiorite and hornblende granodiorite to tonalites as well as young pegmatites (Figure 3-9). These rocks are clearly the oldest metaluminous suite in the Wecho River area, but due to complex dyking of one suite into another and the abundant enclaves and pegmatites, sampling was not possible for fear of contamination.

3.4.2 Wheeler and Germaine Lake Diorites

Genetically related to the Old suite is the Wheeler Lake monzodiorite and Germaine quartz monzodiorite. Both are small, isolated units that are heavily intruded by other granitoid suites. The Wheeler diorite, located to the east of Wheeler Lake, is found as metre scale enclaves intruded by thin veins of the Hickey Suite (Figure 3-10). It is medium grained and composed dominantly of hornblende + plagioclase ± quartz ± K-feldspar ± magnetite. It also exhibits thin millimeter scale epidote veins as well as millimeter scale veins of the intruding granite.

The Germaine Suite is located to the east of Germaine Lake and is cross-cut by two different granitoids, the Mofee Pluton and the Armi Pluton, as well as pegmatite dykes that exhibit coarse grained hornblende crystals growing along their margins. It is a quartz monzodiorite and contains hornblende, plagioclase, quartz and biotite as well as minor K-feldspar, but no magnetite (Figure 3-11). It is also coarser grained, has more plagioclase and has a larger surface expression than the Wheeler Suite.

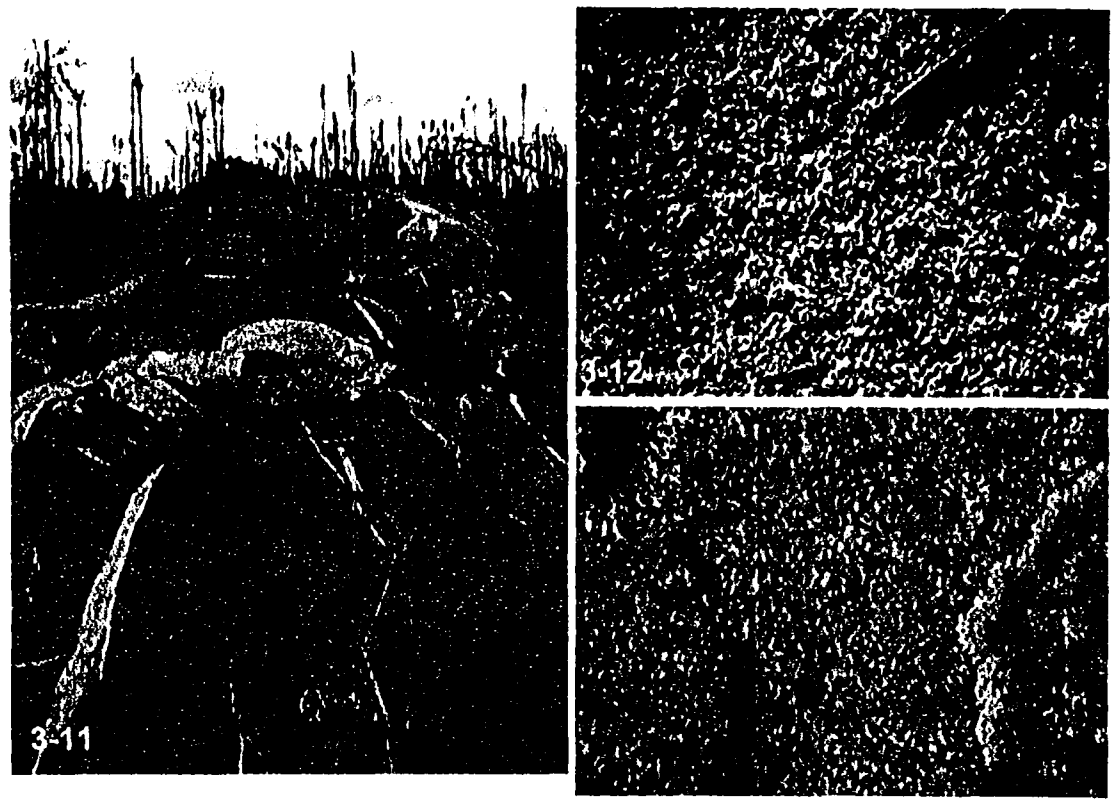

Figures 3-11 to 3-13. 3-11 Germaine Lake monzodiorite with veins of cross-cutting granodiorite and pegmatite. 3-12. Course grained South Suite, a hornblende magnetite granite. Hornblende is often intergrown with biotite and is usually very altered. A K-feldspar stringer is also pictured here. 3-13 The Mag Suite, a magnetite granite.

These suites are similar to the quartz diorites reported in the Snare River area (Jackson, 2003 and Bennett et al., submitted), the Concession Suite near Contwoyto Lake (Davis et al., 1994) as well as a diorite in the Indin Lake area (Pehrsson and Villeneuve, 1999).

3.4.3 South Pluton

In the southernmost portion of the Wecho River area is the South Pluton, a pinkish beige to cream coloured course grained, equigranular hornblende magnetite granite (Figure 3-12). It shows a moderate foliation defined by biotite. Biotite is more abundant than hornblende and the sample has minor disseminated magnetite. The hornblende within the suite is often altered, making it difficult to recognize in outcrop. This suite is faulted along its northern and western margins, which defines the contact between it and the Mosher lake meta-sediments. This suite occurs as enclaves within the 'dirty' granite, and dykes of the Wecho Pluton intrude it.

3.4.4 Hickey Suite

The Hickey Suite is a biotite-magnetite granodiorite to granite suite located primarily in the northern-most portion of the Wecho River area. It is a medium grained, light pink to white, equigranular granodiorite that is distinguished in the field by K-feldspar stringers and a quartz-biotite foliation (Figure 3-13). It is also distinguished by mafic enclaves that range from amphibolite to granulite grade and are hornblende-

plagioclase bearing, and in some cases orthopyroxene-bearing. Enclaves in this suite range from compositionally layered to massive. In some cases there are leucosomes associated with the enclaves within which there are large pyroxene or amphibole crystals (Figure 3-14). It also contains strongly foliated granodiorite to tonalite and sedimentary xenoliths. The sedimentary xenoliths are often at upper amphibolite to granulite grade in the northern regions of the map area, and become much more concentrated near areas where there are remnant meta-sedimentary packages. It is medium to strongly foliated defined by biotite and elongate quartz crystals. The magnetite is found either well disseminated or intergrown with biotite. This pluton has been metamorphosed to granulite grade, recognized in the amphibolite enclaves by the presence of orthopyroxene. In the Wecho River area, the Hickey Pluton is found as enclaves within the 'dirty' granite.

3.4.5 Armi Pluton

Associated with the Armi Lake meta-sedimentary belt is the Armi Lake Pluton a homogenous biotite ± muscovite granodiorite that is medium grained, equigranular and is moderately foliated. This suite contains few enclaves, either meta-sedimentary or mafic depending on the vicinity of the granodiorite to meta-sedimentary and mafic volcanic packages. The foliation of this suite is the same as the biotite-sillimanite foliation in the meta-sedimentary rocks that the granodiorite intrudes, making the age of this suite a maximum age for metamorphism of the meta-sediments (Figure 3-15). Minor muscovite is found in this suite, probably the result of a secondary alteration of the suite or

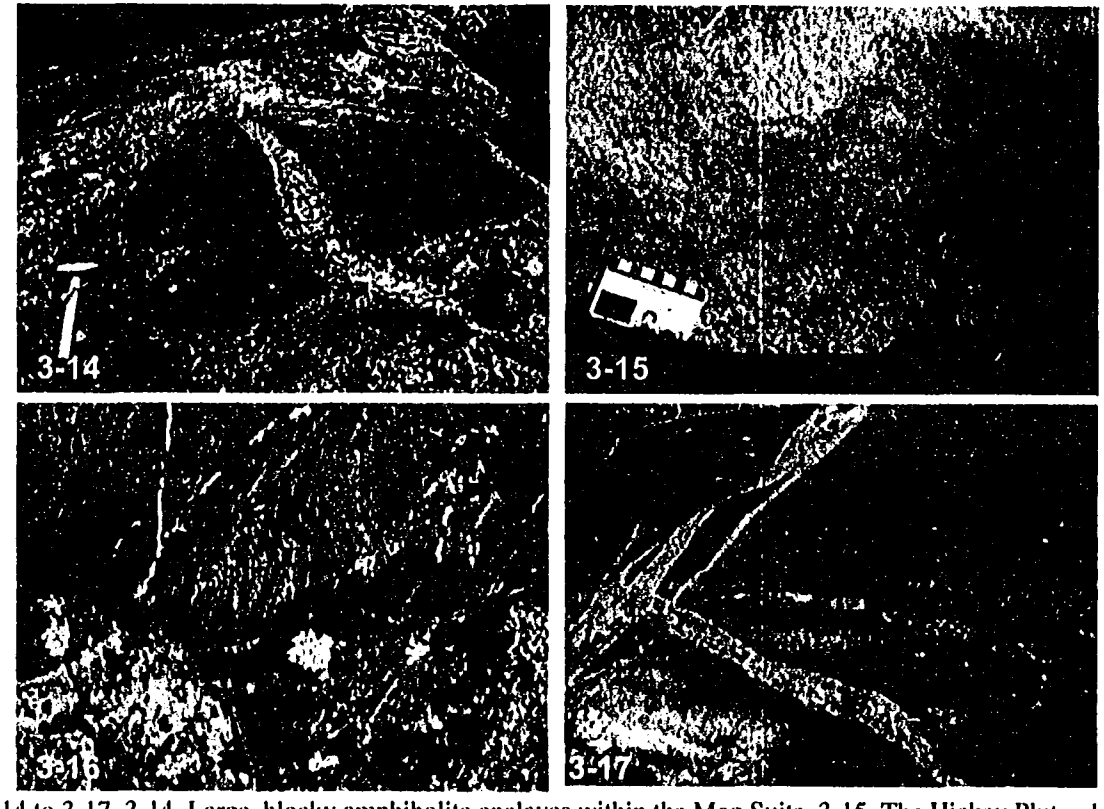

Figures 3-14 to 3-17. 3-14. Large, blocky amphibolite enclaves within the Mag Suite. 3-15. The Hickey Pluton biotite-magnetite granodiorite with a quartz-biotite foliation. This locality shows a gneissic texture. 3-16. Granulite grade layered mafic enclaves within the Hickey Pluton. Enclaves are hornblende + plagioclase + orthopyroxene ± clinopyroxene bearing and have melt stringers in them that often contain macroscopic orthopyroxene crystals. 3-17. The Armi Pluton cross cutting sillimanite-grade meta-sediments with the same foliation as the Armi Suite.

retrograde reactions. Commonly crosscutting this granodiorite are dykes of the Mofee Suite. Other exposures of the Armi Pluton type are found further south near Germaine and Wheeler Lakes.

3.4.6 Mag Pluton

The Mag Pluton is a pluton located in the southernmost part of the Wecho River area. This suite exhibits amphibolite enclaves that are hornblende and magnetite bearing, but shows no K-feldspar stringers (Figure 3-16). It is medium grained and equigranular and exhibits disseminated biotite and magnetite (Figure 3-17). The suite shows a weak foliation defined by biotite.

3.4.7 Inglis Pluton

The Inglis Pluton is an oval pluton surrounding Inglis Lake that is a beige to orange, equigranular hornblende-magnetite granodiorite (Figure 3-18). It is weakly to moderately foliated defined by biotite and hornblende, but its relationship to other suites is unknown.

3.4.8 Dirty Granite

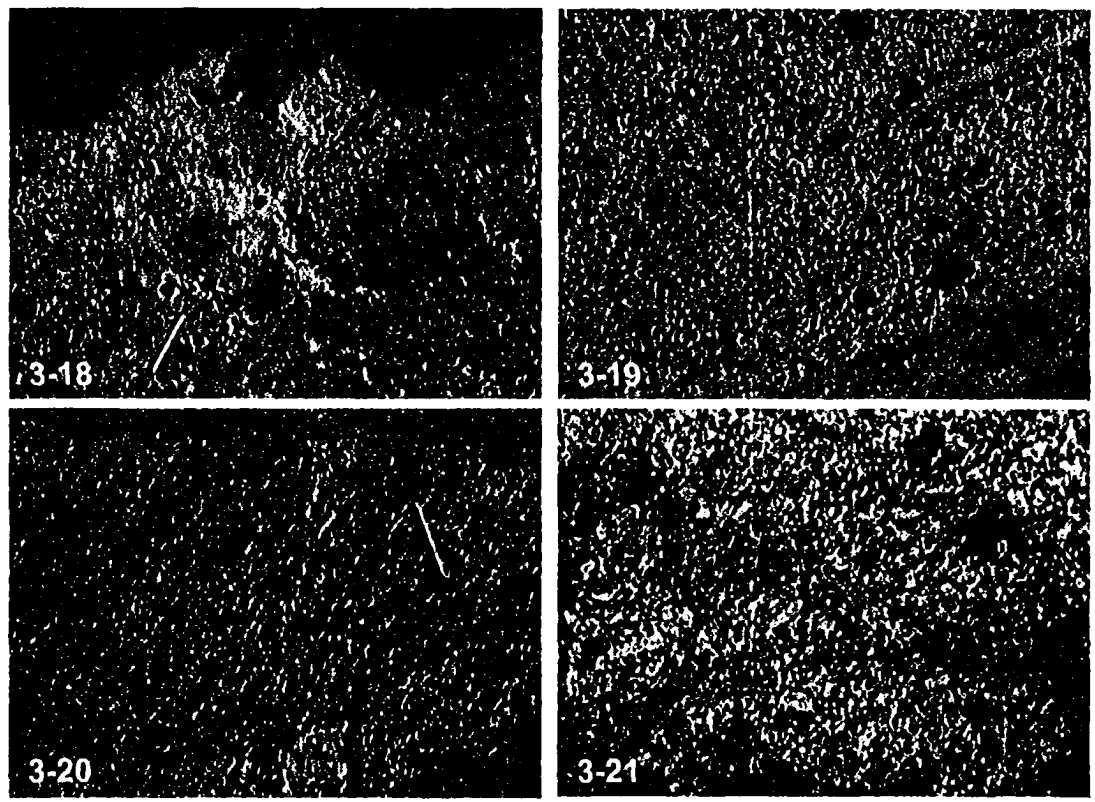

Figures 3-18 to 3-21. 3-18. A vein of the Mosher Pluton intrudes the Dirty Granite. 3-19. The Inglis Lake Pluton, an altered hornblende-biotite granite. Hornblende crystals are the large black crystals. 3-20. A well foliated locality of the 'dirty' granite. 3-21. The Wecho Suite showing 3-4 cm long K-feldspar phenocrysts.

The entire southern portion of the map area is intruded by a young, equigranular biotite granodiorite to granite with abundant sedimentary xenoliths and schlerin termed the 'dirty' granite (Figure 3-19). It is a well foliated and cross cuts many of the plutons.

3.4.9 Mosher Pluton

In the southern portion of the map area, to the north of the Mosher Lake turbidites, is a biotite ± muscovite granite, known as the Mosher Lake Pluton that intrudes the Mosher Lake meta-sediments. This suite is light pink to grey-white, medium grained and equigranular. It is well foliated, the fabric being defined by biotite. There are two main phases, a fine-grained phase and a coarse-grained phase. The fine-grained phase is very grey in colour and is biotite rich. The course grained phase ranges from a granite to granodiorite and has larger plagioclase crystals. Biotite is also abundant in this suite and defines the foliation. Dykes of this suite intrude the 'dirty' granite as well as the supracrustal rocks between Inglis and Mosher lakes (Figure 3-20).

3.4.10 Dauphinee Suite

Unique to the northernmost part of the map area is the Dauphinee Suite, an enderbite to mafic granulite found in small pods, generally confined to the tops of ridges and always underlain by the Wecho Pluton. The enderbite is an orthopyroxene-bearing tonalite with the assemblage of plagioclase + hornblende + magnetite + orthopyroxene ± clinopyroxene ± cummingtonite ± K-feldspar ± quartz ± garnet as well as local

macroscopic orthopyroxene and clinopyroxene. This suite represents one that crystallized under granulite metamorphic conditions. Its texture is granoblastic and the suite is equigranular and medium grained.

3.4.11 Wecho Suite

The Wecho Suite is a K-feldspar porphyritic granite commonly found in association with, but not genetically related to, the Mofee Pluton. This suite extends from the northern most part of the map to the southern most part and is likely an extension of the Stagg Suite (Henderson, 1985) in the Western Plutonic Complex to the south. The K-feldspar porphyritic granite generally has 2-4cm long K-feldspar phenocrysts that range from bright pink to white in colour and show excellent Carlsbad twins. These rocks are very biotite rich with a groundmass composed of biotite + plagioclase + quartz + K-feldspar (Figure 3-21). In the northern portion of the map area the K-feldspar porphyritic granite contains xenoliths ranging in composition from mafic (Figure 3-22) to granitic to granodioritic and tonalitic to meta-sedimentary and range in grade from amphibolite to granulite. The abundance of the meta-sedimentary xenoliths depends strongly on the proximity to remnant sedimentary packages.

Another phase of the Wecho Pluton is commonly associated with the K-feldspar pophyritic granite described previously. This phase is generally finer grained and contains fewer and smaller phenocrysts that are less well formed than in the other suite, although both show Carlsbad twins. The suite is also biotite bearing, but has much less

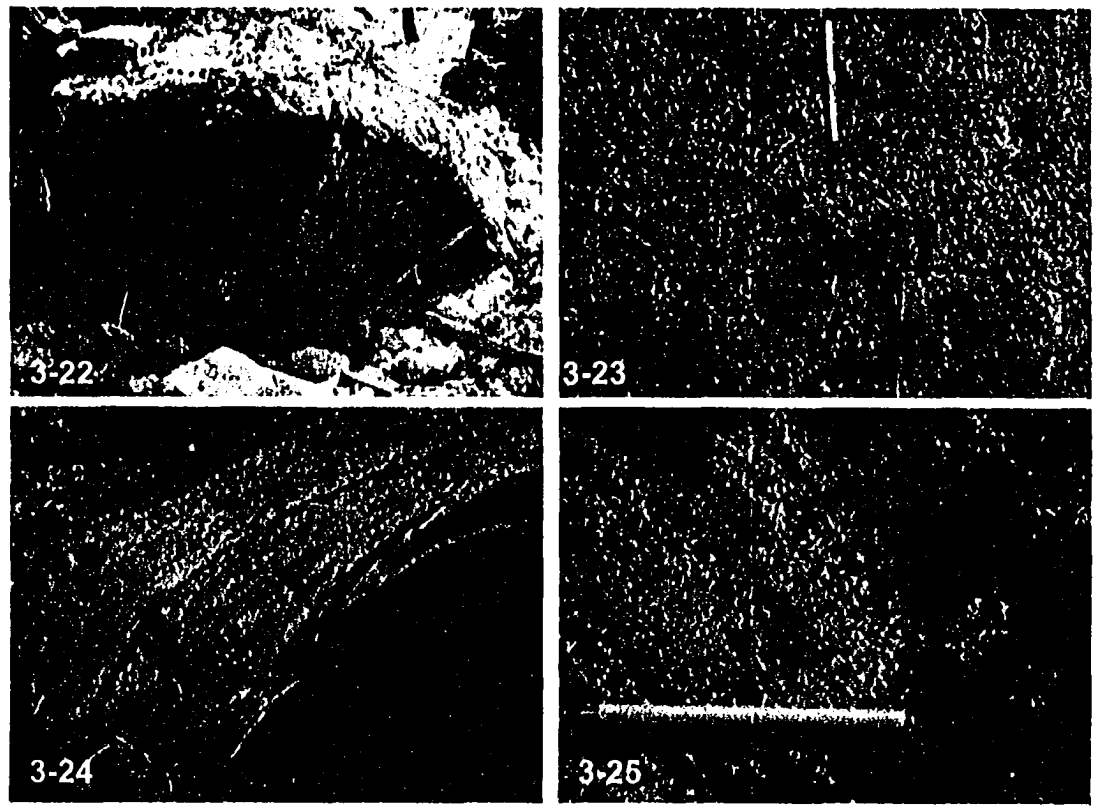

Figures 3-22 to 3-25. 3- 22. Layered mafic xenoliths within the Wecho Suite.3-23. K-feldspar porphyritic granite within a Paleoproterozoic fault zone. The K-feldspar crystals are altered to a bright pink-orange colour and the fractures in the rocks have been in filled and show cataclaysite. 3-24. The Nardin Gneiss being cut by mafic dykes. 3-25. The Nardin biotite-magnetite granodiorite with K-feldspar stringers.

within the groundmass. Magnetite is locally found within the suite and the granite is often altered to a bright pink colour.

3.4.12 Mofee Pluton

The youngest suite in the study area is the Mofee pluton, a biotite-muscovite granite that extensively intrudes the Wheeler and Germaine Lake meta-sediments and occurs throughout the Wecho River area. The two-mica granite is biotite and muscovite bearing and is medium grained and equigranular. It is generally poorly foliated, sometimes exhibiting a foliation defined by weakly aligned micas. It is light pink in colour and it extends to the south towards Wheeler and Germaine lakes. In the northern portions of the map area, it contains sedimentary, mafic, quartz diorite and granodiorite to tonalite xenoliths, but fewer than in other suites.

3.5 Late Features in the Wecho River Area

Evidence for large scale faulting in the Wecho River area includes the presence of large brittle faults that can be traced into neighboring areas. These faults trend NW-SE and generally show sinistral strike slip motion. There are also smaller faults, generally with unknown sense, that are defined by valleys with steep cliffs on either side, slickenlines, or cataclasite (Figure 3-23). Abundant Proterozoic dykes, including the Indin, Dogrib and Mackay swarms, cut all lithologies.

3.6 Geology of the Nardin Complex

Two samples were also collected from the Nardin map sheet (Stubley et al., 1997) located directly to the east of the Wecho River map sheet (Figure 3-26). The Nardin area is the closest location of geologically interpreted basement to the Wecho River area and as such provides an excellent comparison for the samples collected from the Wecho map area.

3.6.1 The Nardin Gneiss

The oldest sample taken is a granodiorite basement gneiss with two generations of deformed mafic dykes (Figure 3-24). The mafic dykes are fine grained, well foliated, with the fabric defined by hornblende. One of the dyke sets is much more foliated than the other indicating their relative age. The gneiss is biotite bearing and shows an excellent foliation defined by biotite and quartz. The quartz is either rounded or elongate within the foliation plane. Millimetre scale granitic veins are parallel to the gneissocity and were unavoidable during sampling. There are also porphyritic dykes intruding the gneiss that are bright pink and include coarse grained plagioclase crystals. This suite has been geologically interpreted as part of the >2.8 Ga Central Slave Basement Complex because of its association with rocks resembling the fuchsitic quartzites and banded iron formation of the Central Slave Cover Group (Stubley, 1997).

3.6.2 The Nardin Granodiorite

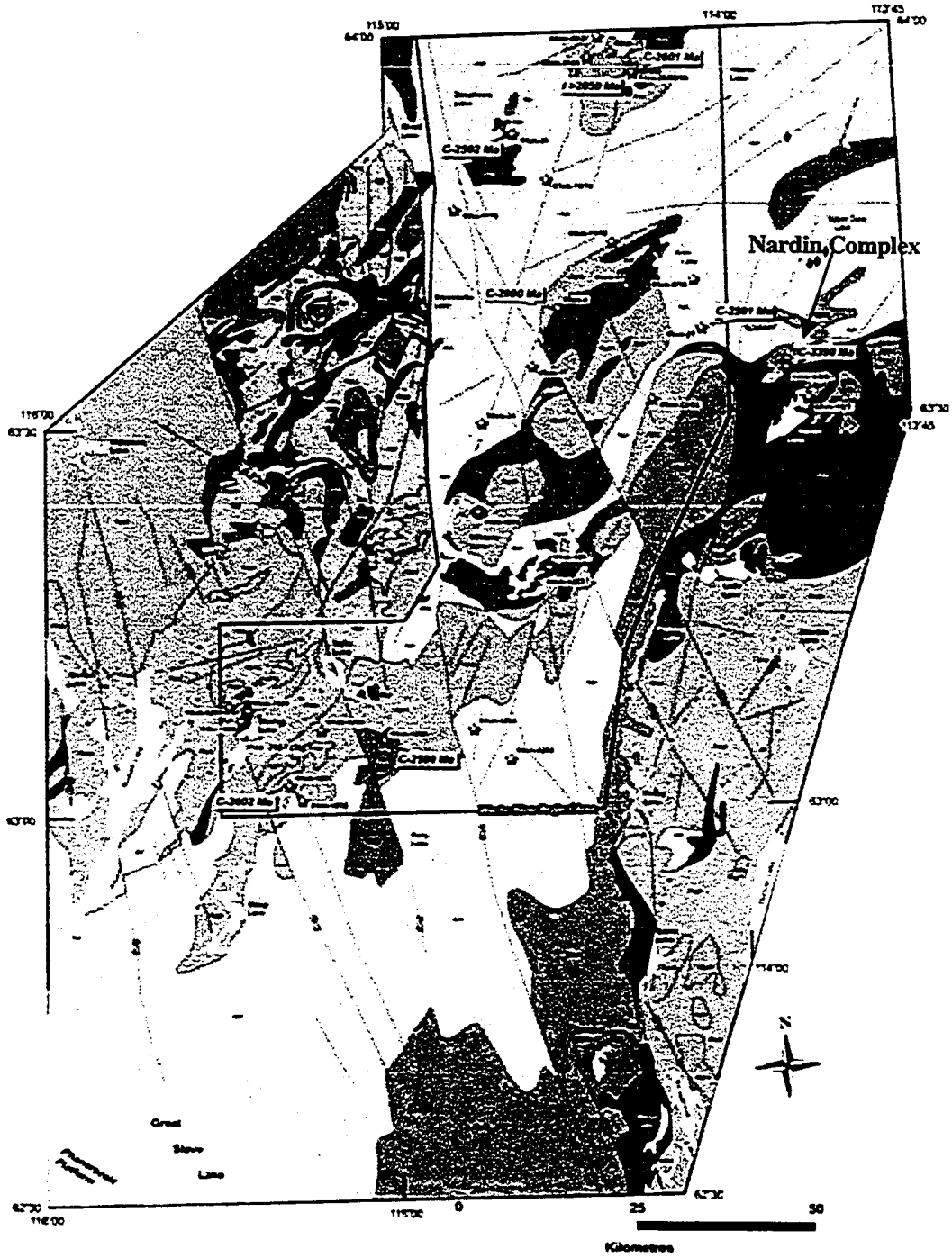

Figure 3-26 Simplified map of the Southwestern Slave Province with Wecho River area samples as well as samples from the Nardin Complex

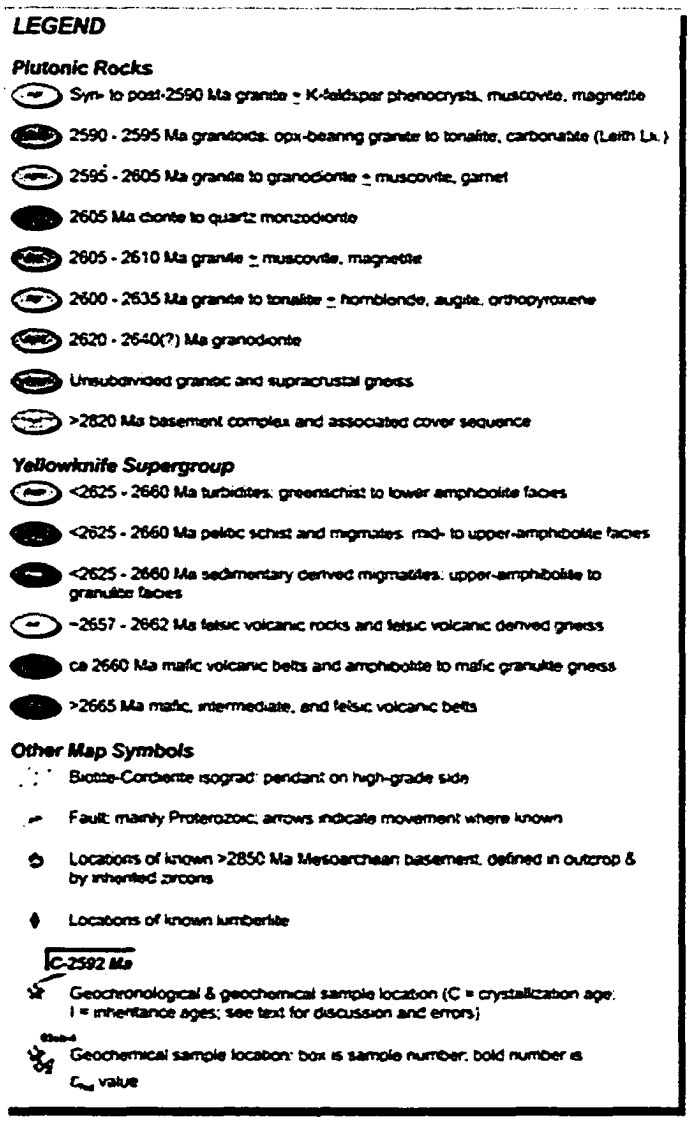

Geology of the Southwestern Slave craton. Modified after Henderson (1985), Stubley (1997), Jackson (2003), and Ootes and Pierce (2005) and references therein

The second suite sampled from the Nardin area is a biotite magnetite granodiorite with local occurrences of hornblende. This suite is well-foliated, medium grained and equigranular and exhibits K-feldspar stringers (Figure 3-25). The foliation is defined by biotite and quartz and the suite strongly resembles the Disco Intrusive Suite from the Snare River area and the Defeat Suite from the Western Plutonic Complex.

Chapter 4 – Petrography

4.1 Introduction

Petrography of the rocks sampled for geochemistry was undertaken to better understand the mineral relationships and textures. A summary of key petrographic characteristics is summarized in Table 4-1 and preparation of thin sections is described in Appendix B1.

4.2 Petrographic Results

4.2.1 The Nardin Gneiss

The Nardin Gneiss is a granodiorite gneiss cut by two generations of gabbro dykes. It contains approximately 45% quartz, 40% plagioclase and 15% microline. Minerals within the gneiss are of two grain sizes with larger plagioclase and quartz, and smaller, interstitial microcline, all of which have highly irregular grain boundaries. Plagioclase is unzoned with some irregular albite twins. Quartz forms elongate, polycrystalline grains (Figure 4-1). Biotite is a minor constituent forming small and ragged grains with few sharp grain boundaries. The gneissic texture is defined by biotite and elongate quartz grains. Accessory minerals include zircon, monazite, epidote and magnetite.

Suite Name	Rock Type	Modal % Quartz	K-feldspar	Plagioclase	Mafic Minerals	Minor Minerals	Grain Size (mm)	Texture
Nardin Gneiss	Grdt Gneiss	45	15	40	Bt	Mag Ep	0.2-2	Gneiss
Nardin Dykes	Gabbro	0	0	100	Hbl, Bt		0.5-1.0	Granoblastic
Mafic Volcanics	Intermediate to Basaltic Volcanics				Hbl, Bt	Qtz, Mag	0.05-0.3	Layered (foliated)
Nardin Granodiorite	Granodiorite	40	15	45	Bt	Ep	0.2-0.9	Equigranuiar
Diorites	Qtz Monzodiorite to Qtz Diorite	15-5	5	80-95	Hbl Bt	Mag Ep	0.3-1.0	Granoblastic
South Pluton	Grdt	45	10	45	Hbl Bt	Mag Ep, Chl	0.4-2.5	Equigranular
Hickey Suite	Grdt	35-45	25-10	30-55	Bt	Mag Ep	0.4-1.5	Panidio-morphic
Mafic Enclaves	Amphibolite				Hbl,	Cum, Mag Opx, Bt	0.1-0.8	Granoblastic to layered
Armi Pluton	Grdt	40-50	15-25	35-45	Bt	Musc	0.4-1.0	Equigranular
Mosher Pluton	Granite	30	40	30	Bt	Ep	0.2-2.0	Equigranular
Mag Pluton	Granite	35	30	35	Bt	Mag Chl, Ep	0.4-2.0	Equigranular
Dauphinee Suite	Enderbite	60	0	40	Opx, Cpx Hbl,Bt	Mag	0.2-1.75	Granofels
Wecho Suite	Granite	30-40	40-50	30-40	Bt	Musc Mag	0.3-40	Phorphyritic
Mofee Suite	Granite	35-40	35-45	30-35	Bt	Musc	0.4-4.0	Equigranular

Grdt=Granodiorite, Qtz=Quartz, Hbl=Hornblende, Bt=Biotite, Opx=Orthopyroxene, Cpx=Clinopyroxene, Musc=Muscovite
Mag=Magnetite, Ep=Epidote, Cum=Cummingtonite, Chl=Chlorite

Table 4-1. Summary of petrographic features for the Wecho River area rocks.

4.2.2 Nardin Mafic Dykes

Two generations of gabbro dykes cross-cut the Nardin Gneiss that can be related chronologically by their degree of deformation. The older dyke set is strongly deformed, with a foliation defined by biotite and hornblende (Figure 4-2). The dykes are gabbroic in composition including subhedral to euhedral plagioclase (15%), hornblende (70%), and biotite (15%). The grain boundaries between minerals are well defined, giving the rock a granoblastic texture. The hornblende is a green to brown colour and exhibits excellent cleavage, and plagioclase is albite twinned.

The later dyke set that cuts the Nardin Gneiss is composed of hornblende (65%), plagioclase (15%), and biotite (20%) and is less deformed (Figure 4-3). Biotite and hornblende are both quite pristine and are elongate within the foliation plane. Plagioclase is also present, but individual grains are much smaller than the other two minerals. The texture of the rock is granoblastic.

4.2.3 Mafic Volcanic Rocks

Mafic volcanic rocks in the Wecho River area are of two types, sheared basalts and mafic to intermediate volcaniclastic rocks. The volcaniclastic rocks include alternating layers of felsic, intermediate and mafic composition. The felsic layers are very coarse grained and consist of only quartz and plagioclase. The quartz is generally aligned in the direction of the layering. The intermediate layers are made up of plagioclase +

quartz + hornblende and are generally more fine grained than the felsic layers (Figure 4-4). The mafic layers are composed of hornblende + plagioclase with minor quartz and magnetite. These layers also include epidote as an accessory mineral. The boundary between intermediate and mafic layers is transitional. The felsic boundaries are more easily distinguished because of the change in grain size.

4.2.4 Wheeler and Germaine Lake Diorites

The Wheeler Lake Diorite is equigranular, consisting of large plagioclase (30%) and hornblende (65%) crystals and smaller, round, anhedral quartz (5%) and magnetite grains. The plagioclase and hornblende grains are all subhedral and the texture is granoblastic. The granoblastic texture is seen well amongst the hornblende crystals but the plagioclase grains are all extremely sericitized making it difficult to see the interlocking granoblastic texture (Figure 4-5). Quartz is a minor constituent and is either interstitial to plagioclase and hornblende or is found as inclusions within plagioclase and hornblende. There is no foliation present. Epidote is abundant and accessory minerals include apatite and zircon.

The Germaine Lake quartz diorite differs from the Wheeler diorite with hornblende(50%), plagioclase (30%), quartz (17%), and microcline (2%) (Figure 4-6). The grain sizes are variable but generally the biotite and hornblende are smaller than the quartz and plagioclase grains. Microcline is a minor constituent, although there are a few larger lath shaped grains. Plagioclase exhibits albite twinning and minor sericitization.

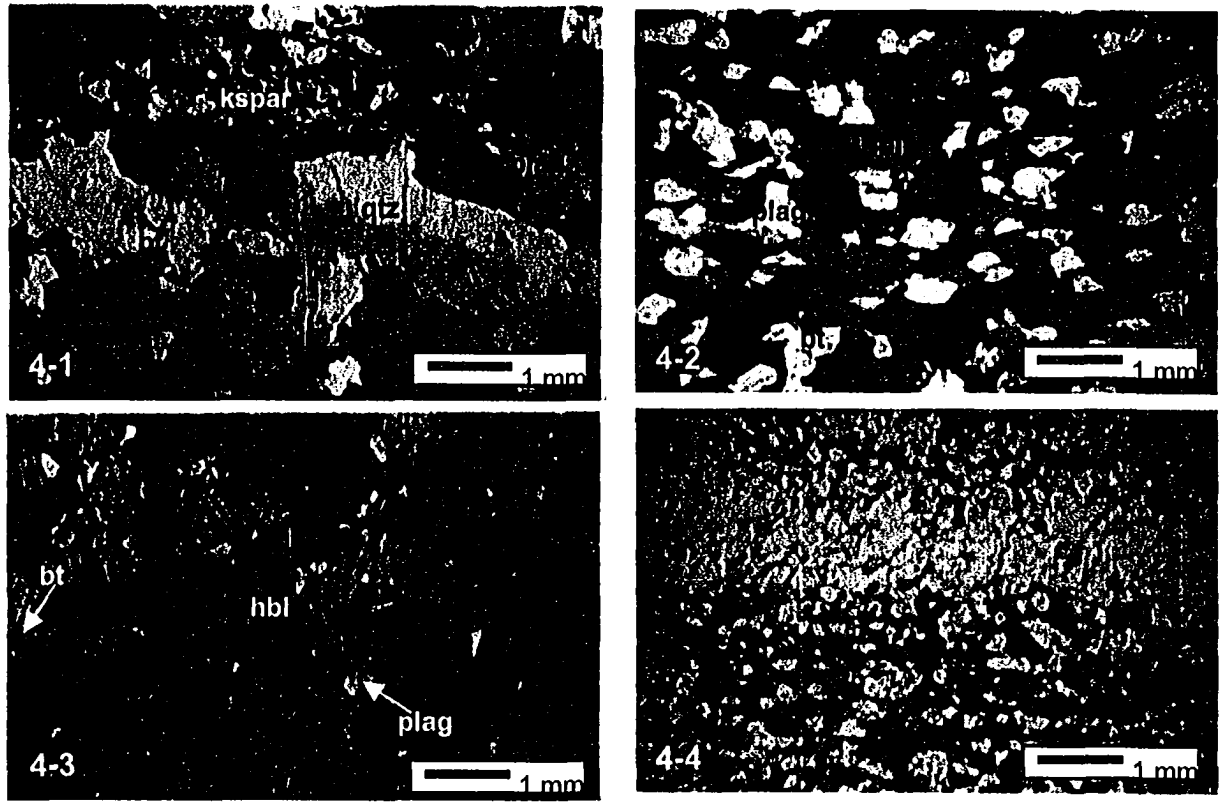

Figures 4-1 to 4-4. 4-1. The Nardin Gneiss in crossed polarized light showing elongate, strained quartz and finer grained biotite, plagioclase, microcline and magnetite. 4-2. Strongly foliated mafic dyke cutting the Nardin Gneiss in plane polarized light showing green hornblende and plagioclase. 4-3. The less deformed mafic dyke cross-cutting the Nardin Gneiss in plane polarized light showing course grained hornblende and biotite and finer grained quartz and plagioclase. 4-4. Germaine Lake mafic volcanics in plane polarized light showing a central, coarse grained layer surrounded above and below by intermediate composition layers.

Quartz is often strained with many different extinction angles observed within a large crystal. Irregularly shaped biotite is also present, and with hornblende defines the foliation. The hornblende is highly altered, going to epidote in some cases. Accessory minerals include zircon and epidote.

4.2.5 Nardin Granodiorite

The Nardin Granodiorite is an equigranular granodiorite entirely made up of anhedral grains of plagioclase (45%), quartz (40%), microcline (15%), biotite and magnetite (Figure 4-7). Plagioclase exhibits albite twins and is slightly sericitized while the quartz shows strain with many different extinction angles within a single crystal. Myrmekite texture is very common along the grain boundaries of small plagioclase and K-feldspar crystals. Biotite is minor, has ragged grain boundaries and is weakly oriented forming the foliation in the rock. Microcline is present, but is generally fine-grained and interstitial. Inclusions of quartz, plagioclase and biotite can be seen within larger grains of plagioclase and quartz. Accessory minerals within this panidiomorphic rock include zircon, monazite and epidote.

4.2.6 South Pluton

The South Suite is a hornblende-magnetite granodiorite that is coarse grained and dominated by subhedral grains of plagioclase (45%), quartz (45%), microcline (10%), hornblende and minor biotite. The plagioclase crystals are large and have albite twins and

show only minor sericitization. Quartz crystals are the same size as plagioclase, but microcline crystals are much smaller and represent a minor, interstitial phase. Hornblende makes up 15% of the rock, and is ragged and highly altered, often to chlorite (Figure 4-8). The hornblende has abundant inclusions of plagioclase and quartz. Biotite within the suite is pristine and quite large, except where in contact with the hornblende. A very weak foliation is defined by biotite. Magnetite, epidote, zircon and titanite are accessory minerals.

4.2.7 Hickey Suite

The Hickey suite ranges from tonalite to granodiorite in composition, and the granitoid includes anhedral grains of two sizes. The suite exhibits large, elongate quartz (35-45%) with smaller microcline (10-25%), plagioclase (30-55%) and minor biotite, all with irregular grain boundaries (Figure 4-10). Grains of plagioclase exhibit albite twinning. with moderate sericitization, and are generally small compared to the quartz. The larger plagioclase grains often include smaller, irregular shaped fragments of plagioclase within them that have the same twin direction, possibly the result of recrystallization (Figure 4-11). Quartz is generally elongate and strained, forming a strong foliation along with biotite. Biotite is small and anhedral to subhedral and is sometimes found as knots intergrown with magnetite. Microcline is rare and is found as interstitial grains between quartz and plagioclase. Inclusions of biotite, plagioclase and quartz are found in plagioclase and inclusions of plagioclase in quartz are common. Myrmekite texture is rare, but occurs

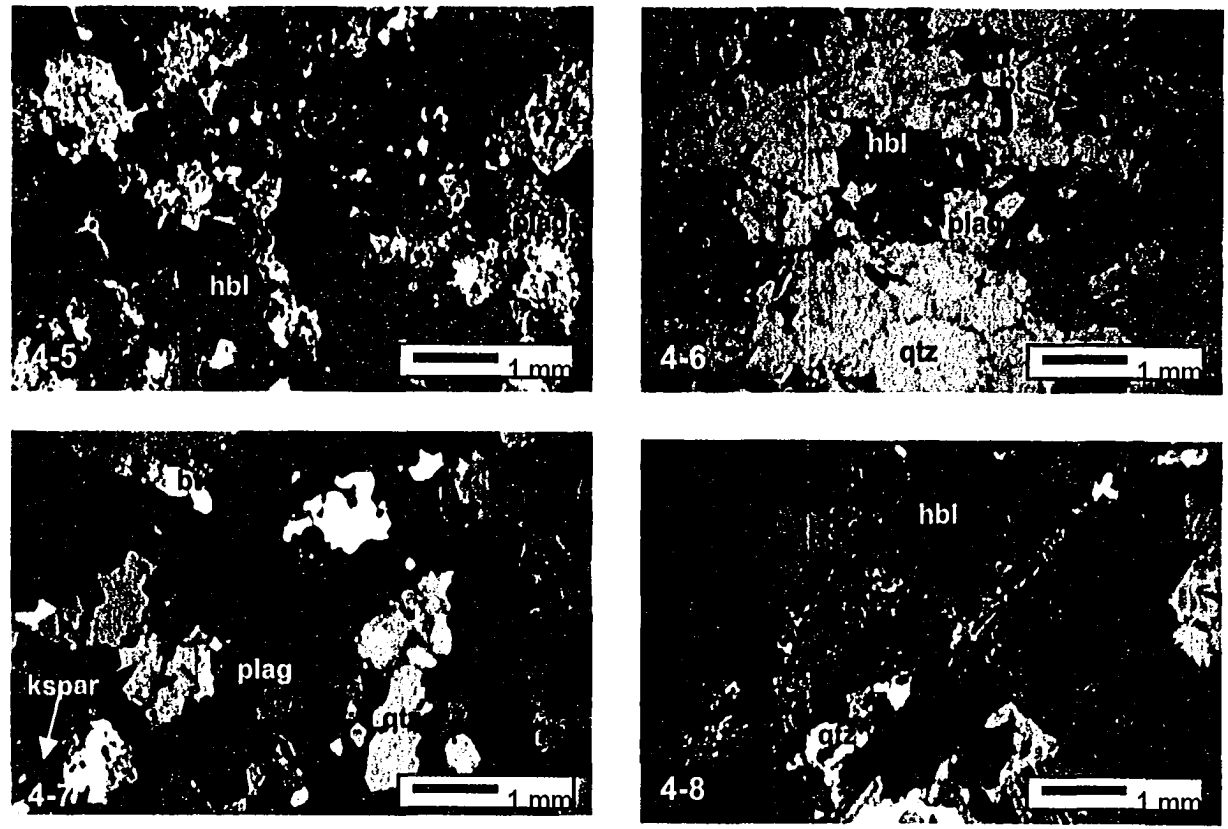

Figures 4-5 to 4-8. 4-5.The Wheeler Diorite under crossed polarized light. 4-6. The Germaine Quartz-Diorite in plane polarized light. 4-7. Representative texture of the Nardin Disco in crossed polarized light . 4-8. A large altered hornblende grain under crossed polarized light from the South Suite.

between larger plagioclase and K-feldspar crystals. Accessory minerals include magnetite, epidote, zircon and monazite.

4.2.8 Mafic Enclaves within the Hickey Suite

Two types of mafic enclaves are found in the Hickey Suite, layered and massive, and they range from amphibolite to granulite in grade. The layered enclaves are granoblastic. The layered enclave sampled for this study is at amphibolite grade defined by the mineral assemblage of plagioclase + hornblende + biotite + quartz +magnetite ± cummingtonite. These enclaves are quite fine grained with the layering defined by plagioclase and hornblende as well as the presence of cummingtonite and biotite (Figure 4-12). The darker layers are more amphibole rich, whereas the lighter layers are plagioclase rich and contain cummingtonite. The foliation is defined by layering as well as the alignment of biotite and hornblende. Hornblende in these rocks is often altered to epidote and is usually ragged. Leucosomes are sometimes associated with this type of enclave and consist of large plagioclase and quartz as well as some fine-grained epidote. Sericitization of plagioclase is common within the leucosomes but the degree of alteration decreases away from the leucosomes, with little to no sericitization of plagioclase in the enclave. Large cummingtonite is common along the leucosome-enclave boundary.

The massive enclaves within the Hickey suite are often quite coarse grained and the ones sampled are at granulite grade, defined by the mineral assemblage of plagioclase + hornblende + orthopyroxene + clinopyroxene + magnetite ± biotite (Figure 4-13). The plagioclase in this sample seems to be interstitial, occurring within holes in the pyroxenes and around other larger grains. The orthopyroxene and clinopyroxene have abundant hornblende and plagioclase inclusions. Magnetite is generally small and round, whereas biotite, when present, is pristine and elongate. Grain boundaries are either straight or slightly rounded giving it a granoblastic texture.

4.2.9 Armi Pluton

The Armi Pluton is an equigranular granodiorite to granite (35-45% plagioclase, 40-50% quartz, 15-25% microcline) with subhedral grains and a moderate foliation defined by biotite (Figure 4-14). The plagioclase is albite twinned and exhibits exsolution lamellae. Similar to the Hickey Suite, plagioclase often includes fragments with the same extinction angles and albite twin directions within a larger plagioclase grain. Quartz grains are strained, and generally round. Microcline shows tartan twinning and has abundant inclusions. Biotite is pristine, similar in size to the other grains, is altered to chlorite locally. In rare cases the biotite is found as fine-grained fragments wrapping around other grains. Myrmekite texture is common. Accessory minerals include muscovite, monazite, zircon and epidote.

4.2.10 Mag Pluton

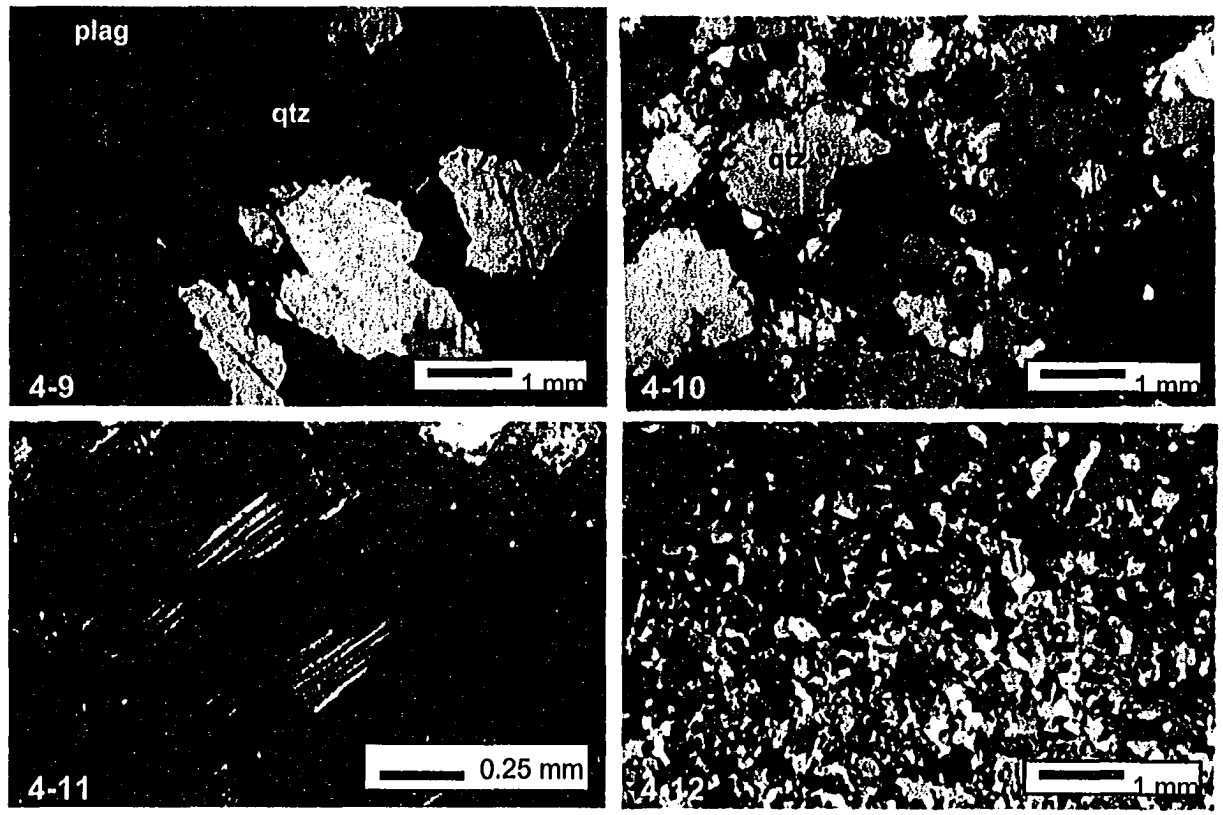

Figures 4-9 to 4-12. 4-9. The coarse grained, equigranular Mag Suite under plane polarized light. 4-10. The Hickey Suite showing multiple grain sizes and sericitization of plagioclase grains under plane polarized light. 4-11. A plagioclase grain under cross polarized light within the Hickey suite that has smaller plagioclase inclusions with irregular grain boundaries but the same optical orientation as the grain it is in. 4-12. Layered mafic enclave at amphibolite grade from the Hickey suite. The top of the photo represents the hornblende rich layers and the lower part shows the plagioclase-cummingtonite rich layers in crossed polarized light.

The Mag pluton is a coarse-grained, equigranular magnetite granite composed of subhedral grains of plagioclase (35%), microcline (30%) and quartz (35%) (Figure 4-9). Plagioclase is moderately altered to sericite, but albite twins can still be deciphered. Quartz is elongated but not strained and biotite grains are ragged to skeletal with rare chlorite replacement. Mineral boundaries are quite sharp. Inclusions of biotite, quartz and magnetite are found within microcline, quartz and plagioclase grains. Magnetite is anhedral and disseminated throughout the rock. Accessory minerals include zircon, monazite, epidote and chlorite.

4.2.11 Mosher Pluton

There are two phases of the Mosher pluton, a coarse-grained and a fine-grained phase. The coarse grained phase is granitic, composed of subhedral grains of quartz (30%), microcline (40%), plagioclase (30%), biotite and magnetite (Figure 4-15). There are many different grain sizes ranging from very small polycrystalline quartz and very large K-feldspar. The plagioclase is quite sericitized although some albite twins can be distinguished and there is often fine-grained myrmekite texture along the grain boundaries. Quartz is polycrystalline, strained, and has many different grain sizes. Biotite is subhedral and defines a weak foliation. Inclusions of quartz, plagioclase and biotite are common in microcline and plagioclase. Accessory minerals include epidote, zircon and monazite.

The fine-grained phase of this pluton is equigranular with subhedral grains. The plagioclase is fresh and has albite twins and the quartz is elongate and strained. Biotite is subhedral with regular grain boundaries and it defines a moderate foliation (Figure 4-16). Microcline is not as common as it is in the coarse-grained suite. Plagioclase has quartz and biotite inclusions and accessory minerals in the suite include zircon and monazite.

4.2.12 Dauphinee Suite

The Dauphinee suite is an enderbite to mafic granulite with a granofels texture and a mineral assemblage of plagioclase + quartz + hornblende + magnetite +orthopyroxene ± clinopyroxene ± biotite. Grains range from anhedral to subhedral and are equigranular with a few orthopyroxene grains larger than the groundmass (Figure 4-17). Plagioclase and quartz are both irregularly shaped and the plagioclase crystals have albite twins. Biotite is often quite large and ranges from euhedral to skeletal and hornblende is often irregular and patchy with abundant inclusions. Orthopyroxene and clinopyroxene, where present, are pristine to altered, sometimes altered to amphibole, and the orthopyroxene contains abundant inclusions of quartz and plagioclase. Accessory minerals include zircon and titanite.

4.2.13 Wecho Pluton

The Wecho Pluton is a K-feldspar porphyritic granite to with 2-4cm long K-feldspar phenocrysts that make up to 30% of the rock and a finer grained,

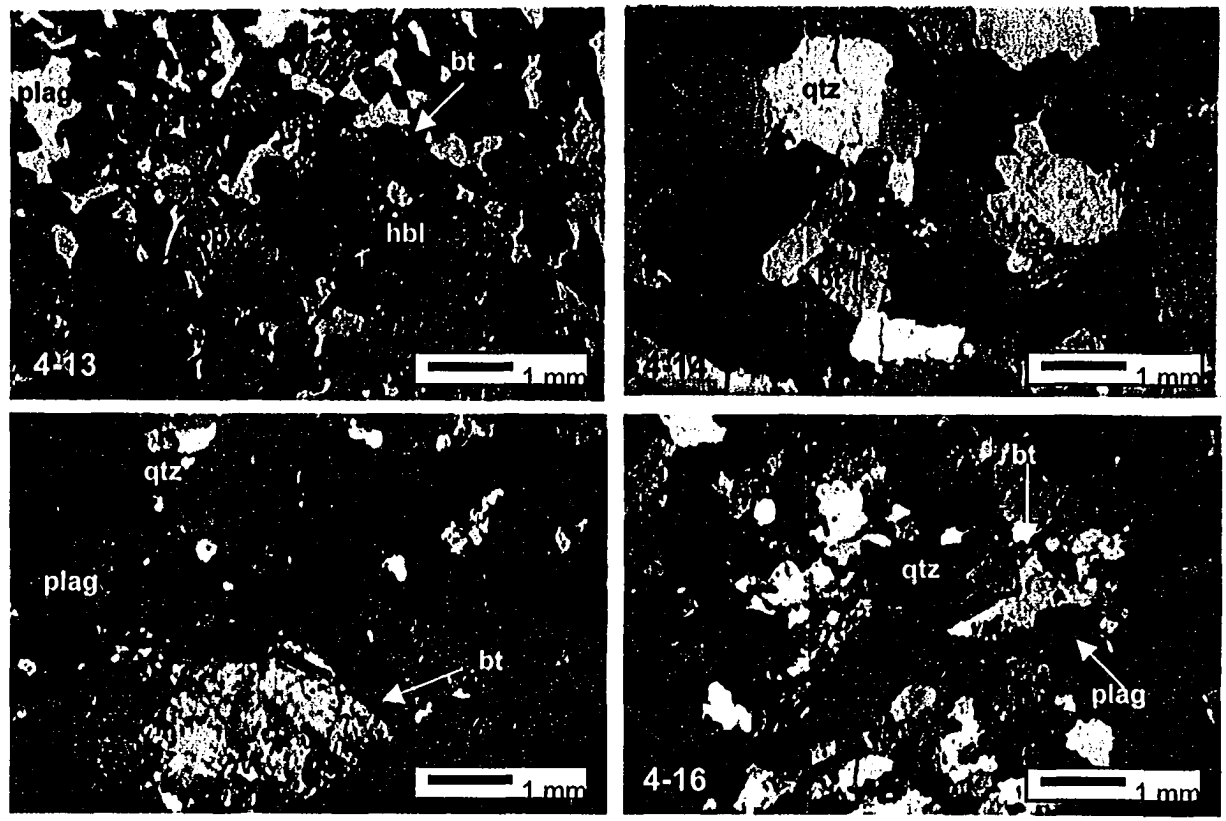

Figures 4-13 to 4-16. 4-13. Massive mafic enclave in plane polarized light at granulite grade from within the Hickey Suite. 4-14. A representative photomicrograph of the Armi Suite under crossed polarized light showing its characteristic equigranular nature. 4-15. Course grained phase of the Mosher Suite. 4-16. Fine grained phase of the Mosher Suite showing a foliation defined by biotite.

equigranular groundmass consisting of plagioclase (20-30%), microcline (40-50%), quartz (20-30%) and biotite (10-15%) (Figure 4-18). The large K-feldspar phenocrysts have Carlsbad twins, but the finer K-feldspar within the groundmass has tartan twins, indicating that it is microcline. The phenocrysts have abundant plagioclase, quartz and biotite inclusions. The quartz ranges from very small to quite large and is strained, showing alternating extinction angles across a single grain. Plagioclase is albite twinned and commonly sericitized. Biotite is abundant within the groundmass and often pristine, and only rarely altered to chlorite. Myrmekite texture is common within this suite, defined by rods or blebs of quartz and plagioclase between grains of plagioclase and K-feldspar (Figure 4-19). Muscovite is present as a secondary mineral in this suite and occurs primarily as ragged fragments along grain boundaries or within fractures. Accessory minerals include magnetite, epidote, zircon and monazite.

4.2.14 Mofee Pluton

The Mofee suite is an equigranular, coarse grained two mica granite (35-45% microcline, 35-40% quartz, 30-35% plagioclase) with subhedral grains (Figure 4-20). Quartz in this suite ranges in size, with the larger grains similar in size to the plagioclase and microcline and is often strained. Plagioclase is highly sericitized but some albite twins can still be seen. Biotite is often chloritized, and is generally smaller than the quartzofeldspathic phases. Muscovite is coarse grained and is present either as large laths or intergrown along cleavage planes with biotite. Inclusions of plagioclase, quartz and

biotite are common in plagioclase, microcline and quartz. Accessory minerals include monazite and zircon.

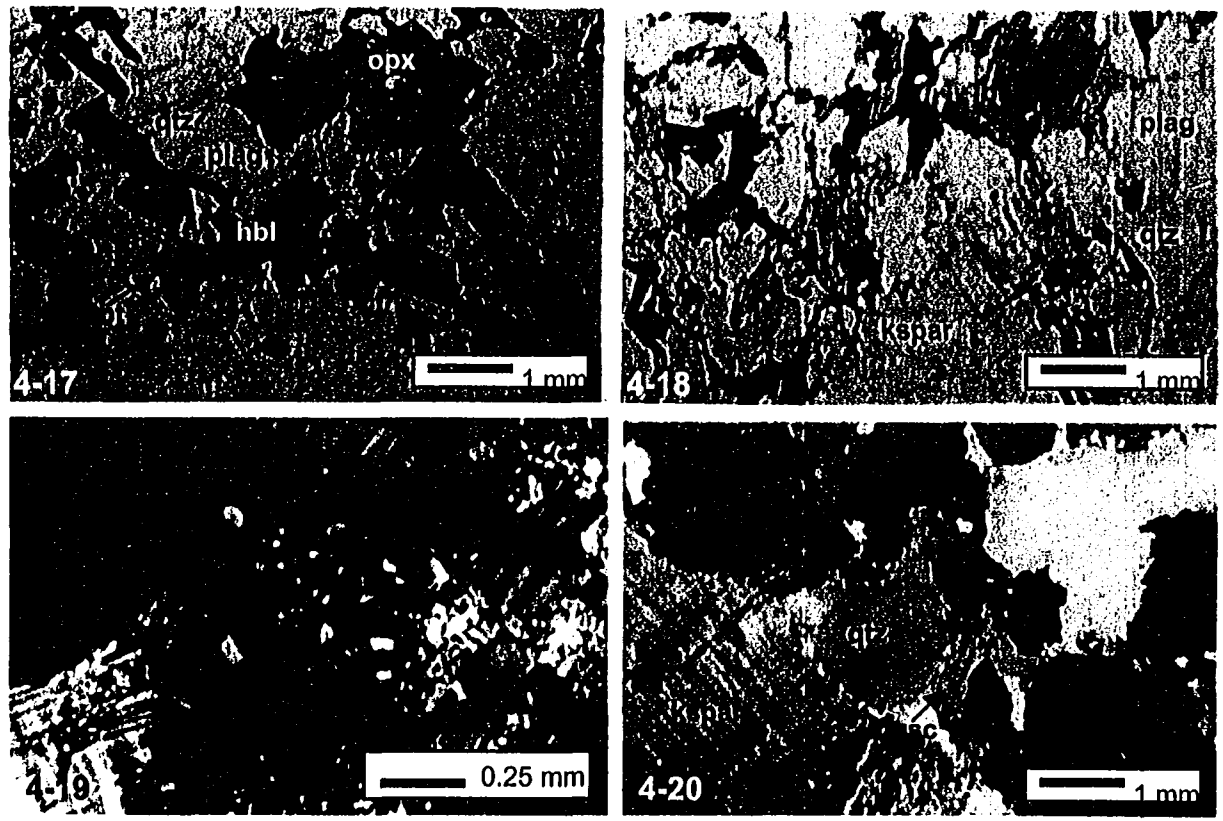

Figures 4-17 to 4-20. 4-17. The Dauphinee Suite under plane polarized light showing orthopyroxene, plagioclase, hornblende and magnetite. 4-18. Representative texture of the Wecho Suite in crossed polarized light showing abundant biotite. 4-19. Myrmekite texture in the Wecho Suite under crossed polarized light. 4-20. The equigranular biotite-muscovite granite, the Mofee Pluton, under crossed polarized light.

Chapter 5: Geochronology

5.1 Introduction

Seven samples were collected for U-Pb geochronology from the Wecho River domain based on their crosscutting relationships and relative timing with other lithologies. Both thermal ionization mass spectrometry (TIMS) and sensitive high resolution ion microprobe (SHRIMP) dating were completed at the Geological Survey of Canada in an effort to pin the crystallization ages of the samples. TIMS and SHRIMP data are summarized in Appendix D. Sampling and preparation of the rocks for U-Pb geochronology is described in Appendices B6, B7 and B8. On concordia diagrams red ellipses represent zircon, blue ellipses represent inherited zircon, green ellipses represent monazite, brown ellipses represent titanite and grey ellipses represent rejected analyses.

5.2 Sample Descriptions and Results

5.2.1 Nardin Gneiss - 03sb005 (z8491)

This Nardin Gneiss geochronology sample is a granodiorite gneiss with two generations of cross-cutting mafic dykes that has been geologically interpreted as part of the CSBC (Stubley, 1997). Thin, millimeter to centimetre scale granitic veins run parallel to the fabric of the gneiss and were unavoidable during sampling. Bright pink porphyritic

dykes are also found locally parallel to the gneissocity, which were avoided during sampling.

Two populations of monazite were analyzed for this suite; M1, rounded, pale yellow, semi-transparent grains, and M2, platy, pale yellow, semi-transparent grains with irregular grain boundaries (Figure 5-1A). Backscattered electron (BSE) images of the monazite show primary, concentric zoning within the grains, often overprinted by irregular, rounded alteration, which is likely secondary (Figure 5-1D). The TIMS data produced from these fractions are all concordant analyses with the M1 fraction yielding ages of 2591.1 Ma and 2593 Ma, within the age range of the 2.6-2.58 Ga Slave Province HT-LP metamorphic event, and the M2 fraction yielded an age of 2552.8 Ma (Figure 5-2B).

Two populations of zircon were also found in this suite: Z1, elongate, brownish-yellow, altered, semi-prismatic grains, and Z2, stubby, semi-prismatic, brownish yellow, altered grains (Figure 5-1B). BSE images of these grains reveal zircon that has some zoning but are generally free of secondary processes such as trace element migration (Pidgeon, 1998) (Figure 5-1C). Otherwise, the zircon is unaltered and would likely represent the crystallization age of the rock.

Three fractions were analyzed yielding discordant ages of 3334.8 Ma and 3203.7 Ma (Figure 5-2B). These ages are typical of ages determined for the CSBC (eg. Yamashita et al., 2000; Ketchum et al., 2004). The data, however, was not conclusive and

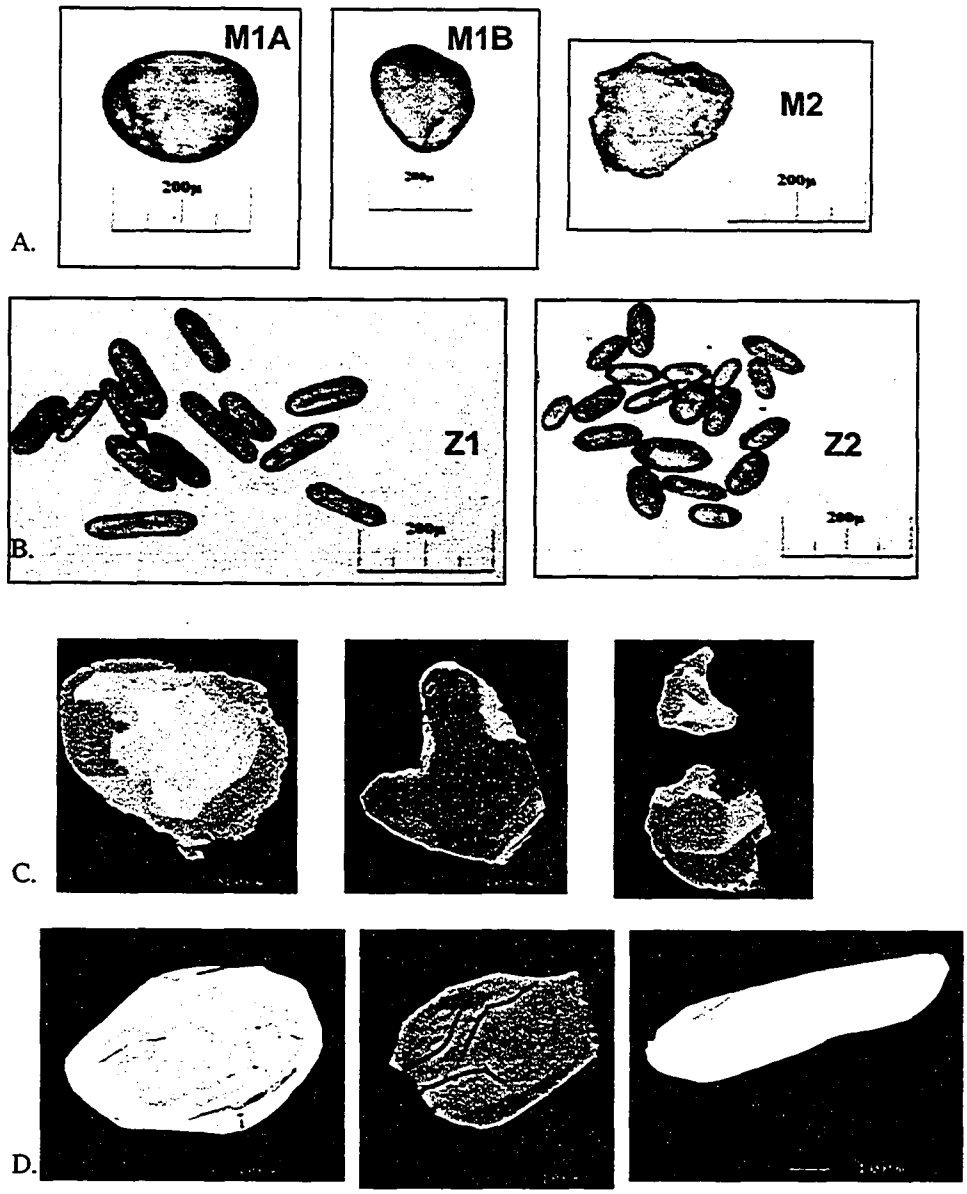

Figure 5-1 A-D. Zircon and monazite populations for the Nardin Gneiss. A. TIMS monazite fractions. B. TIMS Zircon populations. C. BSE images of monazite grains. D. BSE images of zircon grains.

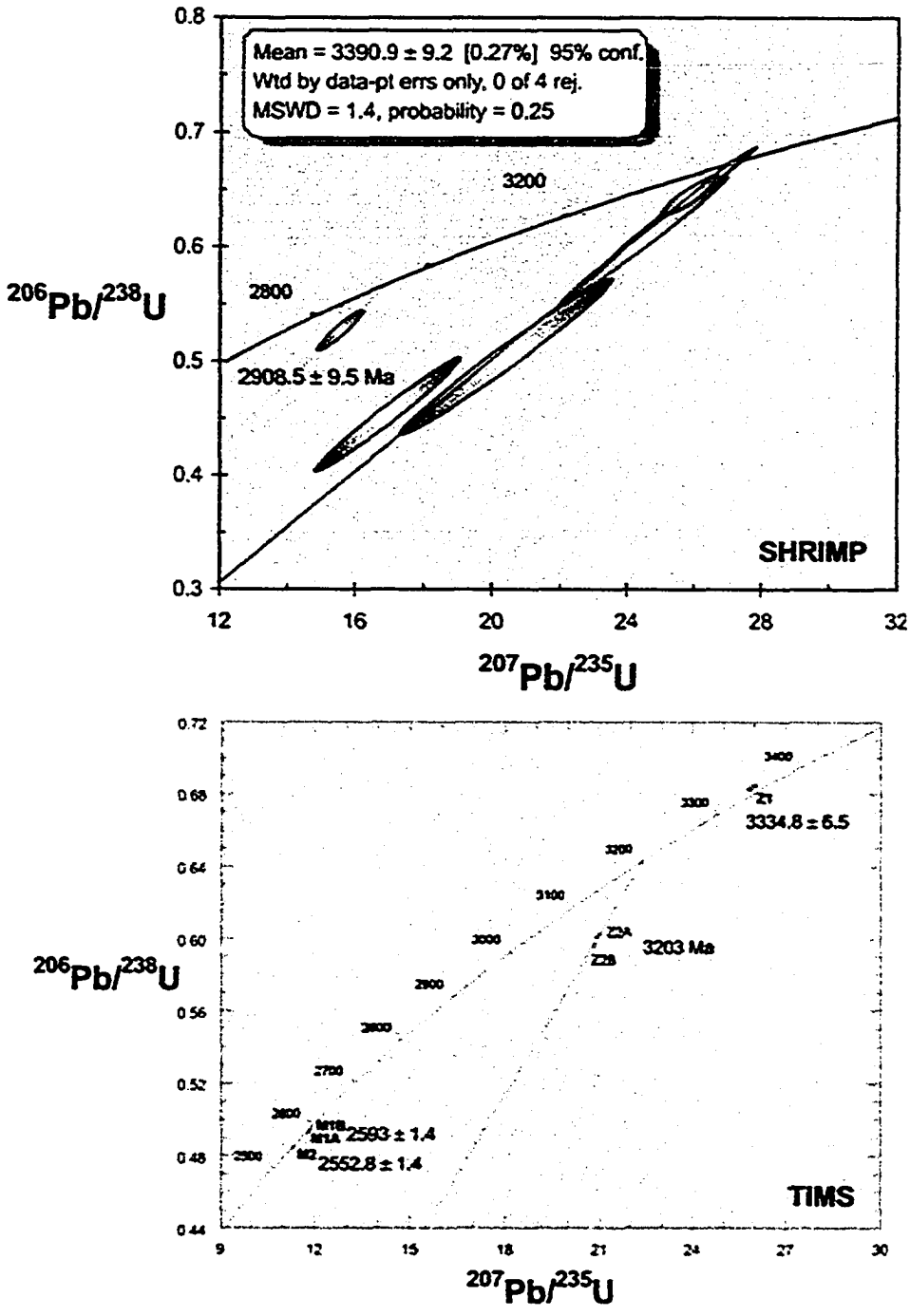

Figure 5-2 A and B. A. SHRIMP concordia diagram showing data from the Nardin Gneiss. B. TIMS concordia diagram showing data from the Nardin Gneiss.

did not constrain a crystallization age, so further analyses were carried out using the SHRIMP.

SHRIMP analyses of grains from this sample yield two ages, the first of which is slightly discordant at 2908.5 ± 9.5 Ma, and is from a single grain with one analysis spot. This age is from a small zircon with no evidence of cores or rims and is undistinguishable from the zircons from the other age population. A second age with a weighted mean of 3390.9 ± 9.2 Ma (MSWD=1.4) was determined from four grains, each with one spot analysis, and is concordant (Figure 5-2A). This data is slightly older than the data determined from the TIMS analysis.

Two interpretations can be made from this data. The first is that 2908.5 ± 9.5 Ma represents the time of crystallization for the gneiss, and the older 3390.9 ± 9.2 Ma age represents zircon inherited from an older source. This however is unlikely because there is no evidence for core-rim relationships or any other signs of inheritance within the grains, nor is there significant amounts of data to support the 2908.5 ± 9.5 Ma crystallization age. The alternate interpretation is that the 3390.9 ± 9.2 Ma represents the crystallization age for the granodiorite gneiss and the 2908.5 ± 9.5 Ma represents the age of the millimeter scale granitic veins within the gneiss. This will be explored further in the Discussion section.

5.2.2 South Pluton – 04sb4261 (z8493)

The South Pluton is a fairly massive, equigranular, medium grained hornblende-magnetite granodiorite. Hornblende within the sample is generally altered to chlorite and minor biotite is present.

The sample contains one population of dark brown titanite that is defined as semi-transparent with irregular surfaces (Figure 5-3A). TIMS analysis of two fractions yield slightly discordant ages of 2601 Ma (Figure 5-4A).

The zircon were of three populations: Z1, elongate, semi-prismatic, light brown grains with fractures, inclusions and zoning, Z2, small, stubby, prismatic, light brown grains; and Z3, large, transparent, light brown, semi-prismatic grains (Figure 5-3B). In transmitted light, most grains are very favorable for TIMS analysis, being large, with no evidence of core-rim relationships (ie. no inheritance). BSE imaging shows large grains with evidence of oscillatory zoning and no core-rim relationships (Figure 5-3C). TIMS data from 3 slightly discordant fractions lie on a cord that yields a mean weighted age of 2602.2 ± 2 Ma.

Both the titanite and the zircon are of the same age within the South Pluton, implying that the suite was cooled and crystallized through 600°C, the nominal closing temperature for titanite (Heaman and Parrish, 1991), by 2602.2 ± 2 Ma.

5.2.3 Hickey Suite - 03sb028 (z7992)

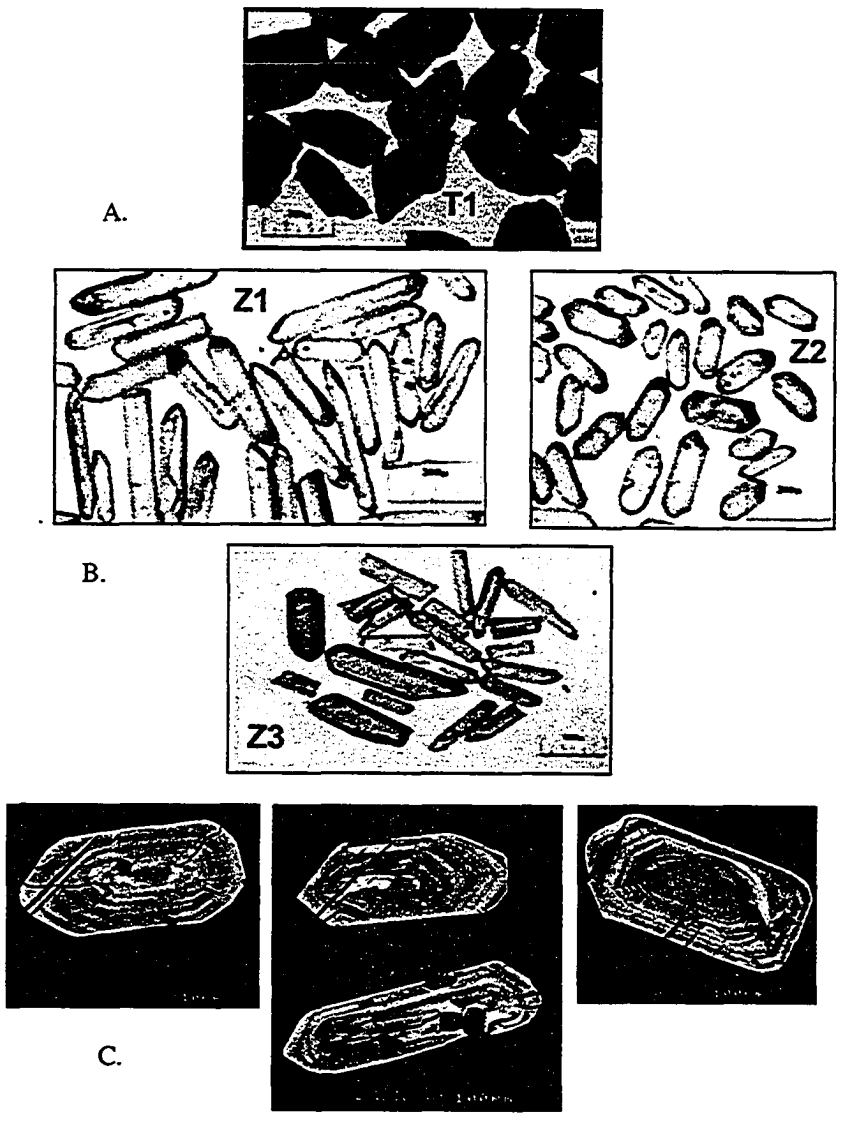

Figure 5-3 A-C. Zircon and titanite populations for the South Pluton. A. TIMS titanite fractions. B. TIMS zircon populations. C. BSE images of zircon grains.

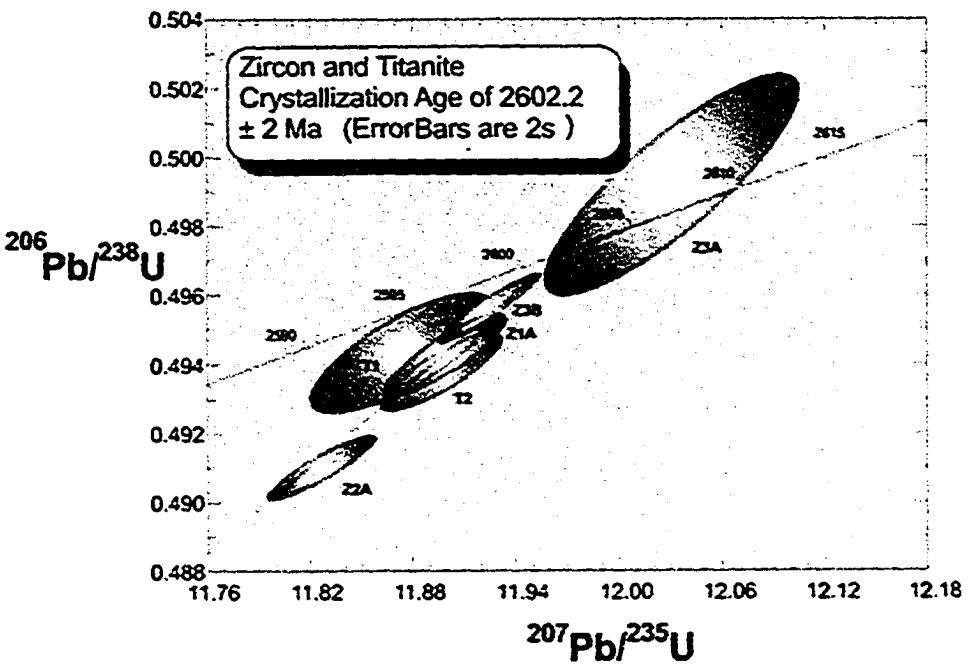

Figure 5-4 TIMS concordia diagram showing data from the South Pluton.

The Hickey Suite is an equigranular, well foliated to gneissic tonalite to granodiorite suite with abundant mafic enclaves. This sample was collected from a gneissic locality, with no surrounding enclaves or characteristic K-feldspar stringers.

Three fractions of monazite were analyzed from the Hickey Pluton: M1, small, rounded, bright yellow grains; M2, pale yellow, blocky grains; and M3, clear, yellow rounded grains (Figure 5-5A). All the grains are highly rounded and exhibit non-faceted surfaces. All three TIMS analyses of these monazites yield overlapping, concordant ages of 2601 Ma (Figure 5-6B) and due to the reproducibility of these ages it likely represents a substantial event in the history of this suite.

Zircons for this rock are of four morphologies: Z1 represents a population including very small, elongate, prismatic grains that are beige and have rounded tips. Z2 consists of beige, stubby, prismatic grains with rounded tips. The Z3 and Z4 populations are small, transparent, prismatic to ovoid grains and brown, semi-prismatic grains with minor inclusions respectively (Figure 5-5B). Backscattered electron imaging of the zircon show grains with no distinct core-rim structures (Figure 5-5C). Rare grains exhibit thin rims, indicating that there may have been two crystallization events of zircon within the suite. These rims, however, are far too small to analyze with the SHRIMP. There are also zones of high and low U contents within the zircon, exhibited by fracture patterns in the darker, more brittle U-poor zones, which is caused by the expansion of U-rich bright coloured zones (Corfu et al., 2003).

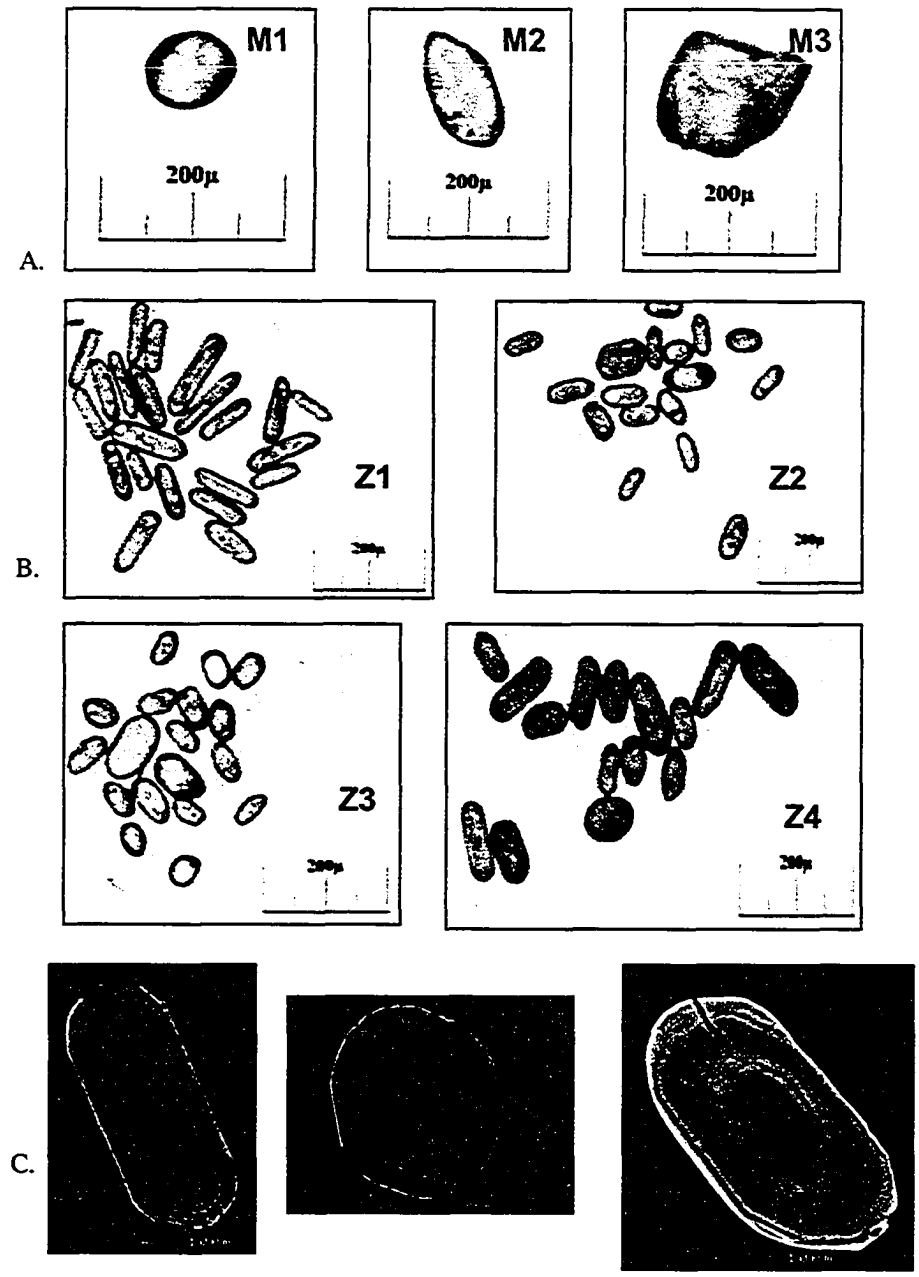

Figure 5-5 A-C. Zircon and monazite populations for the Hickey Suite. A. TIMS monazite fractions. B. TIMS zircon populations. C. BSE images of zircon grains.

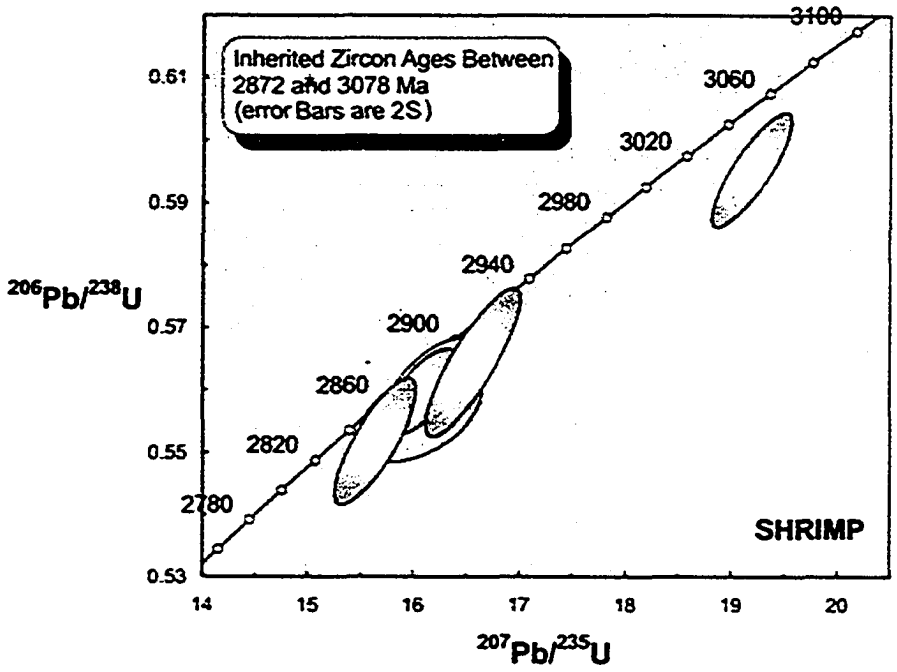

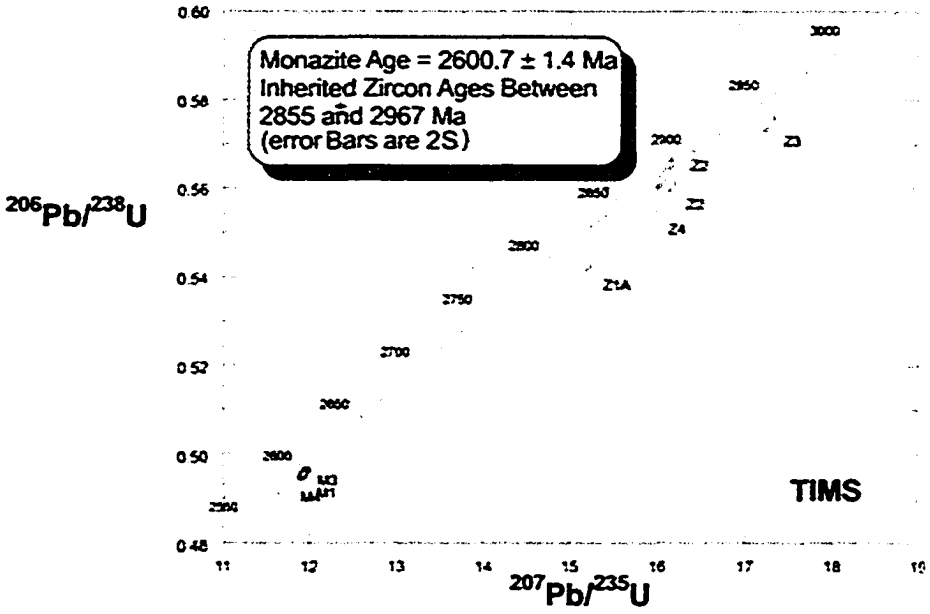

Figure 5-6 A and B. A. SHRIMP concordia diagram showing data from the Hickey Suite. B. TIMS concordia diagram showing data from the Hickey Suite.

The TIMS ages of these zircon fractions yield highly discordant ages between 2855 and 2970 Ma, which are within the age range of the CSBC (Figure 5-6B). It is unlikely that the TIMS data reflect the crystallization age for the Hickey Suite because they show a wide spread along concordia.

The SHRIMP was employed to determine a crystallization age for the sample and to explore the nature of the inheritance. However, because of the small size of the rims on the grains, a crystallization age was not found within the zircons and the data in fact resembled the TIMS data. Eight single spot analyses were completed on eight different grains, with an emphasis on unaltered, unfractured areas. The determined ages were between 3078 and 2872 Ma, again all in the range of ages determined for the CSBC (Figure 5-6A). A cluster of 7 analyses has a weighted mean age of 2899 ± 21 Ma (MSWD=3.5). However, the Th/U ratios of these grains vary between 2.7 and 0.04, which is an extreme spread, making it unlikely that all the grains crystallized from the same source. The MSWD of 3.5 is further evidence that there is excess scatter in the data that is beyond analytical. The zircons are thus interpreted to be inherited from CSBC sources. The monazite age of 2601 Ma from the TIMS analysis likely represents a minimum estimate for the crystallization age of this rock.

5.2.4 Armi Pluton - 03sb008a (z7988)

The Armi Pluton is an equigranular, medium grained biotite granodiorite. It has a weak foliation defined by biotite that is the same as a sillimanite foliation within the Armi Lake meta-sedimentary rocks.

Four populations of monazite were found: M1A, clear with jagged and broken edges, M2A and M3A, pale yellow and transparent with irregular of broken grain boundaries and M4A, pale yellow and anhedral (Figure 5-7A). The ages yielded from these analyses are concordant at 2579.9 +2/-4 Ma and one discordant analysis at 2567 Ma (Figure 5-8B).

Three zircon fractions were described from the Armi Pluton: Z1, large, elongate, brown prisms; Z2, small, elongate prisms with oscillatory zoning; Z3, brown, stubby prismatic grains with abundant oscillatory zoning and inclusions (Figure 5-7B). All of the zircon fractions in this suite show optical evidence for inheritance by the presence of core and rim structures. Further analysis of the grains using BSE imaging on the scanning electron microscope also shows evidence for inheritance by the presence of core-rim structures. Grains exhibit abundant oscillatory zoning as well as fracturing perpendicular to crystal growth (Figure 5-7C).

The TIMS ages collected are highly discordant and include an age of 2931.2±1.4 Ma (Z1), 2580.3±2.2 Ma (Z2) and 2590.9±1.7 Ma (Z3) (Figure 5-8B). The 2931 Ma age is clearly an inherited age, indicating that CSBC or meta-sedimentary rocks may have

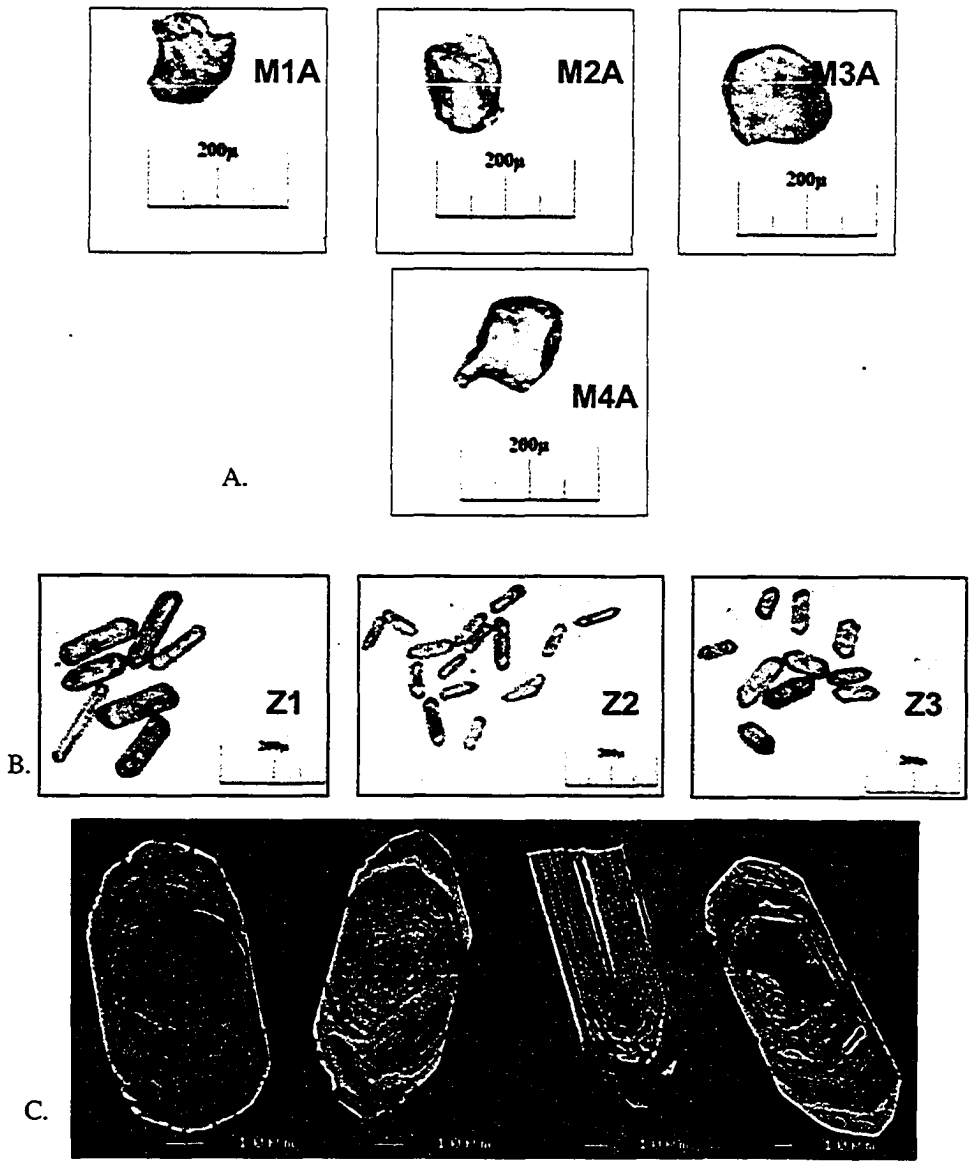

Figure 5-7 A-C. Zircon and monazite populations for the Armi Pluton. A. TIMS monazite fractions. B. TIMS zircon populations. C. BSE images of zircon grains.

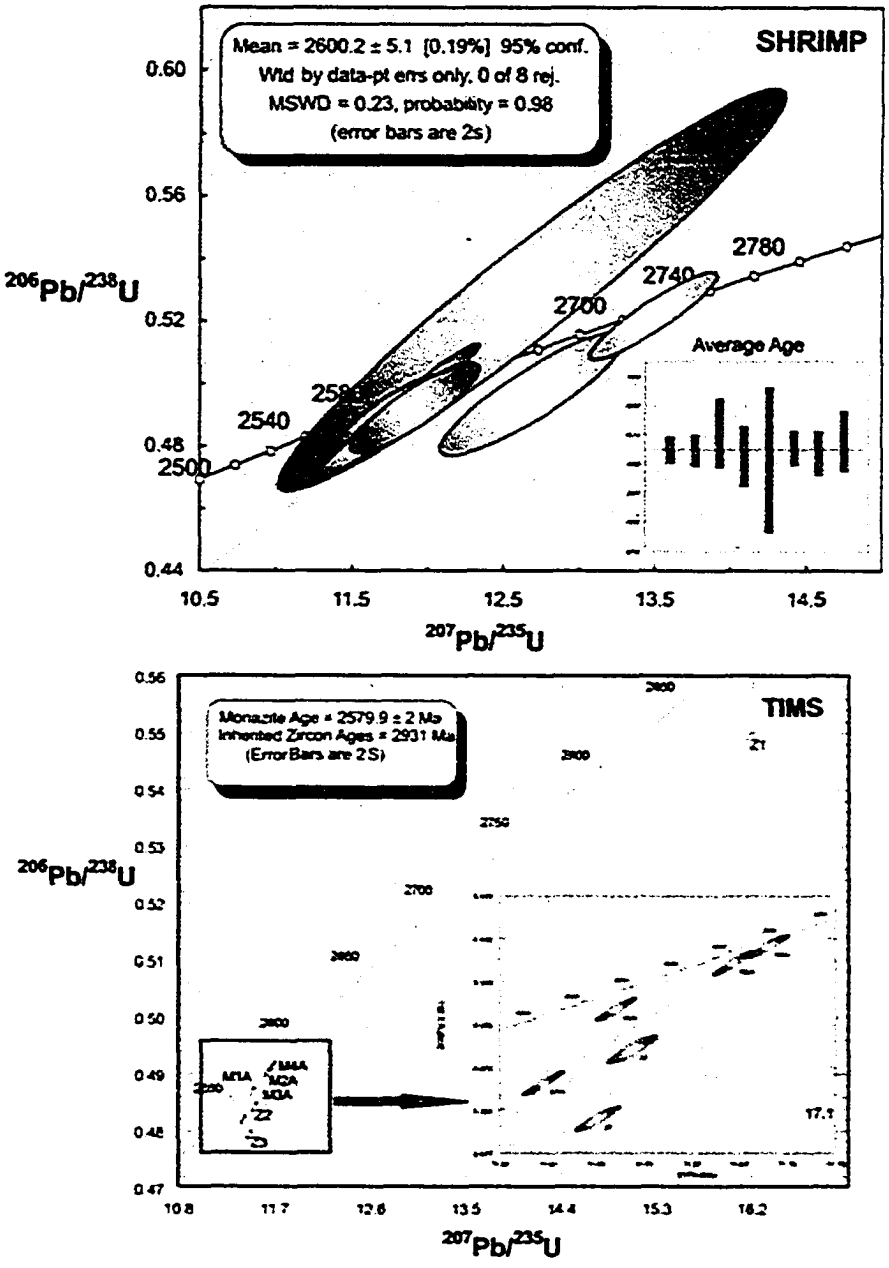

Figure 5-8 A and B. A. SHRIMP concordia diagram showing data from the Armi Pluton. B. TIMS concordia diagram showing data from the Armi Pluton.

had a part in the formation of this suite. The other two ages are within the time of metamorphism in the Slave Province, but do not pin a clear crystallization age.

The SHRIMP data for this suite are more straightforward. Grains with clear cores were analyzed and the cores yielded ages of ca. 2700 Ma while the rims are ca. 2600 Ma. One grain however was analyzed that showed no evidence for cores or rims, but produced an age ca. 2701 Ma and thus is likely a totally inherited grain with no younger rim. Other inherited ages include 2701 Ma and 2720 Ma. The weighted mean of 8 grains yield a concordant age of 2600.2±5.1 Ma (MSWD=0.23) (Figure 5-8A), interpreted as the crystallization age of the rock.

5.2.5 Mag Pluton - 04sb4263 (z8492)

The Mag Pluton is a biotite-magnetite granite with mafic enclaves. It is massive, equigranular and medium grained.

Only one population of monazite was found in this suite, and most grains were highly altered and cloudy. This M1 population is pale yellow, slightly rounded with jagged grain boundaries and is semi-transparent (Figure 5-9A). Two concordant analyses of these grains yield concordant ages of 2575.6 ± 1.4 and 2555.6 ± 1.4 Ma (Figure 5-10B).

Two fractions of zircon were separated; Z1 grains are elongate, prismatic, brown grains that are slightly altered and have abundant fractures; and Z2 grains are stubby, semi-prismatic grains that are very altered and contain abundant fractures. No evidence for cores were evident in transmitted light (Figure 5-9B). TIMS analysis of three fractions yield highly discordant ages that do not suggest a crystallization age (Figure 5-10B).

BSE imaging of this suite shows remnant oscillatory zoning, with some zones broadened by secondary processes. Also, fractures within trace element poor zones of the zircon are common due to the expansion of the trace element rich parts of the zircon (Figure 5-9C). BSE imaging also reveals rare thin cores within the zircons. They are noted by a distinct boundary between the core and the rim.

Due to the inconclusive results from the TIMS analysis, the SHRIMP was utilized to determine a crystallization age for the rock. 17 single spot analyses were carried out on 17 grains yielding a slightly discordant age of 2599.1 ± 4.7 Ma (MSWD=1.2), interpreted as the crystallization age for the pluton. These data were determined from grain rims when there was evidence of inheritance or on homogenous grains as to have a better chance of obtaining a crystallization age. Some cores were also analyzed yielding inherited ages at 2642.9 Ma, 2625.8 Ma and 2656 Ma (Figure 5-10A).

5.2.6 Dauphinee Suite – 03sb020 (z7990)

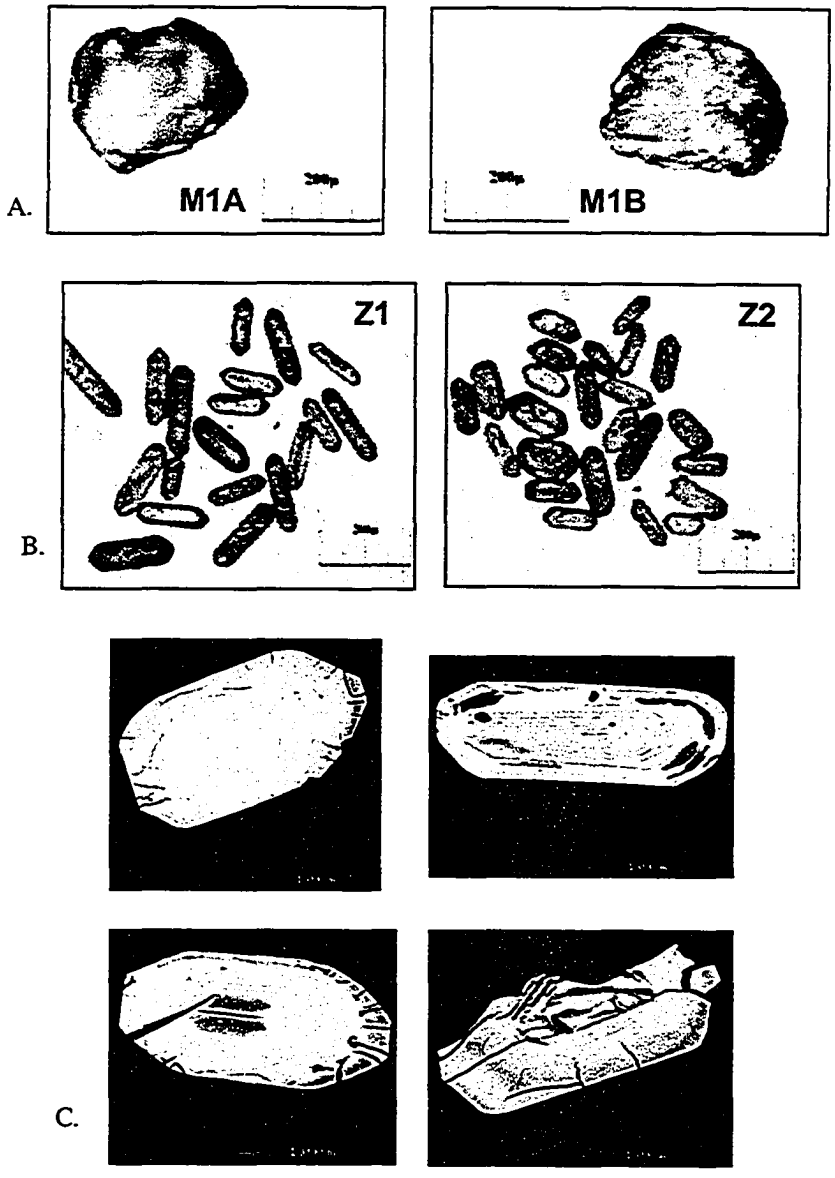

Figure 5-9 A-C. Zircon and monazite populations for the Mag Pluton. A. TIMS monazite fractions. B. TIMS zircon populations. C. BSE images of zircon grains.

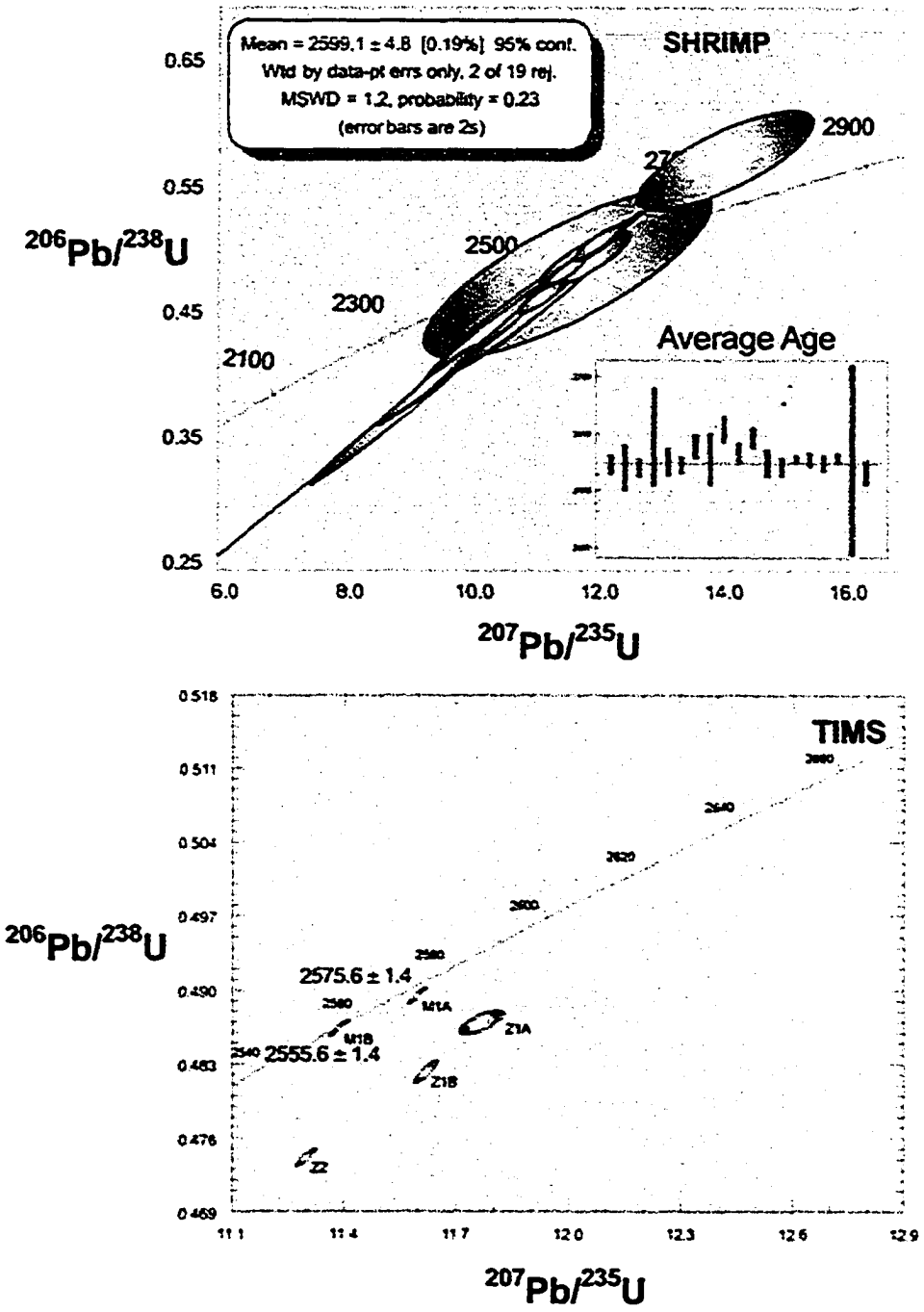

Figure 5-10 A and B. A. SHRIMP concordia diagram showing data from the Mag Pluton. B. TIMS concordia diagram showing data from the Mag Pluton.

The enderbite is an orthopyroxene-bearing tonalite found in the northern-most portion of the Wecho River area and it represents a suite intruded at granulite facies conditions within the Wecho River area. It is equigranular and is made up of plagioclase + hornblende + quartz + pyroxene + biotite.

No monazite is found in this suite, but the zircon grains show a large variety of populations, ranging from very large and corroded to small and unaltered. Six populations were recognized, but only two were analyzed for TIMS because the rest were highly corroded. The Z1A population includes well faceted, small crystals that are elongate, light brown and transparent. The Z1B population also includes small well faceted crystals, but they are generally stubbier, light brown to colourless and fracture free. The Z2 population was originally interpreted as overgrowth zircons and grains from this population are bowl-shaped, irregular, dark brown and slightly fractured (Figure 5-11A). BSE imaging of all the populations show no evidence for inheritance within the grains. Instead most of the grains show effects of differential metamictization causing the expansion of U-rich zones resulting in fracturing of the brittle low U zones (Corfu et al., 2003) (Figure 5-11B).

Five analyses were analyzed using TIMS. The results yielded two discordant age groups, the first at 2590 Ma, the Z1A, Z2A and Z2B populations and the second at 2580 Ma, two Z1B analyses (Figure 5-12B)).

SHRIMP analysis was completed on 12 grains from the Dauphinee Suite sample and all twelve ages yield a concordant weighted mean age of 2591.9±3.6 Ma (MSWD=0.87) (Figure 5-12A). 2580 Ma ages were not found during SHRIMP analysis, making it questionable as to whether they actually exist. The crystallization age for this suite is interpreted to be 2591 Ma, supported by both the SHRIMP and TIMS data.

5.2.7 Wecho Suite - 03sb021 (z7991)

This suite is interpreted through field relations as the youngest suite in the Wecho River area, as it crosscuts most of the other suites. It is a K-feldspar pophyritic granite with a biotite rich groundmass.

Monazite show three distinct populations: M1, flat, transparent, pale yellow to pale brown grains; M2, flat, rounded, slightly cloudy pale yellow grains; and M3, blocky, broken, transparent, yellow, and irregularly shaped grains (Figure 5-13A). All of these grains are rounded and lack prismatic surfaces. Three fractions were analyzed, yielding slightly discordant ages of 2574 Ma, 2565 Ma and 2570 Ma (Figure 5-14B). These monazite ages are similar to those yielded from the biotite granodiorite.

Zircon from this suite were separated into 5 populations, but only Z1, transparent and elongate grains, and Z2, transparent, bowl-shaped grains with irregular surfaces, also interpreted as second generation zircon growth, were analyzed using TIMS. The Z3 fraction is made up of small, stubby grains with dark brown cores, clear rims with small

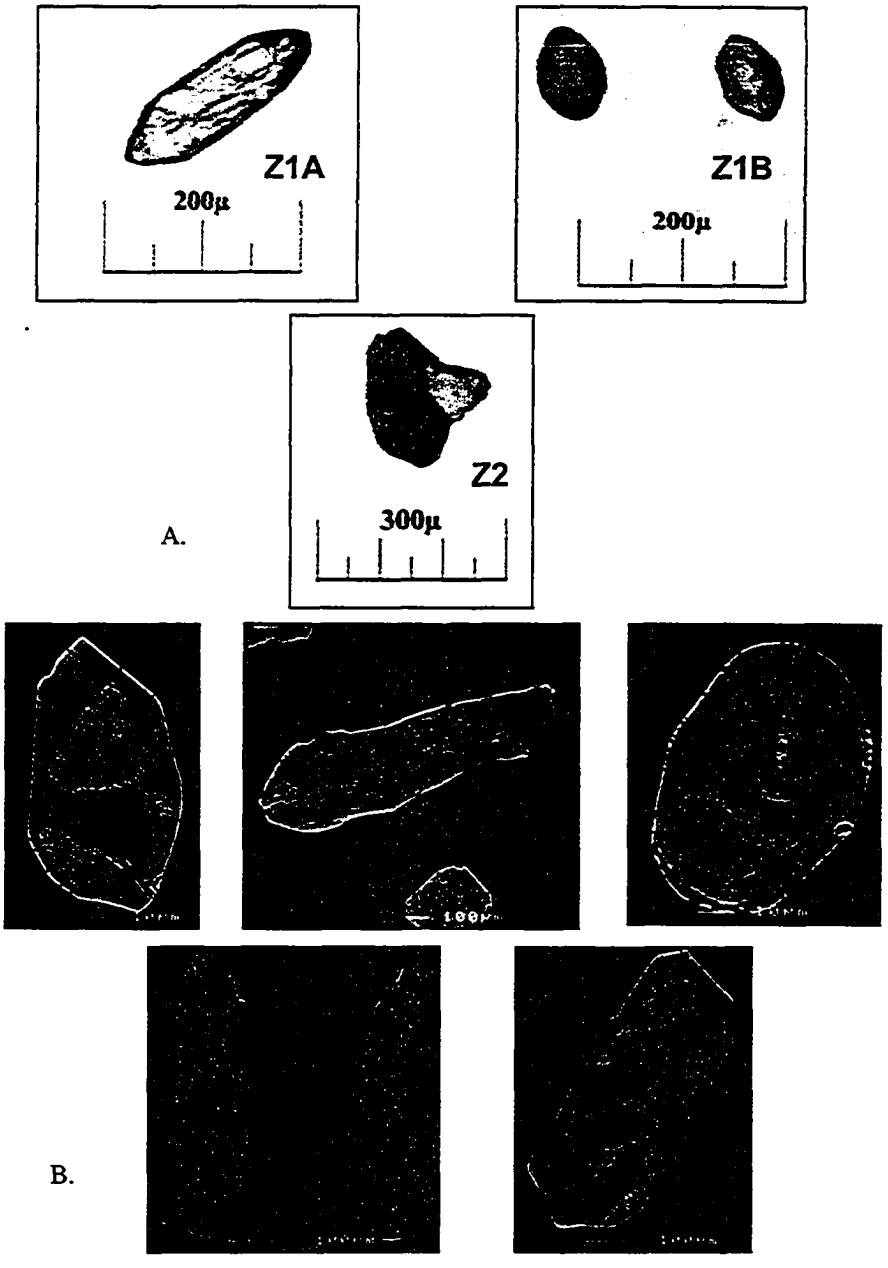

Figure 5-11 A-B. Zircon and populations for the Dauphinee Suite. A. TIMS zircon populations. B. BSE images of zircon grains.

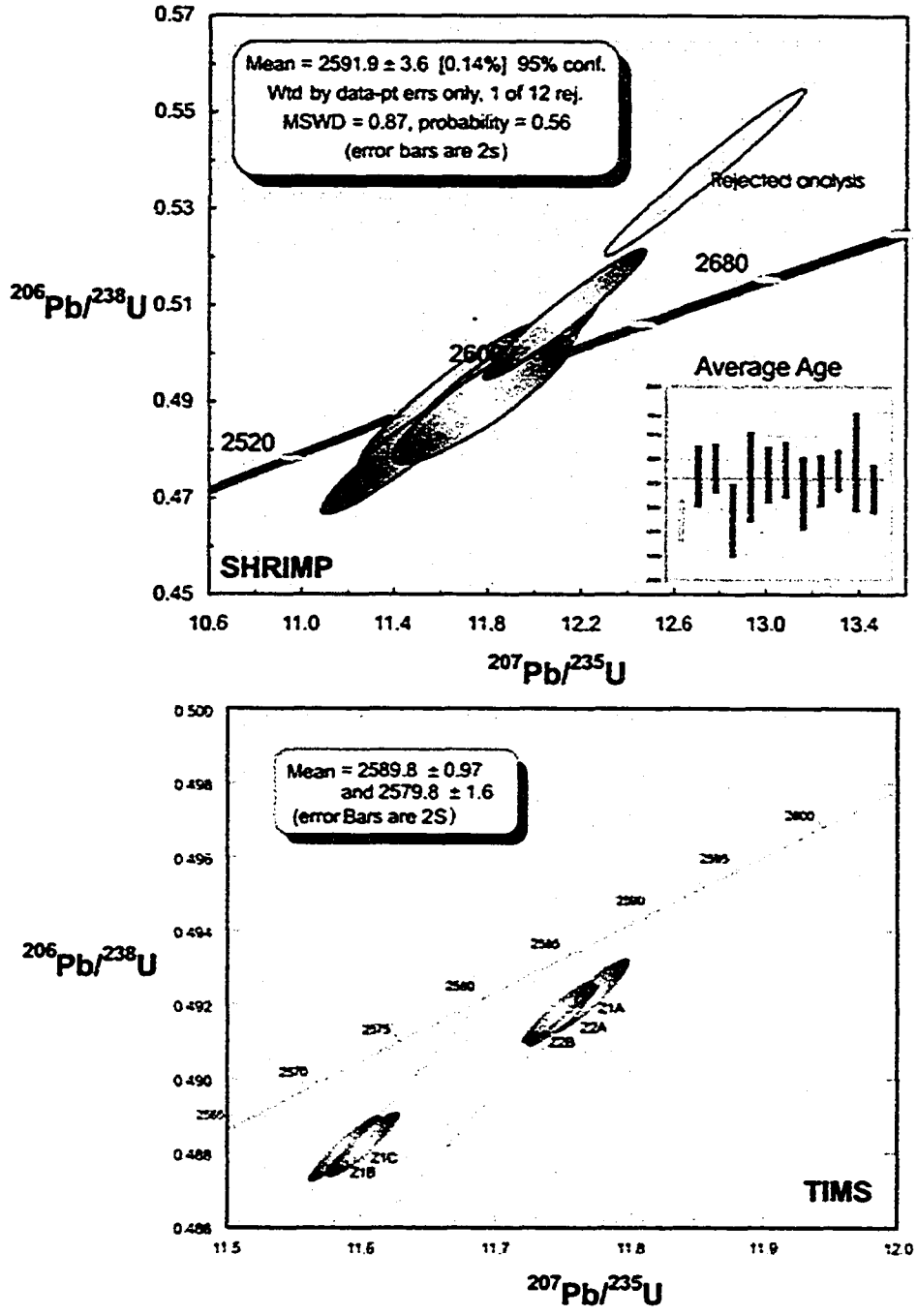

Figure 5-12 A and B. A. SHRIMP concordia diagram showing data from the Dauphinee Suite. B. TIMS concordia diagram showing data from the Dauphinee Suite.

fractures. The Z4 population is small and clear and shows abundant cores and rims. The Z5 grains are generally elongate, light brown and euhedral with fractures parallel to the c-axis of the mineral and show some round cores (Figure 5-13B). Backscattered electron imaging of these grains shows abundant core-rim structures, sometimes with evidence for three growth events (Figure 5-13C), as well as fracturing of the darker trace element poor areas due to expansion of the lighter trace element rich parts of the zircons. There is also some evidence for primary igneous oscillatory zoning, but these zones have often been over-thickened and are largely fractured.

The two TIMS analyses yield discordant ages of 2539.6±3.9 Ma and 2580.6±2.3 Ma (Figure 5-14B). The 2580 Ma age is a likely candidate for crystallization for the pluton, however the Z1 analysis does not represent a plausible age, rendering the TIMS data inconclusive.

Fifteen grains were analyzed on the SHRIMP producing a wide range of ages between 2726 and 2506 Ma (Figure 5-14A). Inherited ages were found in grains with cores, as well as grains with no evidence for cores, which are likely xenocrystic. Inherited ages include 2705 Ma, 2726 Ma, 2684 Ma and 2634 Ma. These ages are found throughout the Slave craton, indicating that other plutonic, mafic volcanic or sedimentary sources were involved in the formation of this suite. The younger ages have a weighted mean of 2591.1±8.2 Ma (MSWD=0.95), which is interpreted as the crystallization age for this suite.

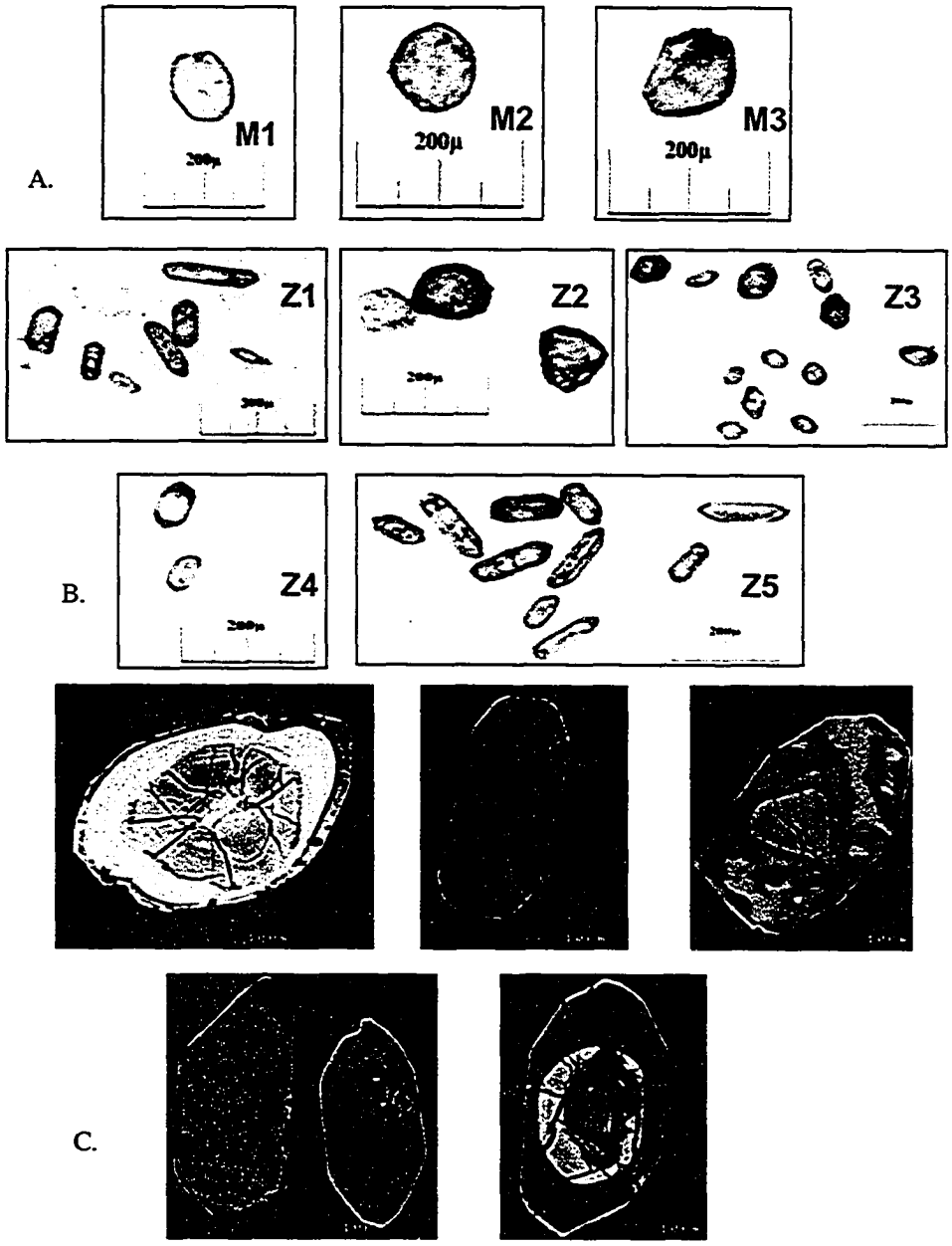

Figure 5-13 A-C. Zircon and monazite populations for the Wecho Suite. A. TIMS monazite fractions. B. TIMS zircon populations. C. BSE images of zircon grains.

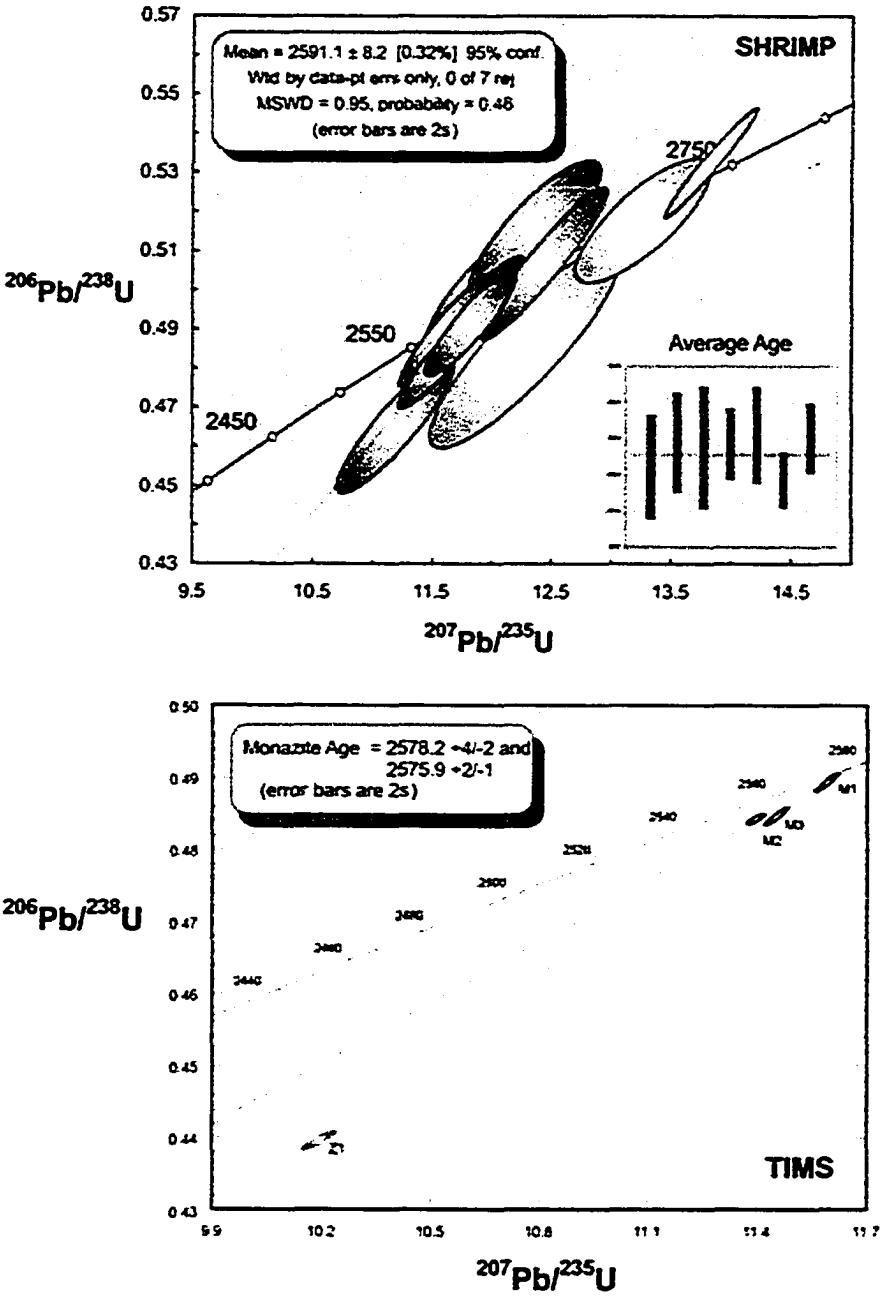

Figure 5-14 A and B. A. SHRIMP concordia diagram showing data from the Wecho Suite. B. TIMS concordia diagram showing data from the Wecho Suite.

Chapter 6 –Geochemistry

6.1 Introduction

The goal of this thesis is to describe the Wecho River granitoids and determine their origin. To do this, major, trace and rare earth element (REE) geochemistry as well as Sm-Nd radiogenic isotope analyses are utilized. Geochemical analyses provide data with which to compare different suites as well as to study source regions. 45 samples taken from suites described in Chapter 3 were analyzed for their geochemical and isotopic properties. Details on sampling practices and analytical methods are found in Appendix B2, B3, B4. Major and rare earth element and Nd isotopic data can be found in Appendix E, and normalization values in Appendix C. A summary of select defining geochemical data are found in Table 6-1 and all figures can be found in the back of this chapter.

6.2 Methodology

6.2.1 Major and Trace Element Data

Major and select trace element analyses were completed using X-ray fluorescence spectrometry (XRF) on fused glass discs at the University of Ottawa. Trace element analyses were completed at the Ontario Geologic Survey in Sudbury using Inductively Coupled Plasma Mass Spectrometry (ICP-MS). Major element analyses are reported as

wt.% oxides and in this thesis are used in discrimination diagrams such as the total alkalis versus silica diagram of Le Maitre et al. (1989), the A/CNK versus silica diagram (Chappell and White, 1974), the Alkali-Iron-Magnesium (AFM) diagram and the Quartz – Alkali Feldspar – Plagioclase (QAP) diagram (Streckheisen, 1976), and bivariate plots, specifically Harker diagrams.

Harker diagrams, such as Figure 6-7, are widely used in this study to indicate differences between suites and to identify trends within suites. These diagrams use SiO_2 versus major elements, trace elements, major element ratios and trace element ratios that may show chemical distinctions between the various suites.

These diagrams are limited however because SiO_2 is the oxide with the highest abundance, and thus creates problems such as deceiving correlations, a reduced scatter of data as SiO_2 increases, and negative trends resulting from an increase in silica relative to other minerals that do not reflect real fractionation trends (Rollinson, 1993). The diagrams are also limited in that they were designed to model a liquid line of decent, but granitoids are not liquids, and more likely are crystal mushes (Miller, 1988).

6.2.2 Rare Earth Element Data

Trace element and specifically rare earth element data are extremely important in understanding petrogenetic processes because they can be modeled mathematically to show the distributions of the various elements in the Earth and are thus useful in

identifying geologic processes and petrogenetic relationships (Rollinson, 1993). They have roughly the same ionic radius and a 3+ charge, meaning that they fractionate to the same extent and they not very mobile, so they reflect their source characteristics. The exception to this is the Eu, which has a 2+ ion that substitutes readily as Ca in plagioclase creating Eu anomalies. A positive Eu anomaly indicates plagioclase accumulation, and a negative Eu anomaly indicates fractionation of plagioclase removing it from the melt. Extended rare earth element diagrams are a useful tool for several reasons such as because REE are immobile during processes such as alteration and low-grade metamorphism (Rollinson, 1993) and they can also indicate fractionation trends determined by the concentration of chondrite normalized light REE to heavy REE (eg. $La/Yb_{(CN)}$). REE are important indicators of source for rocks as well, which can be determined in part by trends in heavy rare earth elements (HREE) relative to light rare earth elements (LREE). An example of this is a strong depletion in HREE relative to LREE, which could indicate a lower crustal melt with garnet as a residue, because garnet preferentially partitions HREE. The multi-element component of these plots adds important incompatible trace elements that also provide clues to the characteristics of a source region. For example, Th-U is depleted in the lower crust, and an Nb-Ta-Ti depletion is characteristic of a subduction zone environment or rutile in the source, as well as certain trends can be indicative of tonalite-trondjhemite-granodiorite series.

The rare earth element data are presented in this thesis as extended rare earth element plots, which include all the rare earth elements as well as selected incompatible elements from multi-element plots. The diagrams are chondrite normalized for the

granitoid suites and primitive mantle normalized for the mafic rocks. Most authors who have published on Slave craton granitoids normalize to chondrite (Taylor and McLennan, 1985), whereas mafic volcanics are generally normalized to primitive mantle (Sun and McDonough, 1989). Chondrite normalization is also used for the granitoid rocks because chondrites represent the least altered, and most primitive, samples from the primordial nebula, making them approximate to the composition of early Earth.

6.2.3 Sm-Nd Isotopic Data

Sm-Nd analyses were completed at Carleton University, with Sm isotopes analyzed on the Finnegan-MAT 261 thermal ionization mass spectrometer and the Nd isotopes analyzed on the Thermal Finnegan TRITON thermal ionization mass spectrometer. The Sm-Nd isotopic system is based on the alpha decay of ^{147}Sm to ^{143}Nd. The system is not very good for dating because the Sm/Nd ratio of the crust and silica-based igneous rocks are roughly the same. However, it is particularly good for examining source regions because the ratio of Sm/Nd in the mantle is higher than in the crust, and thus over time the $^{143}Nd/^{144}Nd$ isotopic ratio in the mantle is greater than the continental crust. Also, both Sm and Nd are relatively immobile so ages and initial ratios remain unaffected by weathering and low-grade metamorphism. The most common way that the data are utilized is Epsilon Nd values, which are calculated using a formula:

$$\varepsilon_{Nd(t)} = \{[(^{143}Nd/^{144}Nd_{rock,t})/(^{143}Nd/^{144}Nd_{CHUR,t})]-1\}*10^4$$

t = time of crystallization

CHUR = Chondritic Uniform Reservoir or Bulk Earth

Error = ± 0.8 units

This equation was created because the range of $^{147}Sm/^{143}Nd$ is quite small for terrestrial rocks and the half-life of ^{147}Sm is quite large, leaving a limited range for the $^{143}Nd/^{144}Nd$ values (DePaulo, 1988). The equation is based on ε_{Nd} values for CHUR always being zero. Nd is preferentially partitioned during partial melting of the upper mantle into the melt phase, which produces a depleted mantle with higher Sm/Nd ratios than CHUR. Thus, negative $\varepsilon_{Nd}{}^{T}$ values are consistent with a crustal source enriched in LREE, meaning that rocks with negative values may have resulted from anatexis of older continental crust. A negative value can also be indicative of enriched mantle, which is also LREE enriched and could be seen in plume-derived rocks. Nb is used to distinguish between crustal and lower, enriched mantle sources, because depletions in Nb relative to Th and La are indicative of crustal rocks. Positive $\varepsilon_{Nd}{}^{T}$ values indicate LREE-depleted mantle sources. Values that show only slightly negative or low positive values may be the result of mixing of sources with enriched and depleted signatures.

This system is particularly useful for the Wecho River area granitoids and mafic volcanics. If ancient crust (>2.9 Ga) is present beneath the Wecho River area, the granitoids should have isotopic evidence consistent with a LREE enriched source or at least interaction with this source.

6.3 Geochemistry Results

The granitoid samples were classified into five groups based on their lithogeochemistry and geochronology. The first, Group A is comprised of the ca.2.66-2.64 Ga mafic volcanics of Germaine and Mosher lakes. The second, Group B, is comprised of the ca. 2625-2600 Ma metaluminous suites, and the Group C rocks are the ca. 2600-2591 Ma, peraluminous younger plutons. Distinguishable from other rocks of its age is the Dauphinee Suite, isolating it as a separate entity, as well as the dated basement sample from the Nardin Complex.

6.3.1. The Nardin Gneiss and Associated Mafic Dykes

The Nardin Gneiss is granodiorite gneiss (Figure 6-1 B) interpreted to be part of the Central Slave Basement Complex (Stubley, 1997) and is supported by new geochronological data presented here. It is a weakly metaluminous suite with molecular $Al_2O_3/CaO+Na_2O+K_2O$ (A/CNK) values between 1.03 and 1.04 (Figure 6-3), and has SiO_2 values between 71 and 73 wt.%. The Nardin Gneiss is rich in alkalis, which is seen in the ternary Na_2O+K_2O-FeO_{total}-MgO (AFM) diagram, which plots trends in calc-alkaline versus tholeiitic rocks (Figure 6-2). K_2O/Na_2O values average 0.75, which is plotted on a graph of K_2O/Na_2O versus SiO_2 with the other Wecho River area granitoids (Figure 6-5). This plot shows the relationship between feldspar composition and SiO_2, which can be utilized to determine magma evolution and plagioclase content. Another tool used to contrast the granitoids is the Rb/Sr versus SiO_2 plot. Rb is a very

incompatible element, even in felsic igneous systems, meaning that it would be concentrated in more evolved granitoids in the upper crust, so higher Rb/Sr values would imply that the granitoid suites crystallized higher up in the crust. Sr preferentially substitutes for Ca in plagioclase, thus higher Sr concentrations would mean that there is more plagioclase present. Higher Sr values would lower the ratio and be indicative of plagioclase rich, less evolved melts. The Nardin Gneiss shows low Rb/Sr values (0.13-0.29), which are similar to values of the Group B magmas (Figure 6-4).

Harker diagrams (Figure 6-7) for the basement samples show distinct differences between the gneissic suite and the other granitoids. Very low MgO (0.31-0.45 wt.%) is noted for the gneissic rocks as well as low CaO (1.9-2.2 wt.%), Fe_2O_3 (1.8-2.5 wt.%), TiO_2 (0.21-1.1) and Nb (1.1-6.3 ppm), Y (4.1-4.7 ppm) and Zr (156-160). The last mentioned oxides and trace elements compositions are comparable to the Group B magmas, with strong comparisons to the Hickey suite.

Extended rare earth element patterns for the Nardin Gneiss shows a strong depletion in Nb relative to Th and a concave up rare earth element pattern, indicating an enrichment in LREE and a depletion in HREE (Figure 6-8 A). The depletion of Nb relative to Th is a crustal signature as Th is enriched in the upper crust relative to the lower crust and Nb is depleted. [$La/Sm_{(CN)}$] values are between 8.7 and 9.6 and [$La/Yb_{(CN)}$] values are between 55 and 71. These $La/Yb_{(CN)}$ values indicate a moderately fractionated rock compared to the other granitoid suites. A plot of $La/Yb_{(CN)}$ versus SiO2 shows the differences in fractionation between suites (Figure 6-6). The gneiss shows

either no Eu anomaly or a slight positive one, indicating that plagioclase was accumulated during its formation.

The Nd isotopic data yield $\varepsilon_{Nd}{}^{T}$ values of -0.42 to -1.64 (Figure 6-9 A). These data are consistent with derivation from an ancient crustal source.

The two generations of gabbroic dykes cross-cutting the Nardin Complex were also analyzed geochemically. The older dyke (03sb007) has 45 wt.% SiO2 while the younger dyke (03sb006) has 46 wt.% SiO_2. Harker diagrams show some similarities between the two generations of dykes such as very low Th (0.22 ppm for the younger dyke, 0.79 ppm for the older dyke) and Nb (1.7 ppm for the younger dyke, 3.9 ppm for the older dyke) (Figure 6-7). They also show low Y values compared to the other mafic rocks (12 ppm for the younger dyke, 15 ppm for the older dyke). Both dykes also have high Fe_2O_3 (11 wt.% for the younger dyke and 15 wt.% for the older dyke), MgO (12 wt.% for the younger dyke, 8 wt.% for the older dyke) as well as high K_2O (0.9 % for the younger dyke, 1.4 % for the older dyke) and CaO (10.5 wt.% for the younger dyke and 9.3 wt.% for the older dyke) compared to the other mafic suites. In general the older dyke suite has higher wt.% oxides and trace element compositions except in the cases of MgO and CaO.

Extended rare earth element diagrams show elevated Rb values relative to Ba and Th (Figure 6-8 B). The older dyke shows a small Sr depletion as well as a positive Eu anomaly as well as a slight depletion in Nb relative to Th and La, indicative of crustal

contamination, while the younger dyke shows only a flat trend. $La/Yb_{(CN)}$ values are very low (1.3 for the younger suite and 4.6 for the older suite) indicating very little fractionation (Figure 6-6). The older dyke does show some fractionation between the LREE and HREE indicating a slightly more complex history.

The Nd isotopic data also differs between samples, with the older dyke showing $\varepsilon_{Nd}{}^{T}$ values of -2.44, while the younger generation of dykes has $\varepsilon_{Nd}{}^{T}$ values of +2.15 (Figure 6-9 A).

6.3.2 Group A Rocks

Group A Rocks consist of the oldest rocks crystallized in the Wecho River area, the Germaine Lake and Mosher Lake mafic volcanic units dated at ca. 2650 Ma relative to the U-Pb dated Mosher Lake meta-sediments (Ootes et al., 2005).

6.3.2.1 Mafic Volcanic Rocks

The Germaine Lake mafic volcanics have 49 wt.% SiO2 and are classified as basalts, (Figure 6-1 A). Harker diagrams show the suite has high MgO (6.09 wt.%) relative to the Mosher volcanics and high Na_2O (3.24 wt.%) relative to all the other mafic units. Its CaO values are very low (8.53 wt.%) in comparison with the other mafic composition suites but high relative to the granitoids. It has moderate TiO_2 (1.31 wt.%),

Nb (4.5 ppm) as well very low Rb (2 ppm), Sr (128 ppm) and Th (1.02 ppm), typical of basalts (Figure 6-6).

Extended rare earth element patterns for this suite are very flat, especially for its rare earth elements ($[La/Sm_{(CN)}] = 1.1$, $[La/Yb_{(CN)}] = 1.3$). The Germaine volcanics, like the Mosher volcanics, show the lowest fractionation between LREE and HREE of all the Wecho River suites. These volcanic rocks also show that Th is slightly elevated relative to Nb, but not significantly. A slight positive Sr anomaly is also present (Figure 6-7 C).

Nd isotopic data for this suite shows ε_{Nd}^{T} values of 0.96 (Figure 6-9 A). The data are consistent with a source that has not been contaminated by continental crust.

The Mosher Lake volcanics have SiO_2 values between 48 and 49 wt.% and, like the Germaine mafic volcanics, are basaltic, but are highly altered, seen by their extremely low Na_2O/K_2O ratios (Figure 6-1 A). Harker diagrams indicate that the suite has high Al_2O_3 (14-15 wt.%), K_2O (0.22-0.56 wt.%), and CaO (8.2-10.0 wt.%) and low and Na_2O (2.4-2.7 wt.%) and MgO (5.1-5.5 wt.%) relative to the Germaine Lake mafic volcanics (Figure 6-7). Sr (150-162 ppm) and Th (0.47-0.84) values are similar to the Germaine Lake volcanics but the Mosher volcanics have lower Y (21-35 ppm) and Zr (61-125 ppm) values.

Extended rare earth element values for this suite are, like the Germaine Volcanics, quite flat, but they have higher values on average for their rare earth and incompatible

elements ([$La/Sm_{(CN)}$] =1.0-1.1, [$La/Yb_{(CN)}$] =1.1-1.3) (Figure 6-8 C). Only minor depletions in Sr and Eu are present within the relatively flat pattern, indicating very little REE fractionation (Figure 6-6).

The ε_{Nd}^{T} for these rocks is between +1.57 and +2.71 (Figure 6-9 A). These values are similar, although greater than the Germaine Lake mafic volcanics, indicating a source with no input from continental crust, and are likely mantle derived.

6.3.3 Group B Rocks

Group B rocks consist of the 2600 to 2630 Ma Hickey Suite, the ca. 2630 Ma Nardin Granodiorite, the ca. 2599 Ma Mag Suite, the ca. 2608 Ma South Suite and the ca. 2608 Ma Wheeler and Germaine diorites. These suites are metaluminous and range in composition from diorite to tonalite to granodiorite to granite. They are the oldest suites in the Wecho River area next to the mafic volcanic suites. They are similar in age and composition to the pre- to syn-deformational plutons in the Western Plutonic Complex and directly east of Yellowknife such as the Defeat suite described by Davis and Bleeker (1999). The general geochemical characteristics that relate these rocks are their low K_2O/Na_2O values (0.25-0.84), SiO_2 values (50 and 74 wt.%), and A/CNK values (0.64 to 1.09). More specifically, the Nardin Granodiorite, Hickey Suite and Mag Pluton are similar and the Wheeler and Germaine Lake Diorites and South Pluton are similar.

6.3.3.1 Nardin Granodiorite

The ca 2630 Ma Nardin Granodiorite (Figure 6-1 B) has SiO_2 values between 71 and 73 wt.% and A/CNK values of 1.02, making it a metaluminous suite (Figure 6-3). It has low K_2O/Na_2O values (0.55-0.84) relative to the other suites (Figure 6-5). Harker diagrams show that the Hickey suite also shows some of the highest values of all the suites for TiO_2 (0.74-1.61 wt.%) and the lowest values for Fe_2O_3 (1.3-2.0 wt.%), MnO (0.01-0.02 wt.%), MgO (0.37-0.65wt.%), Zr (93-147ppm), Y (1-3.5 ppm), Th (2.3-4.9) and Nb (1.6-2.9). Its CaO however shows intermediate values (2.2-2.8 wt.%) between the more mafic compositions of the Dauphinee Suite and mafic volcanics. It also shows low Rb/Sr values (0.21-0.57) (Figure 6-4).

Extended rare earth element patterns for the Nardin Granodiorite show depletions in Nb relative to Th as well as concave up trends indicating an enrichment in LREE and a depletion in HREE (Figure 6-8 D). Fractionation is moderate to high compared to the other suites ($[La/Sm_{(CN)}]$ =7.6-8.7, $[La/Yb_{(CN)}]$ =26.8-59.7) (Figure 6-6). There is also a slight positive Eu anomaly in all the samples collected for the suite indicating plagioclase accumulation. Depletions in Ta, Nb and Ti are also present.

ε_{Nd}^{T} values are between -0.80 and +0.36 for this suite (Figure 6-9 A,B). These data are rather spurious considering that the Nardin Gneiss is located so close to the sample location for the Nardin Granodiorite, indicating that basement likely had only a small effect on the Nardin Granodiorite.

6.3.3.2 Wheeler and Germaine Lake Diorites

These two suites are very similar in their geochemical characteristics, although the Wheeler lake sample is a monzodiorite and the Germaine sample is a quartz monzodiorite. The two suites have SiO_2 values between 51 and 55 wt.% and low K_2O/Na_2O values between 0.42 and 0.43 (Figure 6-5). They also have, like the other Group B suites, low Rb/Sr values (0.08) (Figure 6-4) and low A/CNK values (0.64-0.75) (Figure 6-3). Differences arise however in that they show more of a mixing trend between more mafic compositions, higher in Mg and Fe, and more felsic compositions, higher in total alkalis (Figure 6-2). Besides the more mafic suites (ie. the mafic volcanics and mafic enclaves), Harker diagrams show that the diorites have the highest wt.% MgO (4.5-6.5 wt.%)), CaO (6.7-8.2 wt.%), Y (21-24 ppm) and Fe_2O_3 (7.6-11.4) and low wt.% Al_2O_3 (13.7-15.9 wt.%) and TiO_2 (0.18-0.22 wt.%) They also show low Th (5.4-8.2 ppm) contents (Figure 6-7).

Their extended rare earth element patterns are almost identical with slightly concave-up patterns, a slight depletion in Nb relative to Th (Figure 6-8 F) and moderate fractionation between LREE and HREE ($[La/Sm_{(CN)}] = 2.5\text{-}3.0$, $[La/Yb_{(CN)}] = 17.0\text{-}17.5$). Both the extended REE patterns and the incompatible element patterns are quite similar to those of the South Suite.

The isotopic values for the two diorites are quite different. The Wheeler Lake Diorite has ε_{Nd}^{T} of +1.18, while the Germaine quartz diorite has ε_{Nd}^{T} values of -1.71. This is likely the result of differences in mixing during the petrogenesis of the respected suites, but this will be discussed further in the discussion section.

6.3.3.3 South Pluton

The South Pluton is a hornblende-magnetite granodiorite that can be compared to the Wheeler and Germaine Diorites. It has intermediate SiO_2 values (62 wt.%) and A/CNK values of 0.99, making it metaluminous (Figure 6-1 B). It also falls on a mixing trend between mafic and felsic composition rocks, similar to the Diorite rocks (Figure 6-2), which differ greatly from the other Group B suites. The K_2O/Na_2O values are very low (0.54) (Figure 6-5) and the suite shows some major differences in composition compared to the Nardin Disco and the Hickey Suite. Harker diagrams show that the South suite differs in its high Al_2O_3 values (17.2 wt.%) and very high Zr (263 ppm) values, but quite low Th values (6.7 ppm). CaO (2.2 wt.%), Fe_2O_3 (5.3 wt.%), MgO (1.8 wt.%) and Y (19 ppm) values are higher than those of the Hickey Suite and Nardin Granodiorite, but are lower than those of the mafic volcanics. Rb/Sr values are also low (0.12), but are comparable to the other Group B rocks (Figure 6-4).

The South Suite shows extended rare earth element patterns with slight Nb depletions relative to Th and a slightly concave-up REE pattern (Figure 6-8 F) with a low degree of fractionation ($[La/Sm_{(CN)}] = 3.7$, $[La/Yb_{(CN)}] = 18.8$) (Figure6-6). Incompatible

element trends are very similar to the diorite suites and show depletions in Ta, Nb, Ti and Sr.

Nd isotopic data indicate ε_{Nd}^{T} values of +0.85 (Figure 6-9 A,B). This low positive ε_{Nd}^{T} value indicates that there was some crustal contamination in the petrogenesis of the suite.

6.3.3.4 Hickey Suite and Mafic Enclaves

The Hickey Suite is a tonalite to granite suite (Figure 6-3 B) that has some similarities with the Nardin Granodiorite, such as SiO_2 values between 69 and 71 wt.% and A/CNK values 1.03 and 1.07 (Figure 6-3). The K_2O/Na_2O values are also similar, averaging 0.75 but with a low of 0.25 (Figure 6-5). It also shares the same low values of Fe_2O_3 (1.6-2.4 wt.%), MgO (0.55-1.12 wt.%), Zr (131-499), Y (2.7-8.5) and Nb (131-177 ppm) and moderate CaO values (1.8-3.1 wt.%). Zr and Th also show values higher than any of the other suites. Rb/Sr values are very low (0.08-0.19), comparable with all other Group B rocks (Figure 6-4)

Extended rare earth element diagrams show strong depletions in Nb relative to Th and steep, concave-up patterns (Figure 6-8 D). These are the most fractionated rocks of all the granitoids in the Wecho River area indicated by their large LREE enrichment and depletion of HREE ($[La/Sm_{(CN)}] = 2.4\text{-}11.8$, $[La/Yb_{(CN)}] = 72\text{-}116$) (Figure 6-6). A strong depletion in Nb relative to Th is seen as well as Sr depletion.

ε_{Nd}^{T} values are between -1.31 and -7.58 and are consistent with involvement of an ancient source (Figure 6-9 A,B).

Three samples of mafic enclaves from Hickey plutons were sampled to compare to the Hickey granitoids in order to determine whether they are a possible protolith for the felsic rocks. The enclaves range in SiO_2 from 47-50 wt.% and have very high MgO (7.7-16.4 wt.%). Intermediate values of TiO_2 (0.8-1.17 wt.%) and high CaO (9.3-10.8 wt.%) are characteristic and Harker diagrams show that Y (12-25 ppm) and Fe_2O_3 (11-16 ppm) are varied in composition across the range of all the mafic rocks in the Wecho River area. Th (0.19-1.75 ppm), Zr (57-84 ppm), Na_2O (0.9-2.3 wt.%), K_2O (0.17-0.42 wt.%) and Al_2O_3 (13.3-14.7 wt.%) values are all low relative to the granitoids.

The extended rare earth element patterns of these suites are somewhat varied (Figure 6-8 E). The enclaves show a slight to large negative Sr anomaly and the suites vary in fractionation between LREE and HREE ($[La/Sm_{(CN)}]$ = 1.0-2.7, $[La/Yb_{(CN)}]$ = 0.9-9.0) (Figure 6-6).

Nd isotopic values are also variable indicating differing sources for the enclaves, from dominantly mantle derived positive values to crustally contaminated negative values. The ε_{Nd}^{T} values for the samples have an extreme range from -13.34 to -1.24 to +8.72 (Figure 6-9 A) indicating that they may be the result of an open system.

6.3.3.5 Mag Pluton

The Mag Pluton is a magnetite granodiorite (Figure 6-1 B) dated at ca. 2599 Ma that has a felsic composition, located in the alkali-rich section of the AFM diagram (Figure 6-2). It has 71 wt.% SiO_2 and low Rb/Sr (0.34) and K_2O/Na_2O (0.80) values, similar to the other Group B rocks. It is a metaluminous suite (A/CNK = 1.03) with low TiO_2 (0.18 wt.%), Zr (100 ppm), Nb (2 ppm), Y (4 ppm) and Th (5 ppm) values. Harker diagrams show that the Mag suite has moderate Al_2O_3 (14.9 wt.%), MgO (0.6 wt.%)), Na_2O (3.9 wt.%) and Fe_2O_3 (1.8 wt.%) relative to the other granitoids suites in the Wecho River area. CaO values (2.4 wt.%) are quite high and are comparable with the Hickey Suite and Nardin Granodiorite.

Extended rare earth element patterns show concave-up trends with depletions in Rb relative to Ba and depletion in Nb relative to Th (Figure 6-8 F). Fractionation between the LREE and HREE is quite high ($[La/Sm_{(CN)}] = 8.0$, $[La/Yb_{(CN)}] = 41.1$) (Figure 6-6) and a slight negative Sr anomaly is also seen.

6.3.4 Group C Rocks

The Group C rocks spatially make up about 40% of the Wecho River map area. These intrusions are the youngest group ranging from ca. 2600 to 2591 Ma, and consist of the Mofee Pluton, the Wecho suite, the Armi Pluton and the Mosher Pluton. These are

all weakly metaluminous to peraluminous granites to granodiorites with prominent negative Eu anomalies, and high K_2O/Na_2O and Rb/Sr values compared to the Group A rocks. These suites resemble the post-deformational granitoids defined by Davis et al. (1999).

6.3.4.1 Armi Pluton

The Armi Pluton shows many similarities to the Mosher Suite and the two suites can be readily compared, whereas they are less similar to the Wecho and Mofee Suites. The Armi Suite is a granodiorite to granite (Figure 6-1 B) and has SiO_2 values that are similar to the Group B magmas at 70-72 wt.% as well as A/CNK values between 1.04 and 1.20, making it a weakly metaluminous to peraluminous suite (Figure 6-3). Its K_2O/Na_2O values range from 0.68 to 1.44, higher than the Group B rocks and indicative of K-feldspar being a more dominant phase (Figure 6-5). Al_2O_3 (14.4-15.3 wt.%), CaO (1.2-2.5 wt.%), MgO (0.7-0.8 wt.%), Nb (6.5-9.5 ppm) and Y (5-12 ppm) values are moderate compared to the other Group C suites while the Zr (97-168 ppm) values are all quite low, comparable to the other Group C rocks, but higher than the Group B rocks (Figure 6-7). The Rb/Sr ratios are also higher than the Group B rocks at 0.37-1.38 (Figure 6-4).

Extended rare earth element patterns are concave-up with prominent negative Eu anomalies (Figure 6-8 G). There is also a prominent depletion in Nb relative to Th as well as significant depletions in Ta and Sr. These trends are comparable to the Mosher Suite

trends. The suite has undergone moderate REE fractionation as seen by its depletion in LREE relative to HREE ($[La/Sm_{(CN)}]$ = 4.3-6.4, $[La/Yb_{(CN)}]$ = 21.4-62.9) (Figure 6-6).

ε_{Nd}^{T} values for this suite are highly variable, ranging from -1.43 to +4.41, which will be discussed further in the discussion.

6.3.4.2 Mosher Pluton

The Mosher Suite shows similarities with the Armi Suite in its major and trace element abundances, except that the Al_2O_3 (14.3-15.9 wt.%) is generally higher (Figure 6-7). SiO_2 values are lower than the Armi Suite at 68-71 wt.%. K_2O/Na_2O values are high at 0.74-1.12 (Figure 6-5), consistent with the rest of the group and Rb/Sr values are the same, at 0.35-1.10 (Figure 6-4). A/CNK values are representative of a weakly metaluminous composition (1.02-1.09) (Figure 6-3).

Extended rare earth element patterns show concave-up trends with depletions of Sr, Ta and Nb, as well as enrichment in Th relative to Nb (Figure 6-8 G). It also shows moderate fractionation, but slightly lower than the Armi Suite ($[La/Sm_{(CN)}]$ = 3.8-5.6, $[La/Yb_{(CN)}]$ = 16.8-41.7) (Figure 6-6). Negative Eu anomalies are significant.

The Nd isotopic data for the Mosher suite are more consistent than the other Group C magmas, likely because of the location of the suite in the map area. The values for ε_{Nd}^{T} range from +0.16 to +1.82 (Figure 6-9 A,B).

6.3.4.3 Wecho Suite

The Wecho Suite is the youngest unit in the Wecho River, dated by U-Pb techniques at 2591 Ma. There are two mapped phases of this suite, a highly porphyritic, biotite rich phase, and a less porphyritic, biotite poor phase, both of which are granitic (Figure 6-1 B). The geochemistry of both phases is very similar, so they will be discussed together.

The major and trace element data for this suite show many similarities to the other Group C rocks but they also show a large spread of data, some of which are similar to the Group B rocks. SiO_2 ranges from 66-73 wt.% and Harker diagrams indicate that Al_2O_3 (15-18 wt.%), CaO (1-28 wt.%) and MgO (0.56-1.63) values cover the range of all the granitoid data while Nb (3.9-17.1 ppm), Y (5-21 ppm) and Zr (88-316) values are all quite high, comparable to the other Group C rocks, but higher than the Group B rocks (Figure 6-7). K_2O/Na_2O ratios (0.73-2.00) (Figure 6-5) as well as high Rb/Sr ratios (0.29-1.01) (Figure 6-4) are also higher than those of the Group B rocks. A/CNK values show that the suite is weakly metaluminous to peraluminous with values between 1.00 and 1.42 (Figure 6-3).

Extended rare earth element diagrams show prominent Nb depletions relative to Th as well as prevalent negative Eu anomalies (Figure 6-8 H). LREE are enriched relative to HREE production a moderately fractionated trend ($[La/Sm_{(CN)}] = 3.5\text{-}5.4$, $[La/Yb_{(CN)}] = 13.7\text{-}59.3$) and the REE patterns are concave-up (Figure 6-6).

Nd isotopic data are variable with ε_{Nd}^{T} values between -1.7 and 0.85 (Figure 6-9 A,B).

6.3.4.4 Mofee Pluton

Mofee Pluton is a peraluminous (A/CNK = 1.06-1.13) (Figure 6-3) biotite-muscovite granite (Figure 6-1 B) that has SiO_2 values between 72-74 wt.%. It is the most peraluminous of all the granitoid suites and includes low Zr (91-194 ppm) and Nb (5-12 ppm) as well as moderate Y (5-11 ppm) concentrations relative to the Group C plutons (Figure 6-7). It also has the lowest values of all suites in its TiO_2 (0.11-0.33 wt.%) Fe_2O_3 (1.3-2.1 wt.%), MgO (0.2-1.4 wt.%), CaO (0.8-2.1 wt.%) and Al_2O_3 (13.9-15.3 wt.%). Its K_2O/Na_2O are characteristically high (0.53-1.50) (Figure 6-5) as well as its Rb/Sr values (0.24-3.65) (Figure 6-4).

REE and incompatible element data show depletions in Ta, Sr and Eu as well as a depletion in Nb relative to Th (Figure 6-8 I). The REE patterns for this suite are concave-up with moderate depletions in HREE relative to LREE ($[La/Sm_{(CN)}]$ = 3.3-7.4, $[La/Yb_{(CN)}]$ = 12.1-69.0) (Figure 6-6).

ε_{Nd}^{T} values for this suite ranges from -0.33 to +0.35 (Figure 6-9 A,B). These data are similar to the Wecho suite.

6.3.5 The Dauphinee Suite

The 2592 Ma Dauphinee suite enderbite to mafic granulite alone make up this group and although similar in age to the Group C rocks, its composition and petrogenesis are different enough to place it in a separate group.

The Dauphinee Suite is an enderbite that plots in a tholeiitic trend (Figure 6-2). This suite has a lot of similarities with the diorites, such as its low SiO_2 (52 wt.%) and high CaO (6.88 wt.%), MnO (0.13 wt.%), P_2O_5 (0.54 wt.%) and Fe_2O_3 (12.0 wt.%). It also has moderate MgO (3.6 wt.%) and Zr (153 ppm) values, the highest TiO_2 values at 2.2 wt.% and low Th (1.5 ppm) and high Y (25 ppm) (Figure 6.7). It's A/CNK values make it highly metaluminous with values of 0.81 (Figure 6-3) and it has low K_2O/Na_2O (0.29) and Rb/Sr (0.08) values (Figures 6-5 and 6-6). These low values for the ratios are similar to those of the Group B magmas.

Extended rare earth element patterns are nearly flat ($[La/Sm_{(CN)}] = 2.5$, $[La/Yb_{(CN)}] = 8.4$) showing only slight fractionation (Figure 6-6) and there is no real depletion in Nb relative to Th (Figure 6-8 J). It also shows no Eu anomaly indicating that plagioclase was neither fractionated nor accumulated during its formation.

The Nd isotopic data shows ε_{Nd}^{T} values of +0.40 (Figure 6-9 A,B).

6.4 Summary

Five groups were outlined using the geochemical and isotopic data. The first group, the Nardin Gneiss, has low K_2O/Na_2O and Rb/Sr, similar to the Group B rocks. Similarities with the Group B Hickey Suite and Nardin Granodiorite are common and the extended rare earth element patterns are consistent with moderate fractionation, a slight positive Eu anomaly and depletions in Nb, Ta and Ti. Nd isotopic data are consistent with this suite being ancient crust due to its strongly negative ε_{Nd}^{T} values.

The Group A rocks, the Germaine and Mosher Lake mafic volcanics plot as basalts with flat extended rare earth element patterns and high Mg, Fe, Ca and Ti contents as well as low Th, K and Na values. The ε_{Nd}^{T} values are positive, consistent with a time-integrated LREE-depleted source.

The Group B rocks show mixing between mafic and felsic composition, showing a broad calc-alkaline trend through time on the AFM diagram and are metaluminous diorites to tonalites to granodiorites. They all have low K_2O/Na_2O and Rb/Sr ratios as well as moderate to high La/Yb ratios relative to the Group A and C rocks. In general, Ca, Al and Na values are high relative to the Group C values, and K, Nb, Y and Th are all quite low. Extended rare earth element patterns range from steeply concave up to only slightly concave-up patterns, all with slight to moderate depletions in Nb relative to Th.

$\varepsilon_{Nd}{}^{T}$ values are variable from very negative for the Hickey Suite to positive for the Mag Pluton and South Suite.

The Group C rocks are weakly metaluminous to peraluminous granites. K_2O/Na_2O and Rb/Sr ratios are high. All suites have high K, Th, Y, Zr and Nb and low Ca and Na contents. The extended rare earth element patterns all show prominent negative Eu anomalies and depletions in Ta and Nb relative to Th. The suites have low to moderately fractionated REE, determined by their La/Yb values. $\varepsilon_{Nd}{}^{T}$ data exhibit a range that would be indicative of mixed mantle and crustal sources.

The Dauphinee Suite is metaluminous and shows similarities to the Group B diorites in its K_2O/Na_2O and Rb/Sr ratios as well as its trace and major element compositions. It is, however, much younger than the Group B rocks. Extended rare earth element patterns are quite flat with little fractionation between HREE and LREE and $\varepsilon_{Nd}{}^{T}$ data are low but positive.

Group	Suite	Rock Type	Age Ma	SiO2 wt.%	MgO wt.%	CaO wt.%	Fe2O3 wt.%	Na2O wt.%	Al2O3 wt.%	TiO2 wt.%
Basement	Nardin Gneiss	Granodiorite Gneiss	> 2900	71-73	0.31-0.45	1.9-2 2	1.8-2 5			0.21-1.1
A	Germaine Lake Volcanics	Mafic Volcaniclastic	ca. 2650	49	6.09	8.53	14 9	3.24		1.31
	Mosher Lake Volcanics	Sheered Basalt	ca 2650	48	5.1-5.5	8.2-10.0	13.4-16 6	2.4-2.7	14-15	
B	Nardin Disco	Bt-Mag Grdt	ca 2630	71-73	0.37-0.02	2 2-2.8	1.3-2 0			0.74-1 61
	Diorite Suites	Qtz-Diorite to Qtz Monzodiorite	ca 2608	51-55	4.5-6.5	6.7-8 2	7.6-11 4		13.7-15.9	0.18-0.22
	South	Hbl-Mag-Grdt	ca. 2602	62	1.8	2.2	5.3		17 2	
	Hickey	Bt-Mag Grdt	ca 2601	69-73	0.55-1.12	1.8-3.1	1.6-2.4			
	Mag	Mag-	ca 2599	71	0.65	2.4	1.8	3.9	14.9	0.18
C	Mosher	Bt-Granite	ca 2600	68-71					14.3-15.9	
	Armi	Bt-Grdt	ca. 2600	70-72	0.7-0.8	1.2-2.5			14.4-15.3	
	Wecho	K-spar Porph Granite	ca. 2591	66-73	0.56-1.63	1.0-28 0			15-18	
	Mofee	Bt-Musc Granite	ca. 2591	72-74	0.2-1 4	0.8-2.1	1.3-2.1		13.9-15.3	0.11--.33
D	Dauphinee	Enderbite	ca. 2592	53	3 6	6.88	12			2 2

Suite	Nb (ppm)	Y (ppm)	Zr (ppm)	Th (ppm)
Nardin Gneiss	1 1-6.3	4.1-4.7	156-160	
Germaine Lake Volcanics	4.5			1 02
Mosher Lake Volcanics				0.47-0.84
Nardin Disco	1.6-2.9	1-3.5	93-147	2 3-4.9
Diorite Suites			21-24	5 4-8.2
South		19	263	6.7
Hickey	131-177	2.7-8.5	131-499	18-35
Mag	2	4	100	5
Mosher				
Armi	6.5-9.5	5 - 12	97-168	
Wecho	3.9-17.1	5 - 21	88-316	
Mofee	5.0-12.0	5 0-11.0	91-194	
Dauphinee		25	153	1.5

Table 6-1. Summary of defining geochemical characteristics.

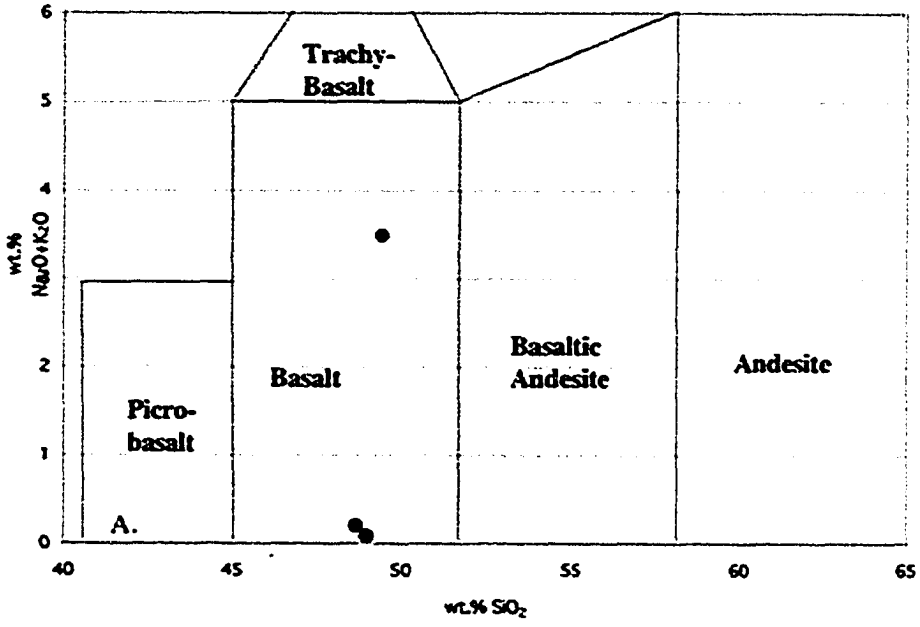

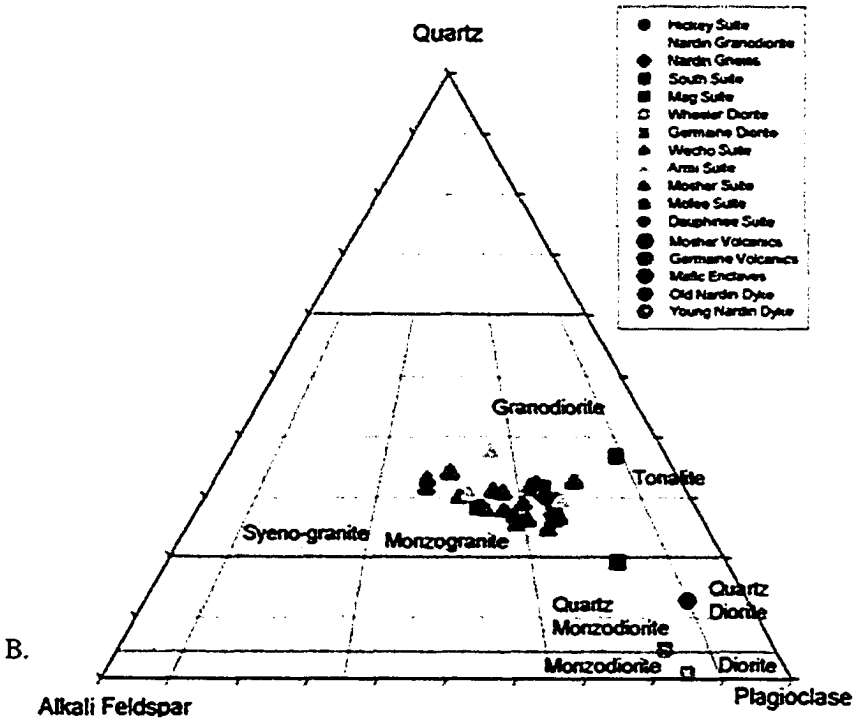

Figure 6-1 A and B. Compositional plots for the Wecho River Rocks. A. The TAS diagram classifying the mafic rocks of the Wecho River area Fields from Le Maitre et al. (1989). B. Ternary QAP diagram showing the compositions of the granitoids. Fields from Streickensen (1976).

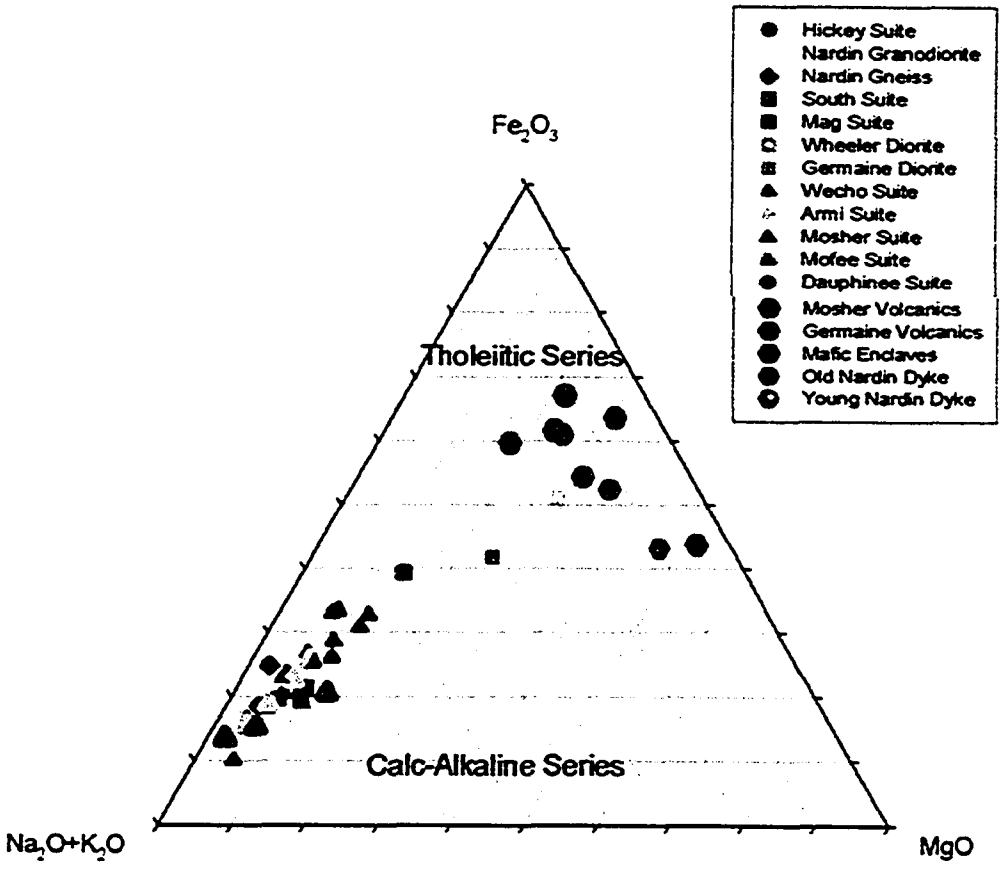

Figure 6-2. Ternary AFM diagram for all the Wecho River area suites (after Irvine and Baragar, 1971).

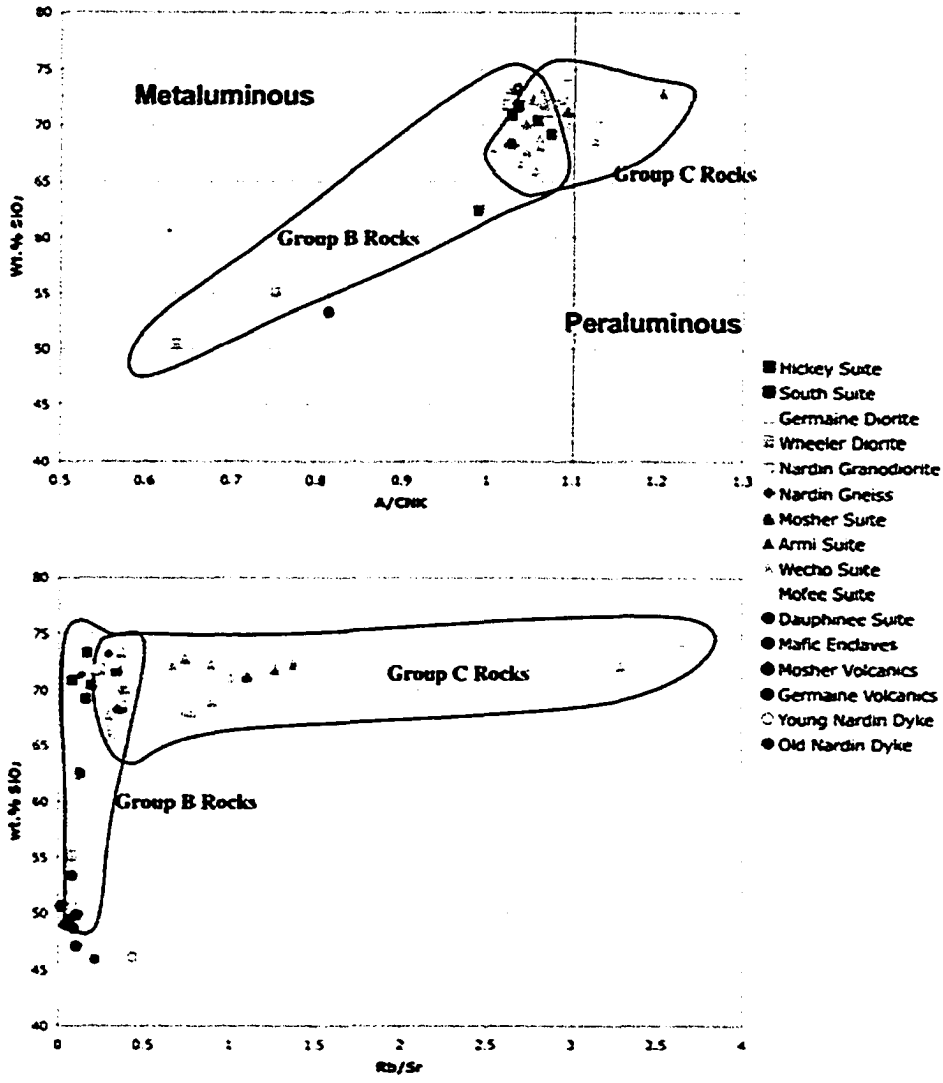

Figures 6-3 and 6-4. 6-3. A/CNK versus SiO_2 plot determining whether a suite is metaluminous (values less than 1.1) or peraluminous (values greater than 1.1). 6-4. Rb/Sr versus SiO_2 plot for all the granitoid suites showing distinctions between the Group B, C and D magmas.

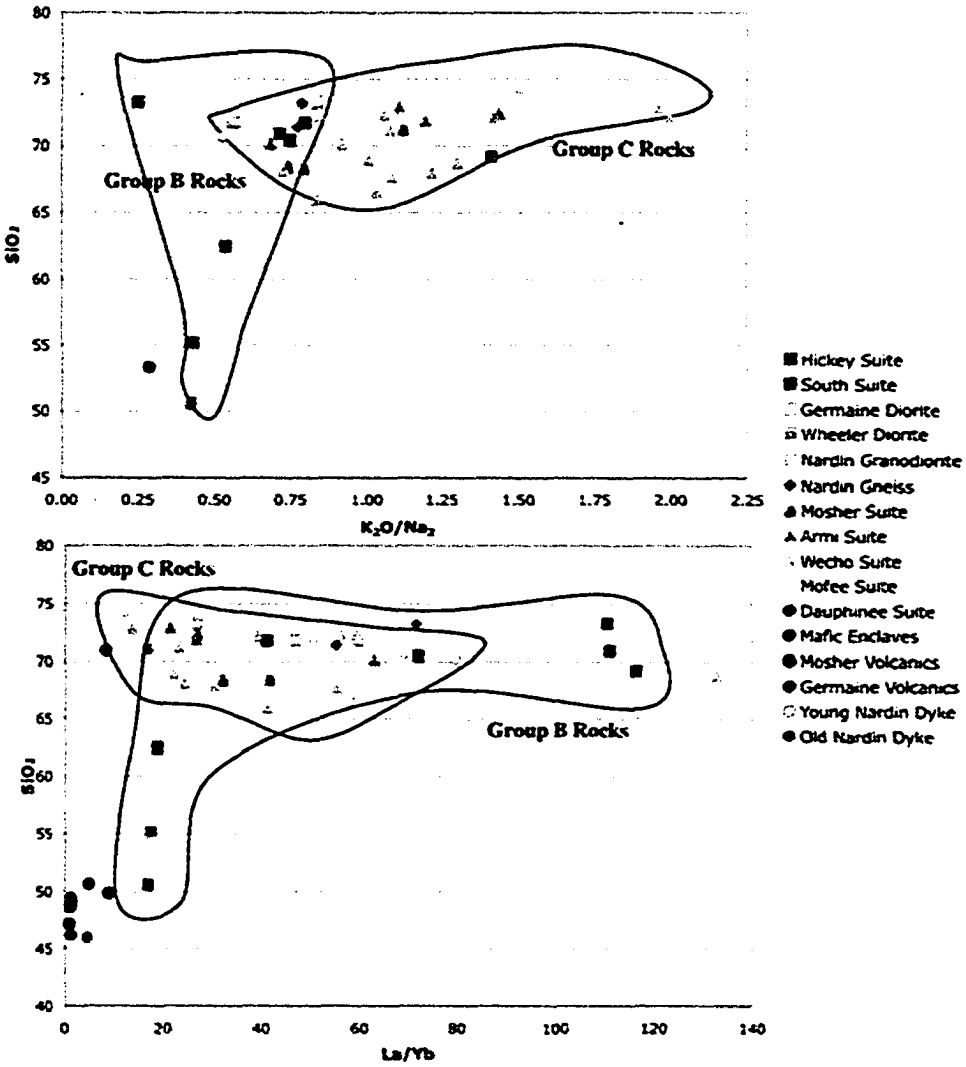

Figures 6-5 and 6-6. 6-5. K_2O/Na_2O versus SiO_2 plot for all granitoid suites showing distinctions between the Group B, C and D magmas. 6-6. La/Yb versus SiO_2 plot for all suites showing distinctions in fractionation between the Group B, C and D magmas.

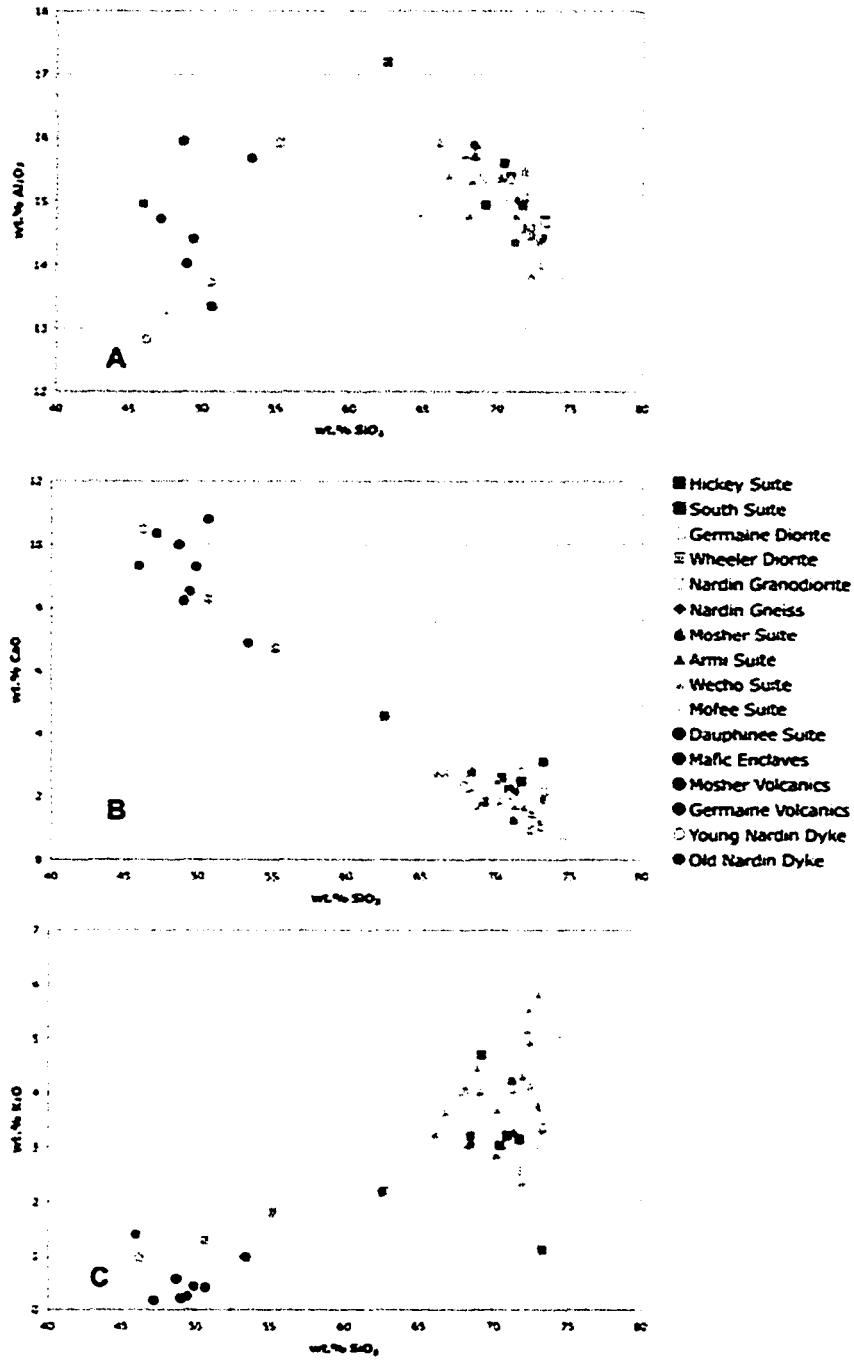

Figure 6-7 A - C. Selected Harker diagrams for all Wecho River area suites. A. SiO_2 versus Al_2O_3 plot. B. SiO_2 versus CaO. C. SiO_2 versus K_2O.

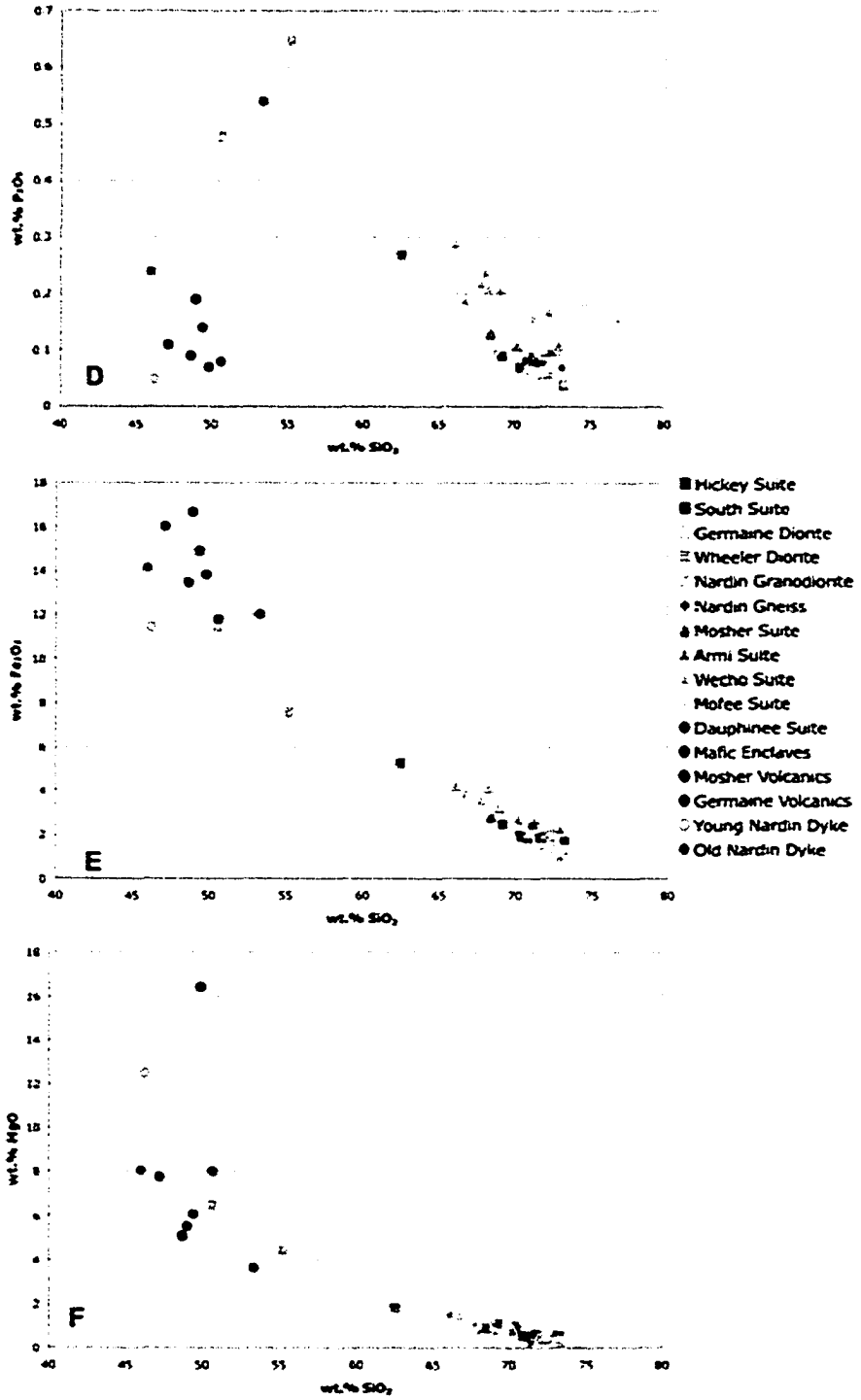

Figure 6-7 D - F. Selected Harker diagrams for all Wecho River area suites. D. SiO_2 versus P_2O_5 plot. E. SiO_2 versus Fe_2O_3. F. SiO_2 versus MgO.

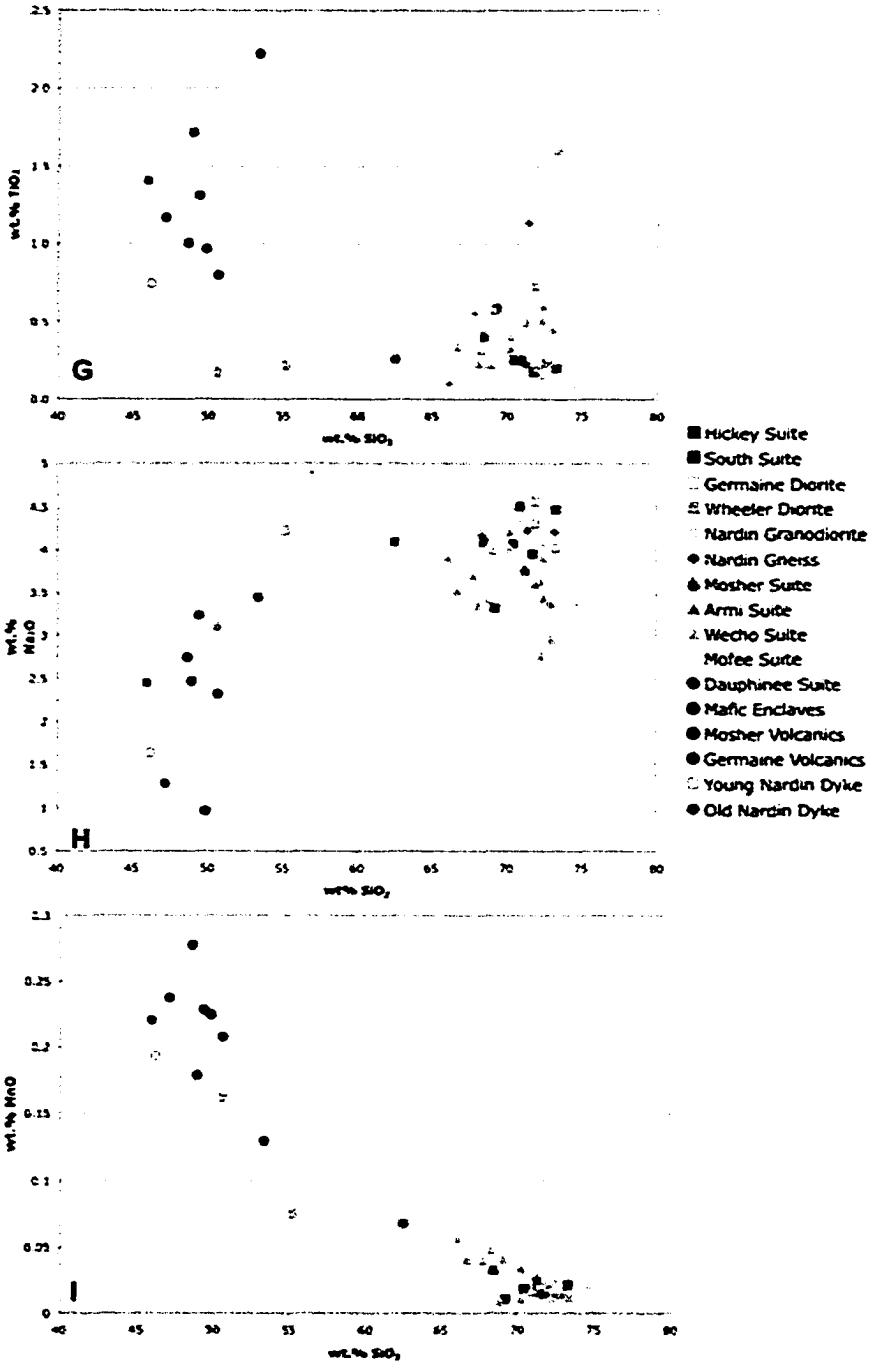

Figure 6-7 G - I. Selected Harker diagrams for all Wecho River area suites. G. SiO_2 versus TiO_2 plot. H. SiO_2 versus Na_2O. I. SiO_2 versus MnO.

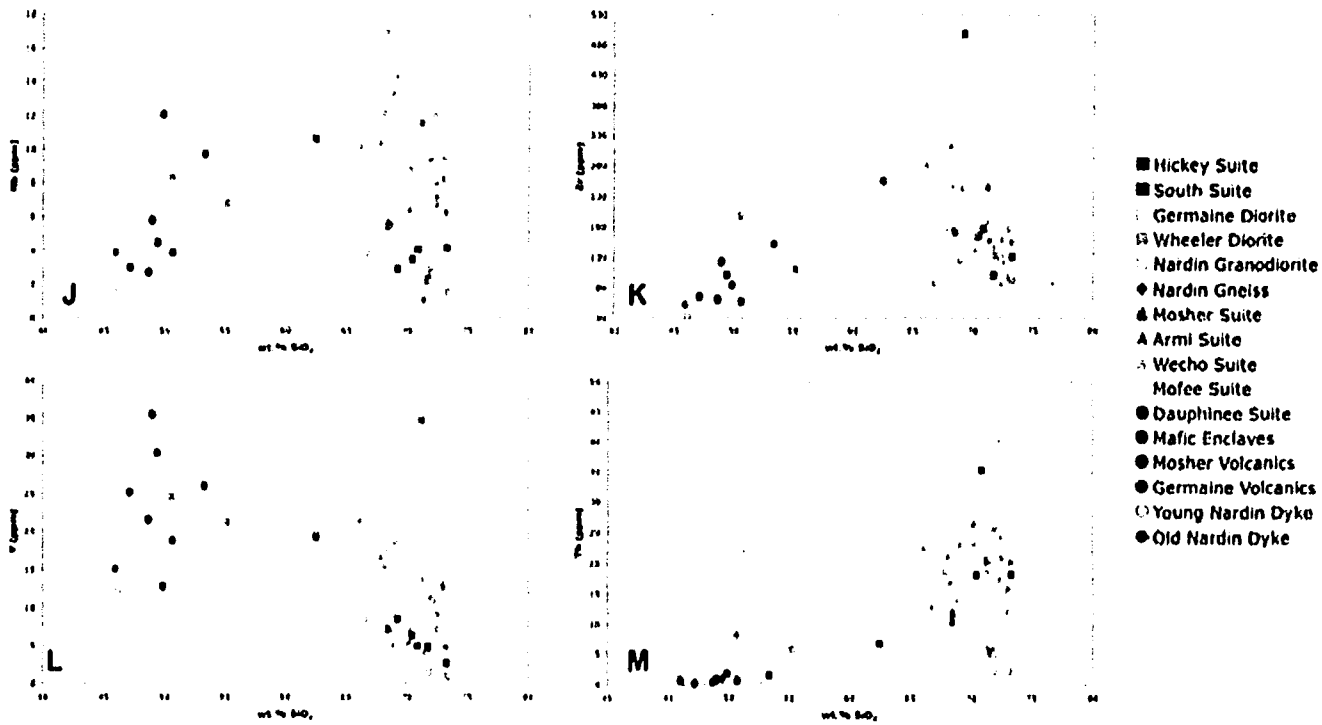

Figure 6-7 J - M. Selected Harker diagrams for all Wecho River area suites. J. SiO_2 versus Nb plot. K. SiO_2 versus Zr. L. SiO_2 versus Y. M. SiO_2 versus Th.

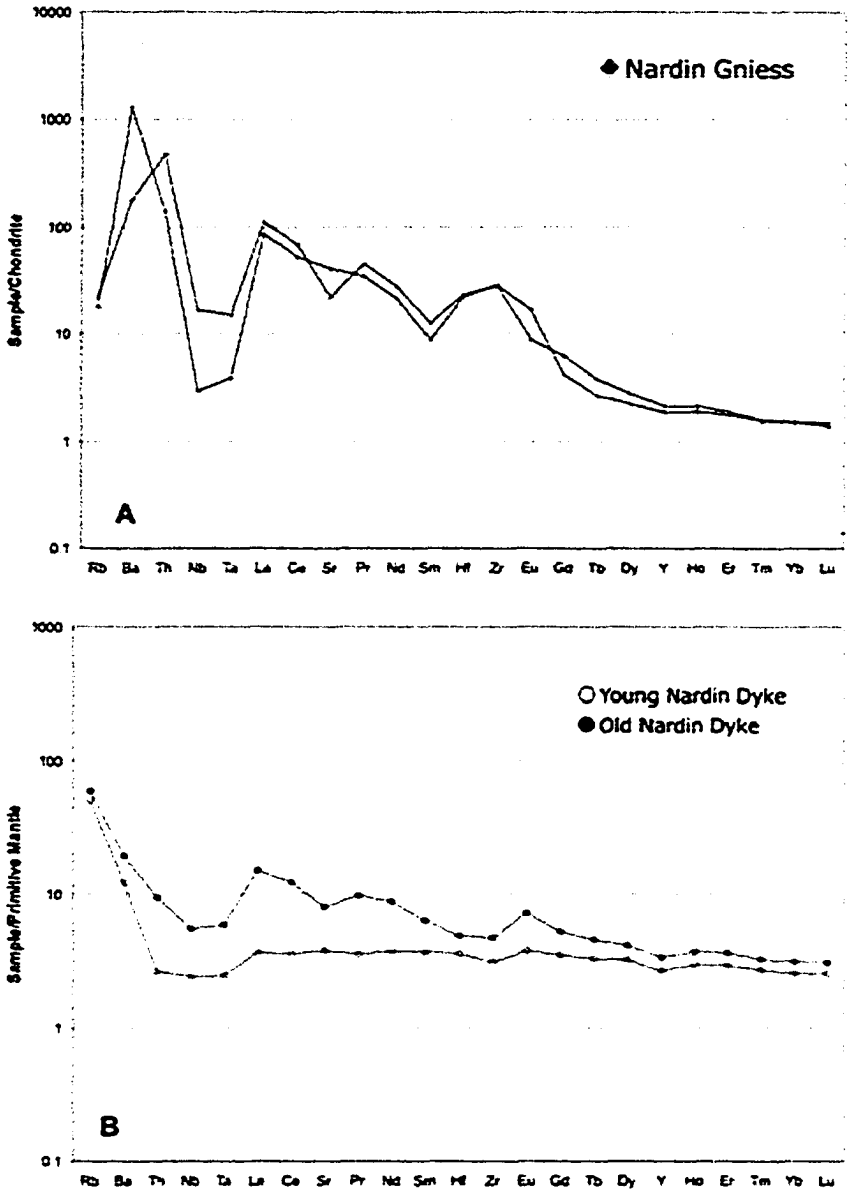

Figure 6-8 A and B. Extended rare earth element diagrams for the suites in the Wecho River area. A. Extended rare earth element patterns for the Nardin Gneiss. B. Extended rare earth element patterns for the Nardin dykes.

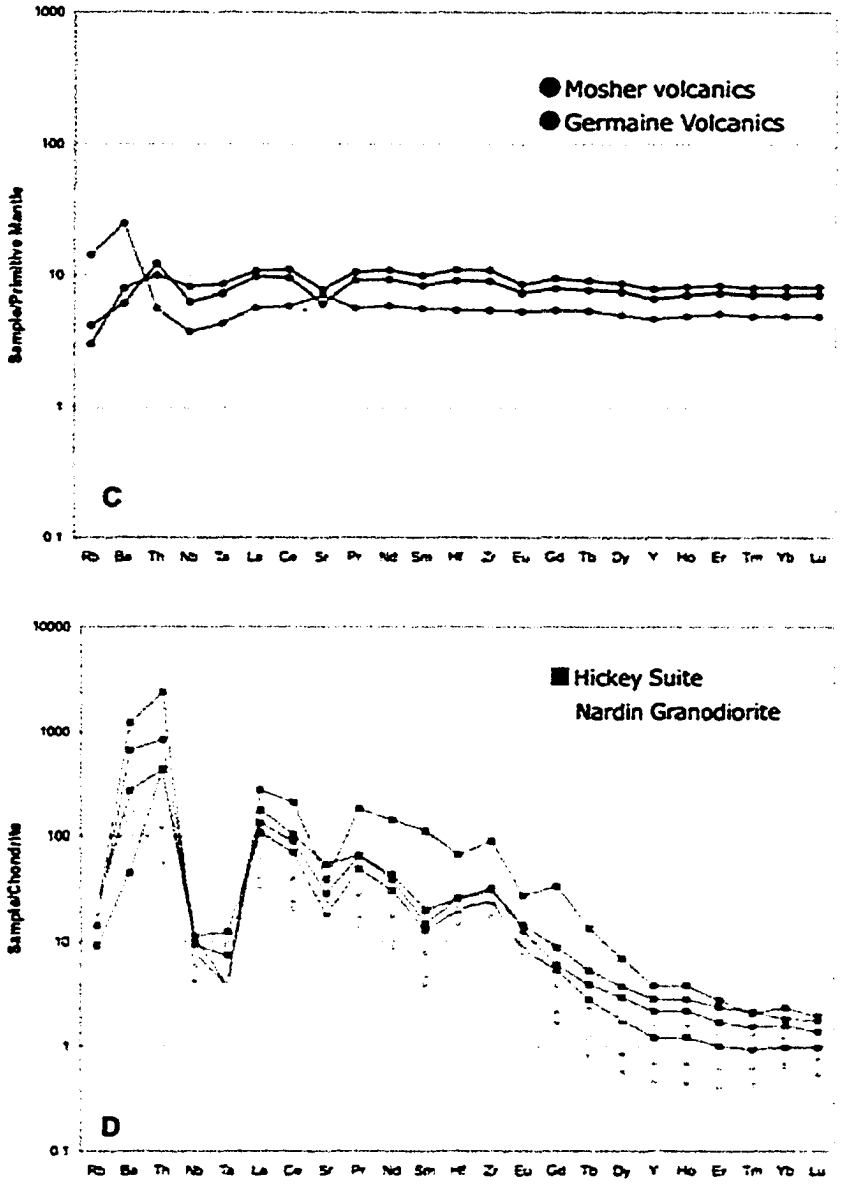

Figure 6-8 C and D. Extended rare earth element diagrams for the suites in the Wecho River area. C. Extended rare earth element patterns for the Mosher and Germaine Lake volcanics. D. Extended rare earth element patterns for the Hickey and Nardin Granodiorite Suites.

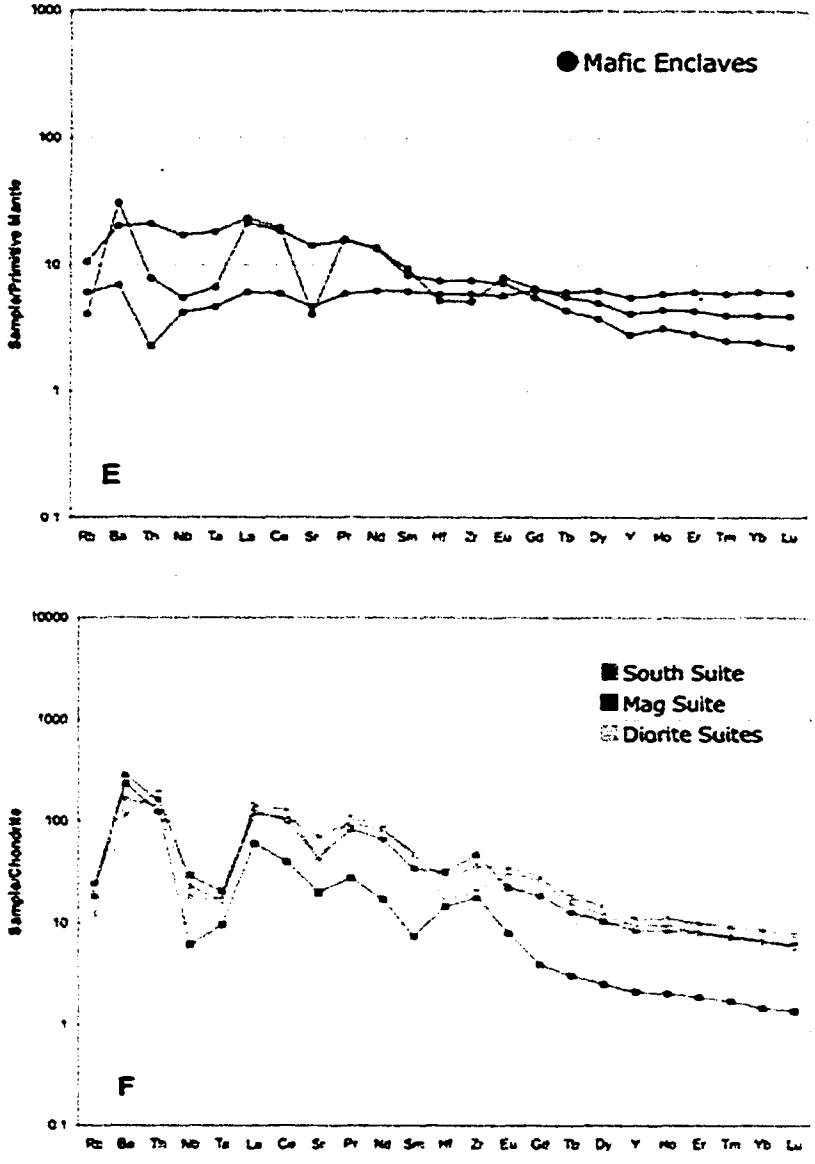

Figure 6-8 E and F. Extended rare earth element diagrams for the suites in the Wecho River area. E. Extended rare earth element patterns for the mafic enclaves. F. Extended rare earth element Patterns for the South, Mag and Diorite Suites.

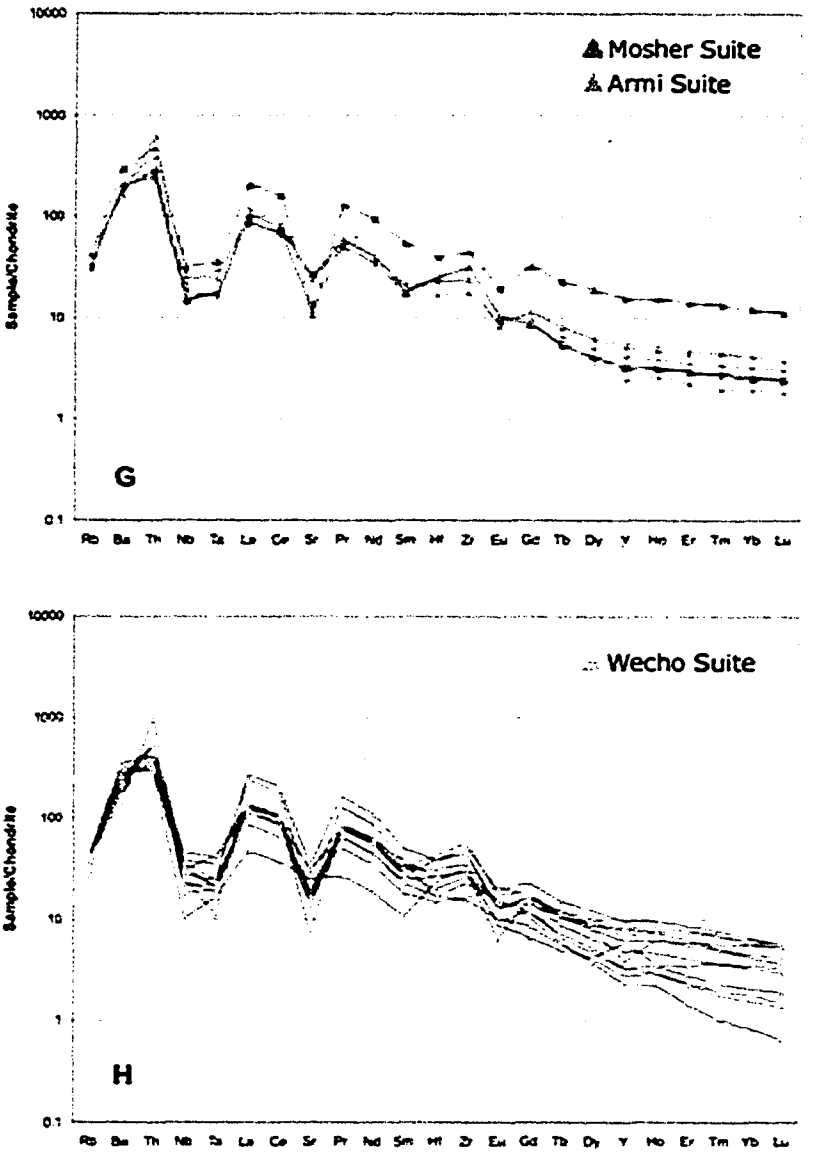

Figure 6-8 G and H Extended rare earth element diagrams for the suites in the Wecho River area. G. Extended rare earth element patterns for the Mosher and Armi Suites. H. Extended rare earth element patterns for the Wecho Suite.

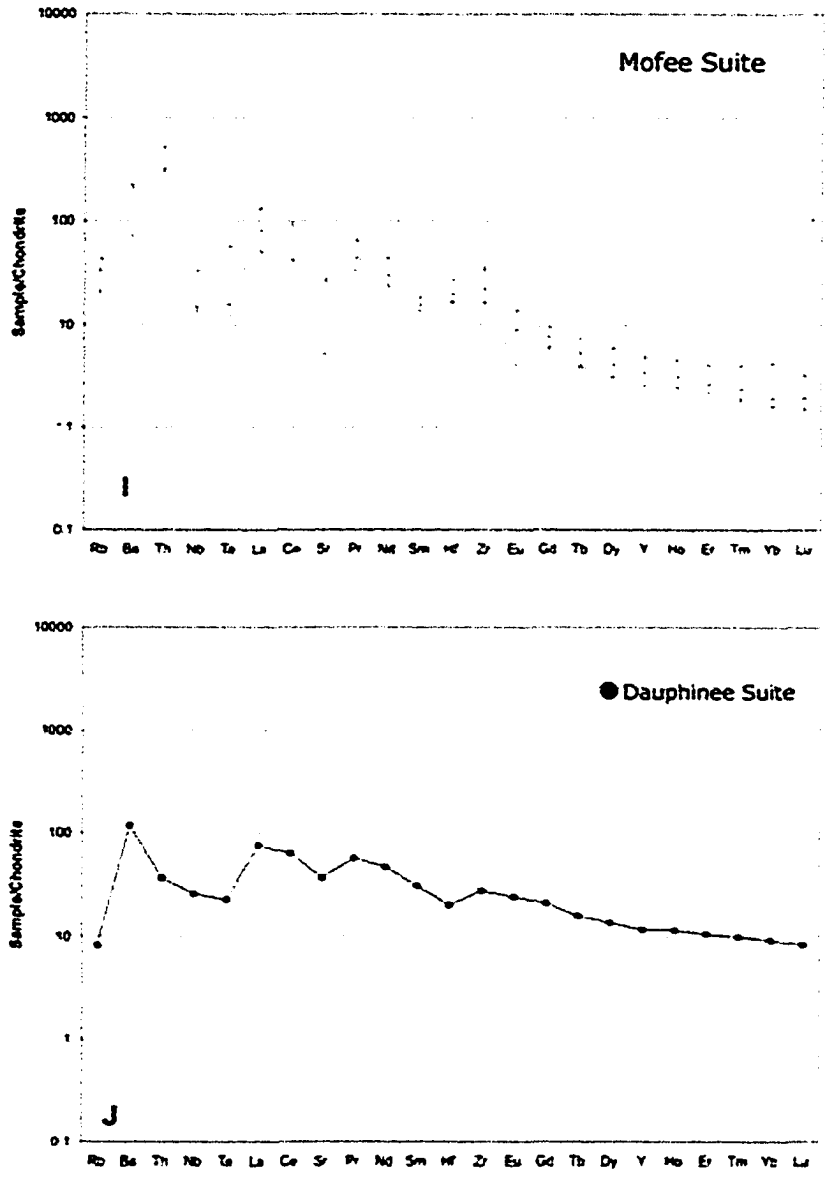

Figure 6-8 I and J. Extended rare earth element diagrams for the suites in the Wecho River area. I. Extended rare earth element patterns for the Mofee Suite. J. Extended rare earth element patterns for the Dauphinee Suite.

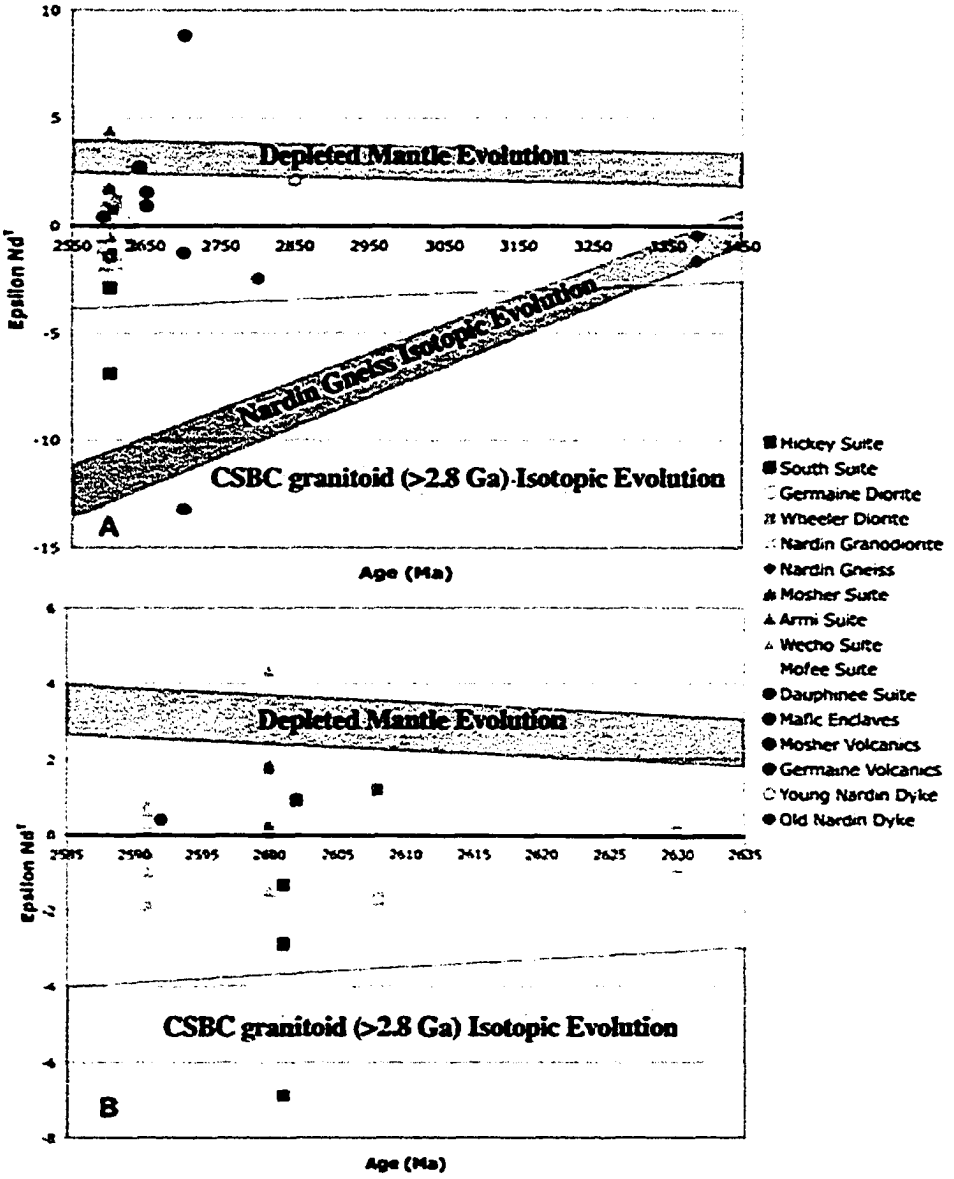

Figure 6-9 A and B. Nd isotopic data. CSBC granitoid isotopic evolution and depleted mantle fields from Davis and Hegner, 1992 A. Age versus Epsilon Nd^T for all suites in the Wecho River area. B. Age versus Epsilon Nd^T for only the Wecho River granitoids. Depleted mantle evolution and CSBC granitoid (pre 2.8 Ga) isotopic evolution are plotted for comparison on each of the plots.

Chapter 7: Discussion

7.1 Introduction

The granitoids described in previous chapters are petrogenetically complex with melting histories defined by their geochronological and geochemical characteristics. Zircon inheritance also plays a key role in defining the granitoids; inherited zircon with ages specific to known times of sedimentation, volcanism and plutonism give important clues as to the derivation of the suites. Sources for granitoids are highly heterogeneous, especially at lower to mid-crustal crustal levels (Miller et al., 1988), evidenced by the complicated geochemical and Nd isotopic data presented in the previous chapter. This section will attempt to explain the origin of the plutonic groups as well as piece together a tectonic model for the Wecho River area within the southwestern Slave Province.

7.2 Petrogenesis of the Nardin Gneiss

The Nardin Gneiss geochronology sample (SHRIMP analyses) yields age of 2909±9 Ma from a single grain and a weighted mean age of 3391±9 Ma from 4 analyses. This sample has a granodiorite bulk composition, but field relations show that the gneiss is dominantly a tonalite with granitic layers. These granitic layers vary in scale from millimeter to centimetre and were unavoidable during sampling. The geochronology data can be explained in two ways. The first explanation is that the crystallization age is 2909±9 Ma and the 3391±9 Ma ages represent zircon inheritance from older crust. This

situation is unlikely because of the abundance of concordant analyses yielded from zircon in the gneiss at ca. 3391 Ma, which make it unlikely that the less abundant ca. 2909 Ma age is the crystallization age. The second explanation implicates a basement age of ca. 3391 Ma for the Nardin Gneiss Complex with a ca. 2909 event responsible for the formation of the granitic layers within the gneiss. This explanation is more reasonable as there are fewer ca. 2909 Ma age zircons and the dominant age is 3391 Ma.

The Central Slave Basement Complex within the Slave Province has been interpreted as a collage of ancient crust with variable ages (Davis et al., 1996 and Yamashita et al., 1999). Typically, the northern parts of the craton have older CSBC ages, >3.4 Ga and the southern portion of the craton has younger ages <3.4 Ga (Davis et al., 1996 and Ketchum et al., 2004). The ca. 3391 Ma age of the Nardin Gneiss described above fit into the current understanding of the distribution of the CSBC within the Slave craton but represent an older age for the CSBC in the southwestern Slave.

The geochemistry of the Nardin Gneiss is representative of TTG-like plutonism, common throughout the Archean (Martin, 2002 and Smithies, 2000). Characteristics include high Al2O3, low Yb and HREE, low K_2O/Na_2O and enrichments in Zr and Hf relative to the REE, similar to many other CSBC exposures (Figure 7-1A). They do not have a negative Eu anomaly, indicating that plagioclase was not a significant fractionating phase during the melt evolution, but the low Sr is indicative of melting with plagioclase as a residual phase. Enrichment in Hf and Zr is indicative, based on

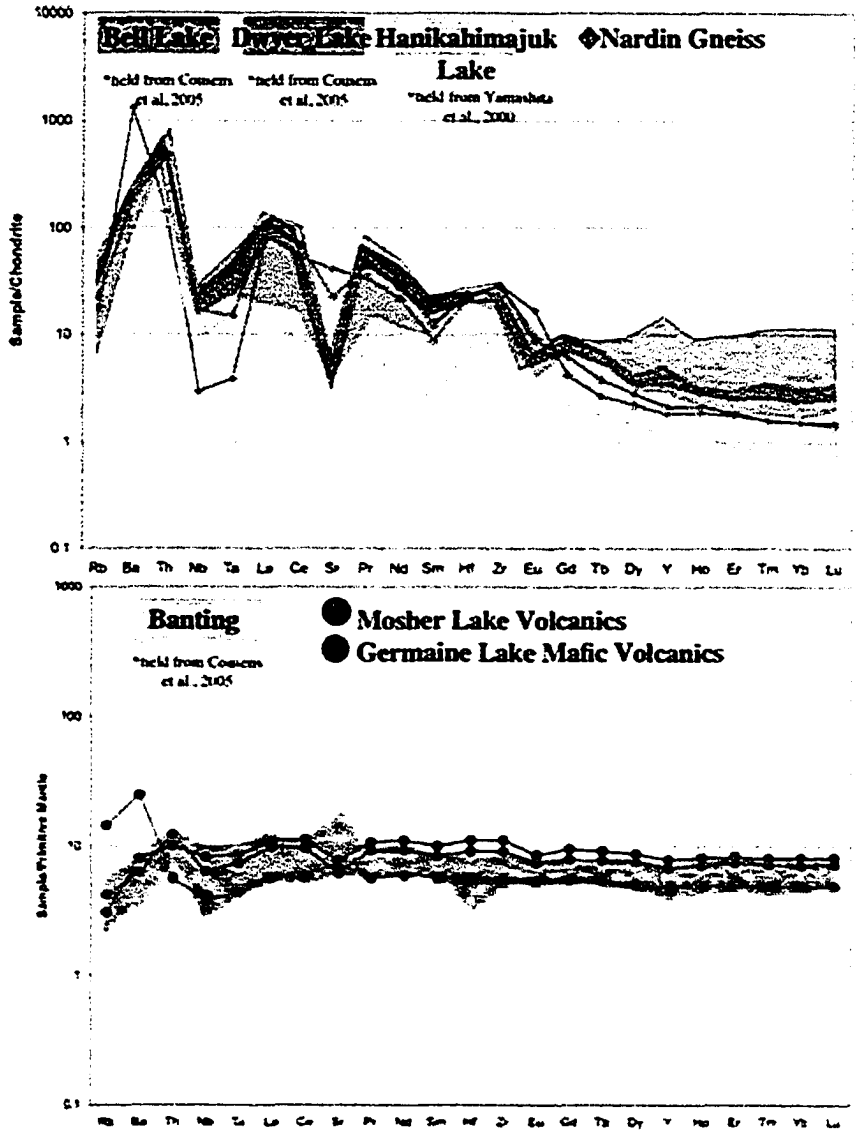

Figure 7-1. A and B. A. Extended rare earth element pattern comparing basement complexes across the Slave craton. B. Extended rare earth element patterns comparing the Banting volcanics with the mafic volcanics from the Wecho River Area.

experimental data, of partial melting of garnet amphibolite because Hf and Zr have been determined to be more incompatible than Nd and Sm during partial melting of this lithology. Low Ni and Cr values indicate that the mantle was likely not involved in the petrogenesis of the gneiss, meaning that a subduction like setting will not explain the gneiss's Nb and Ta depletion and LREE enrichment. Models for TTG production include underplating (Zegers and van Keken, 2001; Smithies et al., 2000 and the suprasubductional mantle wedge model (Kleinhanns et al., 2003). The Nardin Gneiss is thus interpreted to be the result of partial melting of a mafic basement source (ie. an underplate), such as hydrated basaltic crust within the garnet-amphibole stability field, in order to keep the HREE low.

$\varepsilon_{Nd}{}^{T}$ values reported for CSBC throughout the craton ranges from -0.3 to +2.1 in the Hanikahimajuk Lake area (Yamashita et al., 2000), -3.0 to -3.4 for the Dwyer Lake area and -5.3 to +0.7 for the Bell Lake area (Cousens et al., 2005). The positive $\varepsilon_{Nd}{}^{T}$ samples are interpreted as the result of melting of a juvenile source, such as primary basaltic crust, whereas the negative values indicate that there has been a significant amount of time between the formation of parent rock and the analyzed gneiss. This is indicative of crustal working. The strongly unradiogenic Nd isotopic composition of the Nardin Gneiss suggests that it is actually a TTG suite derived from melting of a mafic source with a low positive $\varepsilon_{Nd}{}^{T}$ value. This implies that there was crustal re-working within the Slave craton in the early Archean, prior to 3.4 Ga, which supports data from

other authors such as Yamashita et al. (1999) and Davis et al. (1996) and implies that there were likely many crustal melting events during early Earth history.

The Central Slave Basement Complex has been interpreted as several independent blocks of crust that were amalgamated to form the basement complex. Yamashita et al. (2000) suggest that the northern and Acasta Gneiss are one basement block because of their similarity in ages of their metamorphic events. The Nardin Gneiss, as well as the other Yellowknife area gneisses do not show ages older than 3.4 Ga, and may be unrelated to the basement in the northern part of the craton.

Evidence for two deformational events is present in the Nardin Gneiss, which is implicated by the two generations of dykes that cross cut the gneiss. The dykes are highly deformed, indicating that they are Archean and unlike the younger undeformed Proterozoic dykes that are abundant throughout the craton. The older, more deformed dyke has $\varepsilon_{Nd}{}^{T}$ values of -2.44, indicative of either significant crustal contamination or an enriched mantle source. An enriched mantle source, such as a plume, is unlikely because of the low slope of the REE patterns, as well as depletion in Nb relative to Th and La, indicative of crustal interaction. This dyke is likely from a depleted mantle but has then been highly contaminated, and is not the result of an enriched mantle. The younger dyke is less deformed with $\varepsilon_{Nd}{}^{T}$ values of +2.15, considerably more juvenile, and has flat REE patterns indicating a depleted mantle source. Most basement complexes have at least two generations of mafic dykes (e.g. the Sleepy Dragon Complex (Ketchum et al., 2004)) and

the Nardin dykes are likely similar in age to the Archean dykes found cross-cutting other CSBC exposures (Bleeker et al., 1999a).

7.3 Source of the Group A Rocks

The mafic volcanic rocks in the Wecho River area are relatively dated at ca. 2650 Ma, determined by cross-cutting relationships with the Mosher Lake meta-sedimentary rocks which are dated between 2660 Ma and 2640 Ma (Ootes et al., 2005). The volcanics are commonly highly sheared, with some evidence of pillows to mafic volcaniclastic textures, indicating that they are likely submarine in origin. Geochemically as well as chronologically, they resemble Banting-type volcanism and are likely of mantle origin, possibly the result of extensional volcanism (Cousens, 2002).

REE patterns are extremely flat with extremely low fractionation between heavy and light rare earth elements. The Mosher Lake volcanics have a slight Sr depletion, but otherwise are consistent with mantle origin, similar to the Banting Group (Figure 7-1B). $\varepsilon_{Nd}{}^{T}$ values range between +1.57 and +2.71 for the Mosher lake volcanics and +0.92 for the Germaine lake mafic volcanics, which are also similar to the Banting Group mafic volcanic rocks in the Yellowknife area, determined to be from a depleted source (Cousens et al., 2002)

7.4 Petrogenesis of the Group B Rocks

This plutonic group is defined by age, ca. 2635 to 2600 Ma, as well as broad geochemical characteristics such as low K_2O/Na_2O, low Th, low Rb/Sr and the absence of negative Eu anomalies. Although their ages and geochemistry are comparable the 5 suites have very different petrogenetic origins. Many of the Group B suites within the Wecho River area are correlative to suites found across the Slave Craton.

Also included in this plutonic group are the Old Suite and Inglis Pluton. Both of these suites remain un-dated and no geochemical analyses were preformed on them. However, field relations determine that they are likely related to the metaluminous suites associated with the ca. 2635 to 2600 Ma plutonism in the Wecho River area.

7.4.1 Petrogenesis of the Nardin Granodiorite

The Nardin Granodiorite is highly comparable in geochemical nature to the Defeat Suite in the Western Plutonic Complex, directly south of the Wecho River area as well as the Disco Intrusive Suite found in the Snare River area to the west (Figure 7-1C). Its geochemistry indicates a lower crustal genesis based on its Nb and Ta depletion, Zr and Eu enrichment and steep concave-up REE pattern that are consistent with dehydration melting of a garnet amphibolite at greater than 0.8 GPa. This is consistent with the interpretations of the Defeat Suite by Yamashita et al. (1999) and Cousens et al. (2000) as well as for the Disco Intrusive Suite described by Bennett et al. (in press).

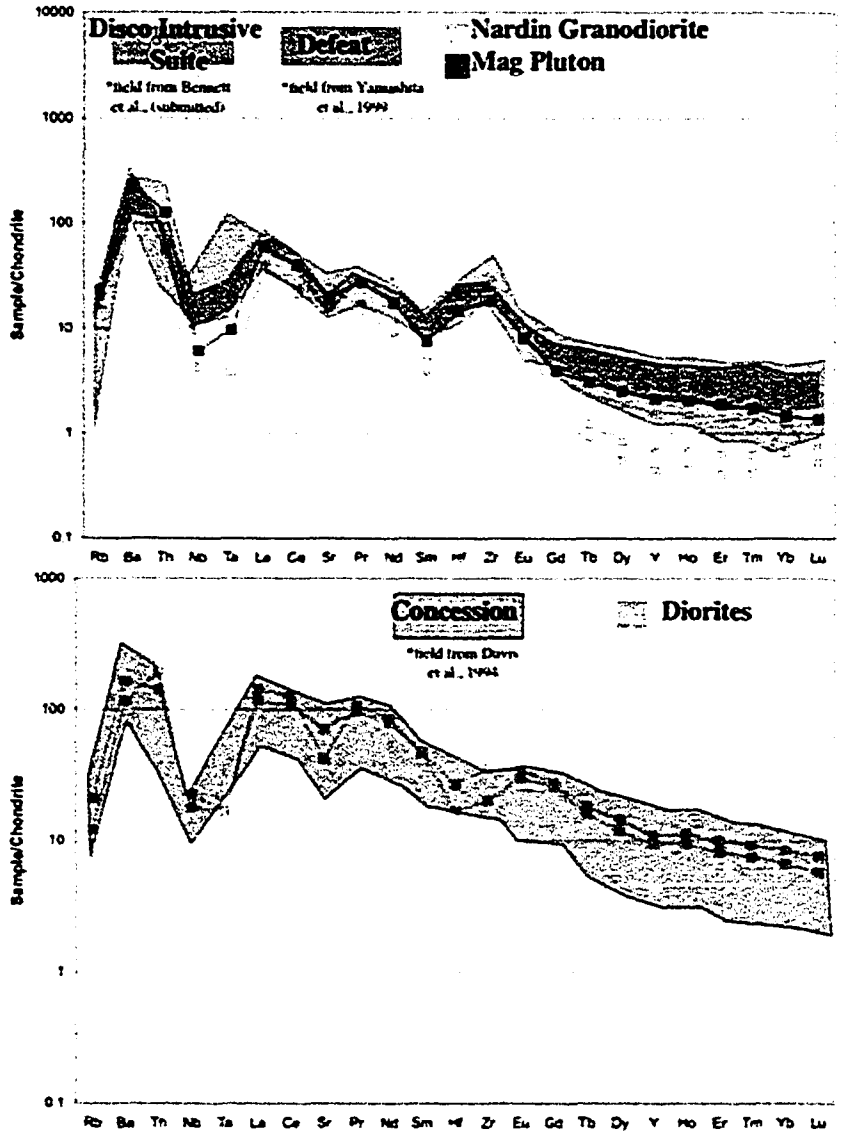

Figure 7-1. C and D. C. Extended rare earth element patterns comparing the Nardin Granodiorite and Mag Granite with the Disco Intrusive Suite and Defeat Suite. D. Extended rare earth element pattern comparing the Concession suite with the Wecho diorites.

The $\varepsilon_{Nd}{}^{T}$ values are also consistent with those of other Defeat Suite plutons in the Western Plutonic Complex with low positive values between 0.36 and 1.67 with endmember values of -0.8. This implies that the source for these rocks would be juvenile, consistent with partial melting of a lower crustal garnet amphibolite.

7.4.2 Petrogenesis of the Diorites and Old Suite

The Wheeler and Germaine Diorites as well as the Old Suite described in the field relations chapter are likely correlative, although no geochemical analyses of the Old suite were attempted due to the complexity of cross-cutting relationships, which were feared to have resulted in contamination of the suite.

The Wheeler and Germaine diorites are correlative to the Concession Suite described by Davis et al. (1994), which are interpreted as sanukitoid like rocks (Figure 7-1D). Geochronology was not conducted on this suite, but Bennett et al. (2005) report similar lithologies in the Snare River area that are ca. 2608 Ma in age and the Concession Suite is also dated at ca. 2608 Ma, making it likely that this is the time of formation for the Wecho River area diorites.

Sanukitoids are defined as high magnesium andesites formed in subduction zones, such as those interpreted in the Superior Province (Stern et al., 1989 and 1991). The high LILE contents are interpreted to be the result of subduction-related mantle enrichment prior to or simultaneous with melting and high Ni and Cr contents are indicative of

mantle interactions. The rocks defined as sanukitoids in the Slave Province do not have the same high Ni and Cr values, although they are higher than a typical granitoid, indicating that significant mantle interaction was not a dominant processes. Davis et al. (1994) interpret the Concession suite to be the result of reaction between slab melts and depleted mantle, creating the depleted signature where the mantle must be previously depleted at the time of formation for the enrichment in LREE. There is no evidence at all for subduction beneath the Wecho River area, so these rocks are likely not directly sanukitoids. Smithies and Champion (2000) suggest that sanukitoids are similar to TTGs except that they are mantle modified, indicated by the high Cr and Ni values. The Wecho diorites do not show this mantle interaction, and they do not show the same amount of HREE depletion as TTGs, but they do have similar Sr, Hf and Zr depletions. The REE patterns also show a Nb depletion relative to Th and La, indicative of a crustal setting or crustal contamination, but the lack of strong HREE depletion rules out a garnet-bearing source. The diorites may instead be melts of a depleted mantle creating a dacitic melt, which then traversed the ultramafic lower crust creating the high Mg, evolved diorites.

$\varepsilon_{Nd}{}^{T}$ values for this suite show extreme variation. The Wheeler Lake diorite has $\varepsilon_{Nd}{}^{T}$ values of +1.18, consistent with a mantle derivation, whereas the Germaine Lake diorite has values of -1.71. This sample location has several cross-cutting granitoid veins and it also includes more K-feldspar in its bulk composition, indicating that it may include more crustal contamination, accounting for its more negative $\varepsilon_{Nd}{}^{T}$ values.

7.4.3 Petrogenesis of the South Pluton

The South Pluton is a hornblende granodiorite dated at 2602 Ma by both zircon and titanite. The zircon from this suite are all pristine and no inheritance is recorded. The closing temperature of titanite is determined to be approximately 600°C and both the zircon crystallization age and the titanite age are ca. 2602 Ma, indicating that the pluton closed at 600°C with no further metamorphic growth or resetting.

The South Suite geochemistry is very comparable to that of the diorites, and the REE patterns are virtually identical. The South Pluton, however, is more evolved compared to the diorites, with more quartz, less hornblende and an overall more felsic bulk composition. Its Nd isotopic ratio is also consistent with melting of a depleted mantle source, with low positive ε_{Nd}^{T} values.

The South Pluton is likely a more evolved member of the diorite suites, with a similar source. If the source is the depleted mantle, followed by a traverse through the lower ultramafic crust, where the diorites are the result of low degrees of partial melting, the South Pluton may be the result of higher degrees of partial melting. LREE are concentrated in melts of low degree, because they are incompatible, and the higher the degree of partial melting the more other elements that will be incorporated, creating a flatter REE signature. The ensuing fractionation of the granitoid would allow for the similarities between the diorites and the South Pluton as well as crustal assimilation would cause the Nb depletion relative to Th and La. This genesis is also supported by the

Nd isotopic data; the south pluton has ε_{Nd}^{T} values of 0.85, which could be the result of melting of a juvenile source and it is also similar to the Wheeler Lake diorite values within error ($\varepsilon_{Nd}^{T} = +1.18$)

7.4.4 Petrogenesis of the Hickey Suite

The Hickey Suite crystallized at ca. 2601 Ma, as determined by a U-Pb TIMS monazite age. Zircons from the suite are scattered between 3078 and 2872 Ma, and as described in Chapter 5, do not reflect a crystallization age. These zircon, however, are all in the age range of CSBC rocks and are interpreted to be inherited from a CSBC source that must be directly underlying the Wecho River area. ε_{Nd}^{T} values for this suite are extremely unradiogenic ranging from -1.31 to -7.48, indicating that they were formed in part from much older crust. REE patterns mimic those of the basement samples found throughout the Slave Province, but they are much more fractionated. From this evidence the Hickey Suite is interpreted to be the result of melting of CSBC rocks, which would provide the old zircon, possibly along with some younger, more juvenile material that would create the less negative values.

Ages of ca. 2600 Ma are not common in the southwestern Slave Province, but the Wecho River area suffered abundant plutonism at this time. Villeneuve and Henderson (1998) report a granodiorite gneiss from north of the Snare River area with xenocrystic zircon at 2605 Ma that may be correlative to the Hickey Suite.

Mafic enclaves were sampled from the Hickey Suite in order to determine whether they are a protolith to the granodiorite. To answer to this question, we must look to the Nd isotopic data. The Hickey Suite is highly unradiogenic, so the enclaves, if they are the protolith must also be unradiogenic. ε_{Nd}^{T} values for the enclaves range from -13.3 to -1.69 to +8.72, which is an extreme range and likely represents an open system. If the enclaves were the source for the Hickey Suite, they would have to be CSBC in age, because of the inherited zircon ages found within the Hickey suite. This is unlikely considering that some of the enclaves are layered, and more likely represent mafic volcanics such as Kam or Banting group equivalents. The massive amphibolite enclaves may be lower crustal rocks that underwent crustal contamination, but it is difficult to determine this because the ε_{Nd}^{T} values cannot be trusted. The enclaves are thus interpreted to be material assimilated into the Hickey magma during its formation and entrained as enclaves within the melt. Some mixing may have occurred between the granodiorite melts and the mafic rocks with more positive ε_{Nd}^{T} values creating the lower negative ε_{Nd}^{T} values.

7.4.5 Petrogenesis of the Mag Pluton

The Mag Pluton is dated at ca. 2599 Ma by U-Pb SHRIMP dating and includes inherited zircon ages of ca. 2625, 2642 and 2656 Ma. These ages are quite young for inherited ages compared to the other Wecho granitoids, and are likely representative of

plutonic and volcanic rather than sedimentary protolith ages. Specifically, the 2625 Ma corresponds to the Defeat Suite and the 2656 Ma age is representative of Banting age mafic rocks.

The geochemistry of the Mag Pluton is very similar to the Nardin Granodiorite, which is interpreted as a partial melt of a garnet amphibolite at high pressures (Figure 7-1A). The Mag Pluton may have a source consisting of buried Banting-age rocks, metamorphosed to a garnet amphibolite at high pressures, followed by partial melting creating the Defeat-like REE signatures.

7.5 Petrogenesis of the Group C Rocks

The Group C rocks are grouped together based on their high K_2O/Na_2O ratios, high Rb/Sr ratios, pronounced negative Eu anomalies, and high Th, all features of more evolved rocks. These geochemical characteristics are indicative of melts from the mid to upper crust as well as significant plagioclase fractionation that creates the negative Eu anomaly. These suites all show varying $\varepsilon_{Nd}{}^{T}$ values indicating differing sources for suites in different geographic locations. Also interpreted to be part of this group is the 'Dirty' Granite that was not sampled.

7.5.1 Petrogenesis of the Armi and Mosher Plutons

The Armi and Mosher Plutons are very similar in composition, and although the Mosher Granite was not dated it is likely genetically related to the Armi Suite. The Armi suite is dated at ca. 2600 Ma and has inherited zircons dated at ca. 2701 and 2720 Ma. These ages are roughly correlative with ages for the Kam mafic volcanics. This implies that the zircons may either be inherited from Kam age felsic volcanic rocks or from the numerous meta-sedimentary belts within the Wecho River area and surrounding terrains.

Geochemistry for these suites shows LREE enrichments and Nb and Ta depletions relative to Th, similar to the Yamba suite in the Contwoyto Lake area (Figure 7-1E). A HREE depletion is also present but the suites show only moderate fractionation, so the depletion is likely not the result of partial melting with a garnet residue. Instead the suite may be the result of mid-crustal melting of a mix of juvenile volcanic, plutonic, meta-sedimentary or basement rocks and their slightly metaluminous nature is likely the result of contribution by metaluminous plutons (White, 1986). This is also supported because melt production is maximized when there is 30-40% biotite in the protolith, so most metaluminous suites are too anhydrous to produce these weakly metaluminous rocks (Patino Douce and Johnston, 1991), indicating that contamination by a sedimentary source is required.

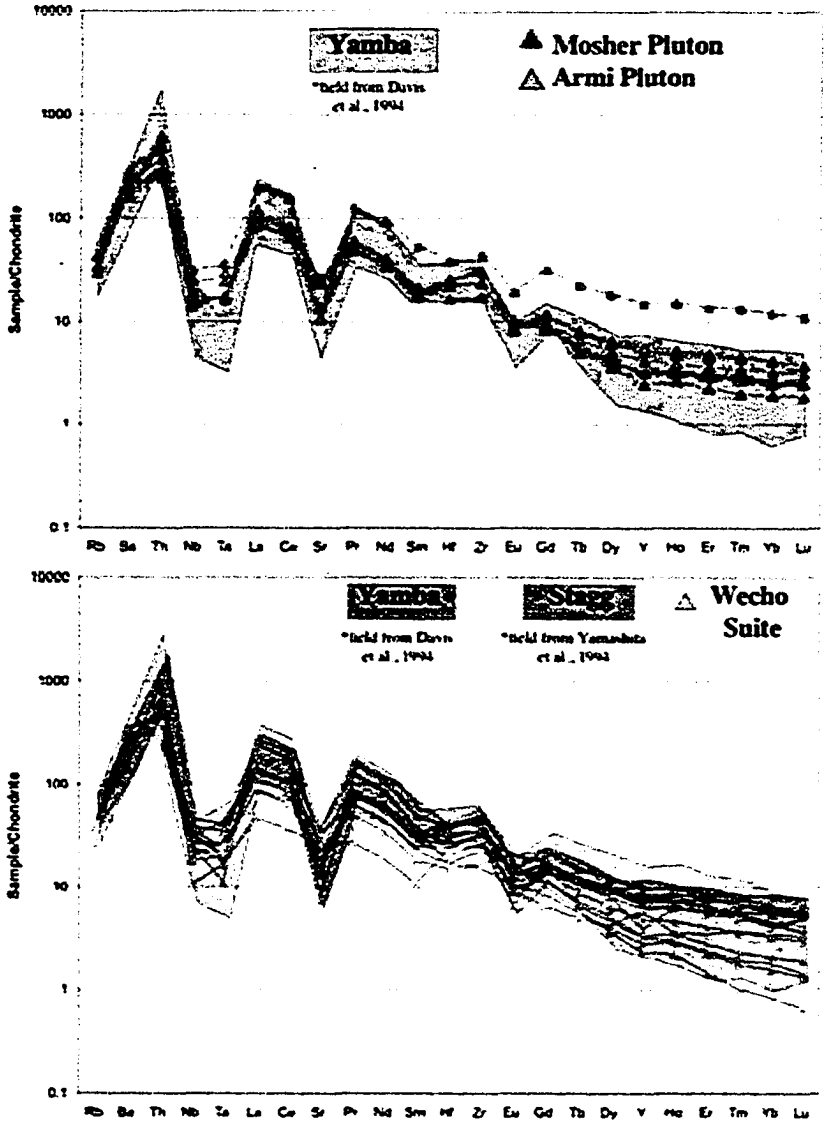

Figure 7-1 E and F. E. Extended rare earth element patterns comparing the Yamba, Mosher and Armi Suites. F. Extended rare earth element patterns comparing the Yamba, Stagg and Wecho Suites.

Further evidence for this is found in the Nd isotopic data. The Armi Suite has $\varepsilon_{Nd}{}^{T}$ values between -1.31 and +4.43 indicative of varying sources ranging from a source with a large component of ancient crustal mixing to very juvenile source rocks. To further support this hypothesis, Th/La ratios, which are indicative of crustal contamination, increase in the Armi Pluton, with decreasing $\varepsilon_{Nd}{}^{T}$ values, indicating that there is indeed crustal contamination of the pluton during petrogenesis and the values are not indicative only of their source. The extremely positive $\varepsilon_{Nd}{}^{T}$ value may be the result of an open system, because it has the highest, most juvenile values in the Wecho River area. The Mosher suite has $\varepsilon_{Nd}{}^{T}$ values between +0.16 to +1.82, more straightforward for a source of mixed origin. These values are likely the result of melting of granitoid and sedimentary sources creating a mixed REE pattern. Both suites show prominent negative Eu anomalies indicating that plagioclase was a major fractionating phase.

7.5.2 Petrogenesis of the Wecho Suite

The Wecho Suite has moderate fractionation, showing depletion in HREE relative to LREE. The Nb depletion relative to Th is indicative of a crustal source and the suite is very comparable in its geochemical characteristics to the Stagg and Yamba suites (Figure 7-1F) and in field characteristics to the megacrystic granite of the Snare River area. The Stagg suite is dated at 2583.5±1 Ma (Davis and Bleeker, 1999) and can be correlated from the Western Plutonic Complex to the Wecho River area. The megacrystic granite from the Snare River area and Ghost domains are dated at 2596±7.6 Ma (Bennett et al.,

2005) and 2598±2 Ma (Villeneuve and Henderson, 1998). These suites can be characterized based on their field relations, but a comparison of their REE patterns show that they are very different.

Inherited zircon for the Wecho Suite yield ages of 2684, 2634 and 2726 Ma. These ages are likely derived from sedimentary sources. The Wecho suite is interpreted to have the same origin as the Yamba suite, a mixture of sources ranging from meta-sedimentary to plutonic with varying Nd values, and like the Mosher and Armi Granodiorites, it is the result of contamination of metaluminous plutons by the meta-sediments (White et al., 1986). The $\varepsilon_{Nd}{}^{T}$ values for this suite show a variety of values from -0.33 to 0.35, which is the result of the source for the granite and not crustal contamination by CSBC rocks because there is no correlation between $\varepsilon_{Nd}{}^{T}$ values and Th/La ratios.

7.5.3 Petrogenesis of the Mofee Pluton

The Mofee Pluton is similar to many late granites across the Slave Province. It is a biotite muscovite granite that resembles the Contwoyto suite from the east-central part of the craton in geochemical characteristics (Figure 7-1G) and to the ca. 2596 Ma Prosperous suite (Davis and Bleeker, 1999) to the southeast of the Wecho River area in field relations. The Contwoyto suite has been compared to the Awry suite by previous authors, but neither the geochemistry nor field characteristics are compatible to the Mofee suite.

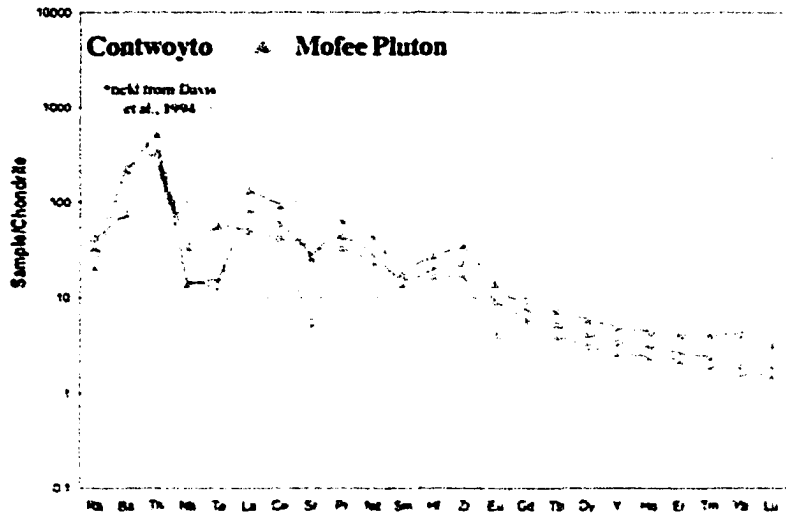

Figure 7-1. G. Extended rare earth element patterns comparing the Contwoyto and Mofee Suites.

The Mofee Suite has compositions similar to melt compositions of granitoids derived from meta-sedimentary rocks. These compositions can be derived by melting of greywackes or quartzofeldspathic rocks, fractional crystallization of less aluminous phases of calc-alkaline liquid and by vapor phase removal of alkalis from weakly metaluminous and weakly peraluminous granitoids (Miller, 1985). Melt fractions for peraluminous granites are maximized from protoliths with ~38% biotite, 32% quartz, 22% plagioclase and 8% aluminosilicate (Patino Douce and Johnston, 1991), which is roughly the same mineralogy as the abundant greywacke turbidites covering the Wecho River area. This suite is interpreted as a mid- to upper-crustal granite requiring a thermal anomaly in the crust during its formation to provide the heat to melt the meta-sediments and crystallize the granite.

$\varepsilon_{Nd}{}^{T}$ values for the Mofee granite range from -0.33 to 0.35, consistent with the values for meta-sedimentary rocks derived from mixed crustal origins. The $\varepsilon_{Nd}{}^{T}$ values determined for the Burwash sediments range between +1.7 to -4.4 (Yamashita and Creaser, 1999), making it likely that they are the source for the Mofee Pluton.

7.6 Petrogenesis of the Dauphinee Suite

The Dauphinee Suite is a unique group of plutonic rocks within the Wecho River area that make up only a small portion of the exposed bedrock. The plutonic group is an enderbite or an orthopyroxene-bearing tonalite that is only found in the northern,

granulite terrain of the Wecho River area. No other suite within the Slave is correlative to the Dauphinee Suite, although mafic granulites from the Snare River area that were originally thought to be comparable are distinctly different in geochemistry from the Dauphinee Pluton (Bennett et al, in press; Perks, 1997).

The rare earth element geochemistry has a unique pattern relative to the other Wecho granitoids, with a low degree of fractionation between heavy and light rare earth elements, a slight Sr depletion and slight depletion in Nb and Ta, but Th is also depleted. The $\varepsilon_{Nd}{}^{T}$ data shows values of +0.40 indicating melting of a juvenile source, but not a depleted upper mantle source. Instead, this suite is likely to be a cumulate rock resulting from a melt of granodiorite composition produced under granulite conditions. Cumulates are the result of crystallizing phases settling out of a melt, which in this case would largely produce a cumulate of plagioclase and amphibole, possibly with some pyroxenes. This would create the flat REE pattern, because the melt would partition the LREE. The macroscopic orthopyroxene and clinopyroxene found in the Dauphinee suite are likely to be metamorphic in origin, formed during the 2600-2580 Ma high temperature-low pressure granulite metamorphic event as the result of the breakdown of amphiboles (Winter, 2001).

7.7 A New Nd Isotopic Boundary in the Slave Province

Nd isotopic data for the intrusive rocks of the Wecho River area represent the missing link in the southwestern Slave craton. Values for these rocks range from

radiogenic for the westernmost magmas to highly unradiogenic for the Hickey suite and other plutons in the eastern part of the map area. The plutons in the middle of the Wecho River have intermediate ε_{Nd}^{T} values. Plutons with variations in their ε_{Nd}^{T} values do not show corresponding changes in their geochemical characteristics indicating that the isotopic variations reflect the granitoid protolith and are not the result of high-level differentiation processes. Some suites, like the Wecho and Mofee Plutons, are consistent with a source with a range of ε_{Nd}^{T} values, such as meta-sediments, that creates a range of values. The Armi Pluton, however, shows evidence for contamination by an increase in Th/La ratios with decreasing ε_{Nd}^{T} values.

Based on the distribution of Nd isotopic data for the plutonic rocks a boundary running roughly through the centre of the Wecho River area can be defined as the western extent of the Central Slave Basement Complex within the southwestern Slave Province (Figure 7-2). This is very similar to the situation that is found in the eastern portion of the craton where a previously defined Nd isotopic boundary is found (Davis et al., 1992). To the north, the isotopic boundary would extend around the Indin Lake Supracrustal belt and connect with the Acasta Gneiss Complex. To the south, the best estimate that can be made is that the boundary would run along the Yellowknife Greenstone Belt, where there are known CSBC exposures.

The oldest plutonic rocks that define this line are the ca. 2608 Ma diorite suites, with ε_{Nd}^{T} values of has +1.20 on the western side of the boundary and -1.67 on the

eastern side of the boundary. This means that the minimum age of a suture between the CSBC and the westernmost rocks must be greater than or equal to 2608 Ma.

7.8 Tectonic Evolution of the Wecho River Area

The Wecho River area was located along the ancient continental margin of the Slave craton at ca. 2608 Ma and represents an area of crust formation and stabilization of the craton. Putting together a tectonic model for this part of the craton is difficult for several reasons. This section will present ideas as to how the Wecho River area may have formed in correlation with the surrounding geologic terrains. A summary of the data for the Wecho River area is presented in a time versus event diagram (Figure 7-4) and a summary of key geochemical features and interpretations can be found in Table 7-1.

Prior to ca. 2900 Ma, CSBC was forming beneath the Wecho River area (Figure 7-3A). Due to the extreme negative $\varepsilon_{Nd}{}^{T}$ values yielded from the Nardin Gneiss, its petrogenesis is the result of melting from an older basement that would have formed from a juvenile mafic source as the protolith prior to 3.4 Ga. Significant time would have passed have in order to evolve the $\varepsilon_{Nd}{}^{T}$ values to more negative. This is important in that there had to have been a significant history within the southern CSBC prior to 3.4 Ga.

At ca. 3.2 to 2.9 Ga there is also evidence for further crustal growth in both the Nardin Complex as well as directly within the Wecho River area beneath the Hickey suite, evidenced from inherited zircons from the Hickey Suite.

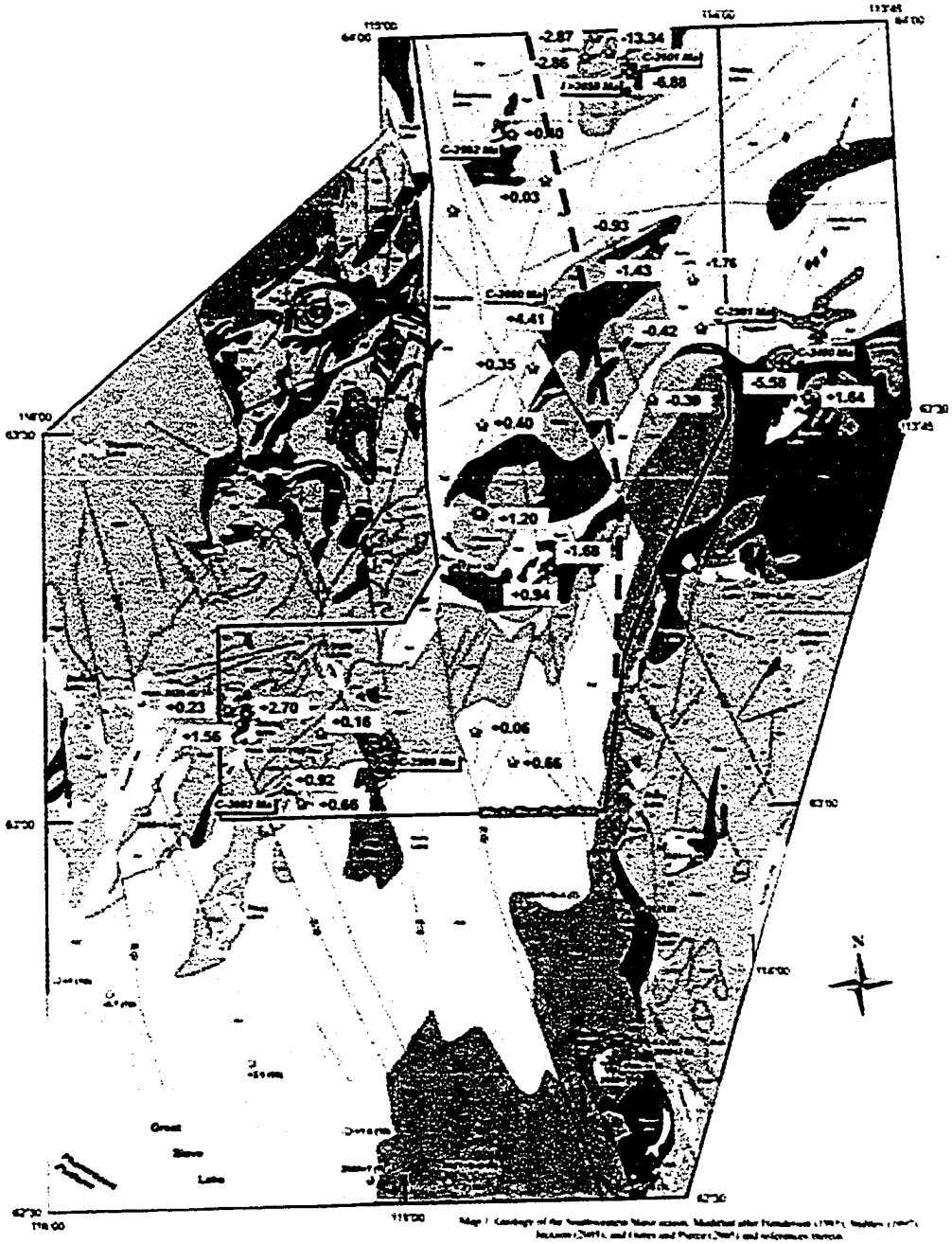

Figure 7-2. Map of the Southwestern Slave Province with the Wecho River area Nd data and Nd isotopic boundary plotted.

Following the end of formation of the basement, deposition of the CSCG on top of the CSBC took place and this sequence is found overlying the Nardin Gneiss. No evidence for CSCG rocks is present within the Wecho River area, although some of the inherited zircons from the Hickey Suite could be from the 2.9-2.8 Ga cover group.

Extensional Kam-type volcanism may also have taken place within the Wecho River area, or along its eastern margins. Although there are no exposures of rocks of Kam age, there are 2720 Ma zircon present within the granitoid suites as well as in the Mosher Lake meta-sedimentary rocks (Ootes et al., 2005). This indicates that although there was no Kam-like volcanism in the western part of the craton (also supported by Pehrsson and Villeneuve, 1999 and Bennnett et al., 2005), there is clearly a distal Kam age component in the meta-sediments or it is from a felsic source, which are less common at that time.

From ca. 2800 Ma until ca. 2660 Ma there is no recorded geologic history in the Wecho River area. To the west of the Wecho River area however, in the Indin Lake and Snare River areas there are ca. 2680 to 2629 Ma sequences that can be correlated from the Russell Lake area to the Grenville-Mesa area (Pehrsson and Villeneuve, 1999). Both areas include ca. 2680 Ma plutonic rocks, such as the Cotterhill gneiss from the Indin Lake area on which the supracrustal sequence lies (Pehrsson and Villeneuve, 1999), the 2650 Ma Hinscliffe complex (Villeneuve and Henderson, 1998), and ca. 2674 to 2654 Ma metaluminous plutonism in the Snare River area (Bennett et al., 2005). Supracrustal

Group	Suite	Rock Type	Age Ma	SiO2 wt.%	La/Sm	La/Yb	Nb/La	Metaluminous/ Peraluminous	K2O/Na2O	Rb/Sr	Epsilon NdT	Slave Equivalent	Interpretation
Basement	Nardin Gneiss	Granodiorite Gneiss	> 2900	71-73	8.7-9.6	55-71	0.03-1.5	Metaluminous	0.77-0.79	0.13-0.29	-7.4 to -5.88	CSBC	TTG
A	Germaine Lake Volcanics	Mafic Volcaniclastic	ca. 2650	49	1.1	1.3	0.66	N/A	0.08	0.06	0.94	Banting Volcanics	Extesional Volcanism
	Mosher Lake Volcanics	Sheered Basalt	ca. 2650	48	1.0-1.1	1.1-1.3	0.65-0.75	N/A	0.09-0.21	0.04-0.09	2.7 to +1.56	Banting Volcanics	Extensional Volcanism
B	Nardin Grdt	Bt-Mag Grdt	ca 2625	71-73	7.6-8.7	26.8-59.7	0.12-0.15	Metaluminous	0.55-0.84	0.21-0.37	0.36	Defeat	Melt of Juvenile Garnet-Amphibolite Lower Crust
	Diorite Suites	Qtz-Diorite to Qtz Monzodiorite	ca 2608	51-55	2.5-3.0	17.0-17.5	0.15	Metaluminous	0.42-0.43	0.08	-1.68 to 1.20	Concession	Sanukatoid
	South	Hbl-Mag-Grdt	ca. 2602	62	3.7	18.8	0.23	Metaluminous	0.54	0.12	0.92	no correlative	Partial Melt of Diorite Composition
	Hickey	Bt-Mag Grdt	ca 2601	69-73	2.4-11.8	72-116	0.02-0.1	Metaluminous	0.75	0.08-0.19	-1.31	no correlative	Melt of TTG basement Rocks
	Mag	Mag-	ca 2599	71	8	41.1	0.1	Metaluminous	0.8	0.34		no correlative	Melt of Juvenile Garnet-Amphibolite Lower Crust/Defeat

Group	Suite	Rock Type	Age Ma	SiO2 wt.%	La/Sm	La/Yb	Nb/La	Metaluminous/ Peraluminous	K2O/Na2O	Rb/Sr	Epsilon NdT	Slave Equivalent	Interpretation
C	Mosher	Bt-Granite	ca. 2600	68-71	3.8-5.6	16.8-41.7	0.14-0.17	Peraluminous	0.74-1.12	0.35-1.10	0.16 to 1.82	Yamba	Mixed Juvenile and Crustal Sources
	Armi	Bt-Grdt	ca. 2600	70-72	4.3-6.4	21.4-62.9	0.14-0.24	Peraluminous	0.68-1.44	0.37-1.38	-1.43 to 4.41	Yamba	Mixed Juvenile and Crustal Sources
	Wecho	K-spar Porph Granite	ca. 2591	66-73	3.5-5.4	13.7-59.3	0.10-0.33	Peraluminous	0.73-2.00	0.29-1.01	-1.76 to 0.85	Stagg/Yamba	Partial Melt of Meta-sediments and Juvenile Sources
	Mofee	Bt-Musc Granite	ca. 2591	72-74	3.3-7.4	12.1-69.0	0.11-0.65	Peraluminous	0.53-1.50	0.24-3.65	-0.33 to 0.35	Contwoyto/	Partial Melt of Greywacke Turbites
D	Dauphinee	Enderbite	ca. 2592	53	2.5	8.4	0.34	Metaluminous	0.29	0.08	0.4	no correlatives	Cumulate

Table 7-1. Summary of distinguishing geochemical features and interpretations for the rock suites.

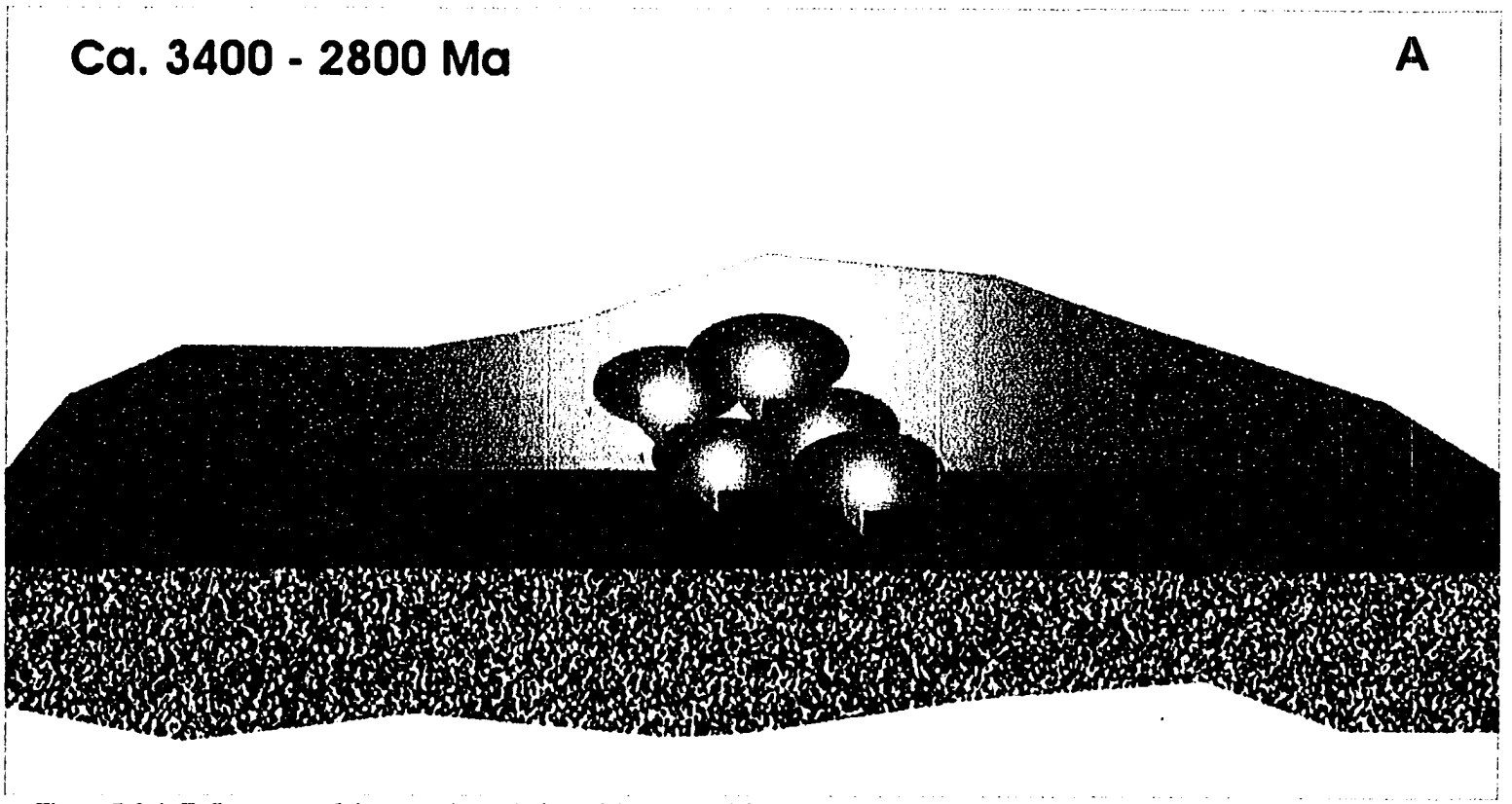

Figure 7-3 A-E. Summary of the tectonic evolution of the Wecho River area in cross-section. A. TTG plutonism creating the Central Slave Basement Complex from mafic juvenile lower crust, with further re-melting of the TTG crust.

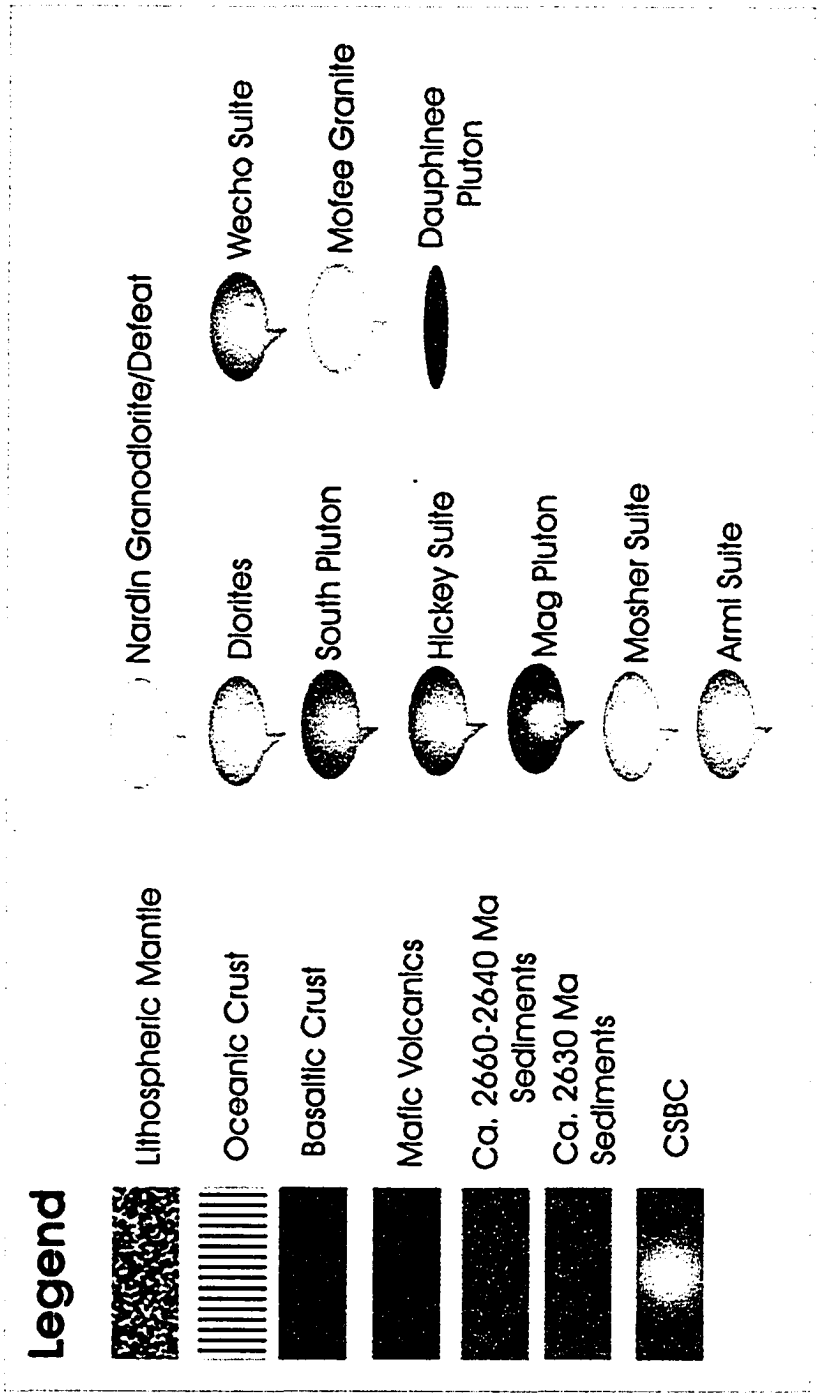

rocks in the Indin Lake area include > 2670 Ma mafic tholeiites, and overlying >2668 Ma mafic, intermediate and felsic volcanic rocks (Pehrrson and Villeneuve, 2005), similar in age to felsic volcanism in the Snare River area (Bennett et al., 2005). The Indin Lake supracrustal belt, as well as the Snare River are have both been proposed to resemble the tectonic setting of the northeastern Slave Province, i.e., terrains accreted to the CSBC.

From ca. 2660 to 2640 Ma sediments were deposited in the Wecho River area equivalent in age to Burwash formation sedimentation (Ootes et al., 2005). This is also the time of Banting type-volcanism in the Slave Province, which is interpreted as a time of waning extension within the southwestern part of the craton (Cousens, 2002). At this time, the Germaine and Mosher Lake volcanics were deposited and the Wecho River area became an area dominated by sediments and mafic volcanic rocks (Figure 7-3B).

Ca. 2660 to 2630 Ma represents the D1 deformation. Late in this deformation event the Defeat Suite and its correlative suites, the Nardin Granodiorite and the Disco Intrusive Suite, were emplaced in the lower crust. This plutonism was widespread across the southwestern Slave Province and likely represents a time at which the Snare and Indin terrains were joined with the Wecho terrain (Figure 7-3C). This implies that at ca. 2630 Ma, or before the onset of Defeat Suite plutonism, collision between a juvenile terrain and the CSBC must have occurred. Thus, the 2680-2630 Ma stratigraphy in the Snare and Indin areas that is not present within the Wecho River domain is likely a juvenile terrain accreted onto the CSBC prior to the end of the D1 deformation or prior to

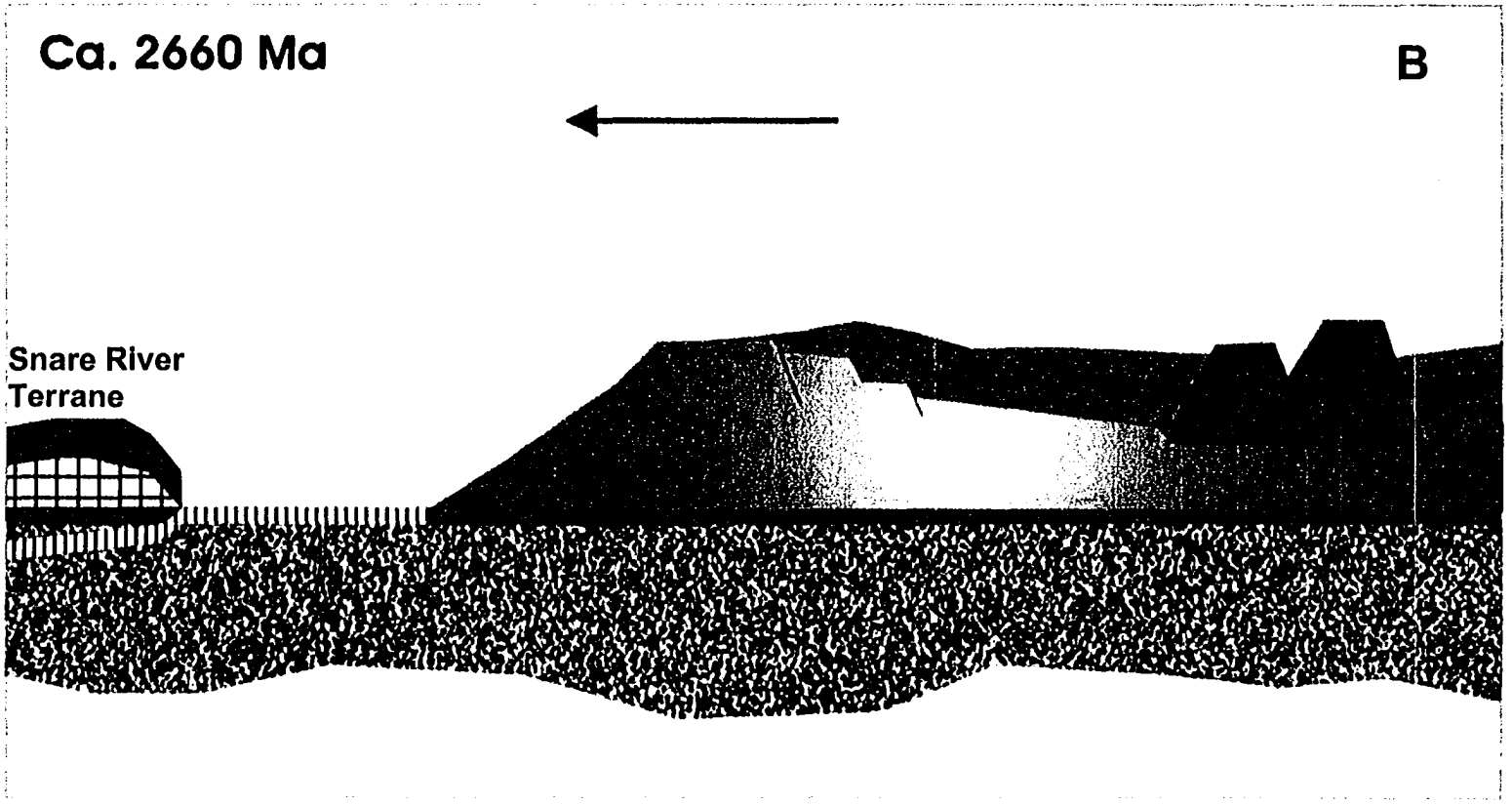

B. Ca. 2650 Ma waning crustal extension causing Banting-type volcanism as well as sedimentation. Also the possible onset of westward subduction beneath the Snare terrain.

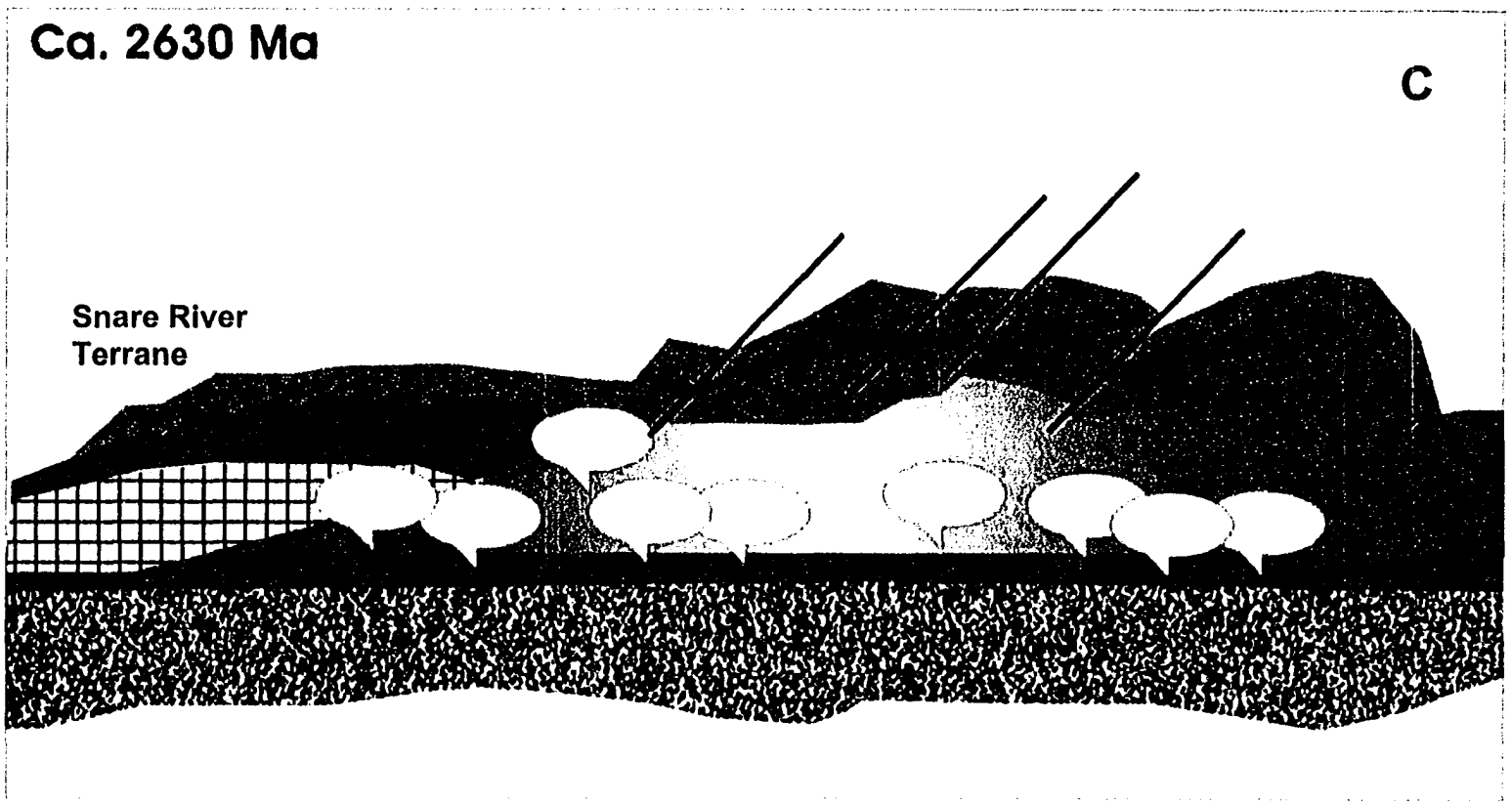

C. The end of D1 deformation (crustal compression), depostion of the ca. 2630 Ma sediments and Nardin granodiorite plutonism. Accretion of the Snare terrain is interpreted to have occurred prior to this time.

the onset of the Defeat plutonism. Accretion of this terrain to the CSBC was likely due to westward dipping subduction because there is no recorded magmatism beneath the Wecho River area prior to 2630 Ma.

A hiatus from ca. 2635 Ma to 2608 Ma occurred in the Wecho terrain but at ca. 2630 Ma sedimentation occurred on the western side of the craton at Russell Lake and Indin Lake. At ca. 2608 Ma the sanukitoid-like diorites are formed that are similar to the Concession suite in the east-central part of the craton (Davis et al., 1994) as well as the quartz diorites present in the Snare River area (Bennett et al., submitted). At this time, from 2608 to 2600 Ma, there is extensive metaluminous plutonism, likely the result of underplating, which initiated lower crustal melting (Figure 7-3D). This may have occurred due to the delamination of a dense ultramafic or eclogitic layer at the base of the crust that had been building since the formation of the Defeat Suite plutonism. It may also have been aided by the hypothesis that the mantle may have been partially molten at the time due to the higher geothermal gradient in the Archean. At ca. 2602 Ma melting of a sanukitoid composition forms the South Pluton, and 2600 Ma brings the melting of basement rocks forming the Hickey suite. Melting of a mixture of meta-sediments and metaluminous plutons caused the formation of the Armi and Mosher Suites. At ca. 2599 Ma the Mag Pluton formed in the lower crust as either a melt of the lower crust or melting of a mixture of lower crust and Defeat-like plutons.

Bennett et al. (2005) suggest that arc-continent collision occurred at the end of metaluminous plutonism responsible for the ca. 2600 Ma 'syn-collisional' magmas. This

is unlikely because the collision had to have occurred prior to 2608 Ma because this is the oldest rock type that shows evidence for contamination.

Following metaluminous plutonism there is a shift to peraluminous plutonism across the entire craton, with equivalent plutonic suites extending from the southern, central and northeastern parts of the craton that act to stitch the entire province, and likely hide the >2608 Ma suture. This could indicate a cratonic event such as delamination, providing the heat to produce the HT-LP peak metamorphic conditions and the Wecho, Stagg, Mofee and Prosperous Plutonism (Figure 7-3E). Is it possible, though, that delamination could be widespread, across the entire Slave craton? And how does the crust compensate for that amount of granitoid being emplaced? Creating space for these plutons could be accommodated by the crustal rebound after delamination, causing expansion and making room for the plutons. An example of this situation is found in the Sierra Nevada batholith, where the rebounding crust following delamination caused enough crustal expansion for plutons to be emplaced (Ducea and Saleeby, 1998).

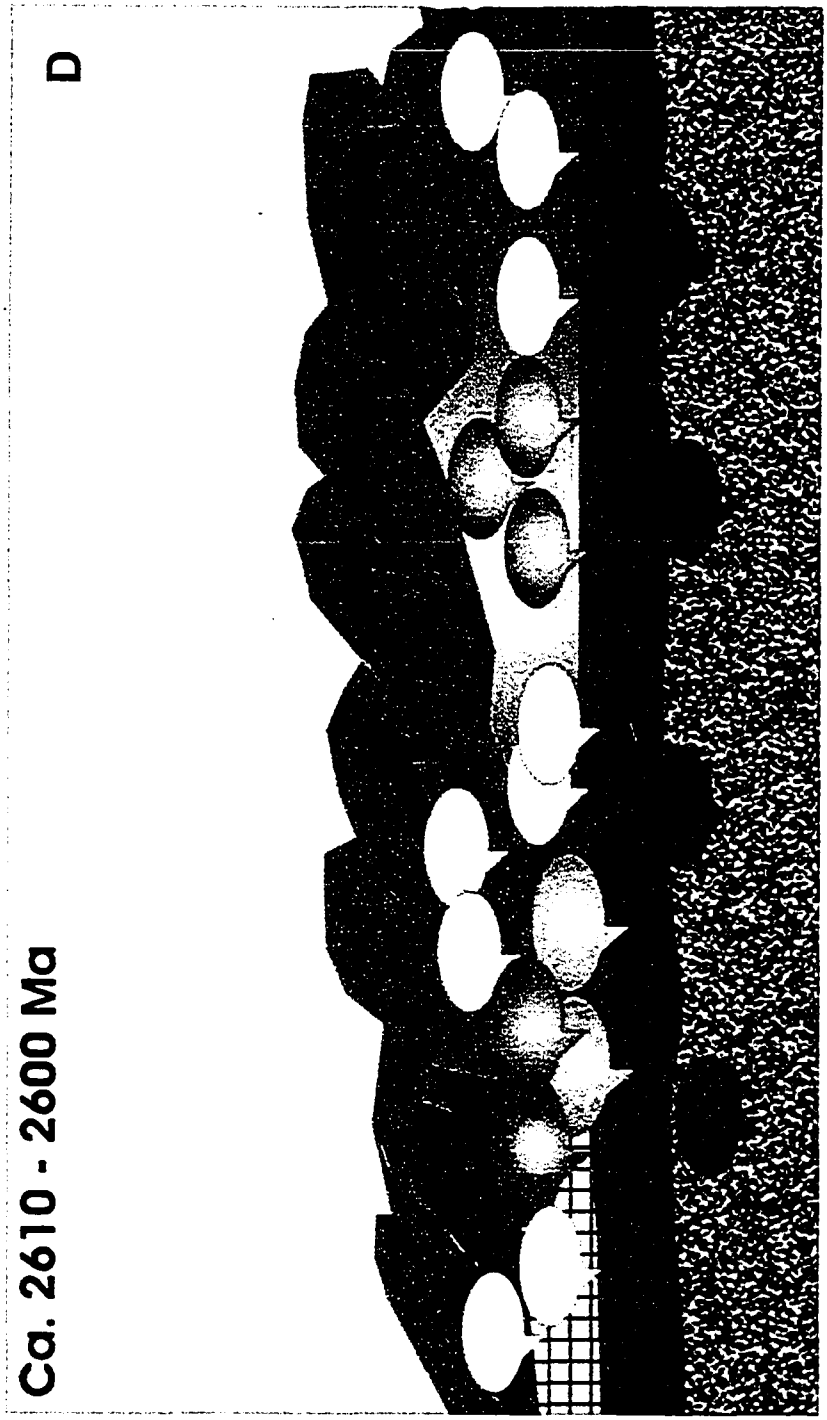

D. Underplating of the crust promoting metaluminous lower to mid-crustal plutonism and D2 deformation (crustal compression).

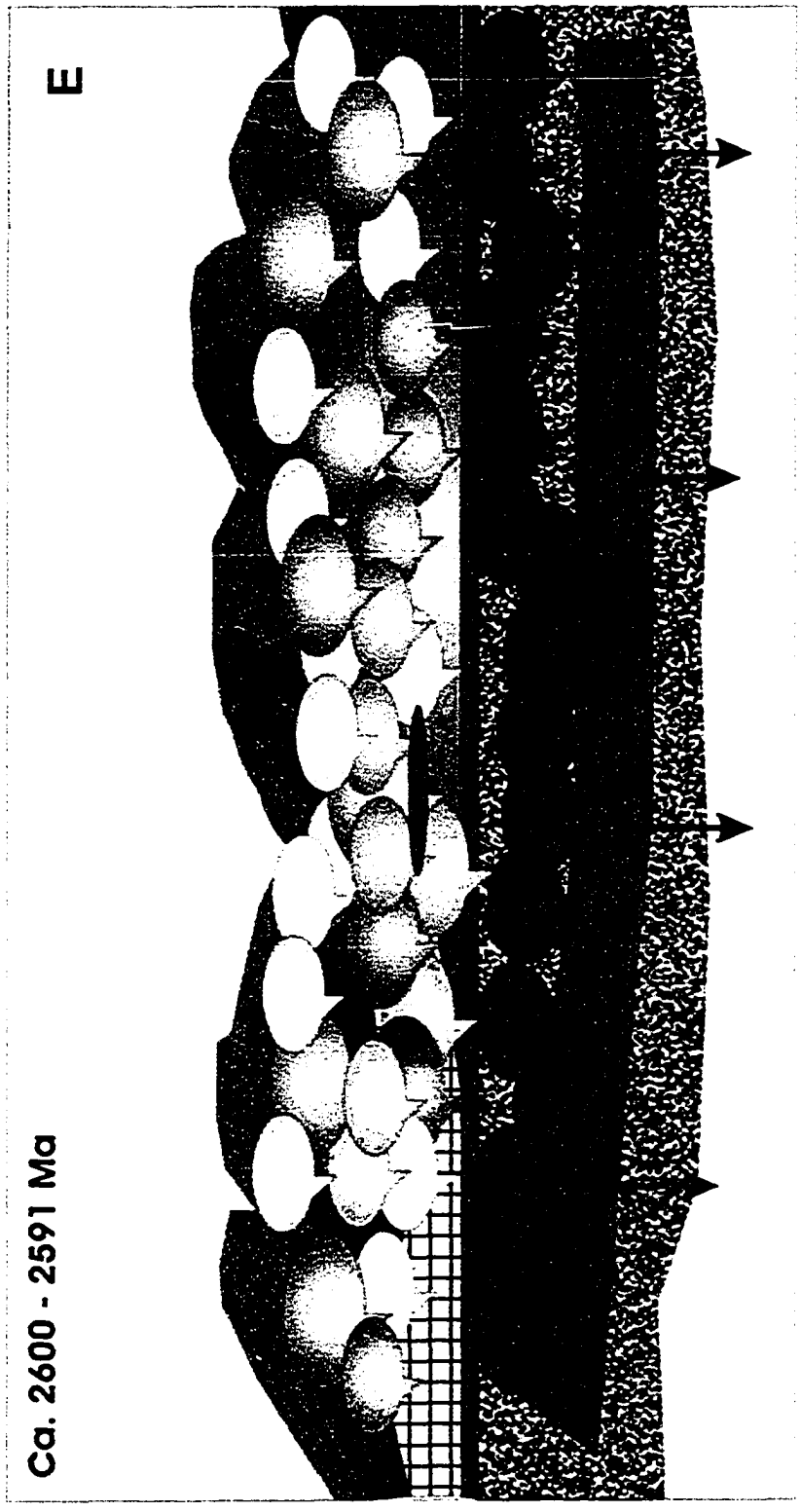

E. Delamination of underplate causing decompression melting and the onset of peraluminous mid- to upper crustal plutonism as well as HT-LP metamorphism.

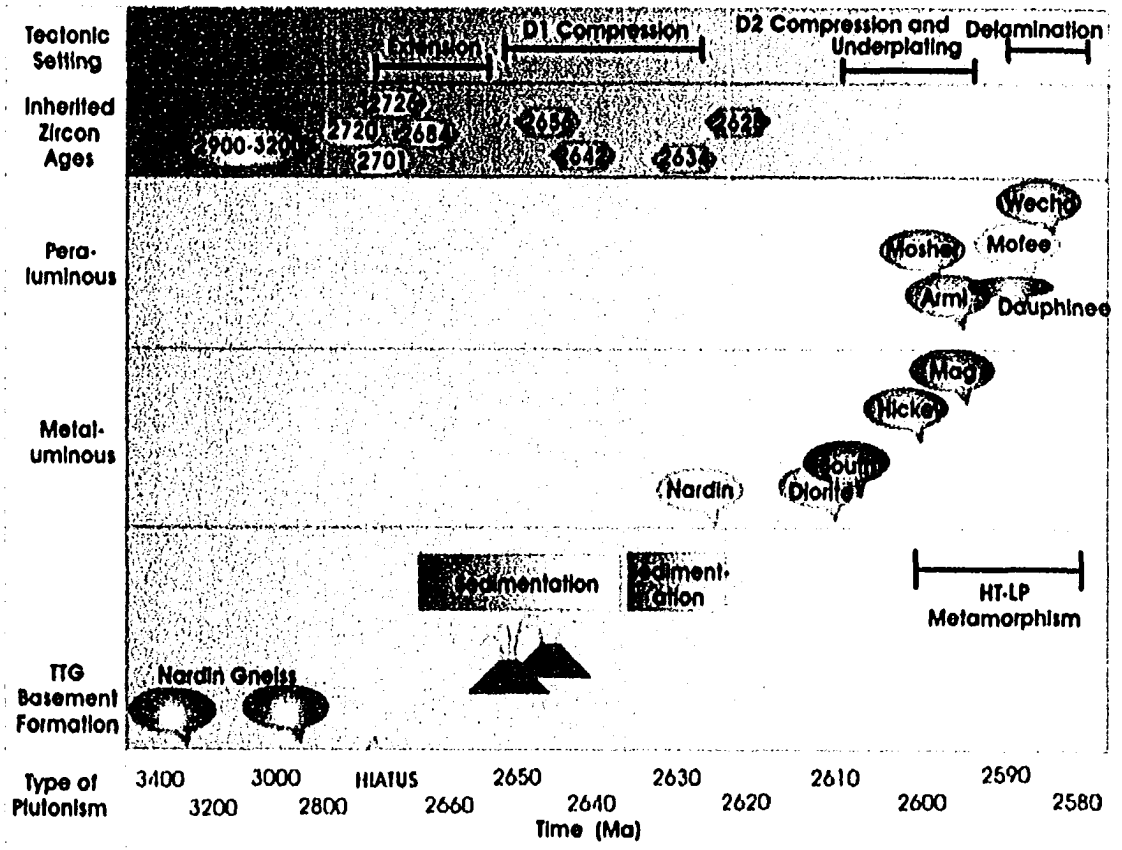

Figure 7-4. Time vs. event diagram summarizing the geologic history of the Wecho River area.

Chapter 8: Conclusions

The Wecho River area is a terrain dominated by plutonic rocks with minor occurrences of meta-sedimentary and volcanic rocks. Plutonism recorded in the Wecho River area is separated into 3 stages: formation of >2.8 Ga CSBC, a ca. 2608 to 2600 Ma metaluminous stage and a 2600 to 2591 Ma peraluminous stage. CSBC beneath the Wecho River area, and directly outboard of it, is composed of TTG plutons. These plutons are highly contaminated indicating that they formed a significant amount of time after the first crustal extraction occurred from a juvenile source, indicating that there was crust formation and growth prior to the 3.4 Ga crystallization of the Nardin Gneiss. The metaluminous plutonism is the result of underplating of the continental crust, which initiated melting of the lower crust. The peraluminous granitoids were formed by anatexis of meta-sedimentary, plutonic and volcanic rocks as a result of delamination of the thickened lower crust, creating a thermal anomaly. These hypotheses are supported by geochemical, geochronological and Nd isotopic data.

The Wecho River area is also extremely important in the formation of the Slave Province. Nd isotopic data defines the edge of the CSBC at ca. 2608 Ma, interpreted to be the edge of a continental margin. This is the minimum age for a suture between the Wecho and Snare terrains, which is not seen due to the voluminous plutonism between 2608 and 2591 Ma. It is likely however that the suture is significantly older, because the ca. 2630 Ma Defeat Suite plutons can be found across the entire southern and southwestern portion of the craton and on both sides of the proposed suture.

The Wecho River area lithologies are not unique to the Slave Province. It is a terrain with plutonism, volcanic activity and sedimentation that is coeval across the south-central and entire craton. The unique part of the area is its Nd isotopic boundary, marking the suture between the westernmost and central parts of the craton. After 2608 Ma, the Wecho River area is a domain involved only in plutonism leading to the stabilization of the craton.

REFERENCES

Bennett, V., Rivers, T., Relf, C., Jackson, V.A and Brannstrom, M. Formation, growth and evolution of Neoarchean crust: geochemical and isotopic constraints from the Snare River terrane, Slave Province, Canada. Journal of Petrology, *submitted.*

Bennett, V., Jackson, V.A., Rivers, T., Relf, C., Horan, P., Tubrett, M., 2005. Geology and U-Pb geochronology of the Neoarchean Snare River terrane: tracking evolving tectonic regimes and crustal growth mechanisms. Canadian Journal of Earth Sciences, 42: 895-934.

Bethune, K.M. and Carmichael, H.D., 1998. Metamorphism along the Slave portion of the SNORCLE transect. In Lithoprobe Slave-Northern Cordillera Lithospheric Evolution (SNORCLE) and Cordilleran Tectonics Workshop Meeting, March 6-8, 1998, Simon Fraser University, Vancouver, B.C. Compiled by F. Cook and P. Erdmer, Lithoprobe Report 64, pp. 17-24.

Bleeker, W., Ketchum, J.W.F., Jackson, V.A., and Villeneuve, M.E., 1999a. The Central Slave Basement, Part I: its structural topology and autochthonous cover. Canadian Journal of Earth Sciences, 36: 1083-1109.

Bleeker, W., Ketchum, J,W,F., and Davis, W.J., 1999b. The Central Slave Basement Complex, Part II: age and tectonic significance of high-strain zones along the basement-cover contact. Canadian Journal of Earth Science, 36: 1111-1136.

Brophy, J. 1992. Geology and gold showings, Wheeler Lake basin, NTS 85O/7; Indian and Northern Affairs Canada, NWT Geology Division, EGS 1992-06, 1 map, scale 1:20,000.

Bowring, S.A. and Williams, I.S. 1999. Priscoan (4.00-4.03 Ga) orthogneisses from northwestern Canada. Contributions to Mineralogy and Petrology, 134: 3-16.

Cairns, S., Relf, C., MacLachlan, K. and Davis, W.J., 2005. Neoarchean decoupling of upper- and mid-crustal tectonothermal domains in the southeast Slave Province: evidence from the Walmsley Lake area. Canadian Journal of Earth Sciences, 42: 869-894.

Chappell, B.W. and White, A.J.R., 1974. Two contrasting granite types. Pacific Geology, 8: 173-174.

Corfu, F., Hanchar, J.M., Hoskin, P.W.O., Kinny, P., 2003. Atlas of zircon textures. Reviews in Mineralogy and Geochemistry, 53: 469-500.

Cousens, B.L., 2000. Geochemistry of the Archean Kam Group, Yellowknife greenstone belt, Slave Province, Canada. Journal of Geology, 108: 181-197.

Cousens, B.L., Facey, K. and Falck, H., 2002. Geochemistry of the late Archean Banting Group, Yellowknife greenstone belt, Slave Province, Canada: simultaneous melting of the upper mantle and juvenile mafic crust. Canadian Journal of Earth Sciences, 39: 1635-1656.

Cousens, B.L., Falck, H., Ootes, L., Jackson, V., Mueller, W., Corcoran, P., Finnigan, C., Alcazar, A., 2005. Regional correlations, tectonic settings, and stratigraphic solutions in the Yellowknife greenstone belt and adjacent areas from geochemical and Sm-Nd isotopic analyses of volcanic and plutonic rocks. Chapter 9 *in* Gold in the Yellowknife Greenstone Belt, Northwest Territories: Results of the EXTECH III Multidisciplinary Research Project, (ed.) C.D Anglin, H. Falck, D.F. Wright and E.J Ambrose; Geological Association of Canada, Mineral Deposit Division, Special Paper.

Davis, W.J. and Bleeker, W., 1999. Timing of plutonism, deformation and metamorphism in the Yellowknife Domain, Slave Province, Canada. Canadian Journal of Earth Sciences, 36: 1169-1187.

Davis, W.J., Fryer, B.J. and King, J.E., 1994. Geochemistry of Late Archean plutonism and its significance to the tectonic development of the Slave craton. Precambrian Research, 67: 207-241.

Davis, W.J., Gariepy, C., van Breeman, O., 1996. Pb isotopic composition of late Archaean granites and the extent of recycling early Archaean crust in the Slave Province, northwest Canada. Chemical Geology, 130: 255-269.

Davis, W.J. and Hegner, E., 1992. Neodymium isotopic evidence for the tectonic assembly of Late Archean crust in the Slave Province, northwest Canada. Contributions to Mineralogy and Petrology, 111: 493-504.

DePaulo, D.J., 1988. Neodymium Isotope Geochemistry: an Introduction. Springer-Verlag, 187 p.

Ducea, M., and Saleeby, J. 1998. A case for delamination of the deep batholithic crust beneath the Sierra Nevada, California. International Geology Review, 40: 1998.

Dudas, F.O., Henderson, J.B. and Mortensen, J.K., 1990. U-Pb ages of zircons from the Anton Complex, southern Slave Province, Northwest Territories. *In* Radiogenic Age and Isotopic Studies: Report 3, Geological Survey of Canada, Paper 89-2, p.39-44.

Heaman, L., and Parrish, R. 1991. U-Pb geochronology of accessory minerals; in Short Course Handbook on Applications of Radiogenic Isotope Systematics to Problems in Geology, Mineral Association of Canada, 19: 59-102.

Henderson, J.B., 1975. Sedimentology of the Archean Yellowknife Supergroup at Yellowknife, District of Mackenzie. Geological Survey of Canada Bulletin, 246, 62.

Henderson, J.B. 1985. Geology of the Yellowknife-Hearne Lake area, District of Mackenzie: a segment across an Archean basin; Geological Survey of Canada, Memoir 414, 135 p.

Henderson, J.B., van Breeman, O. and Loveridge, W.D., 1987. Some U-Pb ages from Archean basement, supracrustal and intrusive rocks, Yellowknife-Hearne area, District of Mackenzie. In Radiogenic Age and Isotopic Studies: Report 1, Geological Survey of Canada, Paper 87-2, p. 111-121.

Hoffman, P.F., 1989. Precambrian Geology and tectonic history of North America. *In* The Geology of North America Vol. A. The Geology of North America – An overview. The Geological Society of America, 65 p.

Isachson, C.E., 1992. U-Pb zircon geochronology of the Yellowknife volcanic belt and subadjacent rocks, N.W.T., Canada: constraints on the timing, duration, and mechanics of greenstone belt formation. Unpub. Ph.D. thesis, Washington University, 164 p.

Isachson, C.E. and Bowring, S.A., 1994. Evolution of the Slave Craton. Geology, 22: 917-920.

Jackson, V.A., 2003. Preliminary compilation of the Snare River (1998-2002 results), Wijinnedi Lake, Labrish Lake and Russell Lake area; parts of 85N and 85O. C.S. Lord Northern Geoscience Centre, Yellowknife, NT. NWT Open Report, 2003-002, 1 map, scale 1:100,000.

Ketchum, J.W.F., Bleeker, W. and Stern, R.A., 2004. Evolution of an Archean basement complex and its allochthonous cover, southern Slave Province, Canada. Precambrian Research, 135: 149-176.

Kleinhanns, I.C., Kramers, J.D., and Kamber, B.S. 2003. Importance of water for Archaean granitoid petrology: a comparative study of TTG and potassic granitoids from Barberton Mountain Lane, South Africa. Contributions to Mineralogy and Petrology, 145: 377-389.

Kusky, T.M. 1989. Accretion of the Archean Slave Province. Geology, 17: 63-67.

LeMaitre, R.W. (editor), 1989. A classification of igneous rocks and glossary of terms. Blackwell Oxford, 193p.

Ludwig, K.R., 2003. User's manual for Isoplot/Ex rev. 3.00: a geochronological toolkit for Microsoft Excel. Berkeley Geochronology Centre, Berkeley, California, Special Publication, 4, 70p.

Martin, H., and Moyen, J-F. 2002. Secular changes in tonalite-trondhjemite-granodiorite composition as markers of the progressive cooling crust. Geology, 30: 319-322.

Miller, C.F. 1985. Are strongly peraluminous magmas derived from pelitic sedimentary sources? Journal of Geology, 93: 673-689.

Miller, C.F., Watson, E.B., and Harrison, T.M. 1988. Perspectives on the source, segregation and transport of granitoid magmas. Transactions of the Royal Society of Edinburgh: Earth Sciences, 79, 135-156.

Ootes, L., Buse, S., Davis, W.J. and Cousens, B., 2005. U-Pb ages from the northern Wecho River area, southwestern Slave Province, Northwest Territories: constraints on late Archean plutonism and metamorphism. Geological Survey of Canada, Current Research-F2, 13p.

Ootes, L., Davis, W.J., and Jackson, V.A. *in review.* Two turbidite sequences in the Russell-Mosher lakes area: SHRIMP U-Pb detrital zircon evidence and correlation with gold-associated iron formation in the southwestern Slave craton, Northwest Territories.

Ootes, L. and Pierce, K. 2005. A GIS digital atlas of the Wecho River area; Northwest Territories Geoscience Office, NWT Open File 2005-003. Digital Files and 1 map, scale 1:125,000.

Parrish, R.R., Roddick, J.C., Loveridge, W.D., and Sullivan, R.W., 1987. Uranium-Pb analytical techniques at the geochronology laboratory, Geological Survey of Canada. Geological Survey of Canada, Paper 87-2, p. 3-7.

Patino-Douce, A.E., and Johnston, A.D. 1991. Phase Equilibria and melt productivity in the pelitic system: implications for the origin of peraluminous granitoids and aluminous granulites. Contributions to Mineralogy and Petrology, 107: 202-218.

Perks, M.A. 1997. The mid crust of the western Slave Province – geological mapping, geochemistry and U-Pb geochronology of the Fork Lake area, southwestern Slave Province, N.W.T.. M.Sc. thesis, University of Alberta, Edmonton, Alta.

Pidgeon, R.T., Nemchin, A.A., Hitchen, G.J. 1999. Internal Structures of zircons from Archaean granites from the Darling Range batholith: implications for zircon stability and the interpretation of zircon U-Pb ages. Contributions to Mineralogy and Petrology, 132: 288-299.

Pehrsson, S.J. and Villeneuve, M.E. 1999. Deposition and Imbrication of a 2670-2629 Ma supracrustal sequence in the Indin Lake area, southwestern Slave Province, Canada. Canadian Journal of Earth Sciences, 36: 1149-1168.

Relf, C., Sandeman, H.A. and Villeneuve, M.E. 1999. Tectonic and thermal history of the Anialik River area, northwestern Slave Province, Canada. Canadian Journal of Earth Sciences, 36: 1207-1226.

Roddick, J.C., Loveridge, W.D., and Parrish, R.R. 1987. Precise U-Pb dating of zircon at the sub-nanogram Pb level. Chemical Geology, 66: 111-121.

Rollinson, H.R. 1993. Using Geochemical Data: evaluation, presentation, interpretation. Longman Scientific and Technical, John Wiley and Sons, 352 p.

Smithies, R.H., and Champion, D.C. 2000. The Archaean High-Mg diorite suite: Links to tonalite-trondhjemite-granodiorite magmatism and implications for Early Archaean crustal growth. Journal of Petrology, 12: 1653-1671.

Stern, R.A. 1997. The GSC Sensitive High Resolution Ion Microprobe (SHRIMP): analytical techniques of zircon U-Th-Pb determinations and performance evaluation. Geological Survey of Canada, Current Research 1997-F, p. 1-31.

Stern, R.A., and Amelin, Y. 2003. Assessment of errors in SIMS zircons U-Pb geochronology using a natural zircon standard and NIST SRM 610 glass. Chemical Geology, 197: 111-146.

Stern,R.A, Hanson, G.N., and Shirey, S.B. 1989. Petrogenesis of mantle-derived, LILE-enriched Archean monzodiorites and trachyandesties (sanukitoids) in southwestern Superior Province. Canadian Journal of Earth Science, 26: 1688-1712

Stern, R.A., and Hanson, G.N., 1991. Archean high Mg granodiorite: a derivative of light rare earth element-enriched monzodiorite of mantle origin. Journal of Petrology, 32: 201-238.

Streckheisen, A.L. 1976. To each plutonic rock its proper name. Earth Science Reviews, 12: 1-33.

Stubley, M.P. 1997. Geological Compilation of the Carp Lake area; NTS 85P and southeastern 85O; Indian and Northern Affairs Canada, NWT Geology Division, EGS 1997-07, 1 map, scale 1:250,000.

Sun, S. and McDonough, W.F. 1989. Chemical and isotopic systematics of oceanic basalts: implications for mantle compositions and processes. Magmatism in the oceanic basins. Geological Society Special Publication 42: 313-345.

Taylor, S.R. and McLennan, S.M. 1985. The Continental Crust: Its Composition and Evolution. Blackwell Oxford.

Thorpe, R.I., Cumming, G.L. and Mortensen, J.K. 1992. A significant Pb isotope boundary in the Slave Province and its probable relation to ancient basement in the western Slave Province. In: Project Summaries, Canada – Northwest Territories Mineral Development Agreement 1987 – 91. Geological Survey of Canada, Open File Report no. 2484: 179-184.

van Breeman, O., Davis, W.J. and King, J.E. 1992. Temporal distribution of granitoid plutonic rocks in the Archean Slave Province, northwest Canadian Shield. Canadian Journal of Earth Sciences, 29: 2186-2199.

Villeneuve, M.E. and Henderson, J.B. 1998. U-Pb geochronology of Wijinnedi Lake area, Slave Province, District of Mackenzie, Northwest Territories. *In* Radiogenic Age and Isotopic Studies: Repost 11; Geological Survey of Canada, Current Research 1998-F, p. 99-106.

White, A.J.R., Clemens, J.D., Holloway, J.R., Silver, L.T., Chappell, B.W., Wall, V.J. 1986. S-types granites and their probable absence in southwestern North America. Geology, 14: 115-118.

Winter, J.D. 2001. An introduction to igneous and metamorphic petrology. Prentice-Hall Inc.

Yamashita, K. and Creaser, R.A. 1999. Geochemical and Nd isotopic constraints for the origin of Late Archean turbidites from the Yellowknife area, Northwest Territories, Canada. Geochimica et Cosmochimica Acta, 63: 2579-2598.

Yamashita, Y., Creaser, R.A., Jensen, J.E., Heaman, L.M. 2000. Origin and evolution of mid- to late-Archean crust in the Hanikahimajuk Lake area, Slave Province, Canada; evidence from U-Pb geochronological, geochemical and Nd-Pb isotopic data.

Yamashita, K., Creaser, R.A., Stemler, J.U. and Zimaro, T.W. 1999. Geochemical and Nd-Pb isotopic systematics of late Archean granitoids, southwestern Slave Province, Canada: constraints for granitoid origin and crustal isotopic structure. Canadian Journal of Earth Sciences, 36: 1131-1147.

Yardley, D.H. 1949. Preliminary map: Wecho River (east half), Northwest Territories; Geological Survey of Canada, Paper 49-14, 1 map, scale 1 inch: 2miles.

York, D. 1969. Least squares fitting of a straight line with correlated errors. Earth and Planetary Science Letters, 5: 320-324.

Zegers, T.E., and van Keken, P.E. 2001. Middle Archean continent formation by crustal delamination. Geology, 29: 1083-1086.

APPENDICES

Appendix A: Field Logistics and Previous Work

A1. Field Logistics

Field mapping was conducted as part of the Wecho River area mapping initiative through the Northwest Territories Geoscience Office. The project took place during the 2003 and 2004 field seasons with emphasis on the northern portion of the map area (NTS 850/9, 10, 15, 16) in 2003 and the southern portion (NTS 850/2, 3, 7 and parts of 85O/1 and 2) in 2004. Each year a four man crew was employed, led by Luke Ootes, and a remote camp was set up on islands or lakeshores of large lakes or river systems in order to maximize the amount of coverage available by boat. Mapping was conducted by foot in teams of two on traverses between 10 and 17km a day. Zodiac, Cessna and Turbo Beaver were the main forms of transportation to traverse each day and a Twin Otter was used to mobilize and demobilize camps. Field seasons were two to three months in length.

Terrain in the Wecho River area is generally quite flat with some hills. It is located below the tree line and the southernmost part of the Wecho River area has abundant forest, but the in the northeastern part of the map sheet trees become sparse and the tundra begins just kilometres to the northeast. Areas of burnt forest are found locally throughout the map sheet producing well-exposed outcrops. Despite the tree coverage,

the outcrop is extensive with up to 90% exposure in some areas. The 2003 map area is covered in a layer of till that dominates a large portion of the area, specifically in the eastern central area.

A2. Previous Work

The eastern portion Wecho River area was first mapped in 1949 by D.H. Yardley, at which point the mapping was likely restricted to river areas and as such many units are missing from his map. The Armi Lake meta-sedimentary belt was also unmapped until recently. In 1992, J. Brophy mapped the Wheeler Lake area with emphasis on mineral showings, primarily the Au-bearing iron formations. Other than these two maps, no other mapping has been done.

Appendix B: Analytical Techniques

B1. Thin Section Preparation

Rock samples were cut at the Northwest Territories Geoscience Office and thin sections were cut, mounted and select sections polished at Carleton University. Petrography was done using a binocular transmitted light microscope at Carleton University.

B2. Geochemical Sampling and Preparation

Samples were taken at the end of each of the two field seasons by helicopter in order to determine the best sample locations based on the entire season's mapping results. Fist size samples were taken and emphasis was put on taking samples far from xenoliths and enclaves as well as ones with no alteration or weathering. The samples were "cleaned" of any surface weathering or lichen in the field and then cut at the Northwest Territories Geoscience Office to remove any other alteration or unwanted material from the samples. They were then washed and dried before shipping to Ottawa.

B3. X-ray Fluorescence (XRF) and Inductively Coupled Plasma Mass Spectrometry (ICP-MS)

Samples were clean crushed using a chipmunk jaw crusher and then ground in an agate ring mill to a fine powder. Before crushing and powdering both machines were pre-

contaminated with small amounts of the sample being crushed. Larger volumes of powder than necessary were produced and then mixed in order to obtain a representative sample. The powders were then split into three parts, one for X-Ray Diffraction analysis at the University of Ottawa, one for Rare Earth Element analysis (ICP-MS) at the Ontario Geological Survey Geochemical Laboratory in Sudbury and one for Sm-Nd isotopic analysis at Carleton University. 45 samples underwent both XRF and ICP-MS analysis as well as several blanks in order to test the reliability of the data.

XRF was carried out at the University of Ottawa by a fused disc technique in order to determine the major element concentrations of SiO_2, TiO_2, Al_2O_3, Fe_2O_3, MnO, P_2O_5, MgO, P_2O_5, Na_2O, K_2O and CaO. A 3:1 flux to sample ratio was heated to approximately 1200°C in a porcelain crucible and the liquid produced was then poured into a platinum disc-shaped mould and then cooled. The product after cooling is an approximately 35mm, homogenous glass disc that is ready for analysis. The data was collected using an automated computer system and the data was reduced using an in-house written program in a spreadsheet.

Rare earth element concentrations as well as Th, U, Hf and Ta concentrations were determined using ICP-MS in Sudbury at the Ontario Geological Survey, by an acid dissolution technique using HF. The resulting residue is then dissolved in nitric acid, dried down and then diluted to the concentration level it will run at prior to taking it to the mass spectrometer.

B4. Sm-Nd Isotopic Analysis

45 samples were analyzed for Sm-Nd isotopic study, and 4 samples were analyzed twice in order to determine the reliability of the data collected. Between 100 and 200 mg of powder was spiked in a Teflon beaker with a mixed ^{149}Sm-^{148}Nd spike solution. The samples were then dissolved with 50% hydrofluoric acid and 16N nitric acid, followed by 8N nitric acid and lastly 6N hydrochloric acid. The sample was left to dissolve for 24 to 48 hours. The resulting solution was then loaded into columns of BioRad cation resin, which retains the REE while removing other major and trace elements. After drying down the collected REE, 0.26N hydrochloric acid was added. This REE solution was added to a column with a 2cm-high bed of Teflon powder coated in HDEHP (di(2-ethylhexyl) orthophosphoric acid and the Nd was collected using 0.26N hydrochloric acid.

Nd was run on a TRITON thermal ionization mass spectrometer, and Sm run on a Finnegan-MAT 261 thermal ionization mass spectrometer, using a double filament technique. Phosphoric Acid was used to load the collected Nd or Sm onto outgassed Re filaments for the mass spectrometer. The isotopic ratios were normalized to $^{147}Nd/^{144}Nd = 0.72190$. A LaJolla standard was used for each analysis, and the results for the standard were consistent with other data collected at this lab on both the TRITON and the Finnegan-MAT 261 mass spectrometers.

B5. Geochronology Sampling and Preparation

Geochronology samples were chosen in the field on the basis of their crosscutting relationships and whether their age would be important in solving timing problems. An approximately 30 kg sample was taken for each suite from areas with no alteration or weathering. Samples were then prepared and analyzed at the Geological Survey of Canada in Ottawa. Heavy mineral concentrates of each sample were prepared through crushing, grinding, Wilfley™ table and heavy liquid separation. Grains were then sorted using the Frantz™ isodynamic separator by magnetic susceptibility. Zircons and monazites were then optically sorted and separated into fractions, defined by morphology.

B6. Thermal Ionization Mass Spectrometry Analysis

For Thermal Ionization Mass Spectrometry (TIMS) analyses, all zircon were air abraded. Analytical methods for U-Pb analyses of zircon and monazite are summarized in Roddick et al. (1987) and Parrish et al. (1987). Analytical errors are determined based on error propagation methods of Roddick (1987). A modified (York, 1969) regression method was used to calculate upper and lower concordia intercept ages and Isoplot v. 3.00 (Ludwig, 2001) was used to calculated weighted mean ages. TIMS analytical results are presented in Table V.

B7. Sensitive High Resolution Ion Microprobe (SHRIMP) Analysis

Analytical procedures for U-Pb zircon analyses using the Sensitive High Resolution Ion Microprobe (SHRIMP II) at the Geological Survey of Canada followed those described by Stern (1997), with standards and U-Pb calibration methods following Stern and Amelin (2003). Zircons were cast in 2.5 cm diameter epoxy mounts (GSC #318) along with fragments of the GSC laboratory standard (z6266, with 206Pb/238U age = 559 Ma). The internal features of the zircons were imaged using the SEM in backscattered electron (BSE) mode prior to analyses. Analyses were conducted using an $^{16}O^-$ primary beam. Two different sized spots were used for analysis, one ca. 15um in diameter and another ca. 9 um in diameter with a beam current of ca. 3.5 and 1 nA respectively. The 1σ external errors of Pb/U ratios incorporate a ±1.0% error in the standard calibration. Isoplot v. 3.00 (Ludwig, 2003) was used to generate concordia plots and calculate weighted means. SHRIMP analytical results are presented in Table X.

Appendix C. Normalization Values Used

Taylor and McClennan, 1985 Chondrite

	chondrite
Rb	3.45
Ba	3.41
Th	0.0425
Nb	0.375
Ta	0.026
La	0.367
Ce	0.957
Sr	11.9
Pr	0.137
Nd	0.711
Sm	0.231
Hf	0.179
Zr	5.54
Eu	0.087
Gd	0.306
Tb	0.058
Dy	0.381
Y	2.25
Ho	0.0851
Er	0.249
Tm	0.0356
Yb	0.248
Lu	0.0381

Sun and McDonough, 1989 Primitive Mantle

	Primitive Mantle
Rb	0.635
Ba	6.989
Th	0.084
Nb	0.713
Ta	0.041
La	0.687
Ce	1.775
Sr	21.1
Pr	0.276
Nd	1.354
Sm	0.444
Hf	0.309
Zr	11.2
Eu	0.168
Gd	0.596
Tb	0.108
Dy	0.737
Y	4.55
Ho	0.164
Er	0.48
Tm	0.074
Yb	0.493
Lu	0.074

Fraction	Description'	# gr	Size (µm)	Wt. (µg)	U (ppm)	Pb* (ppm)
03SB008a Armi Pluton (Z7988)						
M1A (M)	pY,Clr,fFr,Sub,NAbr,M-0.5A	1	125	1	1840	21813
M2A (M)	pY,Alt,Sub,NAbr,M-0.5A	1	125	1	2912	14344
M3A (M)	Y,Alt,Sub,NAbr,M-0.5A	1	200	1	3683	40187
M4A (M)	Y,Alt,An,NAbr,M-0.5A	1	150	1	2792	13737
Z1 (Z)	B,Alt,fFr,E,Pr,Abr,M0°	1	130	1	496	308
Z2 (Z)	pBr,Clr,fFr,cln,Pr,Abr,M0°	2	77	1	462	252
Z3 (Z)	Br,fFr,St,Abr,M0°	1	87	1	586	294
03SB020A Dauphinee Suite (Z7990)						
Z1A (Z)	pBr,Clr,fFr,El,Abr,M1°	1	81	2	231	125
Z1B (Z)	pBr,Clr,rFr,St,Abr,M1°	1	113	2	401	206
Z1C (Z)	pBr,Clr,St,Abr,M1°	2	98	2	484	256
Z2A (Z)	Br,Clr,fFr,Sub,Abr,M1°	1	214	7	402	211
Z2B (Z)	Br,Clr,fFr,Sub,Abr,M1°	1	214	9	307	160
03SB021A Wecho Suite (Z7991)						
M1 (M)	Co,Clr,Eu,NAbr,M-0.5A	1	100	1	14111	16796
M2 (M)	pY,Tb,Sub,NAbr,M-0.5A	1	100	1	9838	11661
M3 (M)	pY,Tb,fFr,Sub,NAbr,M-0.5A	1	150	1	10913	13135
Z1 (Z)	Co,Clr,rFr,El,Ro,Abr,M3°	1	0 8	1	144	72
Z2A (Z)	Co,Clr,Sub,Abr,M3°	1	3 5	3.5	64	40
03SB028A Hickey Suite (Z7992)						
M1 (M)	Co,Clr,Eu,NAbr,M-0 5A	1	100	1	13576	52969
M3 (M)	Y,Tb,rFr,Sub,NAbr,M-0 5A	1	200	1	5697	26453
M4 (M)	Y,Clr,Sub,NAbr,M-0.5A	1	200	1	21255	69892
Z1A (Z)	Co,Clr,fFr,El,Pr,Abr,Dia	7	98	2	301	194
Z2 (Z)	pY,Clr,rFr,St,Abr,Dia	1	66	1	586	362
Z2 (Z)	pBr,Clr,St,Abr,Dia	1	66	1	582	395
Z3 (Z)	Co,Clr,rFr,cln,Ro,Abr,Dia	4	57	2	63	42
Z4 (Z)	Br,Clr,rFr,Ro,Abr,Dia	4	87	3	352	216
04SB4261 South Pluton (Z8493)						
T1 (T)	Br, large	1	200	42	112.48	98.63
T2 (T)	Br, large	4	200	96	107.28	93.98
Z1 (Z)	El, pBr, Clr, fFr	1	253	3	82.02	50.11
Z1A (Z)	El, pBr, Clr, fFr	1	297	3	95.12	54.76
Z2 (Z)	St, pBr, fFr	1	172	2	162.4	89.29
Z2A (Z)	St, pBr, fFr	1	210	4	226.5	134.13
Z3A (Z)	fFr, El, Br, Clr	1	524	10	139.93	79.26
Z3B (Z)	fFr, El, Br, Clr	1	524	28	189.97	105.14
Z3C (Z)	Br,fFr,Pr	1	360	7	181.15	99.64
03sb005a Nardin Gneiss (Z8491)						
M1A (M)	Ro, Y, Akt	1	199	3	6165.6	27264
M1B (M)	Ro, Y, Alt	1	100	3	6366.1	29110
M2 (M)	An, pY,	1	100	3	4358	18881
Z1 (Z)	Br, El, Alt, fFr	1	118	1	395.37	326.34
Z2A (Z)	Pr, St, Br, fFr	1	98	1	194.94	135.65
Z2B (Z)	St, Br, fFr	3	98	2	411.85	278.4
04sb4263 Mag Pluton (Z8492)						
M1A (M)	pY, Tb, An	1	100	5	1969.3	29386
M1B (M)	pY, Tb, An	1	100	5	3237	20732
Z1A (Z)	Br, fFr, Alt	1	158	1	403.41	213.18
Z1B (Z)	Br, An, fFr,	1	158	2	274.88	145.34
Z2 (Z)	St, Br, Pr, Tb	2	104	2	356.2	178.51

1. Description: Z=Zircon, M=Monazite, Co=Colourless, Br=Brown, pBr=Pale Brown, Y=Yellow, pY=Pale Yellow, Alt=Altered, Clr=Clear, Tb=Turbid, fFr=Few Fractures, rFr=Rare Fractures, cln=Clear Inclusions, An=Anhedral, El=Elongate, Eu=Euhedral, Pr=Prismatic, Ro=Rounded, St=Stubby Prism, Sub=Subhedral, Abr=Abraded, NAbr=Not Abraded.

	Pbc (pg)	$^{206}Pb/^{204}Pb$	$^{208}Pb/^{206}Pb$	Radiogenic Ratios (± 1sigma error) $^{207}Pb/^{235}U$	$^{208}Pb/^{232}U$
03SB008a					
M1A (M)	6	8946	27.200	11.394 ± 0.013	0.4819 ± 0.0004
M2A (M)	4	20395	10.420	11 632 ± 0.013	0.4903 ± 0.0004
M3A (M)	7	16817	24.670	11.485 ± 0.013	0.4870 ± 0 0004
M4A (M)	5	18249	10.380	11.676 ± 0.013	0.4914 ± 0.0004
Z1 (Z)	5	4839.8	0.1	16.163 ± 0018	0.5495 ± 0.0005
Z2 (Z)	9	1445.9	0 14	11.506 ± 0016	0.4843 ± 0.0005
Z3 (Z)	6	2612.5	0.05	11.463 ± 0.014	0.4794 ± 0.0005
03SB020A					
Z1A (Z)	4	3273	0.110	11.769 ± 0.015	0.4922 ± 0.0005
Z1B (Z)	4	5628	0.050	11.588 ± 0.014	0.4881 ± 0.0005
Z1C (Z)	10	3103	0.090	11.601 ± 0.014	0.4882 ± 0.0004
Z2A (Z)	8	10034	0.070	11.749 ± 0.013	0.4917 ± 0.0004
Z2B (Z)	10	8567	0.060	11.746 ± 0.013	0.4918 ± 0.0004
03SB021A					
M1 (M)	4	96280	1.640	11.594 ± 0.013	0.4896 ± 0.0004
M2 (M)	4	83489	1.660	11.400 ± 0.013	0.4841 ± 0.0004
M3 (M)	5	72564	1.700	11.448 ± 0.013	0.4846 ± 0.0004
Z1 (Z)	1	1438.4	0.15	10.195 ± 0.023	0.4396 ± 0.0007
Z2A (Z)	6	1275.3	0.26	12.137 ± 0016	0.5107 ± 0.0005
03SB028A					
M1 (M)	15	27850	7 920	11.917 ± 0.013	0 4952 ± 0.0004
M3 (M)	6	28957	9.620	11 933 ± 0.014	0.4961 ± 0.0005
M4 (M)	18	35851	6.490	11 904 ±0.013	0.4952 ± 0.0004
Z1A (Z)	17	1379	0.180	15.218 ± 0.019	0.5420 ± 0.0005
Z2 (Z)	5	2224	0.070	16.171 ± 0.023	0.5602 ± 0.0007
Z2 (Z)	17	440	0.190	16.080 ± 0.052	0.5631 ± 0.0020
Z3 (Z)	4	903	0.130	17.287 ± 0.034	0.5745 ± 0.0010
Z4 (Z)	12	2964	0.080	15.968 ± 0.019	0.5544 ± 0.0005
04sb4263					
T1 (T)	325	460.4	0 88	11.873 ± 0.026	0.4943 ± 0.0008
T2 (T)	385	839.1	0 88	11.896 ± 0.017	0.4937 ± 0.0005
Z1 (Z)	14	96 1	0.23	12.283 ± 0.186	0.5065 ± 0.0086
Z1A (Z)	6	1390	0.18	11.899 ± 0 018	0.4942 ± 0.0005
Z2 (Z)	4	2623.3	0.14	11.629 ± 0.014	0 4870 ± 0.0005
Z2A (Z)	11	2278.4	0.23	11.826 ± 0.016	0.4910 ± 0.0005
Z3A (Z)	115	374.3	0.14	12.031 ± 0.037	0.4991 ± 0.0016
Z3B (Z)	11	14439	0.12	11.924 ± 0.015	0.4956 ± 0.0005
Z3C (Z)	11	3393.8	0.14	11.702 ± 0.015	0.4883 ± 0.0005
03sb005a					
M1A (M)	7	81190	9.15	11.848 ± 0.013	0.4942 ± 0.0004
M1B (M)	9	68144	9.54	11.794 ± 0.013	0.4924 ± 0.0004
M2 (M)	5	73865	9.16	11.316 ± 0.012	0.4842 ± 0.0004
Z1 (Z)	66	267.7	0.13	25.921 ± 0.071	0.6836 ± 0.0008
Z2A (Z)	18	543.3	0.09	20.965 ± 0.036	0.6019 ± 0.0006
Z2B (Z)	11	2055.2	0.06	20.842 ± 0.025	0.5965 ± 0.0005
04sb4263					
M1A (M)	11	26309	33.98	11.596 ± 0.013	0.4894 ± 0.0004
M1B (M)	8	64578	14.02	11.387 ± 0.012	0.4863 ± 0.0004
Z1A (Z)	30	415	0.09	11.768 ± 0.029	0.4869 ± 0.0006
Z1B (Z)	8	1785.8	0.1	11.621 ± 0.016	0.4822 ± 0.0005
Z2 (Z)	7	2370.2	0.06	11.299 ± 0.013	0.4741 ± 0.0005

2. Concentration uncertainty varies with sample weight: >10% for sample weights <10 ug, <10% for sample weights above 10 ug. * = radiogenic Pb.
Pbc = total common Pb in analysis corrected for spike and fractionation.

$^{207}Pb/^{206}Pb$		Age (Ma, ± 2sigma error) $^{207}Pb/^{206}Pb$	% Discord.
	03SB008a Armi Pluton (Z7988)		
0.17149 ± 0.00007	M1A (M)	2572 2 ± 1.4	1.7
0.17207 ± 0.00007	M2A (M)	2577.8 ± 1.4	0 3
0.17100 ± 0.00007	M3A (M)	2567.6 ± 1.4	0.5
0.17231 ± 0.00007	M4A (M)	2580.2 ± 1.4	0.2
0.21335 ± 1.4	Z1 (Z)	2931.2 ± 1.4	4.56
0.17232 ± 2.2	Z2 (Z)	2580.3 ± 2.2	1.62
0.17341 ± 1.7	Z3 (Z)	2590.9 ± 17	3.09
	03SB020A Dauphinee Suite (Z7990)		
0.17342 ± 0.00009	Z1A (Z)	2590.9 ± 1.7	0.5
0.17219 ± 0.00008	Z1B (Z)	2579.0 ± 1.5	0.8
0.17235 ± 0.00009	Z1C (Z)	2580.6 ± 1.7	0.8
0.17331 ± 0.00007	Z2A (Z)	2589.8 ± 1.4	0.6
0.17323 ± 0.00007	Z2B (Z)	2589.1 ± 1.4	0 5
	03SB021A Wecho Suite (Z7991)		
0.17174 ± 0.00007	M1 (M)	2574.6 ± 1.4	0.3
0.17077 ± 0.00007	M2 (M)	2565.2 ± 1.4	0.9
0.17131 ± 0.00007	M3 (M)	2570.5 ± 1.4	1.1
0.16810 ± 3.9	Z1 (Z)	2539.6 ± 3.9	8.94
0.17235 ± 1.7	Z2A (Z)	2580.6 ± 2.3	-3.74
	03SB028A Hickey Suite (Z7992)		
0.17451 ± 0.00007	M1 (M)	2601.4 ± 1.4	0.4
0.17444 ± 0.00007	M3 (M)	2600.7 ± 1.4	0.2
0.17433 ± 0.00007	M4 (M)	2599.7 ± 1.4	0.3
0.20362 ± 0.00012	Z1A (Z)	2855.4 ± 1.9	2.7
0.20934 ± 0.00011	Z2 (Z)	2900.5 ± 1.7	1.4
0.20710 ± 0.00028	Z2 (Z)	2883.0 ± 4.5	0 1
0.21822 ± 0.00019	Z3 (Z)	2967.6 ± 2.8	1.7
0.20888 ± 0.00019	Z4 (Z)	2896.9 ± 1.6	2.3
	04SB4261 South Pluton (Z8493)		
0.17421 ± 0.00025	T1 (T)	2598.5 ± 4.9	0.43
0.17474 ± 0.00014	T2 (T)	2603.5 ± 2.7	0.77
0.17588 ± 0.00151	Z1 (Z)	2614.4 ± 28.4	-1.28
0 17460 ± 0.00013	Z1A (Z)	2602.2 ± 2.5	0.61
0.17318 ± 0.0001	Z2 (Z)	2588.6 ± 1.9	1.44
0.17469 ± 0 00011	Z2A (Z)	2603.1 ± 2 1	1.3
0.17480 ± 0 0003	Z3A (Z)	2604.1 ± 5 8	-0.29
0.17450 ± 0.00007	Z3B (Z)	2601.3 ± 1.4	0.3
0.17381 ± 0.0001	Z3C (Z)	2594.7 ± 1.9	1.46
	03sb005a Nardin Gneiss (Z8491)		
0.17386 ± 0.00007	M1A (M)	2595.1 ± 1.4	0.28
0.17370 ± 0.00007	M1B (M)	2593.6 ± 1.4	0.58
0.16950 ± 0.00007	M2 (M)	2552.8 ± 1.4	0.34
0 27500 ± 0.00057	Z1 (Z)	3334.8 ± 6.5	-0.91
0.25262 ± 0.00028	Z2A (Z)	3201.3 ± 3.5	6.41
0 2534 ± 0.000141	Z2B (Z)	3206.2 ± 1.7	7.42
	04sb4263		
0.17183 ± 0.00007	M1A (M)	2575.6 ± 1.4	0.34
0.16979 ± 0.00007	M1B (M)	2555.6 ± 1.4	0.03
0.17529 ± 0.00032	Z1A (Z)	2608.8 ± 6.2	2 39
0.17477 ± 0.00012	Z1B (Z)	2603.8 ± 2.2	3.1
0.17283 ± 0.00009	Z2 (Z)	2585.2 ± 1.8	3.89

3. Ratios corrected for spike, fractionation, blank and initial common Pb (Cumm Richards, 1975), except 206Pb/204Pb ratio corrected for spike and fractionatio
4. 206Pb/238U age and 207Pb/206Pb age with 2 s absolute error in Ma.

Spot Description	U (ppm)	Th (ppm)	Th/U	Pb* (ppm)	^{204}Pb (ppb)	^{204}Pb/ ^{206}Pb	± ^{204}Pb/ ^{206}Pb	f(206)^{204}	^{208}Pb/ ^{206}Pb
03sb008A Armi Pluton (Z7988)									
7988-166.1	294.81	2 62	0.00917	147	9	0 0000733	1.896E-05	0.00127	0.00254
7988-135 1	906.99	23.17	0.02639	461	7	0 0000182	6.670E-06	0.00032	0 00745
7988-154.1	1022.24	330.07	0.33356	562	4	0.0000093	8.550E-06	0 00016	0.09426
7988-163.1	613.25	200 09	0 33707	355	3	0.0000121	6.570E-06	0 00021	0.09532
7988-140 1	890.04	473.69	0.5498	506	5	0 0000136	6 040E-06	0.00024	0.15123
7988-135.2	210.39	113 8	0.55877	121	10	0.0001062	5.075E-05	0.00184	0 15506
7988-141.1	1019.06	689.03	0.69849	589	51	0.0001195	1.861E-05	0.00207	0 19546
7988-143.1	1007.5	776 57	0.79627	586	22	0 0000540	7.430E-06	0.00094	0.23021
7988-146.1	478.27	431.5	0.93204	291	6	0 0000303	1 524E-05	0.00053	0.25935
7988-155.1	488.46	619.83	1.31089	342	12	0 0000559	1.127E-05	0.00097	0.37180
03sb020A Dauphinee Suite (Z7990)									
7990-95.1	1595.34	554.48	0.35905	941	10	0 0000142	3.690E-06	0.00025	0 10301
7990-110.1	473.85	124.52	0.27146	254	8	0 0000397	1.232E-05	0.00069	0.07650
7990-109.1	827.51	35.91	0.04482	418	3	0.0000079	5.730E-06	0.00014	0.01323
7990-112.1	503.29	287 37	0.58985	284	5	0.0000233	1.293E-05	0.00040	0.16297
7990-107.1	911.27	24.9	0.02823	457	6	0.0000150	5.240E-06	0 00026	0.00821
7990-119.1	1066.9	48 93	0.04738	542	1	0 0000015	2.890E-06	0.00003	0.01369
7990-118.1	872.52	39 01	0.04619	437	2	0.0000049	1.058E-05	0.00008	0.01298
7990-120.1	369.3	110 83	0.31003	192	6	0 0000396	1.725E-05	0 00069	0 08510
7990-125.1	810.04	30.84	0.03934	408	7	0.0000198	6.060E-06	0.00034	0 01097
7990-127.1	992.31	163.62	0.17034	518	2	0.0000058	7.010E-06	0.00010	0 04389
7990-115.1	674.35	71.11	0.10894	342	14	0.0000481	9.150E-06	0.00083	0.02958
7990-121.1	1526.68	902.16	0.61047	898	6	0 0000088	2.860E-06	0.00015	0.17087

Notes (see Stern, 1997): Uncertainties reported at 1s (absolute) and are calculated by numerical propagation of all known sources of error
f206^{204} refers to mole fraction of total 206Pb that is due to common Pb, calculated using the 204Pb-method; common Pb composition used is the surface blank

Spot Description	U (ppm)	Th (ppm)	Th/U	Pb* (ppm)	^{204}Pb (ppb)	^{204}Pb/ ^{206}Pb	± ^{204}Pb/ ^{206}Pb	f(206)^{204}	^{208}Pb/ ^{206}Pb
03sb021A Wecho Suite (Z7991)									
7991-44.1	696.79	10.91	0.01617	353	23	0 0000766	1 955E-05	0.00133	0 00448
7991-60.1	490.99	7 96	0.01676	248	9	0.0000429	1 946E-05	0 00074	0.00620
7991-46.1	1328.22	98.12	0.07632	705	18	0 0000308	1.071E-05	0.00053	0.02342
7991-63.1	627.35	65.88	0.10848	322	7	0.0000267	7 720E-06	0.00046	0.02999
7991-51.1	512.54	59.01	0.11893	248	23	0.0001111	3.863E-05	0.00192	0.03440
7991-68 1	379.23	50.63	0.13793	193	8	0.0000527	1.246E-05	0.00091	0.03781
7991-48.1	647.29	117.03	0.18678	336	3	0.0000101	5.600E-06	0.00018	0.05369
7991-65.1	48.21	9.06	0.19407	25	3	0.0001623	7 317E-05	0.00281	0.05591
7991-66 1	860.87	231.8	0.27816	471	7	0.0000185	7.250E-06	0 00032	0.07672
7991-58.1	311.42	142.89	0.47399	183	12	0.0000863	3 270E-05	0.00150	0.13613
7991-61 1	401.07	199.32	0 51339	222	9	0.0000558	1 152E-05	0.00097	0.15714
7991-73.1	1417.17	868.79	0.63331	885	7	0.0000108	5.230E-06	0.00019	0.17455
03sb028A Hickey Suite (Z7992)									
7992-3.1	514.73	383.59	0.76986	353	8	0.0000341	1.909E-05	0.00059	0.21303
7992-18.1	669.66	28.98	0.04471	393	1	0.0000045	8 230E-06	0.00008	0.01159
7992-21.1	272.89	170.54	0.64557	180	18	0.0001363	3.036E-05	0.00236	0.17113
7992-37.1	388.58	1013.99	2.69572	366	2	0 0000110	1.085E-05	0.00019	0.74030
7992-42 1	372.54	215.23	0.59685	250	1	0 0000081	1.250E-05	0 00014	0.16614
7992-5.1	1153.92	86.58	0.07752	676	433	0.0007824	6.454E-05	0.01356	0.02811
7992-24 1	452.13	113.14	0.25852	302	34	0.0001482	1.802E-05	0.00257	0.07118
7992-13.1	303.23	75.58	0.25748	174	841	0.0056370	1.193E-03	0.09770	0 08520

Spot Description	U (ppm)	Th (ppm)	Th/U	Pb* (ppm)	^{204}Pb (ppb)	^{204}Pb/ ^{206}Pb	± ^{204}Pb/ ^{206}Pb	f(206)^{204}	^{208}Pb/ ^{206}Pb
04sb4262 Mag Pluton (Z8492)									
8492-08.1	1059.4	122.15	0.11911	553	3	0.0000075	4 740E-06	0.00013	0.03356
8492-09.1	268.19	127.64	0.49168	135	4	0.0000403	2.645E-05	0.0007	0.13779
8492-10 1	500 62	106.55	0.21987	208	0	0.0000011	1 243E-05	2.00E-05	0.05796
8492-11.1	3605.1	640 55	0.18355	2184	1	0.0000003	9.300E-07	1.00E-05	0.05156
8492-13 1	855.06	119.67	0.14458	352	4	0.0000141	7 930E-06	0.00024	0.03864
8492-18.1	613.01	82.18	0.13849	240	8	0 0000384	1.535E-05	0.00066	0 03739
8492-22.1	682.89	87.57	0.13247	344	0	0.0000008	1.496E-05	1.00E-05	0 03624
8492-23.1	735.52	162.97	0.2289	357	3	0.0000100	1.000E-05	0.00017	0.06241
8492-26.1	1174.5	41.14	0.03619	590	6	0.0000120	3.350E-06	0.00021	0.0094
8492-28.1	501.85	178.13	0.36668	267	4	0 0000207	1 699E-05	0.00036	0 10021
8492-29.1	363 53	120.55	0.34257	164	3	0.0000210	4.015E-05	0 00036	0.10281
8492-21.1	612.21	149.68	0.25257	304	6	0.0000264	1.136E-05	0.00046	0.07153
8492-8.2.2	598.15	143.76	0.24828	294	1	0 0000056	5.520E-06	0.0001	0 06679
8492-9.1.2	215.62	113.48	0.54369	104	1	0.0000124	1.603E-05	0.00022	0.155
8492-10.2	531.38	63.6	0.12364	279	5	0.0000225	1.088E-05	0.00039	0.03382
8492-26.1.2	693.82	25.92	0.0386	348	2	0.0000084	6.060E-06	0 00014	0.01076
8492-26.1.3	571.28	23.71	0 04287	273	2	0.0000090	8.520E-06	0.00016	0.01255
8492-22.1.2	428.72	57.51	0.13859	220	3	0 0000157	8.410E-06	0.00027	0 04056
8492-22.1.3	368.32	49.95	0.14009	174	4	0.0000304	1.271E-05	0.00053	0.03944
8492-21.1.2	409.41	96.54	0.24359	211	8	0.0000461	1.112E-05	0.0008	0.07066
8492-21 1.3	370.08	87.18	0.24335	172	10	0.0000759	1.453E-05	0 00131	0.06896
03sb005 Nardin Gneiss (Z8491)									
8493-33.1	945.33	193.65	0.21163	717	8	0.0000159	5.410E-06	0.00027	0 05887
8493-35.1	996.24	300.46	0 31156	806	2	0.0000036	3 350E-06	6 00E-05	0 08447
8493-39.1	505.51	289.28	0.59116	387	9	0.0000346	1.244E-05	0.0006	0.14871
8493-40.1	261.27	110.85	0 43831	160	1	0.0000089	1.048E-05	0 00015	0 11423
8493-41.1	303.75	11.22	0.03815	169	11	0 0000830	2 070E-05	0.00144	0.00908
8493-34.1	601.04	168.18	0 28908	315	18	0.0000763	1.862E-05	0.00132	0.08992
8493-32.1	567.34	49.99	0.09103	424	109	0.0003342	1 993E-05	0.00579	0 02627

Spot Description	± $^{208}Pb/^{206}Pb$	$^{207}Pb/^{235}U$	± $^{207}Pb/^{235}U$	$^{206}Pb/^{238}U$	± $^{206}Pb/^{238}U$	Corr Coeff	$^{207}Pb/^{206}Pb$	± $^{207}Pb/^{206}Pb$	$^{206}Pb/^{238}U$
03sb008A Armi Pluton (Z7988)									
7988-166.1	0.00075	11 87127	0 17342	0 49217	0.00610	0.9024	0.17494	0.00111	2580.06
7988-135.1	0.00039	12 03506	0.13460	0.50064	0 00525	0 9691	0 17435	0.00048	2616.55
7988-154 1	0.00103	12.08621	0 14540	0.50352	0.00532	0.9255	0.17409	0.00080	2628 90
7988-163.1	0.00151	12.68812	0.68039	0.53006	0.02634	0.9615	0 17361	0 00258	2741.69
7988-140.1	0.00132	11 97847	0.15171	0 49842	0.00589	0.9657	0.17430	0.00058	2607.02
7988-135 2	0.00256	12.69412	0 24881	0.49682	0 00809	0 8887	0.18531	0.00168	2600.10
7988-141.1	0.00138	11.75401	0.15506	0.49026	0.00532	0.8823	0.17388	0.00109	2571.79
7988-143 1	0.00175	11.56294	0 13150	0.48064	0 00498	0 9499	0.17448	0.00063	2530.03
7988-146.1	0.00320	11.91722	0.17513	0.49230	0.00587	0.8733	0.17557	0.00127	2580 60
7988-155.1	0.00252	13.49034	0.17199	0.52184	0.00580	0.9208	0.18749	0.00094	2707.00
03sb020A Dauphinee Suite (Z7990)									
7990-95.1	0.00079	12.72988	0.17529	0.53764	0 00712	0 9839	0.17172	0.00043	2773.57
7990-110.1	0.00093	11.92901	0.14048	0.49834	0 00533	0.9481	0.17361	0.00066	2606.66
7990-109.1	0.00047	11.86507	0.13995	0.49465	0.00545	0.9663	0.17397	0.00053	2590.78
7990-112.1	0.00120	11.63940	0.15729	0.49151	0 00599	0.9440	0.17175	0.00077	2577.19
7990-107.1	0.00026	11.81903	0.15438	0 49379	0.00550	0.9063	0.17359	0 00097	2587.06
7990-119.1	0.00024	11.90992	0.14683	0.49735	0.00567	0.9599	0 17368	0.00060	2602.41
7990-118.1	0.00048	11.76570	0.13911	0 49070	0.00533	0.9560	0.17390	0.00061	2573.71
7990-120.1	0.00125	11.45686	0.14990	0.48056	0 00563	0.9392	0 17291	0.00078	2529.69
7990-125.1	0.00031	11.81743	0.14425	0.49418	0.00562	0.9650	0.17343	0.00056	2588 75
7990-127.1	0.00047	11.93837	0.13614	0.49797	0.00537	0.9739	0 17388	0.00045	2605.06
7990-115.1	0.00092	11.78053	0.15571	0.49035	0.00539	0.8894	0.17424	0 00106	2572.18
7990-121.1	0.00070	12.12975	0.14145	0.50826	0 00553	0 9655	0.17309	0.00053	2649.20

* refers to radiogenic Pb (corrected for common Pb)
Discordance relative to origin = 100 * (1-(206Pb/238U age)/(207Pb/206Pb age))

Spot Description	± $^{208}Pb/^{206}Pb$	$^{207}Pb/^{235}U$	± $^{207}Pb/^{235}U$	$^{206}Pb/^{238}U$	± $^{206}Pb/^{238}U$	Corr Coeff	$^{207}Pb/^{206}Pb$	± $^{207}Pb/^{206}Pb$	$^{206}Pb/^{238}U$
03sb021A Wecho Suite (Z7991)									
7991-44 1	0.00082	11.92400	0.19489	0 50074	0 00647	0.8553	0.17271	0.00147	2617.00
7991-60 1	0 00077	11.92838	0.17597	0 49680	0 00559	0 8330	0.17414	0 00143	2600.02
7991-46.1	0.00051	12 35325	0.22601	0.51541	0.00726	0.8389	0.17383	0 00174	2679.68
7991-63.1	0.00049	11.88743	0.15724	0.49541	0 00551	0 8968	0.17403	0 00103	2594.03
7991-51.1	0.00176	11.19600	0.20097	0.46516	0 00704	0 8984	0.17456	0.00139	2462.30
7991-68.1	0.00075	11.60794	0.15563	0 48955	0.00588	0.9391	0.17197	0 00080	2568.73
7991-48.1	0.00059	11.81877	0.15594	0 49156	0.00549	0.9016	0.17438	0.00100	2577.40
7991-65.1	0.00339	12.27527	0.32458	0 48524	0 01049	0 8782	0.18347	0.00234	2550.05
7991-66.1	0.00076	12 43745	0.21649	0.50677	0.00797	0.9446	0.17800	0.00102	2642.82
7991-58 1	0.00318	13 26300	0 23052	0 51784	0 00646	0.7945	0.18576	0.00198	2690.00
7991-61 1	0.00236	11.57905	0 14570	0 48268	0.00536	0.9296	0.17398	0.00081	2538.95
7991-73.1	0.00070	13 81863	0.15743	0 53241	0.00577	0.9782	0.18824	0.00045	2751.61
03sb028A Hickey Suite (Z7992)									
7992-3.1	0.00216	16.16593	0.19046	0.55978	0.00349	0.6269	0.20945	0 00194	2865.72
7992-18.1	0.00038	16.10771	0.12194	0 55942	0.00268	0.7195	0.20883	0.00111	2864.24
7992-21.1	0.00248	16.07129	0 23942	0.55610	0.00311	0.4852	0.20960	0.00275	2850.48
7992-37.1	0 00287	16.10815	0.13674	0.55983	0.00279	0.6790	0.20868	0 00131	2865.91
7992-42 1	0.00259	16.57243	0.18198	0.56447	0.00487	0.8519	0.21293	0 00123	2885.06
7992-5.1	0.01264	15.65072	0 15895	0.55178	0.00416	0.8152	0 20571	0.00122	2832.59
7992-24.1	0.00098	19.18966	0.15537	0.59530	0.00375	0.8460	0.23379	0.00102	3010.88
7992-13.1	0.07819	14.71100	5.99310	0.51791	0.10212	0.5861	0.20601	0.06854	2690.30

Spot Description	± $^{208}Pb/^{206}Pb$	$^{207}Pb/^{235}U$	± $^{207}Pb/^{235}U$	$^{206}Pb/^{238}U$	± $^{206}Pb/^{238}U$	Corr Coeff	$^{207}Pb/^{206}Pb$	± $^{207}Pb/^{206}Pb$	$^{206}Pb/^{238}U$
04sb4262 Mag Pluton (Z8492)									
8492-08 1	0.00073	12 022	0.1641	0 5024	0.00597	0 9204	0.17355	0.00093	2624 1
8492-09.1	0 0038	10.609	0.53634	0 44458	0.0211	0.9697	0 17306	0.00216	2371.1
8492-10.1	0 00221	9.3419	0.31869	0.39175	0.01296	0.9886	0.17295	0.0009	2130.9
8492-11.1	0.00128	14 121	0.57889	0 57243	0.01621	0 7709	0.17892	0.00471	2917.8
8492-13.1	0.0083	9.3512	3.44	0.39586	0.10716	0.8098	0.17133	0 03727	2149.9
8492-18.1	0 00194	9 0375	0.6489	0.37645	0.02653	0 9945	0.17412	0.00132	2059 7
8492-22.1	0.00092	11.584	0.15951	0.48417	0.00599	0.9407	0.17353	0 00082	2545.4
8492-23.1	0 00085	11.102	0.52733	0.45469	0.02102	0 9906	0.17709	0 00116	2416.1
8492-26.1	0.00038	11.871	0.29655	0.49308	0.00937	0 8307	0.17462	0.00245	2584
8492-28.1	0.05466	11.777	16.327	0.48503	0.57124	0.9035	0.17611	0.10544	2549.1
8492-29.1	0.0022	10.174	0 57619	0.4091	0.02259	0.9914	0.18036	0 00135	2210.8
8492-21.1	0.0015	11.197	0.15985	0.46231	0 0057	0 9149	0.17566	0.00102	2449.7
8492-8.2.2	0.00746	11 31157	0.24452	0.45899	0.00921	0.9628	0 17874	0 00105	2435.1
8492-9.1.2	0.00218	10.09377	0 55604	0.42113	0.02257	0.9903	0.17384	0.00134	2265.59
8492-10.2	0.001	12.07852	0.16176	0.50601	0.00594	0 9251	0.17312	0.00089	2639 58
8492-26.1 2	0.00029	11.8347	0.39515	0.49172	0.01624	0 9976	0.17456	0.0004	2578.11
8492-26.1.3	0.00061	11 25881	0.4089	0.46804	0.01663	0.9932	0.17446	0.00074	2474.97
8492-22.1.2	0.00059	11.80011	0.32201	0.49236	0.01294	0 985	0.17382	0.00082	2580.88
8492-22.1.3	0.00069	10.93256	0.37044	0 45355	0 01512	0.9957	0.17482	0.00055	2411
8492-21.1.2	0.00369	11.59052	0.94295	0 48166	0.02807	0.7931	0.17453	0.00872	2534.51
8492-21.1.3	0.00146	10.30232	0.40229	0.43431	0.01632	0 9846	0.17204	0.00118	2325.12
03sb005 Nardin Gneiss (Z8491)									
8493-33.1	0 00069	25.763	0.89761	0.65596	0.02245	0.995	0.28485	0.001	3251.4
8493-35.1	0.00068	26.965	0.32396	0.68628	0.00796	0.9861	0.28496	0.00057	3368.4
8493-39 1	0.00288	24.571	1.055	0 61895	0.02594	0.992	0.28791	0 00158	3105 7
8493-40.1	0.00212	20.416	1.3216	0 50509	0 03151	0.9853	0.29316	0.00327	2635 6
8493-41.1	0.00111	15.371	0 26933	0.5299	0.00838	0.9441	0 21039	0.00122	2741
8493-34.1	0.00277	16 793	0.89749	0 44758	0.02296	0.9829	0.27211	0 0027	2384 5
8493-32.1	0.00087	25.975	0.36667	0 66385	0 00827	0.9292	0.28378	0.00149	3282.1

Spot Description	±$^{206}Pb/^{238}U$	$^{207}Pb/^{206}Pb$	±$^{207}Pb/^{206}Pb$	% Discord
03sb008A Armi Pluton (Z7988)				
7988-166 1	26 40	2605.44	10.61	1
7988-135.1	22.60	2599.84	4.64	-0.6
7988-154.1	22.84	2597.36	7 68	-1.2
7988-163.1	111.96	2592.75	25.00	-5.7
7988-140 1	25.39	2599.38	5.54	-0 3
7988-135.2	34.95	2701.00	15.03	3 7
7988-141.1	23.07	2595.39	10.47	0.9
7988-143 1	21.70	2601.11	5.99	2.7
7988-146.1	25.42	2611.45	12 07	1 2
7988-155.1	24.61	2720.28	8.28	0 5
03sb020A Dauphinee Suite (Z7990)				
7990-95.1	29.91	2574 51	4.15	-7 7
7990-110.1	22.97	2592.76	6 31	-0.5
7990-109 1	23.54	2596.18	5.11	0.2
7990-112.1	25.96	2574.78	7.53	-0 1
7990-107.1	23.79	2592.60	9.31	0.2
7990-119.1	24.45	2593.40	5 82	-0.3
7990-118 1	23.10	2595.54	5.84	0.8
7990-120 1	24.57	2586.01	7.58	2.2
7990-125.1	24.30	2591.06	5.39	0.1
7990-127.1	23.14	2595.31	4.36	-0.4
7990-115.1	23.36	2598.84	10.19	1
7990-121.1	23.67	2587.72	5.12	-2 4

Spot Description	±$^{206}Pb/^{238}U$	$^{207}Pb/^{206}Pb$	±$^{207}Pb/^{206}Pb$	% Discord
03sb021A Wecho Suite (Z7991)				
7991-44.1	27.83	2584.10	14.32	-1.3
7991-60.1	24.14	2597.84	13.78	-0.1
7991-46 1	30.97	2594.87	16.84	-3.3
7991-63.1	23 80	2596.78	9.87	0.1
7991-51.1	31.05	2601.90	13.30	5.4
7991-68.1	25.49	2576.93	7.78	0.3
7991-48.1	23.79	2600.14	9.62	0.9
7991-65.1	45.71	2684.52	21 24	5
7991-66.1	34 18	2634.32	9.60	-0.3
7991-58.1	27.50	2705.00	17.66	0.6
7991-61.1	23.36	2596.34	7.82	2.2
7991-73.1	24.34	2726.86	3.93	-0.9
03sb028A Hickey Suite (Z7992)				
7992-3.1	14.43	2901.30	15.08	1.2
7992-18.1	11.07	2896.49	8.62	1.1
7992-21 1	12.88	2902.48	21.44	1.8
7992-37.1	11.53	2895.36	10.23	1
7992-42.1	20.10	2928.01	9.41	1 5
7992-5.1	17 30	2872.08	9.67	1.4
7992-24.1	15.19	3078.19	6.97	2.2
7992-13.1	448.98	2874.40	678.83	6.4

Spot Description	±$^{206}Pb/^{238}U$	$^{207}Pb/^{206}Pb$	± $^{207}Pb/^{206}Pb$	% Discord
04sb4262 Mag Pluton (Z8492)				
8492-08 1	25.68	2592.2	9	-1.2
8492-09.1	94.86	2587.5	20 94	8 4
8492-10.1	60.3	2586 4	8.68	17 6
8492-11.1	66.79	2642.9	44.36	-10.4
8492-13.1	514.91	2570.7	418 88	16.4
8492-18.1	125.45	2597.6	12 65	20.7
8492-22.1	26.06	2592	7.87	1.8
8492-23.1	93.83	2625.8	10.96	8
8492-26.1	40.58	2602.4	23 55	0.7
8492-28.1	2549.1	2616.5	1668.6	2.6
8492-29.1	104.18	2656.2	12.44	16.8
8492-21.1	25.19	2612.3	9.71	6.2
8492-8.2.2	40.84	2641.2	9.81	7.8
8492-9.1.2	103.18	2594.92	12.95	12.7
8492-10.2	25.5	2588.06	8 58	-2
8492-26.1.2	70.55	2601.83	3.85	0.9
8492-26.1.3	73.46	2600.93	7.12	4.8
8492-22.1.2	56.15	2594.78	7.93	0 5
8492-22 1.3	67.42	2604.36	5.29	7.4
8492-21.1.2	123.3	2601.52	85.75	2.6
8492-21.1.3	73.79	2577.61	11.55	9.8
03sb005 Nardin Gneiss (Z8491)				
8493-33.1	88.01	3389.7	5.45	4.1
8493-35.1	30.5	3390 3	3.13	0.6
8493-39.1	104.12	3406.4	8 55	8.8
8493-40.1	136.4	3434.4	17 42	23.3
8493-41.1	35 41	2908.5	9 47	5.8
8493-34.1	103.05	3318.2	15 64	28.1
8493-32.1	32.12	3383.9	8.22	3

Sample:	03sb026	03sb028	03sb029	03sb3149	04sb4261A	04sb4263
Pluton/Suite:	Hickey	Hickey	Hickey	Hickey	South	Mag
Rock Type:	Bt Mag Grdt	Bt Mag Grdt	Bt Mag Grdt	Bt Mag Grdt	Hbl Mag Granite	Mag Granite
Age (Ma):	2601	2601	2601	2601	2602	2599
Easting:	628950	634180	634180	627516	586056	599663
Northing:	7099044	7093817	7093817	7096173	6991244	6997500
		NAD 83				
SiO_2 (wt.%)	70.44	70.89	69.23	73.28	62.52	71.73
TiO_2	0.25	0 26	0.59	0.20	0.74	0.19
Al_2O_3	15 60	15.39	14.94	14.70	17.20	14.94
Fe_2O_3	1 94	1.88	2.50	1.70	5.31	1.89
MnO	0 02	0 02	0 01	0.02	0.07	0.02
MgO	1.00	0 59	1.12	0.55	1.87	0 65
CaO	2.61	2 24	1 84	3.11	4 55	2 48
Na_2O	4.08	4.51	3.33	4.48	4.10	3.96
K_2O	3.05	3.22	4 70	1.13	2.20	3 16
P_2O_5	0.07	0.08	0.09	0.04	0.27	0.08
LOI	0.20	0.00	0 60	0 50		
Total	99.23	99 42	99 02	99.29	99.05	99.23
XRF (ppm)						
Ni	bdl	bdl	bdl	bdl	1	bdl
Ga	17	18	18	16	19	16
Rb	64	48	70	35	62	82
Sr	341	623	442	213	509	241
Y	6	5	4	4	20	6
Zr	165	176	493	128	263	105
Nb	1	3	bdl	2	8	2
Ba	913	2220	4111	151	953	787
Ce	61	89	602	76	99	16
Pb	25	36	46	17	6	16
Th	15	29	161	22	4	5
U	bdl	bdl	3	2	bdl	1
ICP-MS (ppm)						
Nb	3.5	4.1	2 9	4 2	10.6	2.3
Zr	166.9	177 8	499 4	131 6	257	100 7
Y	6.33	4 87	8.55	2.71	19.22	4 78
Sr	336 3	637.9	459.4	206.4	503 4	235 8
Rb	67.55	48.97	62 84	31.25	63.35	79.94

Sample:	03sb026	03sb028	03sb029	03sb3149	04sb4261A	04sb4263
Pluton/Suite	Hickey	Hickey	Hickey	Hickey	South	Mag
Rock Type:	Bt Mag Grdt	Bt Mag Grdt	Bt Mag Grdt	Bt Mag Grdt	Hbl Mag Granite	Mag Granite
Age (Ma)*	2601	2601	2601	2601	2602	2599
Easting.	628950	634180	634180	627516	586056	599663
Northing:	7099044	7093817	7093817	7096173	6991244	6997500
ICP-MS (ppm) cont'd						
Ba					952.04	798
Cr					37.7	13.35
Co	7	4	7	3	11.14	4.08
Cu	15	N D.	N D.	N.D.	13.35	22.08
Ni	13	7	9	4	17.12	4.01
Sc	2.7	1.8	2.8	1.7	10.46	2.22
V	18.9	15.5	29 2	12	88.59	27.17
Zn	34	39	34	27	78.05	33.24
La	48.08	64 17	>100	39.29	45.73	21.91
Ce	85,48	98.56	>200	67.19	96.57	37.74
Pr	8.81	9.04	>25	6 67	11 54	3.73
Nd	30.75	27.48	>100	21.55	46.74	12.24
Sm	4 59	3.42	25 88	2.95	7.85	1.72
Eu	1.26	1.10	2 36	0.74	1 91	0.69
Gd	2.69	1.82	10.15	1.63	5.70	1.20
Tb	0.31	0.23	0 77	0.16	0.74	0.18
Dy	1.43	1.12	2.63	0 68	4.03	0.96
Ho	0.24	0.19	0 32	0.10	0.73	0 17
Er	0.59	0.42	0.69	0.25	1.97	0.47
Tm	0.08	0.05	0 07	0.03	0.26	0.06
Yb	0.45	0.39	0.58	0 24	1.64	0.36
Lu	0.07	0.05	0.07	0.04	0.24	0.05
Th	18.19	35.46	>100	18.20	6.75	5.33
Hf	4.40	4 60	12.00	3.60	5.60	2.60
Ta	0 19	N.D.	N.D.	0.32	0 52	0.25
$(La/Sm)_{CN}$	6.6	11.8	2.4	8.4	3.7	8.0
$(La/Yb)_{CN}$	72.2	111.2	116 5	110 6	18.8	41 1
A/CNK	1.06	1.03	1 07	1 03	0 99	1.03
K2O/Na2O	0.75	0 71	1.41	0.25	0.54	0.80
Rb/Sr	0.19	0.08	0.16	0.16	0.12	0 34

Notes: UTM in Zone 11 NAD 83. Bt-biotite; Mag- Magnetite; Hbl- Hornblende; Grdt- Granodiorite; Kspar Porph- K-feldspar Porphyritic; Musc- Muscovite.
Total Iron calculated as Al2O3. LOI- Loss on Ignition CN- Chondrite normalized.
A/CNK- molar Al2O3/(CaO+Na2O+K20). ND- no detection bdl- below detection limit

Sample:	04sb4266	04sb4267	03sb001	03sb002b	03sb003	03sb004
Pluton/Suite:	Wheeler Diorite	Germaine Diorite	Nardin Granodiorite	Nardin Granodiorite	Nardin Granodiorite	Nardin Gneiss
Rock Type:	Diorite	Quartz Diorite	Bt Mag Grdt	Bt Mag Grdt	Bt Mag Grdt	Grdt Gneiss
Age (Ma):	2608	2608	2630	2630	2630	2900
Easting:	612853	623288	644994	644994	644994	658595
Northing:	7030118	7022776	7050209	7050209	7050209	7054083
SiO_2 (wt.%)	50.62	55 22	71.87	71 91	73.34	71.38
TiO_2	1.61	1.14	0 21	0.26	0.18	0.18
Al_2O_3	13.74	15.94	15.49	15 10	14.67	15 03
Fe_2O_3	11.48	7.63	1.62	2.07	1 36	2 59
MnO	0.16	0 08	0 02	0 02	0.01	0.02
MgO	6.53	4.52	0 47	0 65	0.37	0.31
CaO	8 29	6 73	2.62	2 80	2 22	2.20
Na_2O	3.11	4.24	4.59	4.32	4 03	4.24
K_2O	1.31	1 83	2.60	2 39	3.38	3 28
P_2O_5	0.48	0.65	0 06	0 07	0.04	0.08
LOI			0.50	0 40	0.20	0.40
Total	97.55	98.20	99 66	99.71	99 72	99.83
XRF (ppm)						
Ni	60	29	bdl	bdl	bdl	bdl
Ga	7	19	20	20	18	17
Rb	41	66	60	65	73	65
Sr	504	858	284	262	199	500
Y	26	22	1	3	2	5
Zr	198	111	136	137	87	146
Nb	8	8	bdl	2	3	2
Ba	397	563	630	591	710	4381
Ce	106	119	34	23	20	29
Pb	4	2	15	15	17	10
Th	7	bdl	4	11	6	bdl
U	bdl	bdl	2	3	2	bdl
ICP-MS (ppm)						
Nb	8.4	6.8	2 2	2 9	1.6	1 1
Zr	199.5	112.1	138.1	147.4	93.8	160.1
Y	24.63	21.25	1.52	3.59	1	4 18
Sr	501.6	846.2	271.7	257 7	193 1	488.7
Rb	41.8	72.11	57.97	61.98	70.22	61.72

Sample:	04sb4266	04sb4267	03sb001	03sb002b	03sb003	03sb004
Pluton/Suite:	Wheeler Diorite	Germaine Diorite	Nardin Granodiorite	Nardin Granodiorite	Nardin Granodiorite	Nardin Gneiss
Rock Type	Diorite	Quartz Diorite	Bt Mag Grdt	Bt Mag Grdt	Bt Mag Grdt	Grdt Gneiss
Age (Ma)	2608	2608	2630	2630	2630	2900
Easting:	612853	623288	644994	644994	644994	658595
Northing:	7030118	7022776	7050209	7050209	7050209	7054083
ICP-MS (ppm) cont'd						
Ba	405.22	618 67				
Cr	161.36	42.99				
Co	39.17	27 11	3	5	4	4
Cu	35.66	35 15	N.D.	9	N D	N.D
Ni	102.46	51.94	4	8	4	5
Sc	21.68	18.53	1	1.3	0.9	0 8
V	189.26	193.75	15.4	20.4	8.6	17
Zn	126.66	88.89	39	38	26	27
La	52.69	43.25	14.14	21.60	12 28	31.04
Ce	120.75	102.27	22.40	37.73	19.87	50.53
Pr	14.84	13.30	2.28	3.75	1 96	4.70
Nd	61.04	57.23	7.56	12.45	6.40	15.27
Sm	11.03	10.78	1 08	1 79	0.89	2.03
Eu	3 04	2.62	0 69	0.68	0.73	1 47
Gd	8.42	7.98	0.65	1.15	0 51	1.29
Tb	1.06	0.93	0.07	0 14	0 05	0.15
Dy	5.53	4 58	0.32	0.72	0.22	0.85
Ho	0 96	0.81	0 06	0.13	0.04	0.16
Er	2 49	2.05	0 15	0.35	0.10	0 44
Tm	0.33	0.27	0.02	0.05	0.02	0 06
Yb	2.09	1 67	0.16	0 31	0 31	0.38
Lu	0.29	0.22	0 03	0.05	0.02	0.05
Th	8.22	5.96	2.34	4.94	2 33	5.95
Hf	4.80	3.00	3.70	3.90	2 70	4.00
Ta	0.44	0.43	N.D.	0.24	N.D	N.D.
$(La/Sm)_{CN}$	3.0	2.5	8.2	7.6	8.7	9.6
$(La/Yb)_{CN}$	17.0	17.5	59.7	47.1	26 8	55 2
A/CNK	0.64	0.75	1.02	1.02	1.02	1.04
K2O/Na2O	0.42	0.43	0.57	0 55	0 84	0 77
Rb/Sr	0.08	0.08	0 21	0 25	0.37	0.13

Sample:	03sb005	04sb4259	04sb4260A	04sb4260B	03sb008	03sb022
Pluton/Suite:	Nardin Gneiss	Mosher	Mosher	Mosher	Armi	Armi
Rock Type:	Grdt Gneiss	Bt Granite	Bt Gran	Bt Gran	Bt Grdt	Bt Grdt
Age (Ma):	2900	2600	2600	2600	2600	2600
Easting:	658595	576807	590198	590198	637503	637503
Northing:	7054083	7002321	6998861	6998861	7047285	7047285
SiO_2 (wt.%)	73 21	71.23	68.43	68.47	70 21	71 92
TiO_2	0.22	0.24	0.41	0.41	0.33	0 25
Al_2O_3	14.46	14 39	15.92	15.73	15.39	14.61
Fe_2O_3	1.82	2.55	2.81	2.84	2 74	1.99
MnO	0.02	0.03	0.03	0 03	0 04	0.02
MgO	0 45	0.61	0.97	0.97	0 85	0.60
CaO	1.91	1 30	2.85	2.83	2.57	1 70
Na_2O	4.22	3 78	4.11	4.17	4.22	3 62
K_2O	3 33	4.24	3.27	3 10	2.89	4.32
P_2O_5	0 07	0.09	0.13	0.13	0.11	0.09
LOI	0.60				1 40	0.30
Total	99.85	98.64	99.09	98.84	99.49	99.24
XRF (ppm)						
Ni	bdl	bdl	bdl	bdl	bdl	bdl
Ga	19	19	20	17	20	19
Rb	80	142	111	118	105	166
Sr	273	129	318	312	284	131
Y	3	33	8	9	5	13
Zr	158	214	156	162	157	129
Nb	5	10	6	6	6	8
Ba	607	1004	687	646	664	549
Ce	67	146	52	52	40	72
Pb	27	26	17	15	22	39
Th	24	29	8	12	25	28
U	4	11	bdl	2	2	8
ICP-MS (ppm)						
Nb	6.3	11.7	5 5	5.7	6.5	9 5
Zr	156 8	249.6	175.8	174.2	168 9	133.2
Y	4.75	34.88	7.24	7.3	5.56	11 55
Sr	264.5	133.4	311.5	308.6	281	127.1
Rb	77 06	146 36	111.38	119.08	101.79	>150 00

Sample:	03sb005	04sb4259	04sb4260A	04sb4260B	03sb008	03sb022
Pluton/Suite:	Nardin Gneiss	Mosher	Mosher	Mosher	Armi	Armi
Rock Type	Grdt Gneiss	Bt Granite	Bt Gran	Bt Gran	Bt Grdt	Bt Grdt
Age (Ma)*	2900	2600	2600	2600	2600	2600
Easting:	658595	576807	590198	590198	637503	637503
Northing:	7054083	7002321	6998861	6998861	7047285	7047285
ICP-MS (ppm) cont'd						
Ba		1133.65	799.01	739.96		
Cr		15.37	20.37	19 89		
Co	4	2 64	7.13	6.95	8	5
Cu	3	4 47	11.44	12.78	N.D.	N.D.
Ni	5	3.57	8.45	8.26	11	7
Sc	1.6	5 77	4.99	4.78	3.5	2.7
V	12.8	22.79	55.2	51.91	29.9	15.7
Zn	43	60.22	62.19	61.94	57	49
La	40.29	75.30	30.80	38.27	44.71	40.71
Ce	65.31	153.42	69.34	72 82	80.80	76.62
Pr	6.19	17.70	6.81	7.88	8 35	8.21
Nd	19.83	67.74	24.40	28.27	29.11	28.57
Sm	2 91	12.46	4.01	4.33	4.42	4.97
Eu	0.77	1.71	0.87	0.89	0 93	0.73
Gd	1.92	9.89	2.59	2.78	2.76	3.49
Tb	0.22	1.33	0.32	0.32	0.29	0.46
Dy	1.06	7.13	1.57	1.54	1.38	2.32
Ho	0 18	1.31	0.28	0 27	0.23	0.40
Er	0 47	3.48	0.73	0 74	0.56	1.09
Tm	0.06	0.48	0 10	0 10	0.07	0.16
Yb	0.38	3.02	0.65	0.62	0.48	1.03
Lu	0.06	0.43	0.10	0.09	0.07	0.14
Th	20.19	20 56	10.51	12.12	26.64	25.94
Hf	4.20	7.10	4 50	4.40	4.60	4 10
Ta	0.39	0.94	0.45	0.47	0.45	0.64
$(La/Sm)_{CN}$	8.7	3 8	4.8	5.6	6.4	5.2
$(La/Yb)_{CN}$	71.6	16.8	32.0	41.7	62.9	26.7
A/CNK	1 03	1.09	1.03	1.02	1 04	1.06
K2O/Na2O	0 79	1.12	0.79	0.74	0.68	1.19
Rb/Sr	0 29	1 10	0.35	0.38	0.37	1.27

Sample:	03sb023	03sb031	04sb4262	04sb4264	04sb4265	03sb009
Pluton/Suite:	Arml	Arml	Wecho	Wecho	Wecho	Wecho
Rock Type:	Bt Grdt	Bt Grdt	Kspar Porph Granite	Kspar Porph Granite	Kspar Porph Granite	Kspar Porph Granite
Age (Ma):	2600	2600	2591	2591	2591	2591
Easting:	637503	633719	587686	612413	617413	643544
Northing:	7047285	7063199	6988877	6999441	6999441	7064411
SiO_2 (wt.%)	72.46	72.96	66 71	73.00	68.10	67.82
TiO_2	0.20	0.24	0.58	0 13	0.61	0.51
Al_2O_3	14 51	14.41	15.44	14.03	14.79	15 76
Fe_2O_3	1.62	2.31	3.93	1.06	4 16	3.63
MnO	0 02	0.02	0 04	0.02	0.04	0.04
MgO	0.48	0.74	1.54	0.56	0.91	1.22
CaO	1.52	1 26	2.79	1 09	2 59	2.51
Na_2O	3 45	3.40	3.55	2 98	3.38	3 73
K_2O	4.96	3.77	3.66	5.85	4.11	4.05
P_2O_5	0.10	0.11	0.19	0 10	0.24	0.22
LOI	0.20	0.50				0.60
Total	99.44	99 36	98 64	98.98	99.12	99.73
XRF (ppm)						
Ni	bdl	bdl	bdl	bdl	bdl	bdl
Ga	18	19	14	11	21	19
Rb	175	120	94	155	156	126
Sr	127	162	320	210	201	430
Y	9	14	14	10	15	19
Zr	120	104	205	78	296	224
Nb	7	9	10	2	10	10
Ba	569	737	944	1095	851	1221
Ce	44	34	144	18	102	175
Pb	46	30	13	28	25	20
Th	26	18	14	10	31	21
U	12	6	1	2	5	0
ICP-MS (ppm)						
Nb	7.3	8 3	3.9	9 5	12.3	10.5
Zr	131.9	97.1	90.6	179.2	316.2	180.6
Y	9.42	12 7	8.67	13.42	15 68	16.84
Sr	126.4	163.8	207.2	300.5	197	419
Rb	>150.00	117.75	>150 00	88.47	>150.00	123.7

Sample	03sb023	03sb031	04sb4262	04sb4264	04sb4265	03sb009
Pluton/Suite:	Armi	Armi	Wecho	Wecho	Wecho	Wecho
Rock Type·	Bt Grdt	Bt Grdt	Kspar Porph Granite	Kspar Porph Granite	Kspar Porph Granite	Kspar Porph Granite
Age (Ma).	2600	2600	2591	2591	2591	2591
Eastıng:	637503	633719	587686	612413	617413	643544
Northing:	7047285	7063199	6988877	6999441	6999441	7064411
ICP-MS (ppm) cont'd						
Ba			1028.38	1174.7	870.43	
Cr			29.78	14.79	24.62	
Co	4	5	8 68	2.1	7 54	9
Cu	N D.	N.D	12.39	3.27	12.34	11
Ni	5	11	12.68	4.03	8.26	11
Sc	2 2	2.9	7.92	2.49	7.02	3.9
V	12.3	19 7	65.34	20.07	52 48	49.1
Zn	35	46	63.28	21.2	66.93	59
La	31.87	32 95	89.51	17.45	49.52	92.41
Ce	62.24	64 82	172 38	35.46	100.46	171.03
Pr	6.74	7.21	18.10	3.73	11.48	17.75
Nd	24 19	26.26	62.65	13.40	44.71	59.80
Sm	4 31	4.80	8.48	2.48	7.56	8.80
Eu	0.71	0.76	1.83	0.78	1.56	1.74
Gd	2.99	3 60	5.40	2.05	5.57	5 43
Tb	0.39	0.48	0 64	0.29	0 69	0.70
Dy	1.94	2.46	3.18	1.61	3.45	3.80
Ho	0.33	0.44	0 54	0.30	0.62	0.65
Er	0 89	1.19	1.37	0.87	1.54	1.63
Tm	0.12	0.16	0 18	0.13	0.18	0.20
Yb	0 80	1.04	1.03	0.86	1.10	1.13
Lu	0.12	0.14	0 14	0.13	0.16	0.14
Th	21.11	16 06	13.09	12.18	21.38	18.75
Hf	4.00	3.00	3 00	4.20	7.70	4 40
Ta	0.42	0.77	0.29	0.43	0.52	0.69
$(La/Sm)_{CN}$	4.7	4.3	6.6	4.4	4.1	6.6
$(La/Yb)_{CN}$	26.9	21 4	58 7	13 7	30 4	55 3
A/CNK	1.05	1 20	1 04	1.06	1.00	1.05
K2O/Na2O	1.44	1 11	1 03	1.96	1.22	1 08
Rb/Sr	1.38	0 74	0 29	0 74	0.78	0.29

Sample.	03sb010	03sb011	03sb013	03sb014	03sb015	03sb016
Pluton/Suite:	Wecho	Wecho	Wecho	Wecho	Wecho	Wecho
Rock Type·	Kspar Porph Granite	Kspar Porph Granite	Kspar Porph Granite	Kspar Porph Granite	Kspar Porph Granite	Kspar Porph Granite
Age (Ma):	2591	2591	2591	2591	2591	2591
Easting:	643544	631434	613379	605294	605294	605294
Northing	7064411	7069745	7043385	7043094	7043094	7043094
SiO_2 (wt %)	66 09	72.37	71 27	69 08	72 44	68.29
TiO_2	0.59	0.26	0 32	0.42	0.23	0.52
Al_2O_3	15.95	13.87	14 79	15.38	14.64	15 35
Fe_2O_3	4.31	2 38	2.63	3.28	1.92	4 19
MnO	0.06	0.02	0.03	0.04	0.03	0.05
MgO	1.63	0.79	0.65	0.86	0.57	0.99
CaO	2.80	1.15	1.76	1.95	1.50	2.30
Na_2O	3.93	2 79	3.78	4.01	3.93	4.23
K_2O	3.28	5.58	4.07	4.04	4.16	3.09
P_2O_5	0 29	0.10	0 16	0.21	0.06	0.21
LOI	0.00	0.00	0 30	0.30	0.20	0.20
Total	99.17	99.51	99.64	99.45	99.62	99.37
XRF (ppm)						
Ni	bdl	bdl	bdl	bdl	bdl	bdl
Ga	20	18	22	23	19	26
Rb	135	180	181	176	147	158
Sr	436	270	179	196	165	213
Y	21	11	14	16	6	19
Zr	251	98	184	211	151	256
Nb	9	9	9	13	7	16
Ba	866	1170	712	772	612	594
Ce	214	79	66	81	35	66
Pb	18	27	31	38	44	26
Th	20	24	23	24	31	22
U	1	3	8	11	13	7
ICP-MS (ppm)						
Nb	10.3	8.1	11.5	14.4	6.8	17.1
Zr	283.9	88 4	192 9	246.3	163.2	248.9
Y	21.68	6.37	13.99	18.79	7 5	17 73
Sr	418.5	268	170 3	184.4	159.9	208 2
Rb	133.63	>150 00	>150 00	150	141 91	150

Sample.	03sb010	03sb011	03sb013	03sb014	03sb015	03sb016
Pluton/Suite:	Wecho	Wecho	Wecho	Wecho	Wecho	Wecho
Rock Type.	Kspar Porph Granite	Kspar Porph Granite	Kspar Porph Granite	Kspar Porph Granite	Kspar Porph Granite	Kspar Porph Granite
Age (Ma):	2591	2591	2591	2591	2591	2591
Easting:	643544	631434	613379	605294	605294	605294
Northing	7064411	7069745	7043385	7043094	7043094	7043094
ICP-MS (ppm) cont'd						
Ba						
Cr						
Co	10	5	6	7	4	8
Cu	14	6	N.D	6	N.D.	8
Ni	14	13	8	11	7	12
Sc	6.1	3.2	3.4	4 7	2.9	5.1
V	51.4	20 3	20.2	31	11.3	31.1
Zn	74	43	61	86	48	93
La	>100	32.41	47.12	49.79	44.76	50.64
Ce	>200	62 28	92.71	99 53	84.11	97.21
Pr	22.51	7.02	10.65	11.04	8.98	10.94
Nd	79.72	24.74	39.65	40.99	31.52	40.00
Sm	11.66	4.20	7.18	7 10	5.62	6.30
Eu	1.74	0.89	1.15	1.09	0 84	1.19
Gd	7.03	2.67	5.08	5 10	3.72	4.43
Tb	0 88	0.33	0.60	0 71	0.43	0.62
Dy	4.67	1 52	3.09	3.88	1.99	3.46
Ho	0.82	0.24	0 53	0 71	0.30	0.66
Er	2.15	0.56	1.46	1.96	0.70	1.85
Tm	0.28	0.06	0 20	0 25	0.08	0.24
Yb	1.64	0.39	1.37	1 52	0.51	1.41
Lu	0.21	0.05	0 20	0.22	0.07	0.20
Th	22.70	17.66	19.09	23.36	24 59	17.10
Hf	6.90	2.70	5.70	7 10	4.80	6.80
Ta	0.63	0.57	1 11	0.92	0.51	1.08
$(La/Sm)_{CN}$	5.4	4.9	4 1	4.4	5.0	5.1
$(La/Yb)_{CN}$	41.2	56.2	23.2	22.1	59.3	24 3
A/CNK	1.06	1 09	1 07	1 06	1.07	1.06
K2O/Na2O	0.83	2.00	1.08	1.01	1 06	0 73
Rb/Sr	0.31	0.67	1.01	0.90	0.89	0.74

Sample.	03sb018	03sb019	03sb021B	03sb012	03sb017	03sb024
Pluton/Suite:	Wecho	Wecho	Wecho	Mofee	Mofee	Mofee
Rock Type:	Kspar Porph Granite	Kspar Porph Granite	Kspar Porph Granite	Bt Musc Granite	Bt Musc Granite	Bt Musc Granite
Age (Ma).	2591	2591	2591	2591	2591	2591
Easting	621925	621925	644660	631493	620483	618828
Northing	7078497	7078497	7057427	7069712	7051582	7046533
SiO_2 (wt.%)	70.23	68.86	72.30	72.38	74 54	70.89
TiO_2	0 35	0.46	0.24	0.18	0.12	0.33
Al_2O_3	15.40	15.45	14.49	14 88	13 90	15.37
Fe_2O_3	2.38	3.31	1 84	1.47	1.39	2.09
MnO	0.01	0 01	0.01	0 02	0.02	0.02
MgO	1.00	1.35	0 45	0.57	0 25	1.30
CaO	1.87	1.75	0.97	1.93	0.84	2.11
Na_2O	4.04	3 45	3.66	4.13	3 43	4.40
K_2O	3.72	4.49	5.19	3.47	5.14	2.32
P_2O_5	0.11	0 10	0.17	0.11	0.19	0.07
LOI	0.40	0.50	0 30	0.30	0 00	0.40
Total	99.28	99 43	99.47	99.27	99 93	99.06
XRF (ppm)						
Ni	bdl	bdl	bdl	bdl	bdl	bdl
Ga	20	22	23	19	20	20
Rb	136	142	300	117	248	75
Sr	344	372	91	355	68	310
Y	7	6	11	6	13	8
Zr	142	126	154	109	82	188
Nb	9	12	12	5	12	5
Ba	716	941	492	765	251	733
Ce	102	80	105	10	37	90
Pb	24	26	39	23	35	22
Th	21	20	43	4	17	25
U	bdl	6	14	bdl	9	2
ICP-MS (ppm)						
Nb	8.9	13.4	12 2	5 1	12.9	5.7
Zr	145.2	127.3	161.7	125 4	91.5	194.2
Y	7.3	5.21	10.98	5.91	11.24	7.8
Sr	352.6	378.3	87.4	339	63.4	311.8
Rb	138.5	139.28	150	116 97	150	71.95

Sample	03sb018	03sb019	03sb021B	03sb012	03sb017	03sb024
Pluton/Suite:	Wecho	Wecho	Wecho	Mofee	Mofee	Mofee
Rock Type·	Kspar Porph Granite	Kspar Porph Granite	Kspar Porph Granite	Bt Musc Granite	Bt Musc Granite	Bt Musc Granite
Age (Ma)·	2591	2591	2591	2591	2591	2591
Easting:	621925	621925	644660	631493	620483	618828
Northing.	7078497	7078497	7057427	7069712	7051582	7046533
ICP-MS (ppm) cont'd						
Ba						
Cr						
Co	6	9	4	4	2	6
Cu	N.D.	8	3	N.D.	N.D.	N.D.
Ni	9	16	6	6	N.D.	8
Sc	2.6	2.3	2 4	2	2.2	3.5
V	29.2	53 4	10.6	11.4	4	26.8
Zn	46	53	70	33	37	36
La	53.63	41.28	47.08	30 59	19.15	50 06
Ce	103.61	82.16	101.71	57.07	40 89	88.31
Pr	11.59	8.93	12.04	6 07	4.68	9.06
Nd	41.98	32.24	45.54	21.04	17 14	31.26
Sm	6 46	5.22	8.48	3.18	3.60	4.28
Eu	1.40	1.36	0.57	0 80	0.36	1.23
Gd	3 67	3.23	4.78	1 85	2.86	2.43
Tb	0.39	0.35	0.51	0 23	0.43	0.31
Dy	1.77	1.42	2 47	1.20	2.31	1.60
Ho	0.26	0.19	0.39	0 21	0.38	0.27
Er	0.60	0.36	1.02	0.56	1 03	0 68
Tm	0.07	0.04	0.13	0 07	0.15	0.09
Yb	0.45	0.21	0.81	0.41	1 07	0.49
Lu	0.06	0.03	0.11	0.06	0.13	0.08
Th	23.39	14.19	40.59	14 39	13.40	22.32
Hf	3.60	3.00	4.80	3 60	3.00	5.00
Ta	0.48	0 63	0.55	0.41	1 50	0.33
$(La/Sm)_{CN}$	5.2	5 0	3.5	6 1	3.3	7.4
$(La/Yb)_{CN}$	80.5	132.8	39.3	50.4	12.1	69.0
A/CNK	1.09	1.13	1.08	1 06	1.09	1 13
K2O/Na2O	0.92	1.30	1 42	0.84	1.50	0.53
Rb/Sr	0.40	0 38	3.30	0 33	3.65	0.24

Sample:	03sb020	03sb025	03sb027	03sb030	04lo1026	04lo1069
Pluton/Suite:	Dauphinee	Mafic Enclave	Mafic Enclave	Mafic Enclave	Mosher Volcanics	Mosher Volcanics
Rock Type.	Enderbite	Mafic Enclave	Mafic Enclave	Mafic Enclave	Mafic Violcanic	Mafic Volcanic
Age (Ma)	2592	2700	2700	2700	2650	2650
Easting:	616604	631142	628950	634180	579299	578684
Northing:	7085037	7096865	7099044	7093817	7001458	7000117
SiO_2 (wt.%)	53 35	50.65	47 16	49.86	48.68	48.98
TiO_2	2.22	0.80	1.17	0 97	1 01	1.72
Al_2O_3	15.68	13.35	14.72	6.29	15 95	14 03
Fe_2O_3	12 04	11.81	16.04	13.84	13 49	16.69
MnO	0 13	0.21	0.24	0.23	0.28	0.18
MgO	3.68	8.00	7.74	16 44	5.10	5 52
CaO	6.88	10 80	10.36	9.31	10 00	8.24
Na_2O	3.45	2.32	1.28	0.97	2.75	2.47
K_2O	0.98	0.41	0 18	0.43	0.57	0.22
P_2O_5	0.54	0.08	0.11	0.07	0 09	0 19
LOI	0.10	0 50	0.00	0.50		
Total	99.10	98.57	99.10	98.67	98.03	98.34
XRF (ppm)						
Ni	bdl	68	85	570	68	42
Ga	21	15	18	11	11	16
Rb	33	5	10	9	13	7
Sr	423	290	96	84	149	159
Y	25	21	26	15	24	37
Zr	116	53	61	80	58	114
Nb	8	6	3	12	4	6
Ba	403	213	48	140	173	55
Ce	27	14	9	1	bdl	bdl
Pb	10	9	7	6	1	7
Th	4	2	9	2	5	7
U	2	bdl	5	1	bdl	1
ICP-MS (ppm)						
Nb	9.7	3.9	3	12.1	2.7	5.8
Zr	153.3	57.4	65.8	84.5	61.5	122 7
Y	25.97	18.82	25.17	12 77	21 53	35 5
Sr	438 8	298.1	98.3	86	150.3	162.7
Rb	28.25	2 58	3.83	6.64	9.05	1.94

Sample:	03sb020	03sb025	03sb027	03sb030	04lo1026	04lo1069
Pluton/Suite:	Dauphinee	Mafic Enclave	Mafic Enclave	Mafic Enclave	Mosher Volcanics	Mosher Volcanics
Rock Type.	Enderbite	Mafic Enclave	Mafic Enclave	Mafic Enclave	Mafic Violcanic	Mafic Volcanic
Age (Ma):	2592	2700	2700	2700	2650	2650
Easting:	616604	631142	628950	634180	579299	578684
Northing:	7085037	7096865	7099044	7093817	7001458	7000117
ICP-MS (ppm) cont'd						
Ba					160.65	45 48
Cr					288.84	136.76
Co	28	47	58	74	54 68	46.02
Cu	8	36	145	114	27 16	78.11
Ni	22	102	120	625	107.98	72 56
Sc	14.6	31.9	34	21	46.61	38 44
V	197.8	217.2	291.7	156.8	>300 00	266.76
Zn	135	108	130	116	105 14	129.14
La	27.92	14.67	4.16	16.00	3.92	7.40
Ce	60.59	32 67	10.44	34 40	10.44	19 72
Pr	7.74	4.28	1 62	4.38	1.57	2.92
Nd	33.18	18.44	8.43	18.17	8 01	14 78
Sm	7.13	4.11	2.73	3.67	2.50	4 40
Eu	2.09	1.33	0.95	1.20	0 91	1.43
Gd	6 45	3.89	3.74	3.29	3.26	5.60
Tb	0.92	0.60	0.66	0.47	0.59	0 98
Dy	5.16	3 67	4.58	2.77	3.73	6 35
Ho	0.97	0.72	0.96	0.52	0 81	1.33
Er	2.63	2.08	2.92	1.37	2 48	3.98
Tm	0.35	0.30	0.44	0.19	0.37	0 59
Yb	2.25	1.96	3.01	1.20	2.44	3 98
Lu	0.32	0.29	0 45	0.17	0 37	0.60
Th	1.56	0.65	0.19	1.75	0.47	0 84
Hf	3.60	1.60	1.80	2.30	1.70	3.40
Ta	0.59	0 27	0.19	0.74	0 18	0 35
$(La/Sm)_{CN}$	2.5	2.2	1 0	2.7	1.0	1.1
$(La/Yb)_{CN}$	8.4	5 1	0.9	9.0	1.1	1.3
A/CNK	0.81	0.56	0.70	0 33		
K2O/Na2O	0.29	0.18	0.14	0.44	0 21	0.09
Rb/Sr	0.08	0.02	0.10	0.11	0 09	0.04

Sample:	03lo1192	03sb006	03sb007		
Pluton/Suite:	Germaine Volcanics	Nardin Mafic	Nardin Mafic		
Rock Type.	Mafic Violcanic	Mafic Dyke	Mafic Dyke	**Detection Limits**	**Precision**
Age (Ma).	2650			ppm	Ave, Diff. %
Easting:	622001	658595	658595		*based on runs over
Northing:	7022217	7054083	7054083		the past 5 years
SiO_2 (wt.%)	49.42	46 21	45.97	0.01	0.71
TiO_2	1.31	0.75	1.41	0.01	2.74
Al_2O_3	14.42	12.84	14.96	0 01	3 39
Fe_2O_3	14.93	11.48	14.15	0.01	1.34
MnO	0 23	0 19	0 22	0.01	6 51
MgO	6.09	12.50	8.04	0.01	0.84
CaO	8.53	10.50	9.34	0.01	1.26
Na_2O	3.24	1.64	2.45	0 01	7.45
K_2O	0.25	0.98	1 41	0 01	6.48
P_2O_5	0.14	0.05	0.24	0.01	14.24
LOI	0.70	2.10	1.20	0.01	5.76
Total	98.66	97.36	98.31		
XRF (ppm)					
Ni	42	320	167	0.01	
Ga	18	12	18	0 01	
Rb	8	35	37	0.01	
Sr	125	80	172	0.01	
Y	33	14	16	0.01	
Zr	97	35	51	0.01	
Nb	5	3	5	0 01	
Ba	43	85	135	0 01	
Ce	bdl	23	bdl	0 01	
Pb	6	4	9	0.01	
Th	3	4	2	0.01	
U	2	1	2	0.01	
ICP-MS (ppm)					
Nb	4 5	1 7	3 9	0.2	3
Zr	101	34 5	52.5	4	1.6
Y	30.39	12.04	15 14	0.02	4.52
Sr	128.9	79	168.8	0.5	3.42
Rb	2.68	32 15	37 55	0 5	9.03

Sample:	03lo1192	03sb006	03sb007	Detection Limits	Precision
Pluton/Suite·	Germaine Volcanics	Nardin Mafic	Nardin Mafic	ppm	Ave, Diff. %
Rock Type:	Mafic Violcanic	Mafic Dyke	Mafic Enclave		*based on runs over
Age (Ma):	2650				the past 5 years
Easting:	622001	658595	658595		
Northing:	7022217	7054083	7054083		
ICP-MS (ppm) cont'd					
Ba				0.6	7.05
Cr				8	6.97
Co	44	65	53	0.1	3.92
Cu	85	65	53	0.7	16.51
Ni	67	365	204	0.8	5.32
Sc	31	27 3	21.3	0.6	1.03
V	284.7	199.6	192.4	1	1.76
Zn	121	101	135	3	7.48
La	6.67	2.49	10 29	0.02	4 81
Ce	16.92	6.27	21.70	0.07	3.93
Pr	2 53	0 97	2.68	0.006	5.63
Nd	12.51	5.03	11.84	0.03	2.99
Sm	3.68	1.62	2 81	0.01	5 23
Eu	1.23	0.63	1.21	0.005	11.77
Gd	4.68	2.08	3.11	0.009	10.31
Tb	0.83	0.35	0.49	0 003	9.26
Dy	5.53	2.35	3.03	0.008	5.62
Ho	1.16	0.48	0.60	0.003	1.8
Er	3.54	1 40	1 73	0.008	6.66
Tm	0.53	0.20	0.24	0.003	6.09
Yb	3.46	1.25	1.52	0.01	6.1
Lu	0.53	0 19	0 23	0.003	8.97
Th	1.02	0 22	0.79	0.06	4.91
Hf	2 80	1.10	1.50	0.1	4 48
Ta	0.30	N D	0.24	0.17	5
$(La/Sm)_{CN}$	1.1	1 0	2 3		
$(La/Yb)_{CN}$	1 3	1 3	4 6		
A/CNK		0 56	0 66		
K2O/Na2O	0.08	0.60	0.57		
Rb/Sr	0.06	0.44	0.22		

Pluton/Suite	Sample Number	Age[a] Ma	Nd ppm	$^{143}Nd/^{144}Nd$ [b]	$^{143}Nd/^{144}Nd$ Error 2δ	Sm ppm	$^{147}Sm/^{144}Nd$	$^{143}Nd/^{144}Nd_i$	$E_{Nd}{}^{T}$ [c]
Hickey	03sb028	2601	27 48	0 510713	4 435E-06	3.42	0.2217	0.508913	-6.88
Hickey	03sb029	2601	100.00	0 510872	1 543E-05	25 88	0.2692	0.509197	-1.31
Hickey	03sb026	2601	30 75	0.511153	1 048E-05	4.59	0.2598	0.509117	-2.87
Hickey	03sb3149	2601	21 55	0.511273	1 208E-05	2.95	0.1808	0.509118	-2.86
Hickey	03sb028	2601	27.48	0.510688	7 090E-06	3.42	0 2235	0.508878	-7.58
Mag	04sb4263	2599	12.24	0.510868	1.272E-05	1.72	0 7913	0.510700	28.16
South	04sb4261A	2602	46 74	0.511615	1 350E-05	7.85	0.2961	0.509301	0.85
Germaine Diorite	04sb4267	2608	57.23	0.511639	6 529E-06	10.78	0 3175	0.509166	-1.71
Wheeler Diorite	04sb4266	2608	61 04	0 511735	4 400E-06	11.03	0.2900	0.509313	1.18
Nardin Grdt	03sb002b	2630	12 45	0.511272	1 579E-05	1.79	0.2584	0.509185	-0.80
Nardin Grdt	03sb001	2630	7.56	0.511028	1.039E-05	1.08	0 3297	0.509179	1.67
Nardin Grdt	03sb001	2630	7.56	0 511226	4 924E-06	1.08	0.2325	0.509244	0.20
Nardin Gneiss	03sb004	2900	15 27	0.510439	8 074E-06	2.03	0 2801	0.508364	-1.64
Nardin Gneiss	03sb005	2900	19.83	0 511452	1 023E-05	2.91	0.1410	0.508457	-0.42
Mosher	04sb4259	2600	67.74	0.511741	8 702E-06	12.46	0.3157	0.509277	0.23
Mosher	04sb4260	2600	24.40	0.511286	4.255E-06	4.33	0.4299	0.509273	0.16
Mosher	04sb4260	2600	24.40	0.511285	1.317E-05	4.33	0.3734	0.509357	1.82
Armi	03sb023	2600	24.19	0 511831	3 942E-06	4.31	0.2581	0.509245	-0.39
Armi	03sb022	2600	28.57	0 511752	1.663E-05	4 97	0.2504	0.509269	0.08
Armi	03sb008	2600	29.11	0.511458	1.465E-05	4 42	0.2465	0.509489	4.41
Armi	03sb031	2600	26.26	0.511628	5 119E-06	4.80	0.3128	0.509192	-1.43
Wecho	04sb4262	2591	62.65	0.511154	7.744E-06	8.48	0.3156	0.509310	0.66
Wecho	04sb4265	2591	44.71	0.511449	1.374E-05	7.56	0.3696	0.509288	0 22
Wecho	03sb009	2591	59.80	0.511260	1 121E-05	8 80	0 2468	0.509187	-1.76
Wecho	03sb014	2591	40.99	0.511665	1 933E-05	7.10	0 2789	0.509279	0 04
Wecho	03sb021B	2591	45 54	0.511832	1 004E-05	8.48	0.2706	0 509255	-0.42
Wecho	04sb4264	2591	13.40	0.511693	9 522E-06	2.48	0 3250	0.509279	0.06
Wecho	03sb014	2591	40.99	0 511778	1.570E-05	7.10	0 2364	0.509272	-0.10
Wecho	03sb011	2591	24 74	0 511474	7.525E-06	4.20	0 3115	0.509229	-0 93
Wecho	03sb013	2591	39.65	0.511896	4 526E-06	7.18	0.2385	0.509320	0.85
Wecho	03sb015	2591	31 52	0 511796	9.666E-06	5.62	0.2293	0.509264	-0 25
Wecho	03sb018	2591	41 98	0.511663	9 619E-06	6.46	0 1833	0 509278	0 03

Pluton/Suite	Sample Number	Age[a] Ma	Nd ppm	$^{143}Nd/^{144}Nd$ [b]	$^{143}Nd/^{144}Nd$ Error 2δ	Sm ppm	$^{147}Sm/^{144}Nd$	$^{143}Nd/^{144}Nd_i$	$\varepsilon_{Nd}(T)$ [c]
Mofee	03sb017	2591	17.14	0.512150	8 922E-06	3.60	0.3261	0.509294	0 35
Mofee	03sb012	2591	21.04	0 511701	4 678E-06	3 18	0.1856	0.509260	-0.33
Mofee	03sb024	2591	31.26	0.511217	4.024E-06	4 28	0.2401	0.509268	-0.17
Dauphinee	03sb020	2592	33.18	0.512083	1.273E-05	7.13	0.3354	0.509296	0.40
Mafic Enclave	03sb027	2700	8.43	0.513253	7.702E-06	2.73	0 2925	0.510855	33.10
Mafic Enclave	03sb030	2700	18.17	0 511801	7.712E-06	3.67	0 3438	0 509113	-1.24
Mafic Enclave	03sb025	2700	18.44	0.512213	1.669E-05	4 11	0.3882	0.508520	-13.24
Mafic Enclave	03sb027	2700	8.43	0.513415	5.079E-06	2.73	0.3381	0.509643	8.84
Mosher Volcanics	04lo1026	2640	8.01	0.513212	2.554E-05	2.50	0.3923	0.509350	2.71
Mosher Volcanics	04lo1069	2640	14.78	0.513224	1 050E-05	4.40	0 3552	0 509292	1.57
Germaine Volcanics	03lo1192	2640	12.51	0 512997	7.830E-06	3 68	0.3935	0 509260	0.94
Nardin Mafic	03sb006	2850	5.03	0.513287	4 531E-06	1 62	0.3766	0.508981	2.15
Nardin Mafic	03sb007	2800	11.84	0 511931	7.713E-06	2.81	0.4763	0.508879	-2.44

a Age assumed in initial ratio calculation

b. Measured present day values for 143Nd/144Nd.

c. Errors for Epsilon Nd(T) is ±0.8 based on duplicate runs of samples. i = initial values.

NOTE TO USERS

Oversize maps and charts are microfilmed in sections in the following manner:

LEFT TO RIGHT, TOP TO BOTTOM, WITH SMALL OVERLAPS

This reproduction is the best copy available.

UMI

UNIT DESCRIPTIONS

Quaternary

Q — Undifferentiated Sand and Gravel: reworked eskers and glacial till.

Esker

Proterozoic

Diabase Dyke: undifferentiated; brown; medium grained; locally contains plagioclase phenocrysts up to 3 centimetres; locally magnetic; generally 10 to 30 metres wide, but locally up to 70 metres wide. Individual thickness exaggerated on map due to scale. The ~345° trending dykes are likely part of the Indin swarm (ca. 2200 Ma; Fahrig and West, 1986); the ~70° trending dykes are likely part of the Malley, Mackay, or Dogrib swarm, (Fahrig and West, 1986). The 020° trending dykes are interpreted to be part of a previously undefined swarm (ca. 1885 Ma; Allonson, 2004).

Dyke: interpreted from aeromagnetic signature.

Archean

Plutonic Rocks

Granitic Pegmatite: biotite ± muscovite-bearing; locally contains abundant tourmaline, rare garnet, andalusite, sillimanite, lipidolite, apatite, and uranium staining; north of Germaine Lake, two generations of pegmatite are identified, one generation contains tourmaline and sillimanite, or garnet, the other is generally only tourmaline-bearing.

Syeno- to Monzogranite: medium to coarse grained; equigranular to moderately alkali feldspar porphyritic; biotite ± muscovite-bearing, but generally mica-poor; massive to weakly foliated; commonly contains xenoliths of supracrustal rocks, notably sedimentary rocks and local mafic rocks; locally uranium-stained; may, in part, be equivalent to Awry Suite as defined by Henderson (1985).

Porphyritic Syeno- to Monzogranite: medium to coarse grained; moderately to coarsely microcline porphyritic; biotite ± magnetite, muscovite; weakly to moderately foliated (defined by biotite and microcline phenocrysts), equivalent to parts of Stagg Suite as defined by Henderson (1985); ca 2591 ± 8 Ma (Ootes et al., 2005)

Potassium Feldspar Porphyritic Granite: undifferentiated Agkk and Agkm; generally a mix of both units and not separable on map scale; commonly intermingled with and cutting Agdm.

Charno-enderbite to Enderbite (granodioritic to tonalitic composition): orthopyroxene-bearing; yellow to orange-brown; equigranular to inequigranular; fine to medium grained; contains plagioclase + hornblende + biotite + magnetite ± cummingtonite, clinopyroxene, orthopyroxene, K-feldspar, quartz, garnet; granofels texure; biotite pseudomorphs after megascopic orthopyroxene are common; interpreted to be intrusive rocks that likely intruded during granulite-grade metamorphism; ca. 2590 ± 2.3 Ma (Ootes et al., 2005).

Magnetite Granite: pink; equigranular; medium grained; biotite ± magnetite-bearing; massive; contains abundant, variably magnetic mafic enclaves; relative age relationship with other granites is unknown.

Monzogranite: grey-white to pink-white to pink; fine to medium grained; equigranular to weakly porphyritic; occurs as dykes through Agdm and supracrustal rocks between Mosher and Inglis lakes.

Granite to Granodiorite: grey-brown to grey-white to white; equigranular to seriate to weakly porphyritic; medium to coarse grained; biotite ± muscovite-bearing; abundant (locally up to 80%) enclaves of metasedimentary rocks, biotite-rich schlieren, and local hornblende + magnetite-granodiorite and biotite-tonalite enclaves. Metasedimentary enclaves are generally recrystallized and metamorphic porphyroblasts are rare; locally 'clean' and may in part be equivalent to equigranular phases of Agkm.

Hornblende Granite: dark pink to pink-green; equigranular; medium grained; biotite + hornblende-bearing; magnetite-bearing in the southeastern part of 85O/02; weakly to moderately foliated (defined by biotite and hornblende); may, in part, be equivalent to hornblende granite (Agh) of Jackson (2003).

Magnetite Hornblende Granodiorite: creamy beige to grey-beige; seriate, medium to coarse grained; biotite + magnetite-rich ± hornblende (generally hornblende-bearing), moderate to strong foliation; occurs as map-scale unit southeast of Mosher Lake and as mappable enclaves in Agdm south of Votaw Lake, cut by dykes of Agkk, forms part of Stagg Suite as defined by Henderson (1985), may, in part, be equivalent to hornblende granite (Agh) of Jackson (2003).

Mixed Granodiorite (Agdg) and Hornblende Granodiorite to Tonalite (Agth)

Granodiorite: white to grey-white; equigranular; medium grained; biotite ± hornblende-bearing; strongly foliated (defined by biotite, feldspars, and enclaves), locally contains enclaves of strongly deformed tonalite and hornblende-bearing granodiorite to tonalite (Agth); intrudes and forms injection layering in Asm; ± garnet, cordierite where associated with Asm; highly intruded by Agkm and associated pegmatites; ca. 2600 ± 5 Ma (Ootes et al., 2005).

Magnetite Granite: pink to pink-white; equigranular; medium grained; biotite + magnetite-bearing, moderately foliated (defined by biotite) to locally gneissic; locally contains hornblende-granodiorite to tonalite enclaves (Agth); locally occurs as enclaves in Agdm; some phases are cut by Agdg; in part, equivalent to 'Disco' granite (Abmx) of Jackson (2003); ca. 2607 ± 1.3 Ma (Ootes et al., 2005).

Hornblende Granodiorite to Tonalite: grey-brown, equigranular to weakly hornblende porphyritic; medium grained; biotite + hornblende-bearing, weakly to moderately foliated (defined by biotite and hornblende); generally occurs as enclaves in Agkm and Agdg and locally in Agdm; map scale occurrences are northwest of Germaine Lake, relationship with Agad is currently unknown.

Quartz Monzodiorite to Diorite: black-white to grey-green-pink; equigranular to feldspar porphyritic; medium to coarse grained; hornblende-rich + biotite ± quartz, K-feldspar, locally contains magmatic segregations of feldspar and quartz nodules; intruded into and deformed with Asm; generally occurs as enclaves in Agkm and Agdg, in part, equivalent to quartz diorite (Aqd) of Henderson (2004)

Feldspar Porphyry: creamy white to beige-white; plagioclase porphyritic; medium grained; granodiorite composition; biotite-bearing; moderately foliated; occurs as sills in Aasv and Asm (southeast and north of Wheeler Lake, respectively); highly intruded by Agkm and associated pegmatites.

Yellowknife Supergroup

Metatexite and Diatexite: upper amphibolite to granulite-grade; generally of pelitic to psammitic composition; contains melt + biotite ± sillimanite, cordierite (var. iolite), garnet, spinel, K-feldspar, muscovite (late); metatexite contains compositional bands from centimetres to metres thick; diatexite is massive and locally contains psammitic to intermediate restite; cordierite and garnet are common in mesosome and leucosome and commonly, cordierite has overgrown garnet; locally associated with silicate iron formation (garnet ± magnetite ± amphibole (grunerite?) ± orthopyroxene(?) + melt), amphibolite to mafic granulite (Amq), and intermediate

SYMBOL DESCRIPTIONS

Outcrop Features

Bedding: younging direct

Foliation: main/unknown; cleavage); 3rd generation

Foliation (Dip Unknown); cleavage); 3rd generation

Enclave Foliation: layerin bedding or S1 foliation); foliation or preferential ali

Pillow Flattening: younger

Migmatitic Layering: main melt), injection layering (f

Gneissosity: composition

Axial Plane: unknown; 1s

Ductile Shear: unknown;

Mineral Lineation: unknow in pelites and defines line

Intersection Lineation: ms

Fold Hinge: unknown; 1st

Z-Fold Hinge: unknown g

S-Fold Hinge: unknown; 1

Glacial Striae: pendant in

*Generation refers to the relationship (e.g., S2/F2/L2 indicates that a previ identified at that location). Some ma (1992) and University of Alberta field in the Wheeler and Germaine lakes

Samples

Assay sample location

U-Pb Ages: location and from Ootes et al. (2005): Z = zircon, M = monazite

Dabase dyke ages: from Bc-1939 +89/-92 Ma, Bt = (CHIMES)

Pressure-temperature det

Faults, Shear Zones, and Linear

Fault: unknown sense

Fault: sinistral sense

Fault: dextral sense

Shear Zone: sense unkno

Lineament: interpreted fro maps, and satellite and ae

Isograds (ornament on high-tea

Cordierite-in: first appeara in pelitic rocks

Sillimanite-in: first appear pelitic rocks

Melt-in: first appearance o Tremblay et al. (2003)

Orthopyroxene-in: approx orthopyroxene-bearing ms garnet-iolite-K-feldspar-be

Mineral Showings/Occurrences

Gold: showing (>0.5 g/ton sample label: 3.2ppm/8m.

Gold: anomalous occurrer gold); from Tyhee Develo

SYMBOL DESCRIPTIONS

Outcrop Features

- Bedding: younging direction unknown; upright; overturned
- Foliation: main/unknown; 1st; 2nd generation* (crenulation cleavage); 3rd generation* (crenulation cleavage)
- Foliation (Dip Unknown): unknown; 1st; 2nd (crenulation cleavage); 3rd generation* (crenulation cleavage)
- Enclave Foliation: layering/early foliation (e.g., preserved bedding or S1 foliation); main generation (preserved foliation or preferential alignment of enclaves)
- Pillow Flattening: younging direction unknown
- Migmatitic Layering: main; 2nd generation (in-situ partial-melt); injection layering (foreign granitic veinlets)
- Gneissosity: compositional layering (non-migmatitic)
- Axial Plane: unknown; 1st; 2nd; 3rd generation*
- Ductile Shear: unknown; dextral; sinistral sense
- Mineral Lineation: unknown; 1st generation* (L1 is folded in pelites and defines lineated pillows in mafic volcanics)
- Intersection Lineation: main foliation and bedding
- Fold Hinge: unknown; 1st; 2nd; 3rd generation*
- Z-Fold Hinge: unknown generation
- S-Fold Hinge: unknown; 1st; 2nd generation*
- Glacial Striae: pendant in ice-advancement direction

*Generation refers to the relationships preserved on individual outcrops (e.g., S2/F2/L2 indicates that a previously formed structure was identified at that location). Some measurements adapted from Brophy (1992) and University of Alberta field school (Tremblay et al., 2003) in the Wheeler and Germaine lakes area.

Samples

- Assay sample location
- U-Pb Ages: location and crystallization/inheritance ages from Ootes et al. (2005); sample label: Z-2590 ± 2.3 Ma, Z = zircon, M = monazite, Zi = inherited zircon
- Dubase dyke ages: from Atkinson (2004); sample label: Bc-1939 +89/-92 Ma, Bt = baddeleyite (TIMS), Bc = baddeleyite (CHIMES)
- Pressure-temperature determination: from Scheel (2004)

Faults, Shear Zones, and Lineaments

- Fault: unknown sense
- Fault: sinistral sense
- Fault: dextral sense
- Shear Zone: sense unknown
- Lineament: interpreted from airphotographs, topographic maps, and satellite and aeromagnetic images

Isograds (ornament on high-temperature side)

- Cordierite-in: first appearance of cordierite porphyroblasts in pelitic rocks
- Sillimanite-in: first appearance of fibrolitic sillimanite in pelitic rocks
- Melt-in: first appearance of melt in pelitic rocks; after Tremblay et al. (2003)
- Orthopyroxene-in: approximate southern-limit of orthopyroxene-bearing mafic and intermediate rocks and garnet-sillite-K-feldspar-bearing pelitic rocks

Mineral Showings/Occurrences

- Gold: showing (>0.5 g/ton Au; trenched, or drill indicated); sample label: 3.2ppm/8m; from Brophy (1992)
- Gold: anomalous occurrence (grab sample with >0.5 g/ton gold); from Tyhee Development Corp. (2001) and NORMIN

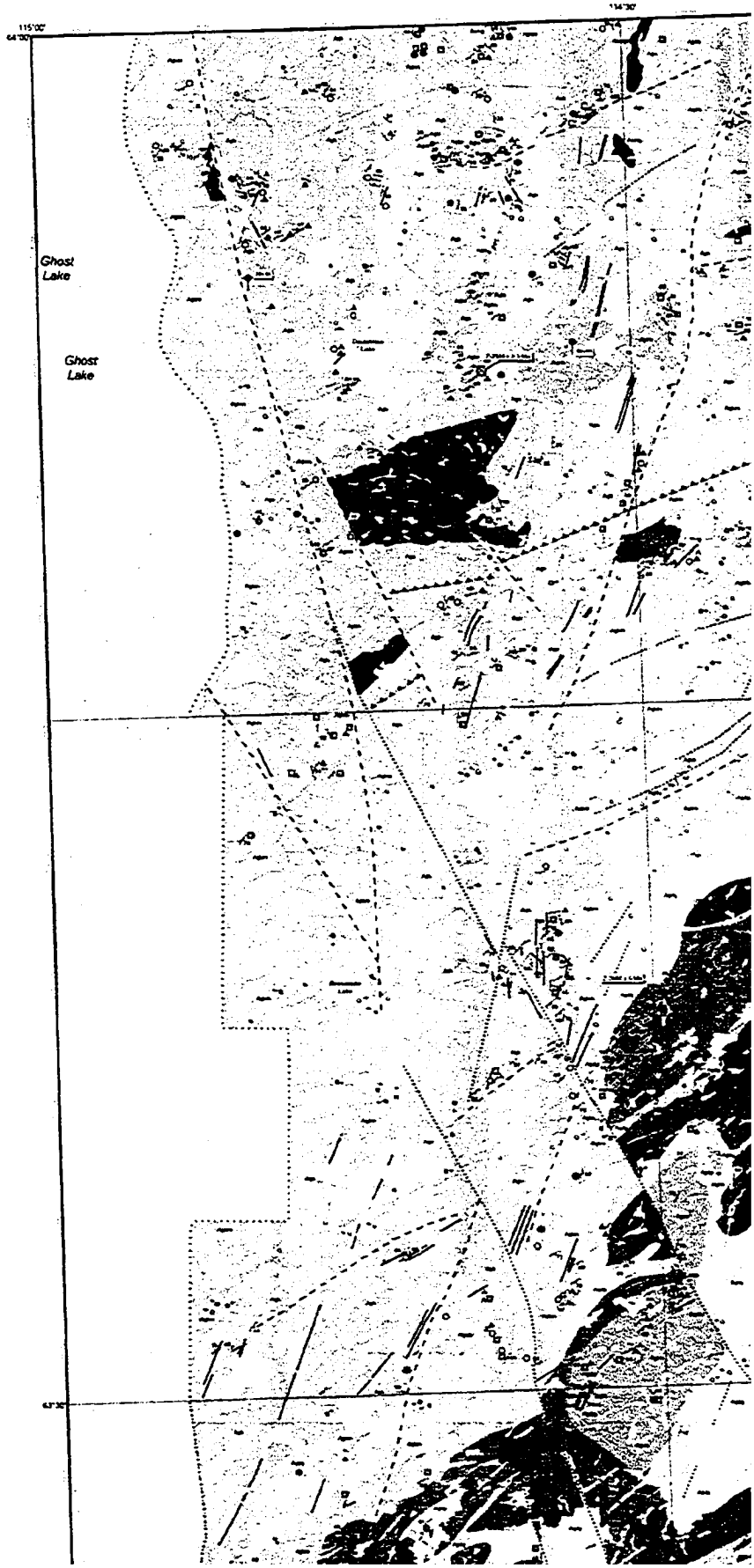

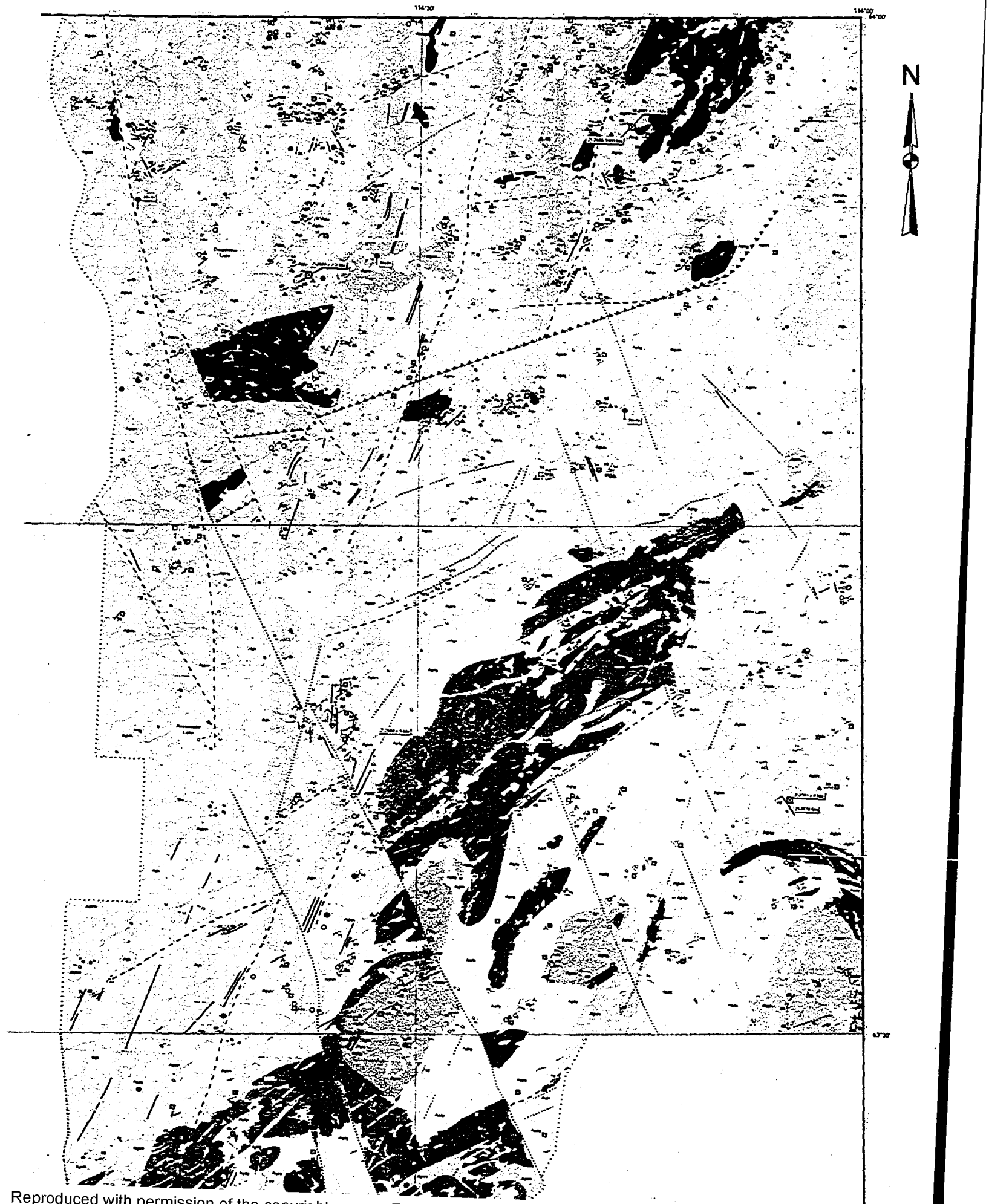

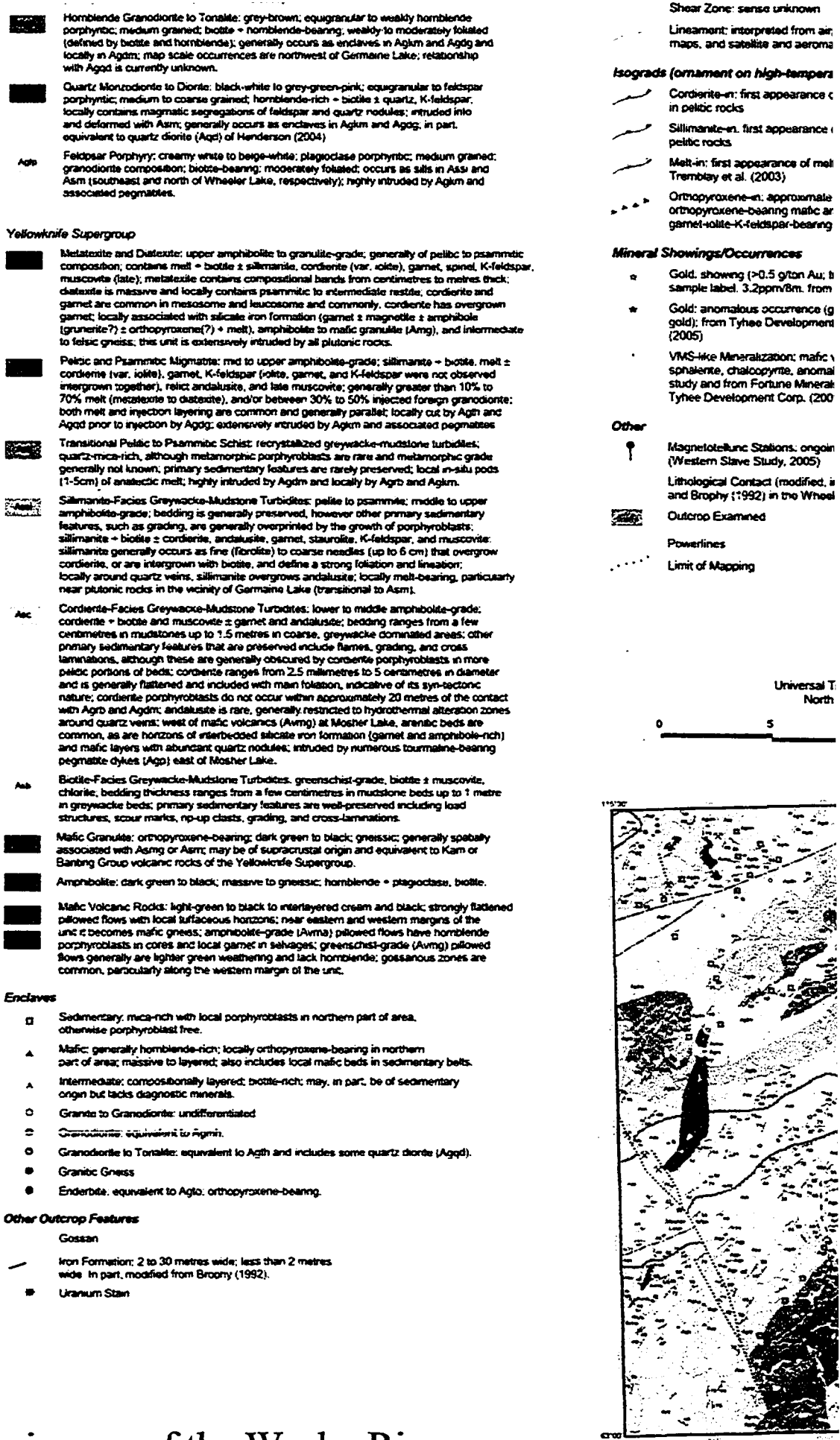

Figure 3-3. Geologic map of the Wecho River area (modified from Ootes and Pierce, 2005).